A cell based GEF assay reveals new insights into the biology of DENN domain proteins and their Rab substrates

Rahul Kumar

The Integrated Program in Neuroscience

Montreal Neurological Institute

McGill University

Montreal, April 2023

A thesis dissertation submitted to McGill University in partial fulfilment of the requirements of the degree of Doctor of Philosophy in Neurological Sciences

Table of contents

Abstract

Membrane trafficking mediated by small GTPases such as Rabs controls the localization and levels of a myriad of proteins and thus numerous cellular functions. Rabs are activated by guanine nucleotide exchange factors (GEFs), including DENN domain-bearing proteins, the largest family of Rab GEFs. To identify new DENN/Rab pairs, we developed a cell-based assay involving DENN domain-mediated recruitment of Rabs to mitochondrial membranes and screened two DENN domain families. Our screening identified 19 novel DENN/Rab pairs, including Rab10 as a substrate for DENND2B, a protein linked to cancer and severe mental retardation. We discovered that DENND2B-mediated activation of Rab10 represses the formation of primary cilia. Primary cilia are essential for cell and organism development and defects in their biogenesis lead to ciliopathies. DENND2B also acts as a GEF for RhoA, regulating primary cilia length. In our second study we uncovered a new function for DENND2B in cytokinesis, the final stage of cell division. Rab35 recruits MICAL1 to accomplish actin depolymerization required for intercellular cytokinetic bridge (ICB) abscission. We found that DENND2B is a GEF for Rab35, activating it at the ICB. The N-terminal region of DENND2B interacts with an active Rab35 mutant, indicating DENND2B is both a Rab35 GEF and effector. Knocking down DENND2B delays abscission, increasing multinucleated cells, F-actin overaccumulation, and chromatin bridge formation. Additionally, DENND2B knockdown (KD) activates Aurora B kinase, a checkpoint activation hallmark. Our research highlights the versatile roles of DENND2B in ciliogenesis and cytokinesis and highlights diversity in DENN domain-mediated activation of Rabs.

Résumé

Le trafic membranaire, qui est médié par de petites protéines GTPases telles que les Rabs, contrôle la localisation et les niveaux d'une myriade de protéines et, par conséquent, de nombreuses fonctions cellulaires. Les Rabs sont activés par des facteurs d'échange de nucléotides guanine (GEFs), y compris les protéines portant le domaine DENN, la plus grande famille de GEFs Rab. Pour identifier de nouveaux couples DENN/Rab, nous avons développé une méthodologie in vivo basée sur le recrutement des Rabs aux membranes mitochondriales par le domaine DENN et nous avons identifié deux grandes classes de famille possédant un domaine DENN. Nous avons identifié 19 nouveaux couples DENN/Rab, y compris Rab10 comme substrat pour DENND2B, une protéine liée au cancer et à la déficience mentale grave. Nous avons découvert que l'activation de Rab10 par DENND2B réprime la formation de cils primaires. Les cils primaires sont essentiels pour le développement cellulaire et les défauts dans leur biogenèse conduisent à des ciliopathies, ce qui en fait un domaine crucial d'étude. DENND2B agit également comme un GEF pour RhoA, régulant la longueur des cils primaires. Dans notre deuxième étude, nous avons découvert une nouvelle fonction de DENND2B dans la cytokinèse, la dernière étape de la division cellulaire. Rab35 recrute MICAL1 pour accomplir la dépolymérisation de l'actine nécessaire à l'abscission du pont cytokinétique intercellulaire (ICB). Nous avons découvert que DENND2B est une GEF pour Rab35, l'activant au niveau de l'ICB. La région N-terminale de DENND2B interagit avec une version mutante de Rab35, indiquant que DENND2B est à la fois une GEF et un effecteur de Rab35. La réduction de DENND2B retarde l'abscission, augmentant la proportion de cellules multinucléées, l'accumulation de F-actine et la formation de ponts de chromatine. De plus, la réduction de DENND2B active la kinase Aurora B, un marqueur d'activation

de point de contrôle. Nos recherches mettent en évidence les rôles polyvalents de DENND2B dans la ciliogenèse et la cytokinèse et soulignent la diversité de l'activation des Rabs médiée par le domaine DENN.

List of figures or tables

List of abbreviations

GTP	Guanosine triphosphate
GDP	Guanosine diphosphate
GEFs	Guanine nucleotide exchange factors
GAPs	GTPase-activating proteins
GDI	GDP-dissociation inhibitor
GDFs	GDI displacement factors
MADD	MAPK-activating protein containing a death domain
ULK	Unc-51-like kinase
Vps23	vacuole protein sorting 23
IFT	Intraflagellar transport
F-actin	filamentous actin
FKBP	FK506-binding protein domain
FRB	FKBP-rapamycin–binding domain
RFP	Red fluorescent protein
γ-tubulin	gamma-tubulin
Ac-tubulin	acetylated tubulin
MO	morpholino
hpf	hours post-fertilization
GST	glutathione S-transferase
MICAL-L2	molecule interacting with CasL-like 2
RBD	Rho-binding domain
LRRK2	leucine-rich repeat kinase 2
MPP9	M-phase phosphoprotein 9
SAG	Smoothened agonist
ANOVA	one-way analysis of variance
ICB	Intercellular bridge
DENN	differentially expressed in normal and neoplastic cells
KD	Knockdown
MICAL-L1	molecule interacting with CasL-like 1
FL	Full length
ROI	region of interest

Acknowledgement

I cannot express enough my gratitude towards my supervisor, **Dr. Peter McPherson**. He has been a constant pillar of support throughout my entire journey, providing me with guidance and encouragement whenever it was needed. I still vividly remember the first two years of my PhD when I was struggling to find a direction, and nothing seemed to be working. During this time, Peter was always there for me, meeting with me multiple times a week to discuss my progress and providing valuable insight. His approachable and understanding nature allowed me to voice my concerns freely and seek guidance when needed. He not only helped me develop my scientific critical thinking skills but also instilled in me a passion for science that I had never experienced before. Dr. McPherson's infectious enthusiasm for science and his ability to deliver scientific presentations with such passion and conviction have been a constant inspiration to me. He provided me with the freedom to develop my skills and pursue growth opportunities, while also ensuring oversight of all my activities. Without his unwavering support and guidance, I would not have been able to achieve what I have today. I feel truly fortunate to have had him as my supervisor and mentor, and I will always be grateful.

The end of my second year in my PhD was a turning point in my journey when Dr. McPherson introduced me to a revolutionary technique using mitochondrial localization of DENN domains to screen for potential Rab GTPase substrate. The idea came from a discussion over lunch between Dr. McPherson and **Dr. Suzanne Pfeffer** from Stanford University, which took place during the Small GTPases meeting. Therefore, I would like to extend my thanks to Dr. Pfeffer as well for her contribution to my research.

I also had the privilege of working with two brilliant committee members, **Dr. Wayne Sossin** and **Dr. Nathalie Lamarche-Vane**. Dr. Sossin's knowledge of molecular and cellular biology was truly inspiring. He challenged me to think critically and deeply about my research questions, and his feedback was always constructive. Dr. Lamarche-Vane's expertise in GTPase mediated signal transduction was equally impressive. She provided me with

invaluable feedback on my experimental design and data interpretation, helping me to refine my ideas. I would like to extend my sincere thanks to both of them for their guidance throughout my entire journey. Thank you for sticking with me throughout PhD.

Going through a PhD journey is an arduous task, filled with long days and nights of research, analysis, and writing. It takes a village of support to make it through, and I was fortunate enough to have an incredible group of friends in Montreal who provided just that. They reminded me to take breaks, to laugh, and to live a little outside the walls of the lab. I cannot express enough gratitude to my dear friend **Shashank Srikanta**. Our friendship goes way back to our days as undergraduates at IISER-Kolkata, India, and he too is pursuing his PhD at IPN. Shashank has been a rock throughout this journey, always there to lend an ear and offer sage advice. I credit him for showing me the ropes on how to craft an effective thesis without sacrificing too much time. His unwavering support has been invaluable to me, and I feel truly blessed to have him by my side. I am also grateful to **Archita Rajasekharan** and **Vincent Francis** for helping me settle in Montreal in the early days. Archita's leadership and organizational skills have been instrumental in our movie nights and restaurant hopping, where we tried out all kinds of Montreal cuisine. Through them, I have “tried” to learn the importance of maintaining a healthy work-life balance. I have great respect for both of them, and I know I can always count on Vincent for advice and support. Further, I want to thank **Dr. Monalisha Nayak**, a 2022 McGill PhD graduate, for her support and advice throughout my doctoral journey. There were many moments when I just needed to vent, to share the highs and lows, and to seek advice. And let's not forget her incredible talent in the kitchen - I am a huge fan of her cooking. Thank you, Mona, for being an amazing friend. My friend **Pratap Singh** has been a beacon of light when it comes to organising big social events. He has hosted many Diwali and Holi parties, which were the perfect stress reliever after a long day in the lab. I am also grateful for **Shibam Debbarma** who always knew just what to say and offered excellent advice, as well as for his encouragement to push me beyond my limits. Thanks to his encouragement, I now participate in multiple sports at the McGill sports complex. And anytime

I crave some spicy food, he is always there to make it for me. Thanks Shibam. Speaking of sports, I can't forget to mention my first and only roommate, **Jemal Yusuf**, who pushed me to do some physical activities and lose some weight. He may think I exaggerate, but it's a fact that I owe him for motivating me to live a healthier lifestyle. I miss those nights when we used to discuss course work topics or fun facts or US politics. Jemal, I cannot thank you enough for being such a kind and wonderful friend to me. In addition, I am grateful for the fun and enjoyable interactions I had with **Dhruv Mehrotra**, a fellow IPN student. Whether it was hanging out at the swimming pool or just spending time together outside, Dhruv was always there to make me laugh and brighten my day. He was also an excellent listener, and I appreciate the support he provided during challenging times. I would also like to thank **Neelima Vaddadi**, an IPN graduate, for the informative discussions we had while working late nights in the lab and for the fun events she organized at her place. Thank you Neelima for being such a wonderful friend.

I realize that I have spoken a lot about the friends I had outside of the lab, but it is important to acknowledge the vital role that lab members play in a successful PhD journey. I want to express my sincere gratitude to **Jacynthe Phillie**, our lab manager, who was always there to offer guidance and support. She was an incredible human being - so kind, compassionate, and down to earth. Whenever I needed help, she always had a solution, and I can't imagine how she managed to keep up with all the demands of the lab, including plating cells for each lab member as per their individual requirements. This level of service was truly exceptional, and it was a testament to Jacynthe's organizational skills and dedication to her work. When she announced her retirement, we were all devastated, but we learned to adapt and carry on without her. Thank you, Jacynthe, for your incredible contributions to the lab and for being such an important part of my PhD journey.

As I progressed in the lab, I came to realize that working collaboratively and helping each other out was key to success. I am also grateful to have had **Vincent**, **Maleeha Khan**, and **Adriana Aguila** as amazing peers who were always there to lend a helping hand and support

me with my experiments. I also have immense gratitude towards **Gopinath Kulasekaran** for the countless discussions we had, from experimental design to data analysis. I also wanted to give a special shoutout to **Dr. Maria S. Ioannou**, a former lab member who has been an incredible help with my second manuscript. Even though she's all the way in Alberta, Maria has always answered my questions and clarified any doubts I may have had. Thanks Maria.

In addition, I will truly miss **Maryam Fotouhi**, our lab technician, who was always so kind and helpful. She was such a great resource and a good listener whenever I had a concern. I will always be thankful for her generosity and warmth. I also want to express my heartfelt appreciation to **Carl Laflamme**, **Emily Banks**, **Armin Bayati**, **Riham Ayoubi**, **Luis Aguilera Luna**, **Sara González Bolívar**, and **Philip Thorne** for being a super supportive and wonderful group of colleagues.

Lastly, I cannot end without expressing my heartfelt gratitude to my family members - my mom, **Kishori Devi**, my dad, **Nand Kishore Baitha**, my late grandfather, **Sriram Baitha**, my grandmother, **Gulabi Debi**, my sister, **Kumari Rajani** and brother-in-law, **Upendra Baitha**. They have been my rocks and cheerleaders throughout this journey. I want to thank them for being my strongest support system, and for always believing in.

Dedication

I would like to dedicate my thesis to my late grandfather, **Sriram Baitha**. He was always eager to see me complete my PhD and would ask about my progress during every phone call. The fact that no one in my family had achieved this highest degree made him even more excited. It was a cruel twist of fate that my grandfather passed away just a month before I submitted my initial thesis, and I couldn't share the news that I was close to obtaining my degree. I miss him dearly and wish he could have been here to witness this accomplishment that he was so invested in. This thesis is a tribute to his unwavering support and encouragement, and I hope to make him proud.

Contributions

Chapter 3

A cell-based GEF assay reveals new substrates for DENN domains and a role for DENND2B in primary ciliogenesis

Rahul Kumar, Vincent Francis, Gopinath Kulasekaran, Maleeha Khan, Gary A B Armstrong, Peter S McPherson
Department of Neurology and Neurosurgery, Montreal Neurological Institute (the Neuro), McGill University, Montreal, Quebec, Canada.

Originally published in *Science Advances*; DOI: 10.1126/sciadv.abk3088

RK	Designed, performed experiments and analysis; wrote the manuscript
VF	Performed experiments and analysis
GK	Performed experiments
MK	Performed experiments
GABA	Performed experiments
PSM	Supervised, designed experiments, and wrote the manuscript

Chapter 4

DENND2B activates Rab35 at the intercellular bridge regulating cytokinetic abscission and tetraploidy

Rahul Kumar*, Vincent Francis*, Maria S. Ioannou, Adriana Aguila, Emily Banks, Gopinath Kulasekaran, Maleeha Khan, Peter S. McPherson
* contributed equally
Department of Neurology and Neurosurgery, Montreal Neurological Institute (the Neuro), McGill University, Montreal, Quebec, Canada.

Preprint published in *BioRxiv*; DOI: https://doi.org/10.1101/2023.01.12.523789

RK	Designed, performed experiments and analysis; wrote the manuscript
VF	Performed experiments and analysis
MSI	Binding assay experiment for DENND2B(N-term) and Rab35
AA	Performed experiments
EB	Generated superposition of alpha-fold DENND1B structure and DENND2B
GK	Performed experiments
MK	Performed experiments
PSM	Supervised, designed experiments, and wrote the manuscript

CHAPTER 1

Introduction

Eukaryotic cells rely on a highly coordinated process of intracellular trafficking to move cargo between organelles. This involves tightly controlled membrane fusion events, which are facilitated by the processes of docking and fusion. Rab GTPases, a key component of budding, transport, docking, and fusion machinery, play a crucial role in ensuring that cargo is delivered accurately to the correct destinations. These small GTPases function in membrane trafficking by toggling between GTP-bound (active; membrane-bound) and GDP-bound (inactive; cytosolic) states. In their GTP-bound state they recruit effector proteins that carry out the membrane trafficking functions downstream of the Rabs. Guanine nucleotide exchange factors (GEFs) mediate the exchange of GDP for GTP, while GTPase-activating proteins (GAPs) accelerate the intrinsic GTPase of the Rabs and end the cycle.

There are around 60 Rabs in the mammalian system, but far fewer GEFs have been described. Given that Rabs play a vital role in defining organelles and regulating membrane trafficking, it is important to understand why there is a discrepancy between the number of Rabs and GEFs. The largest family of GEFs consists of those with a DENN domain, which is a conserved protein module. There are at least 18 members in this family, divided into eight subfamilies, most of which are poorly characterized. Previous in vitro screening of 16 DENN domain proteins against most Rabs led to the identification of a single Rab for each DENN domain subfamily. However, more detailed studies on individual DENN domain proteins have revealed different Rab substrates than those identified in the in vitro screen. In vitro-based screening approaches have limitations, including the potential misfolding and inactivation of

purified Rabs and difficulty in obtaining proper nucleotide loading. Therefore, it is crucial to address these technical challenges to fully understand GEF-mediated regulation of Rabs and membrane trafficking.

In this study, we have developed a cell based GEF assay that utilizes a mitochondrial relocalization technique to identify Rab GTPase substrates for two of the most extensively studied DENN domain protein families (DENND1 and DENND2). The aim of this research is to study the existing Rab GTPase/DENN domain pairs, discover novel targets of the remaining DENN domain proteins, and gain a better understanding of cellular targeting and signaling mechanisms.

CHAPTER 2

Literature review

Endosomal sorting and trafficking

Endosomal trafficking is a conserved cellular process found in all eukaryotes, from single-celled organisms to humans. It involves the internalization of protein and lipid cargo that is then sorted in early endosomes, the first sorting station in the endocytic pathway. From there, the cargo either recycles back to the plasma membrane or progresses through the endosomal system, which matures into late endosomes before fusion with lysosomes for degradation. This system controls the localization and levels of a wide variety of proteins, making it crucial for cellular function. In neurons, endosomal trafficking plays a unique role in controlling processes related to synaptic function. Interestingly, defects in endosomal membrane trafficking pathways have emerged as a common cellular mechanism in neurodegenerative diseases over the past few years.

Rab GTPases

Rab GTPases are the largest family of small GTPases and play crucial roles in regulating membrane trafficking, encompassing all stages of this process. Rab GTPases function as molecular switches that alternate between two conformations: an active state bound to GTP and an inactive state bound to GDP [1][2][3]. Inactive Rabs reside in the cytosol and require GEFs for activation. However, a study by Ioannou et al. has challenged the established view, showing that it is not entirely accurate [4]. The authors demonstrated that Rab13 can associate with and move on

vesicles without C-terminal prenylation, which was previously believed to be necessary. Instead, inactive Rab13 seems to bind to vesicles through protein-protein interactions. It is only after activation that Rab13 associates with the plasma membrane, presumably due to the insertion of the C-terminal prenyl group into the membrane [4]. GEFs interact with the GDP-bound form of the Rab, promoting the exchange of GDP for GTP. Once activated, Rabs translocate to membranes and recruit effector proteins to perform their membrane trafficking functions. However, the activated Rabs are eventually deactivated by GTPase-activating proteins (GAPs), which significantly increase their intrinsic rate of GTPase activity by several orders of magnitude [5][6]. Furthermore, the active and inactive cycle of Rab GTPase works together with the reversible attachment to the cytosolic leaflet of membranes via one or two geranylgeranyl lipid moieties that are covalently attached to C-terminus cysteine residue(s) [7][8][9]. The process of prenylation of Rabs depends on the Rab escort protein (REP), which binds to newly synthesized Rabs and presents them to Rab geranylgeranyltransferase for prenylation [10][11][12]. Once prenylated, the Rabs bind to the GDP-dissociation inhibitor (GDI) in the cytosol and form a complex that is essential for proper membrane targeting (figure 1) [13].

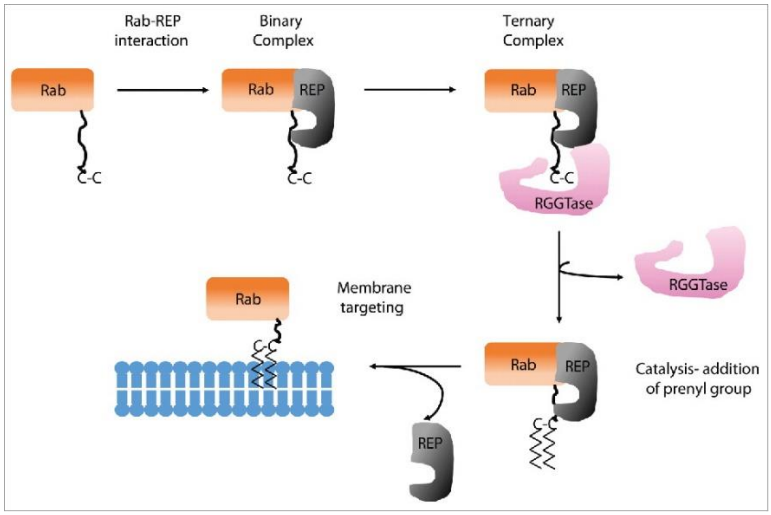

Figure 1: The Prenylation Process of Rab Proteins. Rab proteins initially form a binary complex with REP upon synthesis. Subsequently, RGGTase binds to REP, forming a ternary complex (Rab-REP-RabGGTase), where RGGTase catalyzes the transfer of prenyl groups to Rab's C-terminal cysteine residues. The prenylated Rab stays associated with REP, aiding its targeting to the cell membrane *(Reproduced with permission Taylor and Francis, Shinde et. al. 2018, Small GTPases)*

Rab GTPases are a highly conserved family with around 60 members in mammalian system, and are present in all eukaryotes. Most yeast Rabs have human homologs, highlighting their crucial role in eukaryotic biology [14]. Rab proteins localize to specific intracellular organelles or vesicles and function in specialized trafficking pathways [1]. Their functional impairment is linked to various human diseases [1], such as Charcot-Marie Tooth disease caused by mutations in Rab7 and Niemann-Pick type C disease caused by impaired trafficking by Rab9 [15][16]. In addition, bacterial pathogens exploit Rabs to colonize host cells during infection [17]. For example, Mycobacterium tuberculosis utilizes Rab5 to facilitate iron delivery by fusion with early and recycling endosomes [18], while Legionella pneumophila recruits Rab1 to avoid fusion with the default secretory pathway [19]. In addition, certain Rabs are also linked to cancer. For instance, Rab13 regulates the trafficking and cellular localization of various proteins involved in cancer, such as integrins during cell migration [20][21]. Moreover, the growth of glioblastomas increases and animal survival decreases in the case of loss of function of the endosomal GTPase Rab35 in human brain tumor-initiating cells after implantation in mouse brain [22]. These pathologies associated with impaired Rab trafficking highlight their significance in cell physiology, emphasizing the need for further research on how Rabs function.

Determinants of GTPase recruitment

As stated earlier, the proper insertion of Rabs into their respective membranes is facilitated by the geranylgeranyl lipid moieties obtained through posttranslational modification of cysteine residues at the C-terminus. However, this raises an important query as to what factors determine the specific localization of Rabs. An initial study

proposed that the correct targeting information is contained within the hypervariable region of the Rab's C-terminus [23]. However, this notion was subsequently disputed, with the suggestion that Rab family-specific and Rab subfamily-specific motifs, rather than the hypervariable region, are necessary for Rabs' specific targeting [24]. In addition, it has been proposed that GDI displacement factors (GDFs) localized to the membrane may assist in recruiting Rabs to the correct location by disrupting the stable GDI/Rab complex [25][26], although only one GDF, Yip3, is currently known to function with Rab9, Rab7, and Rab5 [26]. A recent study demonstrated that misplacement of GEFs (Rabex-5, DrrA, or Rabin8) alone to the mitochondria is sufficient to recruit Rab5A, Rab1A, and Rab8A to the mitochondrial membrane [27]. Additionally, targeting the Hps1-Hps4 complex (BLOC-3) to the mitochondria alone is capable of recruiting Rab32 and Rab38 [28]. Therefore, it is evident that the GEF activity of Rab GEFs plays a central role in controlling the membrane localization of Rabs [27][28].

Rab GEFs

In recent years, there have been significant advances in our understanding of how different families of GEFs control the function of Rab GTPases. Several proteins or protein complexes have been shown to act as GEFs for Rab GTPases.

1) Mon1/Ccz1 complex triggering endosomal maturation by acting as a GEF for Ypt7/ Rab7 [29]. Previous research had suggested that the Mon1p-Ccz1p complex in budding yeast played a role in delivering components to the yeast vacuole and was involved in the tethering process, which is known to be Rab-dependent [30]. Later studies in C. elegans and mammalian cells have shed further light on the function of the SAND-1/Mon1 and CCZ-1 complex. It was found that this complex is required for

the maturation of early endosomes into late endosomes and lysosomes, as well as for phagosome maturation [31]. These findings provide additional evidence to support the notion that the maturation of early to late endosomes is linked to a Rab conversion process, whereby Rab5 is replaced with Rab7 [32].

The SAND-1/Mon1 and CCZ-1 complex appears to promote Rab conversion by displacing Rab5 from early endosomes and facilitating the recruitment of the HOPS complex, which is associated with Vps39 Rab7 GEF activity [31]. This process promotes the conversion of early endosomes into late endosomes and ultimately lysosomes. These new findings deepen our understanding of the role played by the SAND-1/Mon1 and CCZ-1 complex in endosome maturation, and provide insights into the mechanisms underlying Rab conversion.

2) Ypt1p/Rab1 is activated by the TRAPP complex on ER-to-Golgi transport vesicles [15][16]. TRAPP-I, a 7-subunit complex, activates Ypt1p and facilitates vesicle tethering via the Ypt1p effector protein Uso1p. In mammalian cells, a similar pathway involving Rab1 and p115, a Uso1p homologue, exists. In budding yeast, there exists another version of TRAPP called TRAPP-II, which consists of 10 subunits. This form of TRAPP is responsible for activating Ypt1p and Ypt31-32p, and is involved in post-Golgi trafficking [33].

3) Sec2p/Rabin8 serves as an activator of Sec4p/Rab8 [34][35][36]. Rab8 is evolutionarily related to yeast Sec4p, and it is not surprising that the Rabin8 protein, mammalian homologues of Sec2p, act as a GEF for Rab8. The Rabin proteins were identified in a proteomic study analyzing components of the BBSome, a complex involved in cilium biogenesis and function, which subsequently demonstrated that Rab8 plays a role in cilium formation [37]. These findings suggest that Sec2-domain

proteins are conserved regulators of the Sec4p/Rab8 GTPases involved in transport to the cell surface.

However, the fruit fly *Drosophila melanogaster*, although having both Rab8 and Rab10 homologues, does not have an obvious Sec2p homologue. This observation suggests that there must be additional GEFs involved in the regulation of the Rab8/10 family of GTPases in fruit flies [6]. The identification and characterization of these additional GEFs may provide insights into the unique trafficking pathways. Further studies are needed to identify these GEFs and understand their mechanism of action.

4) Ric1p-Rgp1p complex functions as a GEF for Ypt6p [20]. Ric1p/Rgp1p is a GEF that activates Ypt6p GTPase and helps in recycling components of the exocytic machinery such as SNAREs from endosomes back into the late-Golgi for reuse [38]. This recycling process is important for maintaining the proper levels of proteins required for efficient exocytosis.

While homologues of Ric1p/Rgp1p have been identified in a wide range of eukaryotes, there has been limited research into their potential GEF activity towards Rab6, which is the equivalent of Ypt6p in humans. Future studies could investigate whether these homologues are capable of activating Rab6 and contributing to intracellular trafficking processes in other organisms.

5) VPS9 domain containing protein: Vps9-domain proteins are a diverse family of GEFs that are known to specifically activate members of the Rab5 subfamily, including Rab5A-C, Rab17, Rab21, Rab22A, and Rab22B in humans [39][40]. Among these GEFs, mammalian Rabex-5 is the most extensively studied. According to cell biological studies, Rabex-5 plays a critical role in regulating membrane fusion dynamics by acting on Rab5 at the early endosome. Rabex-5 is recruited to

endosomes by interacting with ubquitinated cargo molecules and the Rab-effector protein Rabaptin-5, which allows it to confine its GEF activity to the early endocytic pathway where Rab5 is essential [41][42].

Interestingly, in biochemical assays, Rabex-5 has been shown to activate not only Rab5 but also the closely related GTPase, Rab21, but not other Rab proteins. This suggests that Rabex-5 may have some degree of specificity in its GEF activity towards certain Rab proteins. Overall, these findings highlight the importance of Vps9-domain proteins in controlling Rab function and the need for further investigations to fully understand their mechanisms of action and specificity towards different Rab proteins [39].

6) The DENN domain proteins, initially known for their involvement in various signaling pathways, make up the final family known to possess Rab GEF activity. There are eight subgroups of DENN domain proteins in humans, which are discussed in detail below [43].

DENN-domain bearing proteins

The discovery of the first DENN domain protein, MADD (MAPK-activating protein containing a death domain) [44][45], occurred through its identification as a binding partner of a cytoplasmic death domain of the TNF receptor. Subsequent bioinformatic analysis revealed the presence of an N-terminal region of MADD that was similar in other unrelated proteins, leading to the identification of a family of DENN domain-containing proteins that consisted of 18 members based on homology within the DENN domain. These proteins were further categorized into eight families, with the DENN

domain being located at the N terminus in most members except for the DENND2 family, which had it at the C terminus.

Among these eight families, the DENND1 family comprises three members, DENND1A-1C (also known as connecdenn 1-3), which function as GEFs for Rab35. A relationship between connecdenn and Rab35 was first demonstrated in C. elegans, which revealed defective endosomal recycling of the yolk receptor due to mutations in either Rab35 or connecdenn [46]. Later studies in mammalian systems confirmed that all three members of the connecdenn family function as GEFs for Rab35, with variable rates of GEF activity observed among them [47][48]. Interestingly, connecdenn 3 was shown to have specific activity toward Rab13 instead of Rab35 [49].

The DENND2 family consists of four members, DENND2A-2D, with the DENN domain located at the C-terminus. All four members have been demonstrated to function as GEFs for Rab9A/9B [49], which facilitates the retrograde trafficking of the mannose 6-phosphate receptor from the late endosome to the trans-Golgi network [50]. Depletion of DENND2A disrupts mannose 6-phosphate receptor trafficking, while depletion of other DENND2 family members does not influence its trafficking [49]. However, a subsequent study found that DENND2B (also known as ST5) functions as a Rab13 GEF instead of Rab9A/9B [20].

DENND3 functions as a GEF for Rab12 [49][51], and recent studies have revealed that it activates Rab12 upon phosphorylation by Unc-51-like kinase (ULK) [52]. The DENND4 family consists of three members, DENND4A-4C, all of which function as GEFs for Rab10 [49], which regulates basolateral trafficking in polarized cells as well as Glut4 recycling in adipocytes [49][53][54].

The DENND5 family includes DENND5A/5B, also known as Rab6IP1/Rab6IP1-like Protein. DENND5A binds to Rab6 in a nucleotide-independent manner through its first RUN domain [55][56][57]. Both DENND5A and DENND5B function as GEFs for Rab39 [24]. While Rab39A maintains interleukin secretion [58], Rab39B regulates Golgi-derived vesicle trafficking and is critical for neuronal development [59].

The DENND6 family comprises two members, DENND6A/6B (also known as FAM116A and FAM116B), which both function as GEFs for Rab14 [60]. Rab14, activated by FAM116, regulates N-cadherin levels by facilitating transport of ADAM family protease ADAM10 and thereby controls cell migration [60].

MTMR5 and MTMR13, on the other hand, function as GEFs for Rab28 [49]. Rab28 is known to play a role in the late endosomal pathway and partially colocalizes with vacuole protein sorting 23 (Vps23), which is a component of the ESCRT I complex [61].

Finally, the DENN/MADD protein was purified from brain extracts and identified as a Rab3 GEF [44]. Subsequent studies found that DENN/MADD binds to the active form of Rab3 (GTP bound) via its DENN domain, a signature of Rab effector [62]. However, it remains unclear whether DENN/MADD acts as a GEF, an effector, or both toward Rab3. Additionally, DENN/MADD has been shown to have GEF activity for Rab27A/B in addition to its role as a GEF for Rab3 [49][63]. With that being said, it is important to note that several of the DENN/Rab pairs mentioned earlier have not undergone detailed cell biological studies and have only been reported based on in vitro assays.

Thus, DENN domain proteins play a crucial role in regulating the activity of Rabs and thereby controlling various cellular processes such as endosomal recycling, vesicle trafficking, and cell migration. The specificity of DENN domain proteins towards

individual Rab proteins highlights the complexity of Rab GTPase signaling and the need for further research to fully understand these processes.

Effectors and Rab cascade

Effectors are proteins that interact specifically with the GTP-bound from of a Rab GTPase and are involved in at least one aspect of its downstream effects. They are identified by their ability to bind selectively to a specific Rab in its GTP-bound state and have been discovered through various methods such as the yeast two-hybrid system, genetic screens, and affinity purification. The growing collection of Rab effectors is a testament to their importance in regulating membrane trafficking pathways [64].

Each Rab appears to signal through a variety of different effectors that work together to translate the signal from one Rab protein to various aspects of membrane transport. This coordination of effectors is critical to the specificity of membrane traffic. Effector proteins play a crucial role in establishing membrane domains that are marked by a specific Rab. Additionally, effectors are involved in maturing these domains through a Rab cascade mechanism.

For example, once a Rab has reached its destination, it needs to be activated and stabilized in its active, GTP-bound form to ensure proper vesicle transport and fusion. One way to achieve this is through the formation of a complex between the Rab, its GEF, and one or more of its effectors. A well-studied example is the Rabex5-Rab5-Rabaptin5 complex. Rab5 is required for endocytic vesicle transport and fusion with early endosomes [65]. For Rab5 to function properly, it needs to be localized to both

endocytic vesicles and early endosomes [65]. This localization is achieved through the actions of Rabex5, the Rab5-GEF, and one of its effectors, Rabaptin5 [65].

Initially, Rab5 is recruited to the membrane, followed by Rabex5-mediated activation [66][67]. Once activated, GTP-bound Rab5 can interact with its effectors, including Rabaptin5 [68]. Rabaptin5 not only binds to Rabex5 but also enhances its exchange activity on Rab5 [69], creating a positive feedback loop that prevents GAP inactivation and GDI-mediated membrane extraction, thereby ensuring that Rab5 remains in its active, GTP-bound form attached to endocytic vesicles or the early endosome. Similar positive feedback loops have been identified in other systems as well, such as the Vps33p effector of the Rab GTPase Ypt7p and the Vps39p GEF [70]. The existence of the GEF-Rab effector complex indicates that it is a recurring mechanism for Rab activation and localization.

Rabs appear to be required for all steps of membrane traffic, so it's essential that these transport steps are coupled to ensure transport continuity and specificity. One way this coupling can occur is through Rab cascades and Rab conversions. Rab cascades and conversions refer to a mechanism where the GEF of a downstream Rab GTPase also serves as an effector of an upstream Rab protein. In simpler terms, the protein that binds one activated Rab also activates the next Rab in the transport pathway [71].

For example, a Rab cascade was identified in yeast through the analysis of the final stage of the exocytic pathway. Two Rabs, Ypt31p and Ypt32p, are involved in several trafficking events at the Golgi [72]. The protein Sec2p is an effector of these Rabs and is also the GEF for Sec4p, another Rab required for transport of secretory vesicles from the trans-Golgi network to the plasma membrane in yeast [73][74][35]. Thus, Ypt31/32p and Sec4p are functionally linked in a regulatory Rab cascade through the

exchange protein Sec2p. This coupling ensures that distinct trafficking events, such as vesicle formation and delivery, are functionally coupled, providing greater specificity and continuity in membrane traffic.

Another interesting aspect of Rab cascades and conversions is that they can cause the conversion of one type of endosome to another. A recent study observed that early endosomes containing Rab5 protein converted into late endosomes containing Rab7 protein. This conversion appears to be the result of a Rab cascade involving the Vps11p and Vps39p proteins in the conserved class C VPS/HOPS complex [32][75][76][77][78].

Overall, Rab cascades and conversions are important mechanisms for efficient intracellular membrane transport in cells. They ensure that different transport steps are coupled for greater specificity and continuity, and they can even cause the conversion of one type of organelle into another.

Rab GTPases and primary cilia formation

The deep phylogeny of eukaryotes is a complex problem in evolutionary biology. Multiple attempts were made to root the tree of eukaryotes by identifying shared derived characteristics, such as unique fusions of conserved genes. One widely accepted model resulting from this approach is the unikont-bikont phylogeny. The unikont branch includes Metazoa, Choanozoa, Fungi, and Amoebozoa, while the rest of eukaryotes belong to the bikonts [79]. Unikont organisms possess one cilium, while bikonts have two [80][79]. However, there are notable differences in the evolution of cilia among unikonts. For instance, the slime mold *Dictyostelium* (Amoebozoa) and some fungi have lost cilia and ciliary genes [81]. In contrast, in mammals, cilia and

ciliary genes have diversified to serve diverse roles in the development and maintenance of cells, tissues, and organs [81].

Primary cilia are tiny hair-like structures that protrude from the surface of almost every vertebrate cell. These cilia function as sensors and enable cells to receive signals from light, chemical, or mechanical stimuli [82]. They are involved in several signaling pathways that play an essential role in tissue development and homeostasis. For example, the Sonic hedgehog and Wnt signaling pathways rely on primary cilia to function properly (figure 2) [83].

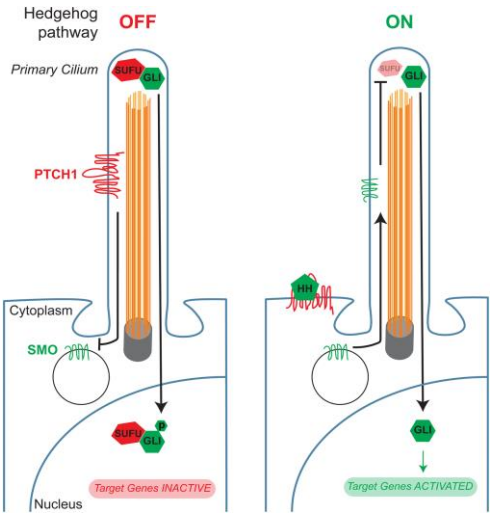

Figure 2: Activation of hedgehog signaling through primary cilia. In the inactive state of the Hedgehog pathway, Patched (PTCH1) localizes to the primary cilium, impeding the entry of Smoothened (SMO) into the cilium. Meanwhile, the Suppressor of Fused homolog (SUFU) interacts with glioma-associated oncogene homolog (GLI) transcription factors, effectively suppressing their activity. Activation of the Hedgehog pathway is initiated when Hedgehog ligands (HH) bind to PTCH1, causing it to disengage from the cilium. This allows SMO to translocate into the cilium where SMO triggers a cascade of events that lead to the activation of GLI proteins. Subsequently, the activated GLI proteins function as transcription factors, prompting the transcription of Hedgehog target genes. (*Reproduced from Choudhury et. al. 2020, Dermatology and Therapy, open access, licensed under a Creative Commons Attribution-NonCommercial 4.0, http://creativecommons.org/licenses/by-nc/4.0/*)

A functional primary cilium is essential for cells to activate these signaling pathways correctly. Therefore, any defects in primary cilia can lead to cellular dysfunction. Scientists have linked abnormalities in primary cilia to a group of related human diseases known as ciliopathies. These disorders, including Bardet-Biedl syndrome, Joubert syndrome, Meckel-Gruber syndrome, nephronophthisis, and Sensenbrenner syndrome, share overlapping genetic and phenotypic characteristics.

Ciliopathies can manifest in different ways, with symptoms that include brain malformations, skeletal abnormalities, retinal degeneration, and cystic kidney disease. These disorders can be severe and debilitating, making it challenging for individuals

to perform daily activities. Understanding the role of primary cilia in cellular signaling pathways and the link between ciliopathies and disease is a critical area of research that may lead to better treatments and therapies for affected individuals [84][85][86][87].

Primary cilia are specialized structures that are present on nearly all quiescent cells in the human body. These structures are composed of microtubule bundles, referred to as the ciliary axoneme, which forms the central core of the cilium. The ciliary axoneme of primary cilia has a distinct "9 + 0" configuration, comprising a radial arrangement of nine doublet microtubules with no central pair of singlet microtubules (figure 3) [88]. The basal body, which is a cytoplasmic microtubule organizing center, serves as the origin of the microtubule axoneme, and is derived from the mother centriole [88]. The mature centriole can docks at the plasma membrane, acting as a basal body to anchor the primary cilium on quiescent cells [88][89].

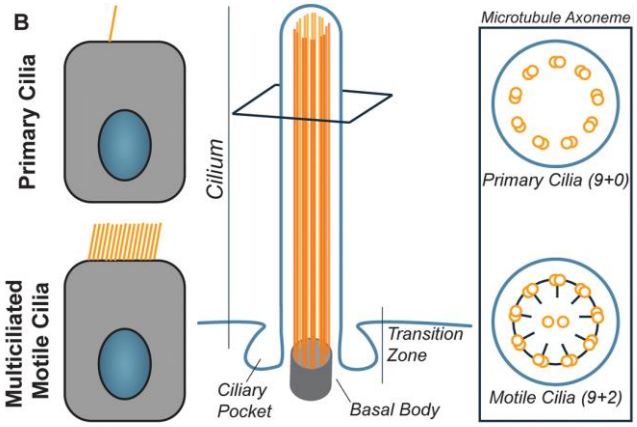

Figure 3: Schematic of axoneme of primary cilia. In contrast to motile cilia, where multiple cilia can be found on a cell's surface, each cell typically possesses only one primary cilium. Furthermore, the primary cilium's axoneme lacks central microtubule singlets that are commonly found in motile cilia. (Reproduced from Choudhury et. al. 2020, Dermatology and Therapy, open access, licensed under a Creative Commons Attribution-NonCommercial 4.0, http://creativecommons.org/licenses/by-nc/4.0/)

Ciliogenesis relies on several small GTPases that play essential roles in different stages of the process such as ciliary vesicle formation, centriole uncapping, and ciliary membrane elongation. Rabs such as Rab8, Rab10, Rab11, Rab23, Rab29, and Rab34, are involved in the process of ciliogenesis [90][37][91][92][93][94][95].

Nonetheless, our understanding of all the membrane trafficking mechanisms that contribute to ciliogenesis remains incomplete.

Rab8 is a key regulator of exocytosis and has been linked to cilia formation and transport. Overexpression of Rab8 GAP or inactive Rab8 blocks cilium formation [96], while depletion of Rabin8, which is a Rab8 GEF, results in the complete inhibition of ciliogenesis [37]. Conversely, overexpression of active Rab8 stimulates the extension of the ciliary membrane [37]. These observations highlight the crucial role of Rabin8 in regulating ciliogenesis and suggest that Rab8 activation is necessary for the formation and elongation of cilia. However, Rab8 knockout mice do not display ciliopathy-like phenotypes, suggesting redundancy with other Rab GTPases [97][98]. Rab8 associates with ciliary membranes, localizing to the ciliary base and axoneme. Studies have shown that Rab8 works with other proteins, including Rabin8 and Rab11, in a complex chain reaction to activate and target Rab8 to the cilium base [90][99]. Rab11 plays a significant role in recruiting and stimulating the GEF activity of Rabin8 to the mother centriole [90][99]. As a result of this process, Rab8 is also recruited and activated at the mother centriole [90][99].

Rab29 also plays an important role in cilia formation. Rab29 is located near the base of the cilium, and when it is depleted, the cilia become shorter and fewer in number [92]. Interestingly, Rab29 has been uncovered as a binding partner of Rab8 and Rab11 during a coimmunoprecipitation experiment. Notably, all these proteins are implicated in cilia formation [92].

Similarly, Rab23 is found in primary cilia and flagella and may regulate transport events within the cilium [100][101][102][103]. Although it does not directly regulate intraflagellar transport (IFT), studies suggest that Rab23 negatively regulates the

levels and transport of Smoothened [100]. Smoothened is a protein that plays a crucial role in the Hedgehog signaling pathway, which is important in embryonic development and tissue repair [104]. This suggests that Rab23 may play a role in inhibiting the Hedgehog signaling pathway. Additionally, it is worth noting that despite Rab23's involvement in cilia and flagella, its depletion or loss does not seem to affect cilia/flagella formation and length in various mammalian cells, zebrafish, trypanosomes, and mice [101][105][103][102]. This implies that Rab23's role may be more specific or limited to certain functions within the cilium. Another GTPase involved in cilia formation is Rab34. Rab34 is specifically located in the ciliary sheath of intracellular cilia and may play a role in the formation of ciliary vesicles [94][95]. During ciliogenesis, Rab34 is dynamically recruited to the mother centriole and helps establish the membrane identity of distal appendage vesicles and the ciliary sheath. Because the ciliary sheath faces the cytoplasm, Rab34 may also promote vesicular trafficking to the nascent cilium and/or fusion of the ciliary sheath with the plasma membrane [94][95]. These findings provide insight into the complex and intricate mechanisms involved in cilia formation and function. A range of Rab GTPases can play a role in regulating processes related to cilia, including basal body maturation, ciliary axoneme extension, intraflagellar transport, and ciliary signaling (figure 4).

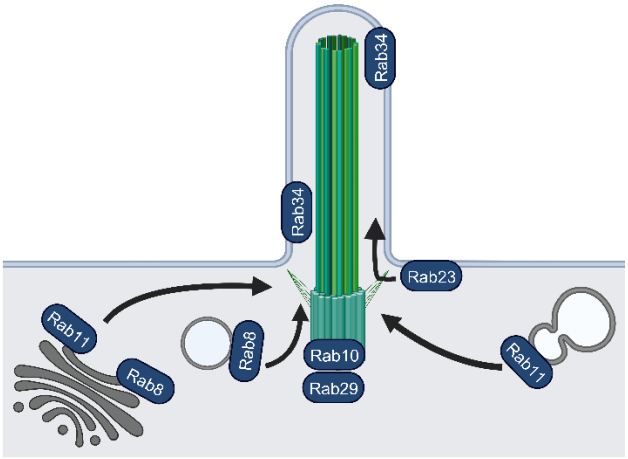

Figure 4: Schematic of various Rab GTPases regulating primary cilia formation. The illustration displays Rab proteins positioned along primary pathways of ciliary membrane protein trafficking.

Rab GTPases in cytokinesis

Cytokinesis, the final step of cell division, which involves studying diverse cellular processes, such as cytoskeletal regulation, membrane dynamics, signaling, and cell mechanics. Various approaches and model organisms, including bacteria, archaea, yeast, plants, and animal cells, are used to better understand the process of cytokinesis in eukaryotic cells. Although the precise mechanism of daughter cell separation remains a challenge, significant progress has been made with the discovery of more than one hundred genes that contribute to cytokinesis.

Cytokinesis, the process of cell division, is not solely dependent on actin filaments and myosin-II to create the furrow required for the separation of two daughter cells. It involves other cytoskeletal elements like microtubules and septins, which work together to play an essential role [106]. Despite this, numerous questions about cytokinesis remain unanswered. During the early stages of cytokinesis, the actomyosin contractile ring drives the ingression of the cleavage furrow and results in the formation of a narrow cytoplasmic bridge that connects the two daughter cells. This intercellular bridge is filled with anti-parallel microtubule bundles and is eventually severed in a process called abscission, which is the least understood step of cytokinesis [107].

The midbody, an electron-dense structure at the center of the bridge, serves as a platform for recruiting proteins essential for abscission. Recent research suggests that the assembly of ESCRT-III filament helices on the side of the midbody, drives the final bridge constriction and leads to cytokinetic abscission [108][109]. For successful abscission, the ESCRT machinery must constrict the plasma membrane by clearing cytoskeletal elements, including microtubules and filamentous actin (F-actin)

[110][107]. ESCRT-mediated delivery of Spastin is necessary for removing microtubules from the ICB, while Rab35 is responsible for F-actin clearance [111]. Rab35 drives F-actin depolymerization through MICAL1, which oxidates and depolymerizes F-actin [108][112], and prevents accumulation of F-actin through its effector Oculo-Cerebro-Renal syndrome of Lowe, an inositol (4,5)P_2 5-phosphatase [113][114]. Rab35/MICAL1-dependent actin depolymerization also facilitates ESCRT recruitment [108]. The ICB recruits a scaffold protein Rab11FIP1 following Rab35 recruitment, which helps to maintain Rab35 at the site [115]. Membrane trafficking plays a vital role in the process of abscission. Specifically, the incorporation of new membrane material into the cleavage furrow is critical to this process, and endosomes have been identified as a key source of this material. Through the incorporation of new membrane material, endosomes contribute to the formation of the midbody at the site of the cleavage furrow and plays a critical role in the final stages of cytokinesis.

Multiple Rabs localize at the furrow or intercellular bridge including Rab1, Rab6, Rab8, Rab10, Rab11, Rab14, Rab21, Rab24 [116][117][118][119][120][121]. Rab11 is indeed one of the most extensively studied Rab GTPases in cytokinesis, in addition to Rab35. The involvement of Rab11 in cytokinesis has been observed in a variety of organisms, including C. elegans, Drosophila, and mammalian cells. In C. elegans, Rab11 and its GEF REI-1 are crucial for the proper ingression of the furrow during cell division [121][122]. Similarly, in Drosophila, the involvement of Rab11 in cytokinesis has also been observed, with its effector FIP3 playing a role in regulating endosomal recycling [123][124][125][126][127][128][129][130]. The increasing interest in identifying and characterizing their GEFs is driven by Rabs' growing association with diseases [131][132]. Understanding the roles of these Rabs (figure 5) and their activators and effectors during cytokinesis is vital for unraveling the complex

mechanisms underlying this fundamental process and may have implications for the development of new therapeutic strategies for diseases associated with abnormal cell division.

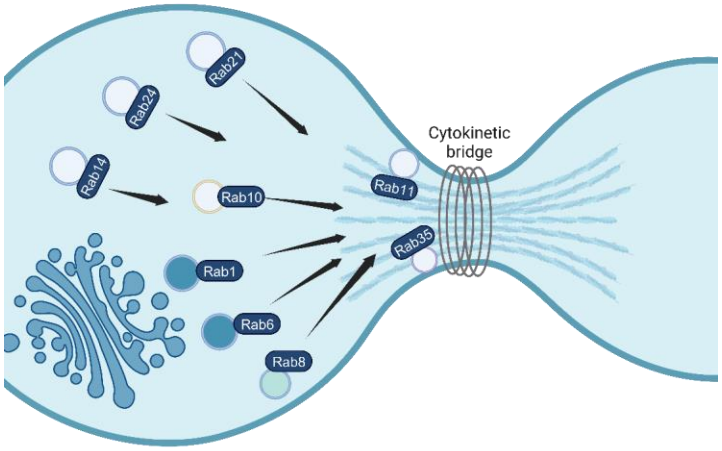

Figure 5: Schematic diagram illustrating the involvement of different Rab GTPases in cytokinesis.

CHAPTER 3

A cell-based GEF assay reveals new substrates for DENN domains and a role for DENND2B in primary ciliogenesis

Rahul Kumar, Vincent Francis, Gopinath Kulasekaran, Maleeha Khan, Gary A B Armstrong, Peter S McPherson

Department of Neurology and Neurosurgery, Montreal Neurological Institute (the Neuro), McGill University, Montreal, Quebec, Canada.

Originally published in *Science Advances*

DOI: 10.1126/sciadv.abk3088

Abstract

Primary cilia are sensory antennae crucial for cell and organism development, and defects in their biogenesis cause ciliopathies. Ciliogenesis involves membrane trafficking mediated by small guanosine triphosphatases (GTPases) including Rabs, molecular switches activated by guanine nucleotide exchange factors (GEFs). The largest family of Rab GEFs is the DENN domain–bearing proteins. Here, we screen all 60 Rabs against two major DENN domain families using a cellular GEF assay, uncovering 19 novel DENN/Rab pairs. The screen reveals Rab10 as a substrate for DENND2B, a protein previously implicated in cancer and severe mental retardation. Through activation of Rab10, DENND2B represses the formation of primary cilia. Through a second pathway, DENND2B functions as a GEF for RhoA to control the length of primary cilia. This work thus identifies an unexpected diversity in DENN domain–mediated activation of Rabs, a previously unidentified non-Rab substrate for a DENN domain, and a new regulatory protein in primary ciliogenesis.

Introduction

Vesicle trafficking is a fundamental cellular process involving the transport of lipids and proteins throughout cells using a series of trafficking events including vesicle budding from donor organelles, vesicle transport, and fusion of vesicles with acceptor compartments. The spatial and temporal control of these events is largely mediated by the Rab family of small guanosine triphosphatases (GTPases), which regulate all aspects of membrane trafficking at all cellular locations (1).

Mammalian cells have approximately 60 Rabs (2). Rabs switch between a guanosine triphosphate (GTP)–bound active state and a guanosine diphosphate (GDP)–bound inactive state (3). These switches are controlled by guanine nucleotide exchange

factors (GEFs) and GTPase-activating proteins (GAPs). Upon activation by GEFs, Rabs carry out their appropriate membrane trafficking functions, recruiting effector proteins that drive trafficking events (3). The association of Rab GTPases with membranes requires insertion of hydrophobic geranylgeranyl groups, attached to one or two cysteine residues at the C terminus of Rabs into the cytosolic leaflet (4). Upon inactivation by GAPs, which stimulate the intrinsic GTPase activity, Rabs are extracted from the membrane and interact reversibly with the molecular chaperone GDP dissociation inhibitor (GDI) to form a cytosolic complex, protecting the hydrophobic moieties (5, 6).

Because the presence of a specific Rab on an organelle is a defining feature of that organelle, a key question relates to how Rabs are targeted to their appropriate cellular location. Early studies suggested a role of the hypervariable region at the C terminus of the Rab as a targeting signal (7). However, this was challenged as the hypervariable region can be dispensable for Rab membrane targeting (8). It has also been postulated that GDI displacement factors (GDFs) drive dissociation of Rab-GDP/GDI complexes, catalyzing Rab membrane delivery (9). However, only one GDF has been identified (10). It is thus unclear how this process could mediate the distinct membrane targeting of multiple Rabs. It was subsequently demonstrated that the GEF DrrA recruits Rab1 to membranes by catalyzing GTP loading, leading to displacement of GDI, without the need of a GDF (11). Moreover, when GEFs are artificially relocated to membranes of different organelles, such as mitochondria, substrate Rabs are mistargeted to these new locations (12). GEF-mediated activation of Rabs drives Rab membrane association and allows the GTPases to recruit and trap effector proteins (13). These experiments suggest that GEFs are solely responsible for controlling the spatial and temporal localization of Rab GTPases and thus their effectors.

There are far fewer GEFs than Rabs (14). The largest family of GEFs are those bearing a DENN (differentially expressed in normal and neoplastic cells) domain, an evolutionary conserved protein module (15). There are minimally 18 members in the DENN domain family that are further divided into eight subfamilies, most of which are poorly characterized (15). A screen of 16 DENN domain proteins against most Rabs using an in vitro approach led to the assignment of a single, unique Rab to each DENN domain subfamily (16). However, subsequent cell biological studies focused on individual DENN domain proteins including DENND1C (17, 18) and DENND2B (19) revealed different Rab substrates than those identified in the in vitro screen. In vitro GEF assays are challenging in that purification of recombinant Rabs can lead to inactivation and altered nucleotide loading (20), and purified DENN domains may also be misfolded.

Here, we develop a cell-based GEF assay to identify Rab GTPase substrates of the seven members of the DENND1 and DENND2 families, using a mitochondrial relocalization approach. Screening against 60 Rabs reveals that each member of the DENND1/DENND2 families activates multiple GTPases, changing the notion that each DENND family targets one common Rab (16, 18).

Multiple Rab GTPases are associated with trafficking of proteins regulating the formation of primary cilia (21). Primary cilia are microtubule-based nonmotile sensory organelles present in most vertebrates. These organelles are critical in regulating signal transduction pathways including Hedgehog (Hh) signaling (22). Disruption in ciliogenesis leads to a spectrum of disorders known as ciliopathies, including polycystic kidney disease, skeletal malformations, retinal degeneration, mental retardation, and cancer (23). Cells form primary cilia by two pathways: (i) the extracellular pathway where the basal body (matured mother centriole) docks to the

apical plasma membrane and cilia form from the apical plasma membrane and (ii) the intracellular pathway in which the basal body fuses with ciliary vesicles, allowing cilia formation in the cytoplasm, which eventually fuse with the apical plasma membrane (24). The maturation of the mother centriole requires encapsulation by ciliary vesicles from the Golgi (25), implicating Rab-mediated trafficking. Several Rab GTPases and their GEFs have been described as positive regulators of ciliogenesis (26). In addition, there is a critical negative regulatory pathway in ciliogenesis. Specifically, the centriolar coiled-coil protein of 110 kDa (CP110), along with associated proteins, caps the basal body and prevents cilia growth. How this pathway is regulated is unknown.

Here, we found that DENND2B (also known as suppression of tumorigenicity 5), via activation of Rab10, inhibits primary cilia formation through Rab10-dependent recruitment of the inhibitor CP110 to the mother centriole. Through a second pathway, involving direct enzymatic activation of RhoA, DENND2B controls ciliary length. The importance of DENND2B is illustrated with the finding that patients with a loss-of-function mutation in DENND2B display mental retardation and multiple congenital abnormalities (27). Thus, we have found unexpected diversity in DENN domain control of small GTPases leading to a new regulatory mechanism for primary ciliogenesis.

Results

Identification of Rab substrates of the DENND1 and DENND2 families

To identify DENN substrates, we screened all members of the DENND1 and DENND2 subfamilies against all 60 Rab GTPases using a mitochondrial recruitment assay. Given that the isolated DENN domain is solely responsible for GEF activity (18), the assay involves targeting DENN domains to the mitochondrial outer surface by fusion with amino acids 141 to 187 of ActA from Listeria monocytogenes (Fig. 1A) (28). We

verified that the mitochondrial targeted DENN domain of DENND1A [DENN(1A)-mito] is recruited selectively to mitochondria (fig. S1), where it leads to a near-complete steady-state relocalization of cotransfected GFP-Rab35 (Fig. 1, B and C). A nonprenylatable form of Rab35 lacking the two C-terminal cysteines (GFP-Rab35 C_C del) is not recruited to the mitochondria (Fig. 1D), indicating that mitochondrial recruitment of the GTPase requires membrane insertion of prenyl groups. This indicates that Rab35 is inserted into the mitochondrial membrane via a GEF activity and is not simply trapped via DENN domain binding. To visualize Rab35 recruitment in real time, we developed an inducible system based on heterodimerization of the FK506-binding protein domain (FKBP) from the human FKBP12 protein and the FKBP-rapamycin–binding domain (FRB) of mTOR (mammalian target of rapamycin) (fig. S2A). Upon addition of rapamycin, each of DENN1A, DENN1B, and DENN1C rapidly translocates to mitochondria where they recruit Rab35, indicating that all three DENND1 DENN domains function as Rab35 GEFs (Fig. 1E; fig. S2, B to D; and movie S1).

We next cotransfected HeLa cells with individual DENN-mito and GFP-Rab constructs (Fig. 2A and fig. S3) in a 7 by 60 screen and compared the mitochondrial localization of the GFP-Rabs in the presence of the DENN domain red fluorescent protein (RFP)–mito (Fig. 2, A to F) or a control RFP-mito (fig. S4). All three members of the DENND1 family (1A/1B/1C) recruit Rab35 to the mitochondria (Fig. 2B and fig. S5, A and B). Unexpectedly, the screen also revealed Rab15 as a substrate for all three DENND1 DENN domains (figs. S5, C to E, and S6). Note that Rab35 and Rab15 have largely overlapping subcellular localizations (early and recycling endosomes) and function (endocytic recycling) (18, 29, 30). Apart from Rab35 and Rab15, the three DENND1

DENN domains recuit no other Rabs (fig. S6). Notably, DENN(1C) does not recruit Rab13 (Fig. 2, B and C) (16).

Screening of the four members of the DENND2 subfamily against all 60 Rabs (Fig. 2A) revealed an array of Rab substrates. DENND2A selectively recruited Rab15 (figs. S7A and S8). DENND2B recruited Rab8A, Rab8B, Rab10, Rab13, Rab15, Rab27A, Rab27B, and Rab35 (Fig. 2D and figs. S7, B to F, and S8). DENND2C recruited Rab8A, Rab8B, Rab10, Rab15, and Rab35 (figs. S7, G to J, and S8). Last, DENND2D recruited Rab8A and Rab10 (figs. S7, K and L, and S8). There is commonality among these substrates as they all function in delivery of cargo to the plasma membrane, either through recycling pathways or directly via the secretory pathway (18, 19, 31). However, there is no obviously phylogenetic or structural relationship such that substrate specificity remains unclear. Among the targets for DENN(2B) was Rab13 (Fig. 2D) (19). In contrast, we did not detect recruitment of Rab9 to mitochondria by DENN(2B) (Fig. 2, D and E) (16) or other members of the DENND2 family (Fig. 2F and fig. S8).

Loss of DENND2B promotes primary cilia formation and enhanced cilia length

A loss-of-function mutation in DENND2B is seen in a patient with submucous cleft palate, unilateral cystic kidney dysplasia, sensorineural hearing loss, persistent ductus Botalli, mental retardation, and other anomalies (27), symptoms associated with a ciliopathy. Ciliopathies are a group of disorders caused by the dysfunction of primary cilia (23, 32). In addition, DENND2B has a role in cancer invasion (19), a phenotype associated with primary cilia defects (33). Rab8, Rab10, and Rab35 each regulate distinct aspects of primary ciliogenesis (26, 34–36), and all were recruited to

mitochondria with the DENND2B DENN domain. Thus, we sought to explore whether DENND2B regulates the formation or function of primary cilia.

The formation of primary cilia is induced in cultured cells by serum starvation (37). We transfected human alveolar epithelial cells (A549), a model for primary cilia formation (38) with GFP-DENND2B; induced ciliogenesis by serum starvation; and labeled cells with markers of the centrosome and primary cilia. The centrosome is the major microtubule-organizing center in animal cells and is composed of two centrioles, the mother and daughter centrioles, MC and DC, respectively. Each centriole has a proximal and a distal end. Upon serum starvation, the distal end of the mother centriole matures into a basal body and initiates primary cilia formation (39). While most DENND2B localizes to the cell periphery (19), a pool of approximately 2% colocalizes with gamma-tubulin (γ-tubulin), a marker of the proximal end of the basal body (Fig. 3, A and B). This DENND2B pool is proximal to CEP164, a marker of the distal appendage (a structural protrusion at the distal end of the basal body involved in membrane docking) of the mother centriole (Fig. 3, C and D) (40). DENND2B does not localize to the cilium proper as marked by acetylated tubulin (Ac-tubulin) (Fig. 3E). As revealed by staining for Ac-tubulin, cells overexpressing DENND2B have a reduced percentage of primary cilia compared to GFP transfected cells (fig. S9, A and B). Moreover, the length of the cilia is reduced (fig. S9C). In addition, note that most cells having DENND2B localized at the ciliary base lack primary cilia (fig. S9A). These data suggest that DENND2B functions as a repressor of primary cilia formation.

We used CRISPR-Cas9 to knockout (KO) DENND2B in A549 cells, which we validated with genomic sequencing and immunoblot (fig. S10, A to C). A549 KO cells had a higher percentage of ciliated cells and longer primary cilia as compared to wild-type (WT) cells (Fig. 4, A to C). Similar results were seen in DENND2B KO human retinal

pigment epithelial-1 (RPE-1) cells (fig. S10, D to F, and Fig. 4, D to F). Expression of GFP-DENND2B in the DENND2B KO cells rescues both the percentage of ciliated cells and ciliary length, thus ruling out the possibility of off-target effects (fig. S11, A to C). Collectively, the overexpression and KO/rescue studies indicate that DENND2B plays an inhibitory role in primary cilia formation and length.

We next examined whether the function of DENND2B in primary ciliogenesis is evolutionarily conserved and observable in an in vivo model. Alignment of full-length DENND2B from zebrafish and human revealed ~65% sequence identity with ~90% identity in the DENN domain. We injected either an antisense morpholino (MO) oligonucleotide blocking translation of the dennd2b transcript or a standard control MO oligonucleotide into the one-cell stage of zebrafish embryos. At the eight-somite stage, 13 hours post-fertilization (hpf), we labeled embryos with Ac-tubulin. Similar to phenotypes in the DENND2B KO cells, embryos injected with the dennd2b MO displayed an increased percentage of ciliated cells and enhanced cilia length (Fig. 4, G to I). At 27 hpf, we observed that dennd2b morphants were shorter in length and displayed a greater proportion of a delayed tail-straightening phenotype compared to WT/control MO (Fig. 4, J to L). The phenotypes were rescued by the co-injection of DENND2B mRNA (Fig. 4, G to L). The larval length and tail phenotypes overlap with defects seen in other studies involving depletion of ciliary proteins in zebrafish, thus suggestive of a ciliopathy (41). Thus, DENND2B appears to play a role in development via regulation of primary cilia.

DENND2B inhibits primary cilia formation by functioning as a GEF for Rab10

Our screen reveals that the DENND2B DENN domain recruits Rab8, Rab10, and Rab35 to the mitochondria. Decreasing Rab8 function through expression of inactive

Rab8 or depletion of the Rab8 GEF Rabin8 reduces cilia formation (26, 34). Silencing of Rab35 does not alter cilia formation but decreases cilia length (35). DENND2B KO increases both the percentage of ciliated cells and cilia length. Thus, it is unlikely that either Rab8 or Rab35 are the mediators of the DENND2B activity. In contrast, the loss of Rab10 causes a significant increase in the percentage of ciliated cells (36) but does not alter cilia length (fig. S12, A to D). We thus sought to investigate the role of Rab10 in DENND2B-mediated ciliary phenotypes. Flag-DENND2B DENN domain efficiently immunoprecipitates the inactive form of Rab10 (T23N) but not the active form of Rab10 (Q68L) (fig. S13A), a hallmark of a GEF. Mutations in the catalytic site of the DENN domain of DENND2B, determined from the structure of Rab35-bound DENND1B (42, 43), abolishes the recruitment of Rab10 to mitochondria (fig. S13B). An effector binding assay using a glutathione S-transferase (GST) fusion with a C-terminal fragment of MICAL-L2 (molecule interacting with CasL-like 2, also known as GST-MICAL-L2 C), which selectively binds the active form of Rab10 (44), reveals no changes in active Rab10 levels when we compared WT and DENND2B KO cells (fig. S13, C and D). This is not unexpected as other GEFs including DENND4C and Rabin8 are also known to function on Rab10 (44, 45). We did however observe enhanced active Rab10 in lysates from cells transfected with GFP-DENND2B when compared with untransfected cell lysate (fig. S13, E and F), strongly supporting a GEF/substrate relationship for DENND2B and Rab10.

KO of DENND2B results in two distinct cilia phenotypes, enhanced cilia formation and increased cilia length. Overexpression of an active mutant of Rab10 (GFP-Rab10 Q68L) in DENND2B KO RPE-1 cells rescues the percentage of ciliated cells to a level similar to WT but does not rescue the enhanced cilia length phenotype (Fig. 5, A to C). This rescue is not seen with a nonprenylatable form of active Rab10 (GFP-Rab10

Q68L C_C del). Thus, membrane recruitment of active Rab10 is required for the rescue of the cilia formation phenotype resulting from DENND2B KO (fig. S14, A to C).

We next sought to examine the localization and dynamics of Rab10 relative to the primary cilia. GFP-Rab10 localizes at the ciliary base marked by γ-tubulin (fig. S15). Using fluorescence recovery after photobleaching (FRAP), we observed that green fluorescent protein (GFP)–Rab10 is rapidly recruited to the centriole (marked by centrin) after bleaching with a half-time of ~4.5 s (fig. S16, A to D). This could represent rapid vesicle trafficking of Rab10 to the centriole or recovery by recruitment from a cytosolic pool. Analysis of the localization of endogenous Rab10 using a KO-validated antibody revealed a bright puncta located exclusively to the mother centriole marked by partial overlap with CEP164 (Fig. 5, D and E), consistent with the localization of DENND2B.

Given that Rab10 inhibits cilia growth, we predicted that induction of ciliogenesis would remove Rab10 from the base of the cilia. WT and DENND2B KO A549 cells were serum-starved and stained for Ac-tubulin and endogenous Rab10. While endogenous Rab10 staining at the mother centriole was obvious in most growing WT cells (Fig. 5, D and E), upon serum starvation, a subtle (~9%) but significant percentage of WT cells had Rab10 puncta at the base of primary cilia (Fig. 5, F to H), suggesting that most cells had lost Rab10 from the basal body. In contrast, we did not observe a single DENND2B KO cell with Rab10 puncta at the base of primary cilia (Fig. 5, F and G), consistent with the idea that GEFs control the localization of Rabs (46) and that the loss of DENND2B disrupts Rab10 localization. Subsequently, expression of GFP-DENND2B in the KO cells resulted in ~8% of cells showing Rab10 staining at the ciliary base (fig. S17, A and B). In addition, we also demonstrate that GFP-DENND2B

(~1.5-fold overexpression; fig. S18B) and Rab10 colocalize proximal to CEP164 (fig. S18A). Together, these data suggest that DENND2B activates Rab10 and that activated Rab10 localized at the mother centriole controls primary cilia formation.

DENND2B controls cilia length by activating RhoA

Following DENND2B KO, expression of Rab10 rescues defects in the percentage of ciliated cells (Fig. 5B) but does not rescue defects in cilia length (Fig. 5C). We thus sought to understand the mechanism by which DENND2B controls cilia length. The physiological need for primary cilia of a defined length is not clear, but a genetic mutation altering cilia length represses Hh signaling (47). Consistently, as monitored by the expression of the Gli1 transcription factor (48, 49), Hh signaling is repressed in the absence of DENND2B (fig. S19). Activation of RhoA has been linked to cilia length, specifically, cells with higher levels of active RhoA have shorter cilia, possibly through the formation of stress fibers (50, 51), whereas reduced RhoA activity leads to longer cilia (52). We thus considered that DENND2B could control cilia length by acting as a GEF for RhoA. DENN(2B) relocates RhoA to the mitochondria, inducing gross morphological changes (Fig. 6A). The GEF dead mutant of DENN(2B) does not recruit RhoA, reinforcing that catalytic activity of the DENN(2B) is required for mitochondrial recruitment (Fig. 6A). Mitochondrial recruitment of RhoA is independent of Rab10 and occurs as normal in the absence of endogenous Rab10 (fig. S20, A and B). We next measured levels of active RhoA in DENND2B KO cells using GST fused to the Rho-binding domain (RBD) of the effector protein Rhotekin, which selectively recognizes cellular RhoA in the active, GTP-bound form (53). There is a significant decrease in active RhoA in DENND2B KO cells as compared to WT cells, whereas total RhoA remains unchanged (Fig. 6, B and C). Conversely, overexpression of DENND2B increases the levels of active RhoA (Fig. 6, D and E). In coimmunoprecipitation

experiments, DENND2B interacts preferentially with inactive RhoA (T19N) as compared to active RhoA (Q63L) (Fig. 6F), a hallmark of GEFs. Thus, the substrates of DENN domains may now be expanded beyond Rab GTPases.

We next asked whether increasing the levels of GTP-loaded RhoA could rescue the cilia length phenotype resulting from DENND2B KO. RhoA activation using CN03 restored cilium length to normal in DENND2B KO A549 cells as did the expression of active RhoA (RhoA: ~1.5-fold; Fig. 7, A to C, and fig. S21). RhoA activation by CN03 in DENND2B KO cells overexpressing active Rab10 (GFP-Rab10 QL; Rab10: ~2-fold; fig. S21) rescued both the percentage of ciliated cells and ciliary length (Fig. 7, A to C) as did coexpression of both active GTPases (fig. S22, A and B). Thus, DENND2B controls cilia length by controlling the GTP status of RhoA and the percentage of ciliated cells by controlling the GTP status of Rab10.

DENND2B controls recruitment of CP110 via Rab10

Proteins critical for negative regulation of primary cilia formation are CP110 and its interacting partner centrosomal protein of 97 kDa (CEP97) (54). CP110 is recruited by binding to CEP97 at the distal ends of both the mother and daughter centrioles (54). Upon serum starvation or in the G0 phase, CP110 uncapping from the distal end of the mother centriole is required for it to mature into a basal body and initiate primary cilia formation (39). However, the mechanisms regulating CP110 recruitment are not fully understood.

γ-Tubulin marks the centriolar region containing the mother and the daughter centrioles. In the absence of DENND2B, only ~5% of A549 cells had both mother and daughter centrioles capped with CP110 (two dots) as compared to WT cells where ~50% of the cells had both centrioles capped (Fig. 8, A and B). We next analyzed the

capping of CP110 specifically at the distal end of the mother centriole. A significantly smaller proportion of DENND2B KO cells had CP110 localized at the distal appendage of the mother centriole, as marked by CEP164 (Fig. 8, C and D). These results demonstrate that DENND2B sets up a permissive environment for the accumulation of CP110 to the distal end of the mother centriole as a mechanism to control capping status and primary cilia formation.

We next sought to determine whether Rab10 functions downstream of DENND2B in the capping function of CP110 at the mother centriole. An active mutant of Rab10 is located at the mother centriole marked by CEP164 (Fig. 8, E and F) and in DENND2B KO cells, where CP110 no longer caps the mother centriole, expression of GFP-tagged active Rab10 restores recruitment of CP110 to the mother centriole seen by colocalization with γ-tubulin (Fig. 8, G and H). Furthermore, in coimmunoprecipitation experiments, CP110 binds to both the active and inactive mutants of Rab10 (fig. S23). Because it is the membrane-bound active form of Rab10 that rescues the formation of cilia, we propose that DENND2B-mediated activation of Rab10 drives the recruitment of CP110 to the mother centriole.

Rab10 functions in Parkinson's disease associated with autosomal dominant mutations in the leucine-rich repeat kinase 2 (LRRK2) gene. Dominant mutations in LRRK2 autoactivate the LRRK2 kinase, which phosphorylates active Rab10 (36, 55, 56). Phospho-Rab10 (p-Rab10) localizes to the mother centriole, where it blocks the release of CP110 and inhibits cilia formation (36, 57). We thus investigated the levels of p-Rab10 in A549 cells as they contain high levels of WT LRRK2. We did not find any changes in overall p-Rab10 levels between A549 WT and DENND2B KO cells (fig. S24A), which is not unexpected as DENND2B KO had no influence on the overall active Rab10 levels (fig. S13, C and D). However, we did find an increase in p-Rab10

levels in cell lysates overexpressing WT LRRK2 and DENND2B when compared to cell lysates overexpressing WT LRRK2 alone, indicating that LRRK2 phosphorylates active Rab10 after activation by DENND2B (fig. S24B). In addition, treatment of A549 cells with the LRRK2 inhibitor MLI-2 reduced p-Rab10 levels, demonstrating that phosphorylation of Rab10 is mediated by LRRK2 (fig. S24A). Thus, it is possible that DENND2B-activated Rab10 is phosphorylated by LRRK2 to inhibit cilia formation.

Discussion

The identification of GEFs for Rab GTPases is critical for understanding membrane trafficking and, by extension, the pathophysiology of multiple human diseases. Most mammalian Rabs have no assigned GEF. Here, we use a cell-based GEF assay to screen for all Rab substrates of the seven members of the DENND1 and DENND2 DENN domain–containing protein subfamilies. The large number of substrates identified were not seen using more traditional in vitro approaches. The most important advantage of the cell-based system is that the Rab substrates have all of the cellular requirements to retain their endogenous nucleotide status, something that is often lost following their purification. However, the degree of overexpression of both the GEFs and the Rab substrates may drive lack of specificity even in cells. For example, DENND4C is present in multiple cell lines at very low levels and yet it is a potent GEF for Rab10 (45). In addition, we cannot rule out that some of the identified Rabs are recruited to mitochondria as part of Rab cascades downstream of true Rab substrates. Given the unexpected diversity of Rab substrates for the seven DENN domains tested, our approach likely explains why there are far fewer GEFs compared to the total number of Rab GTPases (14).

In addition to confirming four known DENN/Rab pairs, we identify 19 novel pairs: DENND1A/B/C with Rab15; DENND2A with Rab15; DENND2B with Rab8A, Rab8B, Rab10, Rab15, Rab27A, Rab27B, and Rab35; DENND2C with Rab8A, Rab8B, Rab10, Rab15, and Rab35; and DENND2D with Rab8A and Rab10. This indicates that individual DENN families are not selective for a single Rab. Of all the newly identified Rab GTPases, only Rab8A, Rab8B, Rab10, Rab13, and Rab15 have a strong phylogenetic correlation belonging to one subfamily (2), suggesting no specific phylogentic pattern in regard to pairs identified in association with the DENND1 and DENND2 families. Furthermore, although both Rab8A and Rab8B were identified as substrates for DENND2B and DENND2C, only Rab8A and not Rab8B was identified with DENND2D, despite very high sequence similarity. Thus, there is a high degree of specificity inherent in the screen and in DENN domain recognition of substrates. In contrast, all but one of the DENN domains screened activated Rab15, suggesting a certain promiscuity that could function to enhance combinatorial possibilities in cell signaling events. While most members of the DENND2 family are not well studied, we now know that all members of the DENND1 family activate Rab35 at different cellular locations. DENND1A and DENND1B are largely restricted to the endocytic system, whereas DENND1C is associated with the actin cytoskeleton (17). Another possibility is tissue-specific functions of the DENN domain proteins. For example, a cascade of Rabs (Rab35, Rab8A, and Rab13) and effector proteins (MICAL-L1/L2) controls neurite outgrowth (58). Given that DENND2B interacts with MICAL-like proteins (19), it would be worth investigating whether DENND2B plays a role in such signaling mechanisms.

Several Rab GTPases have been associated with primary cilia, either in stimulatory or inhibitory roles (21). Here, we demonstrate that Rab10 is a physiologically relevant

substrate of DENND2B and that DENND2B activates Rab10 to inhibit primary cilia formation. Furthermore, we found that Rab10 controls recruitment of CP110, a repressor of ciliogenesis, at the distal appendage of the mother centriole, thereby explaining the inhibition of cilia formation (Fig. 9A).

The extracellular pathway for ciliogenesis involves docking of the basal body with the plasma membrane with formation of cilia from the surface. In contrast, the intracellular pathway requires ciliary vesicles derived from the Golgi to encapsulate the mother centriole at an early stage of cilia formation within the cytoplasm (24, 25). Subsequently, accumulation of ciliary vesicles forms a double-membrane sheath around the basal body (matured mother centriole), and the growing axonemal microtubules form a nascent intracellular cilium, which then migrates and fuses with the plasma membrane, exposing the cilium to the external environment (24). Rab10 and DENND2B are involved in the trafficking of endosomal/Golgi vesicles to the plasma membrane (31). While it is unclear how DENND2B is recruited to the proximal end of the mother centriole, we propose that DENND2B activates and recruits Rab10 that further recruits CP110 to the mother centriole, and it is the recruitment of CP110 to the distal end of the mother centriole that prevents the maturation of the mother centriole to the basal body and ultimately cilia formation.

Two independent studies provide evidence that the nucleotide status of RhoA controls cilia length (50, 52). In addition, high levels of active RhoA induce the formation of stress fibers that prevent primary cilia outgrowth (51). Although nearly 80 RhoGEFs are known to regulate signaling events (59), none have been linked to ciliogenesis. We now demonstrate that DENND2B activates RhoA and controls cilia length, and we provide compelling evidence that DENND2B is a GEF for RhoA (Fig. 9B). Last, overexpression of active RhoA mutant reverses normal cilia length resulting from

DENND2B KO. Thus, the substrates for DENN domain proteins must be expanded beyond Rab GTPases. Although we provide evidence of DENND2B functioning as a GEF for RhoA using the mitochondrial recruitment assay and other standard protocols for the identification of Rho GEFs (60, 61), we cannot rule out the possibility of another Rab getting recruited by DENND2B, which further recruits RhoA through a GTPase cascade.

In addition, our analysis reveals that Hh signaling is suppressed in DENND2B KO cells. Any alteration in Hh signaling is known to cause a diverse spectrum of disorders, known as primary ciliopathies (62). A patient with a DENND2B loss-of-function mutation presents a diverse set of severe anomalies related to ciliopathies (27, 32), and it is likely that defects in primary cilia contribute to the disease phenotype. KD of dennd2b in zebrafish reveals reduced larval length and a curved tail along with ciliary defects, indicating that dennd2b-mediated regulation of primary cilia might be contributing to the developmental defects. KO mice for M-phase phosphoprotein 9 (MPP9), a protein involved in the recruitment of CP110 to the mother centriole, also showed decreased body weight/length and a twisted body axis at midgestation (63), suggesting that DENND2B and MPP9 may be part of a common pathway. DENND2B recruits multiple other Rabs to the mitochondria (Rab8A/B, Rab15, Rab35, and Rab27A/B), and therefore signaling mechanisms governed by the remaining GTPases are yet to be found.

An intriguing question relates to how multiple DENN domains can target a single Rab and how the same DENN domain can target multiple Rabs. This may be explained, in part, by different DENN domain proteins acting on a common Rab but at different subcellular compartments. For example, DENND1A/B activates Rab35 at endosomes, whereas DENND1C activates Rab35 at the actin cytoskeleton (17). For Rab10, there

are multiple GEFs including DENND2C and DENND2D, newly demonstrated in this study, and DENND4C (45) and Rabin8 (44). It is possible that all GEFs are present in any given cells but that they activate Rab10 at different subcellular locations. When we performed KO of DENND2B, we saw no change in the total cellular levels of the active form of Rab10, likely due to the presence of multiple other Rab10 GEFs. Immunofluorescence analysis indicates that the pool of Rab10 at the centriole is a relatively minor component of the overall cellular pool of Rab10. This further stresses that DENND2B selectively activates Rab10 to function at the centriole. In addition, the answer for the broad diversity in substrate specificity within and between families could be unveiled once we solve the structure of the individual DENN domains. While we have screened two major families of DENN domains in this manuscript, all the remaining DENN domain family members must be screened using a similar approach to understand the full complement of substrates. Because DENN domains are no more specific for Rabs, they must be screened across all the small GTPase families in the future.

As our study finds new aspects of DENN domains in membrane trafficking, it also poses several questions related to DENND2B. DENND2B is known to promote cancer invasion (19). Coincidently, numerous cancer cells lack primary cilia (64). Given the inhibitory role of DENND2B in primary cilia, is it possible that the disrupted function of DENND2B gives rise to cancer phenotypes via defective primary cilia? In addition, previous studies have reported that Rab8A and Rab10 have opposite effects on cilia formation. Because both Rab8A and Rab10 are substrates for DENND2B, it will be important to investigate factors contributing to context-specific GEF activity that leads to Rab10-specific phenotype but not Rab8A. The Parkinson’s disease gene LRRK2 phosphorylates a subset of Rabs (65). Of all the Rabs, Rab10 has been recently

associated with an emerging Parkinson's disease cellular phenotype, inhibition of primary cilia formation by p-Rab10 (36). Note that overexpression of DENND2B increases the levels of Rab10 phosphorylated by LRRK2. DENND2B KO cells show increased cilia formation, and reduced p-Rab10 fits the model published by other groups showing that increased LRRK2-mediated phosphorylation of Rab10 inhibits cilia formation (36, 57). This finding raises important questions that need further investigation: (i) Does DENND2B interact with LRRK2 to modulate its activity and, if so, under what circumstances? (ii) Does DENND2B function upstream of LRRK2 in known cell biological events such as in macropinocytosis to mediate immunological responses in phagocytes (66)?

In summary, we demonstrate that DENN domains have a wide spectrum of GTPase substrates, even outside the Rab family. More specifically, we have uncovered DENND2B as a GEF localized at the base of the primary cilia, negatively regulating primary cilia formation and ciliary length by controlling activation of Rab10 and RhoA. In addition, with the DENND2B zebrafish showing developmental defects, a thorough analysis must be performed to understand the impact of Hh signaling, with the possibility of extending the analysis to mice. Last, it is still unanswered as to how DENND2B is inhibited under normal physiological conditions to allow primary cilia formation. Understanding the DENN/GTPase-mediated complex trafficking mechanisms will have potential implications in multiple disease paradigms, from developmental disorders to neurodegeneration and cancer.

Materials and methods

Cell lines

Human embryonic kidney (HEK) 293T, HeLa, A549, and RPE-1 cells were from the American Type Culture Collection (CRL-1573, CCL-2, CCL-185, and CRL-4000).

Cell culture

All cell lines were cultured in Dulbecco's Modified Eagle's medium (DMEM) high-glucose (GE Healthcare, catalog no. SH30081.01) containing 10% bovine calf serum (GE Healthcare, catalog no. SH30072.03), 2 mM l-glutamate (Wisent, catalog no. 609065), 100 IU of penicillin, and streptomycin (100 µg/ml) (Wisent, catalog no. 450201). Serum starvation media are as follows: DMEM high-glucose containing 2 mM l-glutamate, 100 IU of penicillin, and streptomycin (100 µg/ml). Cell lines were routinely tested for mycoplasma contamination using the mycoplasma detection kit (biotool, catalog no. B39038).

DNA constructs

GST-MICAL-L2-C and all 60 GFP-Rab constructs were gifts from M. Fukuda (Tohoku University) (44, 67–69). RFP-mito was generated, replacing venus in mVenus-N1 vector (table S1). DENN(1A)-mito, DENN(1B)-mito, DENN(1C)-mito, DENN(2A)-mito, DENN(2B)-mito, DENN(2C)-mito, and DENN(2D)-mito were cloned into RFP-mito. Lenti GFP-Rab10 Q68L construct was generated using the QuickChange lightning site-directed mutagenesis kit (Agilent Technologies) on lentivirus vector pSLQ1371 containing GFP-Rab10 (36). GFP lentivirus construct was generated by subcloning GFP in pLVX-M-Puro vector at Xho I and Xba I sites by Synbio Technologies. Plasmids from Addgene are as follows: GFP-RhoA Q63L (Addgene, 12968), GFP-RhoA T19N

(Addgene, 12967), 2XMyc-LRRK2-WT (Addgene, 25361), GFP-Rab10Q68L (Addgene, 49544), GFP-Rab10T23N (Addgene, 49545), dTomato-centrin-1 (Addgene, 73332), and pMito-mCherry-FRB (Addgene, 59352). Lenti GFP-RhoA Q63L was cloned into pLVX-M-puro vector (Addgene, 125839). Amplified insert of the coding sequence of Rab35 having double-cysteine residues deleted at the C terminus was cloned into the pEGFP-C1 vector. GST-Rhotekin RBD (murine 7 to 89) was obtained from M. Olson. GFP-DENND2B, mCh-DENND2B, and Flag-DENN(2B) were described previously (19). Human CP110 (GenBank, BC036654.2) was synthesized and subcloned into pCMV-tag2B vector by Synbio Technologies. GFP or GFP-DENND2B was subcloned into pLVX-M-puro vector by Synbio Technologies. Flag-CP110 was synthesized by SynBio. Successful cloning of constructs were verified by sequencing. Refer to table S1 for cloning strategies and oligo sequences.

Table S1: Cloning strategy and oligonucleotides used in this study

Cloning	**Primers (5' → 3')**
RFP-mito: Amplifying RFP-mito from Addgene 11702 and inserting in the digested vector from Addgene 27793 using SalI and NotI	RFP_Fwd (SalI): CATAGTCGACCACCATGGCCTCCTCCGAGGACGTC Mito_Rev (NotI): GCGCGCGGCCGCTTAATTATTTTTTCTTAATTGAATAATTTTGATAAACGCCCC
DENN(1A)-mito in RFP-mito Amino acid: 1-403 Mouse (66)	DENND1A Fwd (NheI): CATAGCTAGCCACCATGGGCTCCAGGATCAAG DENND1A Rev (HindIII): GCGCAAGCTTCTGATGGTACAGTTTGTC
DENN(1B)-mito in RFP-mito Amino acid: 2-412 Human (66)	DENND1B Fwd (NheI): CATAGCTAGCCACCATGGACTGCAGGACCAAG

	DENND1B Rev (EcoRI): GCACGAATTCGAAGCTTATCATATTGTAACTTGTCTTTAC
DENN(1C)-mito in RFP-mito Amino acid: 1-424 Human (66)	DENND1C Fwd (NheI): CATAGCTAGCCACCATGGAATCCAGAGCTGAAG DENND1C Rev (HindIII): GCGCAAGCTTGAGCTGATAGGATCGAAGG
DENN(2A)-mito in RFP-mito Amino acid: 571- 961 Human, GenBank: BC132875	DENND2A Fwd (NheI): CATAGCTAGCCACCATGGTGTCTTTGCACAAGAAGCAGGC DENND2A Rev (HindIII): GCGCAAGCTTCTCCTGGATGAAGCCCCG
DENN(2B)-mito in RFP-mito Amino acid: 687–1,121 Human, GenBank: BC036655	DENND2B Fwd (NheI): CATAGCTAGCCACCATGGAGCTGCTGGAGTGGCAGG DENND2B Rev (HindIII): GCGCAAGCTTCTTATTCATTCCACTCTGCTCAG
DENN(2C)-mito in RFP-mito Amino acid: 481–887 Mouse, NM_177857.2	DENND2C Fwd (NheI): CATAGCTAGCCACCATGGAGCAGCAGCTCTTTGAAC DENND2C Rev (EcoRI): GCACGAATTCGAAGCTTCCGGACTTCAAACAAACC
DENN(2D)-mito in RFP-mito Amino acid: 57–459 Mouse, NM_028110.2	DENND2D Fwd (NheI): CATAGCTAGCCACCATGGGCCAGCACTTCTTTGAATAC DENND2D Rev (HindIII): GCGCAAGCTTTTTCTTTTGGAAGTAGCCTG
SDM: Lenti-Rab10 Q68L	Fwd: GTGTGAAATCGCTCCAGGCCTGCTGTATCCC Rev: GGGATACAGCAGGCCTGGAGCGATTTCACAC
SDM: Lenti-Rab10 Q68L C_C del	Fwd: TGACAGGCTGGAAGAGCAAATGACCTAGGATAAC Rev: GTTATCCTAGGTCATTTGCTCTTCCAGCCTGTCA
SDM: DENN(2B)-RFP-mito P946R	Fwd: CCAACCAGGAAGCGGGTGGGACAGC Rev: GCTGTCCCACCCGCTTCCTGGTTGG

SDM: DENN(2B)-RFP-mito Q1080A	Fwd: GGATGAAGCCAGCAAACATCGCAGACTCCATAAAAACCTCAA Rev: TTGAGGTTTTTATGGAGTCTGCGATGTTTGCTGGCTTCATCC
Modified mVenus-N1 vector for **BFP-FKBP** (Venus was replaced with FKBP using SalI and NotI sites, amplified from Addgene 46944) and BFP was inserted using EcoRI and SalI, amplified from Addgene 80086	BFP Fwd (EcoRI): CATAGAATTCTGATGAGCGAGCTGATTAAG BFP Rev (SalI): GTATGTCGACTGATTAAGCTTGTGCCCCAG FKBP Fwd (SalI): ATACGTCGACGGGAGTGCAGGTGGAAAC FKBP Rev (NotI): GCGCGCGGCCGCTTATTCCAGTTTTAGAAGCTCCAC
DENN(1A)-BFP-FKBP using BFP-FKBP construct	DENND1A Fwd (NheI): CATAGCTAGCCACCATGGGCTCCAGGATCAAG DENND1A Rev (HindIII): GCGCAAGCTTCTGATGGTACAGTTTGTC
DENN(1B)-BFP-FKBP using BFP-FKBP construct	DENND1B Fwd (NheI): CATAGCTAGCCACCATGGACTGCAGGACCAAG DENND1B Rev (EcoRI): GCACGAATTCGAAGCTTATCATATTGTAACTTGTCTTTAC
DENN(1C)-BFP-FKBP using BFP-FKBP construct	DENND1C Fwd (NheI): CATAGCTAGCCACCATGGAATCCAGAGCTGAAG DENND1C Rev (HindIII): GCGCAAGCTTGAGCTGATAGGATCGAAGG
Lenti-GFP RhoA Q63L: GFP-RhoA Q63L in pLVX-M-puro vector (RhoA QL was amplidfied using Addgene 12968	GFP Fwd (XhoI): CATACTCGAGCCACCATGGTGAGCAAGGGCGAGG RhoA Rev (BamHI): GTGCGGATCCTCACAAGACAAGGCAACCAG
Lenti-mSc Rab10 Q68L: mScarlet(mSc)-Rab10 Q68L in pLVX-M-puro vector (Rab10 QL	Cloning of Rab10 QL into mScarlet-I-C1 vector: Rab10 Fwd (XhoI): CATACTCGAGCTGCGAAGAAGACGTACGAC Rab10 Rev (KpnI): GCGCGGTACCTCAGCAGCATTTGCTCTTC Cloning mSc-Rab10 QL into pLVX-M-puro:

was amplified using Addgene 49544	mSc Fwd (BamHI): CATAGGATCCGCCACCATGGTGAGCAAGGGCGAGG Rab10 Rev (EcoRI): GTGCGAATTCTCAGCAGCATTTGCTCTTCC
GFP-Rab35 C_C del cloned into pEGFP-C1 vector Human Rab35 (NM_006861)	GFP Rab35 _C_C_del Fwd (XhoI): ATACTCGAGCTGCCCGGGACTACGACCAC GFP Rab35 _C_C_del (BamHI): ATATGAATTCTTAGCGTTTCTTTCGTTTACTGTTCTTC

Generation of DENND2B KO line (A549 and RPE-1)

Two guide RNAs (gRNAs) (Target_1-318: CGTCTCTCTTGCACGCCGAA; Target_2-442: CGGGTCAGCAAGACGCCCCG) were obtained from Applied Biological Materials and separately cloned into pLenti-U6-sgRNA-SFFV-Cas9-2A-Puro to increase the chances of generating a KO line. Lentivirus-based delivery of gRNA and Cas9 was used to KO DENND2B from A549 and RPE-1 cells. One 15-cm plate containing 107 HEK-293T cells were transfected with 7.5 µg of each gRNA constructs, 15 µg of psPAX2 (obtained from S. Pfeffer), and 7.5 µg of pMD2 VSV-G (obtained from S. Pfeffer) using calcium phosphate. At 8 hours post-transfection, the culture medium was replaced with collection medium [15 ml per plate; regular medium supplemented with 1× nonessential amino acids (Gibco) and 1 mM sodium pyruvate (Gibco)]. The medium was collected at 24 and 36 hours and replaced with fresh medium (15 ml per plate) with each collection. The collected medium at 24 hours was stored at 4°C until the last collection. The collected culture media were then filtered through a 0.45-µm α-polyethersulfone (PES) membrane. A total of 5 × 104 A459 and RPE-1 cells were seeded in one well of a 24-well plate. The next day, regular culture media were replaced with the filtered supernatant containing lentivirus (2 ml each well)

and incubated for 48 hours. Following incubation, puromycin-resistant cells were selected with puromycin (2.5 μg/ml) in the culture medium for 48 hours. After selection, cells were isolated by clonal dilution. Following the expansion of selected colonies, KOs were confirmed by sequencing of the PCR-amplified genomic DNA.

Transfection

HeLa, A549, and RPE-1 cells were transfected using the jetPRIME Transfection Reagent (Polyplus) according to the manufacturer's protocol. HEK-293T cells were transfected using calcium phosphate.

Small interfering RNA–mediated KD of Rab10

HeLa cells were plated at ~80% confluency. Cells were transfected using Lipofectamine RNAiMax (catalog number: 13778-150) from Thermo Fisher Scientific according to the manufacturer's guidelines and were used 48 hours after KD. Control small interfering RNA (siRNA) (ON-TARGETplus; D-001810-10-20) and Rab10 siRNA-targeting genome pool (SMARTpool:ON-TARGETplus; L-010823-00-0010) were purchased from Dharmacon/Horizon Discovery.

Antibodies and reagents

Mouse monoclonal Flag (M2) antibody is obtained from Sigma-Aldrich (F3165). Rabbit polyclonal GFP (A-6455) is obtained from Invitrogen, and rat monoclonal HSC70 antibody [Western blot (WB)-1:10,000] is from Enzo (ADI-SPA-815-F). Alexa Fluor 488– and Alexa Fluor 647–conjugated rabbit secondary antibodies are from Invitrogen. Purified anti-calnexin antibody (W17077C) is from BioLegend [immunofluorescence (IF)-1:1000], anti-PMP70/ABCD3 antibody (sc-514728) is from Santa Cruz Biotechnology (IF-1:500), anti-CP110 antibody (methanol fixation; IF-1:100) is from Proteintech (12780–1-AP), anti-CEP164 antibody

(methanol/paraformaldehyde fixation, IF-1:100) is from Santa Cruz Biotechnology (sc-515403), anti-LAMP1 antibody (IF-1:200) is from Cell Signaling Technology (D2D11), anti-TOM20 antibody (IF-1:500) is from Abcam (ab186734), anti-EEA1 antibody (IF-1:100) is from BD Transduction Laboratories (610456), anti-GM130 antibody (IF-1:500) is from BD Transduction Laboratories (610822), anti-Rab10 antibody (WB-1:1000) is from Cell Signaling Technology (D36C4), anti-Rab10 antibody (IF-1:1000) is from Abcam (ab237703), anti–p-Rab10 antibody (WB-1:1000) is from Abcam (ab230261), anti-LRRK2 antibody (WB-1:1000) is from Abcam (ab133518), anti-RhoA antibody (WB-1:1000) is from Cell Signaling Technology (67B9), anti–Ac-tubulin antibody (IF-1:1000) is from Cell Signaling Technology (D20G3), anti-DENND2B antibody (WB-1:1000) is from GeneTex (GTX55282), anti–γ-tubulin antibody (1:100) is from Sigma-Aldrich (T6557), and MLI-2 is from Tocris Bioscience (5756).

Lentivirus production

For each virus, 10 cm by 15 cm plate containing 107 HEK-293T cells were transfected with 30 μg of lenti construct containing protein of interest, 30 μg of psPAX2, and 15 μg of pMD2 VSV-G using calcium phosphate. At 8 hours post-transfection, the culture medium was replaced with collection medium (15 ml per plate; regular medium supplemented with 1× nonessential amino acids and 1 mM sodium pyruvate). The medium was collected at 24 and 36 hours and replaced with fresh medium (15 ml per plate) with each collection. The collected medium at 24 hours was stored at 4°C until the last collection. The collected culture media were then filtered through a 0.45-μm PES membrane and concentrated by centrifugation (16 hours at 7000 rpm), and the resulting pellets were resuspended in DMEM in 1/5000 of the original volume. Concentrated viruses were aliquoted and stored at −80°C until use.

Protein overexpression using lentivirus

Concentrated lentivirus was added to the cells with minimum culture media (for example, 200 µl of the medium for each well in a four-chambered dish or 1 ml of medium in a well of six-well dish), and the medium was replaced with a fresh culture medium the following day. The expression of the target protein was verified by GFP fluorescence.

Confocal imaging

HeLa cells were plated on poly-l-lysine–coated coverslips, and A459/RPE-1 cells were seeded on collagen-coated coverslips. Cells were fixed with warm 4% paraformaldehyde for 10 min at 37°C, permeabilized for 5 min in 0.1% Triton X-100, and blocked for 1 hour in 2% bovine serum albumin in phosphate-buffered saline (PBS) (blocking buffer). Coverslips were incubated in a blocking buffer containing diluted primary antibodies and incubated overnight at 4°C. Cells were washed three times for 10 min with blocking buffer and incubated with corresponding Alexa Fluorophore–conjugated secondary antibodies diluted 1:1000 in blocking buffer for 1 hour at room temperature. Cells were washed three times for 10 min with blocking buffer and once with PBS. Coverslips were mounted on a microscopic slide using fluorescence mounting medium (Dako, catalog no. S3023).

Imaging was performed using a Leica SP8 laser scanning confocal microscope and Zeiss LSM880 with AiryScan. Images of primary cilia are presented as maximum intensity projections. Image analysis was done using ImageJ. All the images were prepared for publication using Adobe Photoshop (adjusted contrast and applied 1-pixel Gaussian blur) and then assembled with Adobe Illustrator.

Live-cell imaging rapamycin-based DENN recruitment

Live-cell imaging was performed using LSM-880 confocal microscope upon addition of 100 nM rapamycin (Sigma-Aldrich). Cells were kept at 37°C in 5% CO2. Frames were captured every 8 s.

Calculation of degree of colocalization

The degree of colocalization of RFP (DENN or RFP alone in the control) with the GFP-Rab constructs was quantified using Imaris Software at the Analysis Workstation of Advanced BioImaging Facility (McGill). RFP-DENN (mitochondrially localized protein) was masked such that only the mitochondrial area is evaluated. Furthermore, images were thresholded automatically using the Imaris algorithm, and the Pearson correlation coefficient (PCC) was calculated between the two indicated fluorescent signals.

Quantification of recruitment rate of DENN domains or GFP-Rab

We used Imaris software to calculate PCC for each frame over time between mCherry and TagBFP. The degree of colocalization (PCC) represents the recruitment of DENN domain on the mitochondria over time. Similarly, PCC was calculated between mCherry and GFP, which represents the recruitment of Rab35 on the mitochondria over time.

Screening of 60 GFP-Rabs

HeLa cells (9000 cells per 100 ml of culture medium) were seeded in each well of a 96-well plate CellCarrier-96 Ultra Microplates (6055302, PerkinElmer). Cells were cotransfected with 100 ng each of individual GFP-Rabs and DENN(x)-mito or RFP-mito using jetPRIME. At 24 hours post-transfection, cells were fixed with 4% paraformaldehyde, washed three times with PBS, and permeabilized for 5 min in 0.1% Triton X-100 in PBS. Following permeabilization, cells were stained with 4′,6-

diamidino-2-phenylindole (DAPI) for 5 min diluted in PBS. Last, cells were washed gently with PBS, and 100 µl of PBS was added to each well.

Each transfected well of the 96-well plate was divided into grids and between 70 and 100 images were acquired by the Opera Phenix HCS microscope using a 63× objective. A qualitative assessments of colocalization of GFP-Rabs and DENN or RFP alone at the mito were performed on all the images by eye estimation. Furthermore, all potential hits were further confirmed by imaging each pair using Leica SP8, which provides much higher resolution.

FRAP imaging

FRAP experiments were carried out on a Zeiss LSM780 laser scanning confocal microscope (Carl Zeiss, Germany). Cells were cultured in 35-mm glass-bottom petri dishes (Lab-Tek II Chamber, USA) and maintained on the microscopy incubator at 5% CO2 and 37°C. Imaging was performed using a 100×/1.46 numerical aperture Plan-Apochromat oil objective at 5× optical zoom. FRAP conditions were optimized as follows: A region of interest encompassing the centriole was selected (~2.3 µm by 2.3 µm) and photobleached at 100% laser power (488-nm argon laser) with 200 iterations. Prebleach and postbleach time series images were collected at 2-s intervals for 5 to 8 min. Cells were excited by a 488-nm argon laser for GFP-Rab10 or GFP and a 561-nm diode pumped solid state (DPSS) laser with dTomato-Centrin-1, centriolar marker, respectively.

FRAP image analysis

For quantification of the centrosome FRAP experiments, fluorescence intensity was measured using ImageJ software with plugins provided by Stowers Institute. The square measurement region was set to ~2.3 µm by 3 µm. The average intensity of the

image was subtracted at each time point as background. Recovery intensities were fit to an exponential curve, described by the following equation: $I(t) = b + IE\ (1 - e^{-t/\tau})$, where I is the intensity, IE is the maximum intensity, t is the time, and τ is an intermediate variable. IE was identical to the fraction recovered, and τ was used to calculate a recovery half-time (t½), by the following equation: $t½ = -\ln 0.5 \times \tau = 0.69\ \tau$. The fluorescence recovery curves were calculated from the averaged values. Statistical analysis of fraction recovered (%) and t½ was performed in Microsoft Excel (Microsoft Corporation, USA).

Primary cilia induction

A549 or RPE-1 cells were grown in regular culture media until they became fully confluent. Both cell lines were serum-starved for 24 hours. Following starvation, cells were fixed and stained for cilia marker (Ac-tubulin).

SAG treatment

WT or DENND2B KO cells were grown to confluency and cultured in serum-free medium for 24 hours to induce ciliogenesis. Next, serum-free culture medium containing 200 nM Smoothened agonist (SAG) (EMD Milipore, catalog # 566661) was added to cells for 24 hours. Then, cells were washed in PBS, and RNA was extracted as per the method described in the quantitative polymerase chain reaction (PCR) protocol.

Rho activator II (catalog no. CN03) treatment

WT or DENND2B KO cells were grown to confluency and cultured in serum-free medium for 24 hours to induce ciliogenesis. After 24 hours of starvation, serum-free culture medium containing CN03 (1 µg/ml) was added to cells for 6 hours. Then, cells were processed for confocal imaging.

Real-time quantitative PCR

Total RNA was extracted from A549 cells using the RNeasy Mini Kit (QIAGEN), and 500 ng of RNA was used for the cDNA synthesis using the iScript Reverse Transcription Supermix (Bio-Rad Laboratories). Real-time quantitative PCR was performed using the Bio-Rad CFX Connect Real-Time PCR Detection System with SsoFast EvaGreen Supermix (Bio-Rad Laboratories). The values were expressed as fold change in mRNA expression in cells relative to control WT cells (untreated) using TATA-box binding protein and β-2-microglobulin as endogenous controls. The primer sequences (5′ → 3′) used in this study were as follows: Gli1 (forward) GAAGACCTCTCCAGCTTGGA and Gli1 (reverse) GGCTGACAGTATAGGCAGAG.

Protein purification

GST-MICAL-L2-C and GST-Rhotekin RBD proteins were expressed in Escherichia coli BL21 (500 μM isopropyl β-d-1-thiogalactopyranoside; Wisent Bioproducts; at room temperature for 16 hours) and purified using standard procedure in tris buffer [20 mM tris (pH 7.4), 100 mM NaCl, 10 mM MgCl2, and 1 mM dithiothreitol] supplemented with protease inhibitors.

Biochemical assays

Immunoblot of cell lysate

To analyze levels of p-Rab10, cells were lyzed in phospho-lysis buffer [20 mM Hepes, 100 mM NaCl, 1 mM dithiothreitol, 1% Triton X-100 (pH 7.4), 5 mM sodium pyrophosphate, 500 nM okadaic acid, 1 mM Na3VO4, and 10 mM NaF], supplemented with protease inhibitors [0.83 mM benzamidine, 0.20 mM phenylmethylsulfonyl fluoride, aprotinin (0.5 mg/ml), and leupeptin (0.5 mg/ml)]. Cell lysates were

centrifuged at 21,130g for 10 min at 4°C, and the supernatant was resolved by SDS–polyacrylamide gel electrophoresis (PAGE) and processed for Western blotting.

Coimmunoprecipitation

HEK-293T cells grown to 60% confluency in 15-cm dishes were transfected with Flag-tagged or GFP-tagged constructs. At 24 hours post-transfection, cells were gently washed with PBS, scraped into lysis buffer [20 mM Hepes, 100 mM NaCl, 0.5 mM dithiothreitol, 10 mM MgCl2, and 1% Triton X-100 (pH 7.4)] supplemented with protease inhibitors, incubated for 20 min on a rocker at 4°C, and the lysates were centrifuged at 305,000g for 15 min at 4°C. For Flag immunoprecipitation, supernatants were incubated with prewashed protein G beads–Sepharose beads (GE Healthcare) for 1 hour (preclearing step). Following preclearing, supernatants were incubated with protein G–Sepharose beads and the anti-Flag antibody for 2 hours at 4°C. Beads coupled to the Flag antibody were washed three times with the same lysis buffer, eluted in SDS-PAGE sample buffer, resolved by SDS-PAGE, and processed for immunoblotting.

Effector pull-down assay

Cells were gently washed with PBS, lyzed in lysis buffer [20 mM Hepes, 100 mM NaCl, 20 mM MgCl2, and 1% Triton X-100 (pH 7.4)] supplemented with protease inhibitors, and incubated for 20 min on a rocker at 4°C, and the lysates were centrifuged at 305,000g for 15 min at 4°C. For GST pull-down experiments, supernatants were incubated with GST fusion proteins precoupled to glutathione-Sepharose beads for 1 hour at 4°C. GST beads attached to the fusion proteins were washed three times with the same lysis buffer, eluted in SDS-PAGE sample buffer, resolved by SDS-PAGE, and processed for immunoblotting.

Immunoblot

Lysates were run on large 10% polyacrylamide gels and transferred to nitrocellulose membranes. Proteins on the blots were visualized by Ponceau staining. Blots were then blocked with 5% milk in tris-buffered saline with 0.1% Tween 20 (TBST) for 1 hour followed by incubation with antibodies O/N at 4°C diluted in 5% milk in TBST. The next day, blots were washed three times with TBST. Then, the peroxidase-conjugated secondary antibody was incubated in a 1:5000 dilution in TBST with 5% milk for 1 hour at room temperature followed by washes.

Zebrafish

WT TL zebrafish (Danio rerio) were bred and maintained according to standard procedures (70). All experiments were performed in compliance with the guidelines of the Canadian Council for Animal Care. An antisense MO was designed (Gene Tools) to bind and inhibit specifically the ATG site of the zebrafish dennd2b transcript targeting the following sequence (CTGTCAAAGGG AGATGACTGCCAAC). The standard control MO (CCTCTTACCTCAGTTA CAATTTATA) was used as a control. Injections of 1 nl volumes of an antisense or control MO at a concentration of 0.1 mM were made directly into one-cell stage embryos. For confocal examination, larvae aged 13 hpf were fixed in 4% paraformaldehyde overnight at 4°C. After fixation, the larvae were rinsed several times (1 hour) with PBS, then incubated in freshly prepared block solution containing primary antibody against Ac-tubulin antibody (IF-1:1000) from Cell Signaling Technology (D20G3) overnight at 4°C, washed, and followed by 4 hours of incubation with block solution containing a secondary antibody (1:4000; Alexa Fluor 488 nm, Invitrogen). Labeled zebrafish were washed several times with PBS and mounted on a slide in 70% glycerol before imaging.

Rescue experiment

Human DENND2B mRNAs were transcribed from Not I–linearized pCS2+ using SP6 polymerase with the mMESSAGE Machine Kit (Thermo Fisher Scientific). The mRNA was diluted in nuclease-free water with 0.05% Fast Green (Sigma-Aldrich) to a final concentration of 30 ng/μl and backfilled in a pulled (Sutter Instrument Company) thin-walled bromosilicate capillary tube and pressure-injected into the cell using a PicoSpritzer III (General Valve).

Statistics

Graphs were prepared using GraphPad Prism software. All statistical tests were performed using SPSS. For all data, normality test was performed before determining the appropriate statistical test. For normally distributed data, comparisons were made using either t test or one-way analysis of variance (ANOVA) with either Tukey's post hoc multiple comparisons test or Dunnett's test. For nonnormally distributed data, comparisons were made using Mann-Whitney U test or Kruskal-Wallis test. All data are shown as the means ± SEM with $P < 0.05$ considered statistically significant.

Acknowledgments for Chapter 3

We thank H. McBride for comments on the manuscript, S. Pfeffer for providing us with the idea of a cell-based GEF assay and lentiviral Rab10 overexpression constructs, and M. Fukuda and J. Bonifacino for providing us all 60 GFP-Rab and GST-MICAL-L2 C constructs. We also thank J. Philie and M. Fotouhi for excellent technical assistance. We acknowledge N. Vuillemin from the McGill University Advanced BioImaging Facility (ABIF; RRID:SCR_017697), M. Fu and S. Bo Feng from the RI-MUHC Molecular Imaging Platform for technical support, and the Neuro Microscopy Imaging Centre at the McGill University.

Funding: This work was supported by a Canadian Institutes of Health Research Foundation Grant to P.S.M. G.A.B.A. was supported by a project grant funding from the Canadian Institutes of Health Research and ALS Canada. R.K. is supported by a studentship from ALS Canada. V.F. was supported by a fellowship from the Fonds de recherche du Quebec–Sante (FRQS). G.K. was supported by FRQS and a Jeanne Timmins Costello Fellowship. P.S.M. is a Distinguished James McGill Professor and a Fellow of the Royal Society of Canada.

References for Chapter 3

1. M. Zerial, H. McBride, Rab proteins as membrane organizers. Nat. Rev. Mol. Cell Biol. 2, 107–117 (2001).

2. Y. Homma, S. Hiragi, M. Fukuda, Rab family of small GTPases: An updated view on their regulation and functions. FEBS J. 288, 36–55 (2021).

3. H. Stenmark, Rab GTPases as coordinators of vesicle traffic. Nat. Rev. Mol. Cell Biol. 10, 513–525 (2009).

4. H. Stenmark, V. M. Olkkonen, The Rab GTPase family. Genome Biol. 2, REVIEWS3007 (2001).

5. A. D. Shapiro, S. R. Pfeffer, Quantitative analysis of the interactions between prenyl Rab9, GDP dissociation inhibitor-α, and guanine nucleotides. J. Biol. Chem. 270, 11085–11090 (1995).

6. Y.-W. Wu, K.-T. Tan, H. Waldmann, R. S. Goody, K. Alexandrov, Interaction analysis of prenylated Rab GTPase with Rab escort protein and GDP dissociation inhibitor explains the need for both regulators. Proc. Natl. Acad. Sci. U.S.A. 104, 12294–12299 (2007).

7. P. Chavrier, J.-P. Gorvel, E. Stelzer, K. Simons, J. Gruenberg, M. Zerial, Hypervariable C-terminal domain of rab proteins acts as a targeting signal. Nature 353, 769–772 (1991).

8. F. Li, L. Yi, L. Zhao, A. Itzen, R. S. Goody, Y.-W. Wu, The role of the hypervariable C-terminal domain in Rab GTPases membrane targeting. Proc. Natl. Acad. Sci. U.S.A. 111, 2572–2577 (2014).

9. A. Barbara Dirac-Svejstrup, T. Sumizawa, S. R. Pfeffer, Identification of a GDI displacement factor that releases endosomal Rab GTPases from Rab-GDI. EMBO J. 16, 465–472 (1997).

10. U. Sivars, D. Aivazian, S. R. Pfeffer, Yip3 catalyses the dissociation of endosomal Rab-GDI complexes. Nature 425, 856–859 (2003).

11. S. Schoebel, L. Katharina Oesterlin, W. Blankenfeldt, R. Sidney Goody, A. Itzen, RabGDI displacement by DrrA from Legionella is a consequence of its guanine nucleotide exchange activity. Mol. Cell 36, 1060–1072 (2009).

12. J. Blümer, J. Rey, L. Dehmelt, T. Mazel, Y.-W. Wu, P. Bastiaens, R. S. Goody, RabGEFs are a major determinant for specific Rab membrane targeting. J. Cell Biol. 200, 287–300 (2013).

13. F. A. Barr, Rab GTPases and membrane identity: Causal or inconsequential? J. Cell Biol. 202, 191–199 (2013).

14. J. Cherfils, M. Zeghouf, Regulation of small GTPases by GEFs, GAPs, and GDIs. Physiol. Rev. 93, 269–309 (2013).

15. A. L. Marat, H. Dokainish, P. S. McPherson, DENN domain proteins: Regulators of Rab GTPases. J. Biol. Chem. 286, 13791–13800 (2011).

16. S.-i. Yoshimura, A. Gerondopoulos, A. Linford, D. J. Rigden, F. A. Barr, Family-wide characterization of the DENN domain Rab GDP-GTP exchange factors. J. Cell Biol. 191, 367–381 (2010).

17. A. L. Marat, M. S. Ioannou, P. S. McPherson, Connecdenn 3/DENND1C binds actin linking Rab35 activation to the actin cytoskeleton. Mol. Biol. Cell 23, 163–175 (2012).

18. P. D. Allaire, A. L. Marat, C. Dall'Armi, G. Di Paolo, P. S. McPherson, B. Ritter, The Connecdenn DENN domain: A GEF for Rab35 mediating cargo-specific exit from early endosomes. Mol. Cell 37, 370–382 (2010).

19. M. S. Ioannou, E. S. Bell, M. Girard, M. Chaineau, J. N. R. Hamlin, M. Daubaras, A. Monast, M. Park, L. Hodgson, P. S. McPherson, DENND2B activates Rab13 at the leading edge of migrating cells and promotes metastatic behavior. J. Cell Biol. 208, 629–648 (2015).

20. A. K. Gillingham, R. Sinka, I. L. Torres, K. S. Lilley, S. Munro, Toward a comprehensive map of the effectors of rab GTPases. Dev. Cell 31, 358–373 (2014).

21. O. E. Blacque, N. Scheidel, S. Kuhns, Rab GTPases in cilium formation and function. Small GTPases 9, 76–94 (2018).

22. P. Satir, S. Tvorup Christensen, Overview of structure and function of mammalian cilia. Annu. Rev. Physiol. 69, 377–400 (2007).

23. J. F. Reiter, M. R. Leroux, Genes and molecular pathways underpinning ciliopathies. Nat. Rev. Mol. Cell Biol. 18, 533–547 (2017).

24. M. Mirvis, T. Stearns, W. James Nelson, Cilium structure, assembly, and disassembly regulated by the cytoskeleton. Biochem. J. 475, 2329–2353 (2018).

25. R. Rohatgi, W. J. Snell, The ciliary membrane. Curr. Opin. Cell Biol. 22, 541–546 (2010).

26. A. Knödler, S. Feng, J. Zhang, X. Zhang, A. Das, J. Peränen, W. Guo, Coordination of Rab8 and Rab11 in primary ciliogenesis. Proc. Natl. Acad. Sci. U.S.A. 107, 6346–6351 (2010).

27. I. Göhring, A. Tagariello, S. Endele, C. C. Stolt, M. Ghassibé, M. Fisher, C. T. Thiel, U. Trautmann, M. Vikkula, A. Winterpacht, D. R. FitzPatrick, A. Rauch, Disruption of ST5 is associated with mental retardation and multiple congenital anomalies. J. Med. Genet. 47, 91–98 (2010).

28. S. Pistor, T. Chakraborty, K. Niebuhr, E. Domann, J. Wehland, The ActA protein of Listeria monocytogenes acts as a nucleator inducing reorganization of the actin cytoskeleton. EMBO J. 13, 758–763 (1994).

29. I. Kouranti, M. Sachse, N. Arouche, B. Goud, A. Echard, Rab35 regulates an endocytic recycling pathway essential for the terminal steps of cytokinesis. Curr. Biol. 16, 1719–1725 (2006).

30. D. J. Strick, L. A. Elferink, Rab15 effector protein: A novel protein for receptor recycling from the endocytic recycling compartment. Mol. Biol. Cell 16, 5699–5709 (2005).

31. B. D. Grant, J. G. Donaldson, Pathways and mechanisms of endocytic recycling. Nat. Rev. Mol. Cell Biol. 10, 597–608 (2009).

32. N. A. Zaghloul, S. A. Brugmann, The emerging face of primary cilia. Genesis 49, 231–246 (2011).

33. L. Liu, J.-Q. Sheng, M.-R. Wang, Y. Gan, X.-L. Wu, J.-Z. Liao, D.-A. Tian, X.-X. He, P.-Y. Li, Primary cilia blockage promotes the malignant behaviors of hepatocellular carcinoma via induction of autophagy. Biomed. Res. Int. 2019, 1–14 (2019).

34. M. V. Nachury, A. V. Loktev, Q. Zhang, C. J. Westlake, J. Peränen, A. Merdes, D. C. Slusarski, R. H. Scheller, J. F. Bazan, V. C. Sheffield, P. K. Jackson, A core

complex of BBS proteins cooperates with the GTPase Rab8 to promote ciliary membrane biogenesis. Cell 129, 1201–1213 (2007).

35. S. Kuhns, C. Seixas, S. Pestana, B. Tavares, R. Nogueira, R. Jacinto, J. S. Ramalho, J. C. Simpson, J. S. Andersen, A. Echard, S. S. Lopes, D. C. Barral, O. E. Blacque, Rab35 controls cilium length, function and membrane composition. EMBO Rep. 20, e47625 (2019).

36. H. S. Dhekne, I. Yanatori, R. C. Gomez, F. Tonelli, F. Diez, B. Schüle, M. Steger, D. R. Alessi, S. R. Pfeffer, A pathway for parkinson's disease LRRK2 kinase to block primary cilia and sonic hedgehog signaling in the brain. eLife 7, e40202 (2018).

37. R. W. Tucker, A. B. Pardee, K. Fujiwara, Centriole ciliation is related to quiescence and DNA synthesis in 3T3 cells. Cell 17, 527–535 (1979).

38. J. Lee, D. H. Oh, K. C. Park, J. E. Choi, J. B. Kwon, J. Lee, K. Park, H. J. Sul, Increased primary cilia in idiopathic pulmonary fibrosis. Mol. Cell 41, 224–233 (2018).

39. D. K. Breslow, A. J. Holland, Mechanism and regulation of centriole and cilium biogenesis. Annu. Rev. Biochem. 88, 691–724 (2019).

40. S. Graser, Y.-D. Stierhof, S. B. Lavoie, O. S. Gassner, S. Lamla, M. L. Clech, E. A. Nigg, Cep164, a novel centriole appendage protein required for primary cilium formation. J. Cell Biol. 179, 321–330 (2007).

41. B. Delaval, L. Covassin, N. D. Lawson, S. Doxsey, Centrin depletion causes cyst formation and other ciliopathy-related phenotypes in zebrafish. Cell Cycle 10, 3964–3972 (2011).

42. X. Wu, M. J. Bradley, Y. Cai, D. Kümmel, E. M. De La Cruz, F. A. Barr, K. M. Reinisch, Insights regarding guanine nucleotide exchange from the structure of a DENN-domain protein complexed with its Rab GTPase substrate. Proc. Natl. Acad. Sci. U.S.A. 108, 18672–18677 (2011).

43. G. Kulasekaran, M. Chaineau, V. E. C. Piscopo, F. Verginelli, M. Fotouhi, M. Girard, Y. Tang, R. Dali, R. Lo, S. Stifani, P. S. McPherson, An Arf/Rab cascade controls the growth and invasiveness of glioblastoma. J. Cell Biol. 220, e202004229 (2021).

44. Y. Homma, M. Fukuda, Rabin8 regulates neurite outgrowth in both GEF activity-dependent and -independent manners. Mol. Biol. Cell 27, 2107–2118 (2016).

45. H. Sano, G. R. Peck, A. N. Kettenbach, S. A. Gerber, G. E. Lienhard, Insulin-stimulated GLUT4 protein translocation in adipocytes requires the Rab10 guanine nucleotide exchange factor Dennd4C. J. Biol. Chem. 286, 16541–16545 (2011).

46. M. Cabrera, C. Ungermann, Guanine nucleotide exchange factors (GEFs) have a critical but not exclusive role in organelle localization of rab GTPases. J. Biol. Chem. 288, 28704–28712 (2013).

47. S. Yoshida, K. Aoki, K. Fujiwara, T. Nakakura, A. Kawamura, K. Yamada, M. Ono, S. Yogosawa, K. Yoshida, The novel ciliogenesis regulator dyrk2 governs hedgehog signaling during mouse embryogenesis. eLife 9, e57381 (2020).

48. G. B. Carballo, J. R. Honorato, G. P. F. de Lopes, T. C. L. de Sampaio E Spohr, A highlight on Sonic hedgehog pathway. Cell Commun. Signal. 16, 11 (2018).

49. P. Niewiadomski, R. Rohatgi, Measuring expression levels of endogenous gli genes by immunoblotting and real-time pcr. Methods Mol. Biol. 1322, 81–92 (2015).

50. A. J. Streets, P. P. Prosseda, A. C. M. Ong, Polycystin-1 regulates ARHGAP35-dependent centrosomal RhoA activation and ROCK signaling. JCI Insight 5, e135385 (2020).

51. A. Pitaval, Q. Tseng, M. Bornens, M. Théry, Cell shape and contractility regulate ciliogenesis in cell cycle–arrested cells. J. Cell Biol. 191, 303–312 (2010).

52. L. Rangel, M. Bernabé-Rubio, J. Fernández-Barrera, J. Casares-Arias, J. Millán, M. A. Alonso, I. Correas, Caveolin-1α regulates primary cilium length by controlling RhoA GTPase activity. Sci. Rep. 9, 1116 (2019).

53. X.-D. Ren, W. B. Kiosses, M. A. Schwartz, Regulation of the small GTP-binding protein Rho by cell adhesion and the cytoskeleton. EMBO J. 18, 578–585 (1999).

54. A. Spektor, W. Y. Tsang, D. Khoo, B. D. Dynlacht, Cep97 and CP110 suppress a cilia assembly program. Cell 130, 678–690 (2007).

55. D. R. Alessi, E. Sammler, LRRK2 kinase in Parkinson's disease. Science 360, 36–37 (2018).

56. Z. Liu, N. Bryant, R. Kumaran, A. Beilina, A. Abeliovich, M. R. Cookson, A. B. West, LRRK2 phosphorylates membrane-bound Rabs and is activated by GTP-bound Rab7L1 to promote recruitment to the trans-Golgi network. Hum. Mol. Genet. 27, 385–395 (2018).

57. Y. Sobu, P. S. Wawro, H. S. Dhekne, W. M. Yeshaw, S. R. Pfeffer, Pathogenic LRRK2 regulates ciliation probability upstream of tau tubulin kinase 2 via Rab10 and RILPL1 proteins. Proc. Natl. Acad. Sci. U.S.A. 118, e2005894118 (2021).

58. H. Kobayashi, K. Etoh, N. Ohbayashi, M. Fukuda, Rab35 promotes the recruitment of Rab8, Rab13 and Rab36 to recycling endosomes through MICAL-L1 during neurite outgrowth. Biol. Open 3, 803–814 (2014).

59. H. Bagci, N. Sriskandarajah, A. Robert, J. Boulais, I. E. Elkholi, V. Tran, Z.-Y. Lin, M.-P. Thibault, N. Dubé, D. Faubert, D. R. Hipfner, A.-C. Gingras, J.-F. Côté, Mapping the proximity interaction network of the Rho-family GTPases reveals signalling pathways and regulatory mechanisms. Nat. Cell Biol. 22, 120–134 (2020).

60. C. Guilluy, A. D. Dubash, R. García-Mata, Analysis of RhoA and Rho GEF activity in whole cells and the cell nucleus. Nat. Protoc. 6, 2050–2060 (2011).

61. M. S. Sajib, F. T. Zahra, R. G. Akwii, C. M. Mikelis, Identification of Rho GEF and RhoA activation by pull-down assays. Methods Mol. Biol. 2193, 97–109 (2021).

62. E. M. Valente, R. O. Rosti, E. Gibbs, J. G. Gleeson, Primary cilia in neurodevelopmental disorders. Nat. Rev. Neurol. 10, 27–36 (2014).

63. N. Huang, D. Zhang, F. Li, P. Chai, S. Wang, J. Teng, J. Chen, M-Phase Phosphoprotein 9 regulates ciliogenesis by modulating CP110-CEP97 complex localization at the mother centriole. Nat. Commun. 9, 4511 (2018).

64. M. Higgins, I. Obaidi, T. M. Morrow, Primary cilia and their role in cancer. Oncol. Lett. 17, 3041–3047 (2019).

65. M. Steger, F. Tonelli, G. Ito, P. Davies, M. Trost, M. Vetter, S. Wachter, E. Lorentzen, G. Duddy, S. Wilson, M. A. S. Baptista, B. K. Fiske, M. J. Fell, J. A. Morrow, A. D. Reith, D. R. Alessi, M. Mann, Phosphoproteomics reveals that Parkinson's disease kinase LRRK2 regulates a subset of Rab GTPases. eLife 5, e12813 (2016).

66. Z. Liu, E. Xu, H. T. Zhao, T. Cole, A. B. West, LRRK2 and Rab10 coordinate macropinocytosis to mediate immunological responses in phagocytes. EMBO J. 39, e104862 (2020).

67. T. Matsui, T. Itoh, M. Fukuda, Small GTPase Rab12 regulates constitutive degradation of transferrin receptor. Traffic 12, 1432–1443 (2011).

68. T. Tsuboi, M. Fukuda, Rab3A and Rab27A cooperatively regulate the docking step of dense-core vesicle exocytosis in PC12 cells. J. Cell Sci. 119, 2196–2203 (2006).

69. M. Ishida, N. Ohbayashi, Y. Maruta, Y. Ebata, M. Fukuda, Functional involvement of Rab1A in microtubule-dependent anterograde melanosome transport in melanocytes. J. Cell Sci. 125, 5177–5187 (2012).

70. M. Westerfield, The Zebrafish Book. A Guide for the Laboratory Use of Zebrafish (Danio rerio) (University of Oregon Press, ed. 3, 1995).

Figures for Chapter 3

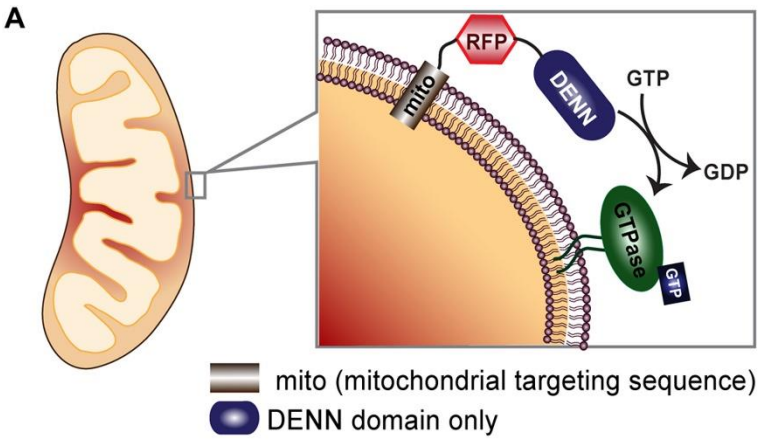

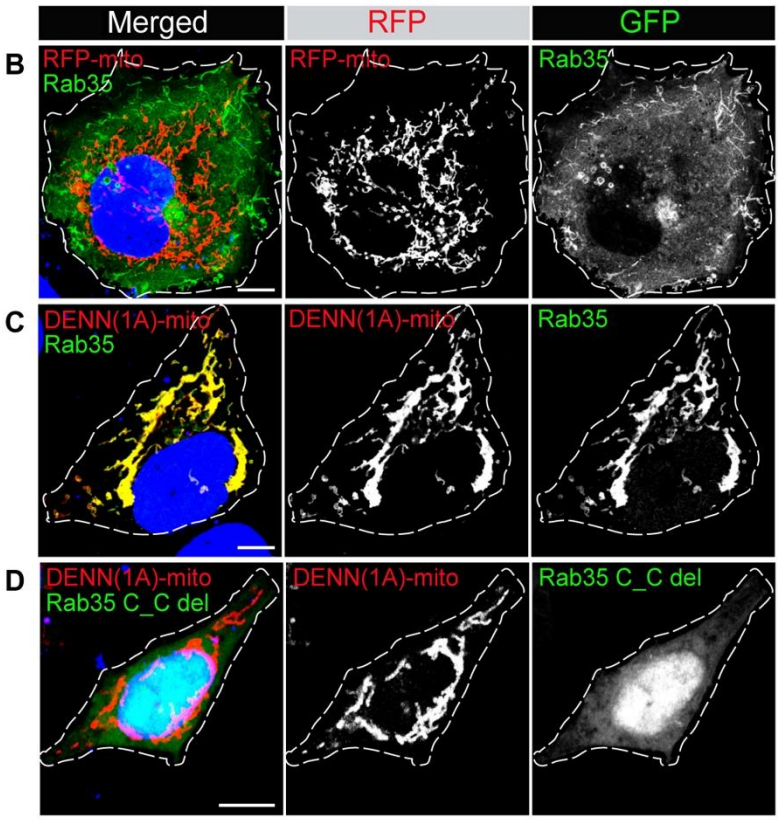

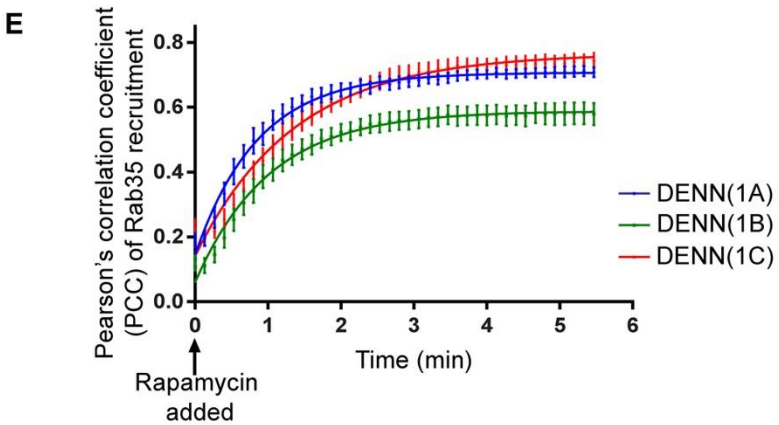

Figure 1: DENN domains targeted to mitochondria recruit their Rab substrates.

(A) Schematic model of the cell-based GEF assay. (B and C) HeLa cells cotransfected with GFP-Rab35 and RFP-mito (B) or GFP-Rab35 and DENN(1A)-mito (C) were stained with 4′,6-diamidino-2-phenylindole (DAPI) to reveal nuclei. (D) HeLa cells cotransfected with DENN(1A)-mito and GFP-Rab35 C_C del were stained with DAPI (blue) to reveal nuclei. Scale bars, 8 μm. (E) Curves demonstrating the recruitment kinetics of Rab35 (means ± SEM from 12 independent experiments). Recruitment curves were fit by a nonlinear regression one-phase association.

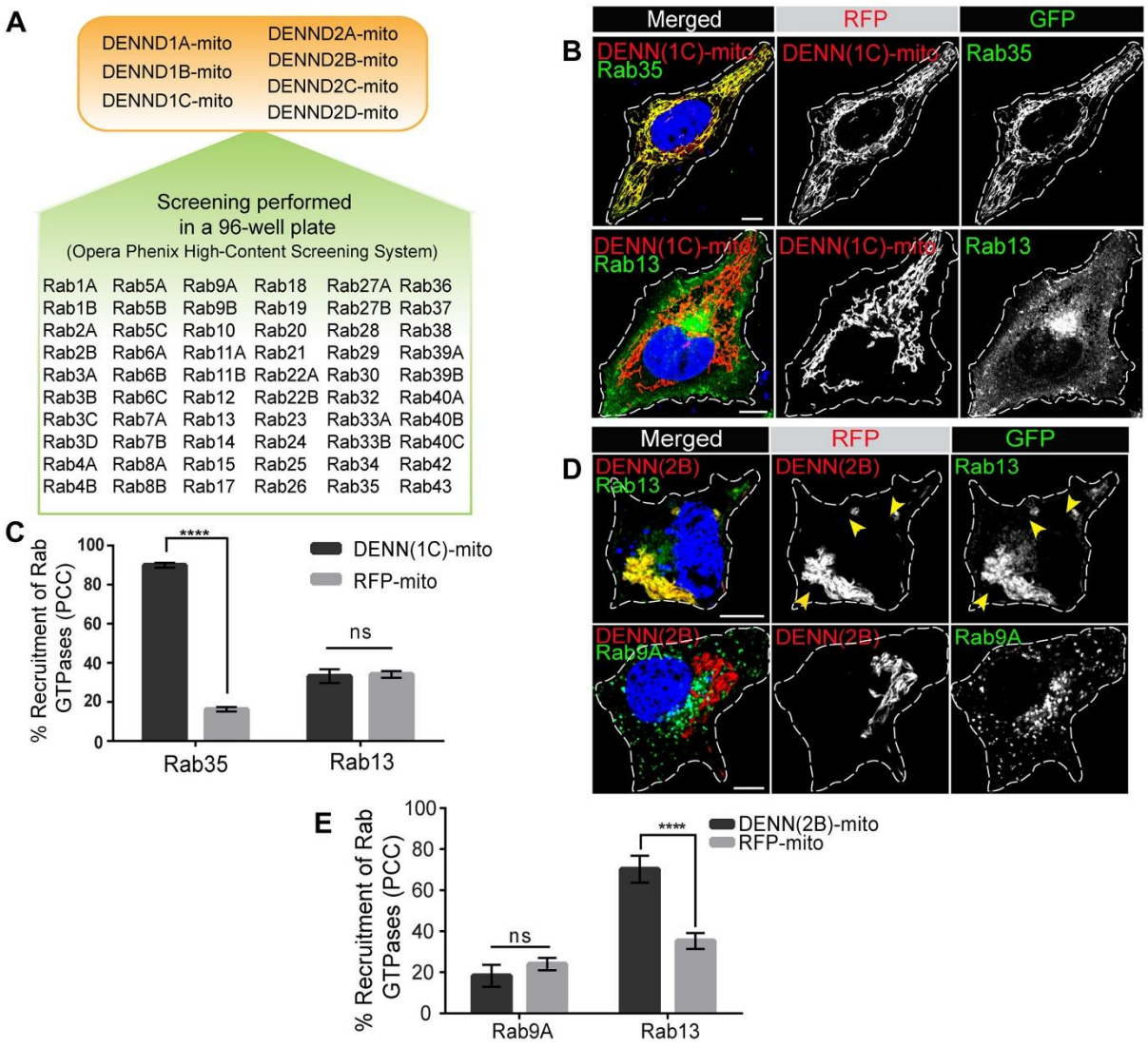

F

	Screening using DENN domains only	Previously reported Rab substrates	Newly identified and confirmed substrates
DENND1	DENND1A	Rab35	Rab35, Rab15
	DENND1B	Rab35	Rab35, Rab15
	DENND1C	Rab13/Rab35	Rab35, Rab15
DENND2	DENND2A	Rab9	Rab15
	DENND2B	Rab9/Rab13	Rab8A, Rab8B, Rab10, Rab13, Rab15, Rab27A, Rab27B, Rab35, **RhoA**
	DENND2C	Rab9	Rab8A, Rab8B, Rab10, Rab15, Rab35
	DENND2D	Rab9	Rab8A, Rab10

Figure 2: High-content screening reveals GEF activity of DENND1 and DENND2 DENN domains.

(A) Schematic representation of a comprehensive screen of DENN(1A/1B/1C) and DENN(2A/2B/2C/2D) against 60 GFP-Rabs. (B) HeLa cells coexpressing DENN(1C)-mito and GFP-Rab35 or GFP-Rab13 were stained with DAPI to reveal nuclei. Scale bars, 8 μm. (C) Quantification of percentage recruitment of Rab35 and Rab13 by DENN(1C) by analyzing colocalization using PCC (Pearson correlation coefficient) measuring cells from six independent experiments as shown in (B); means ± SEM; unpaired t test (for Rab35) and Welch t test (for Rab13); ****P < 0.001; ns, not significant. (D) HeLa cells expressing DENN(2B)-mito and GFP-Rab13 or GFP-Rab9A were stained with DAPI to reveal nuclei. Scale bars, 8 μm. (E) Quantification of percentage recruitment of Rab9A and Rab13 by DENN(2B) by analyzing colocalization using PCC, measuring cells from five independent experiments as shown in (D); means ± SEM; unpaired t test (for Rab13) and Mann-Whitney U test (for Rab9A); ****P < 0.001. (F) Tabular representation of all the newly identified or confirmed GTPases recruited by the respective DENN domain proteins versus previously reported GTPases.

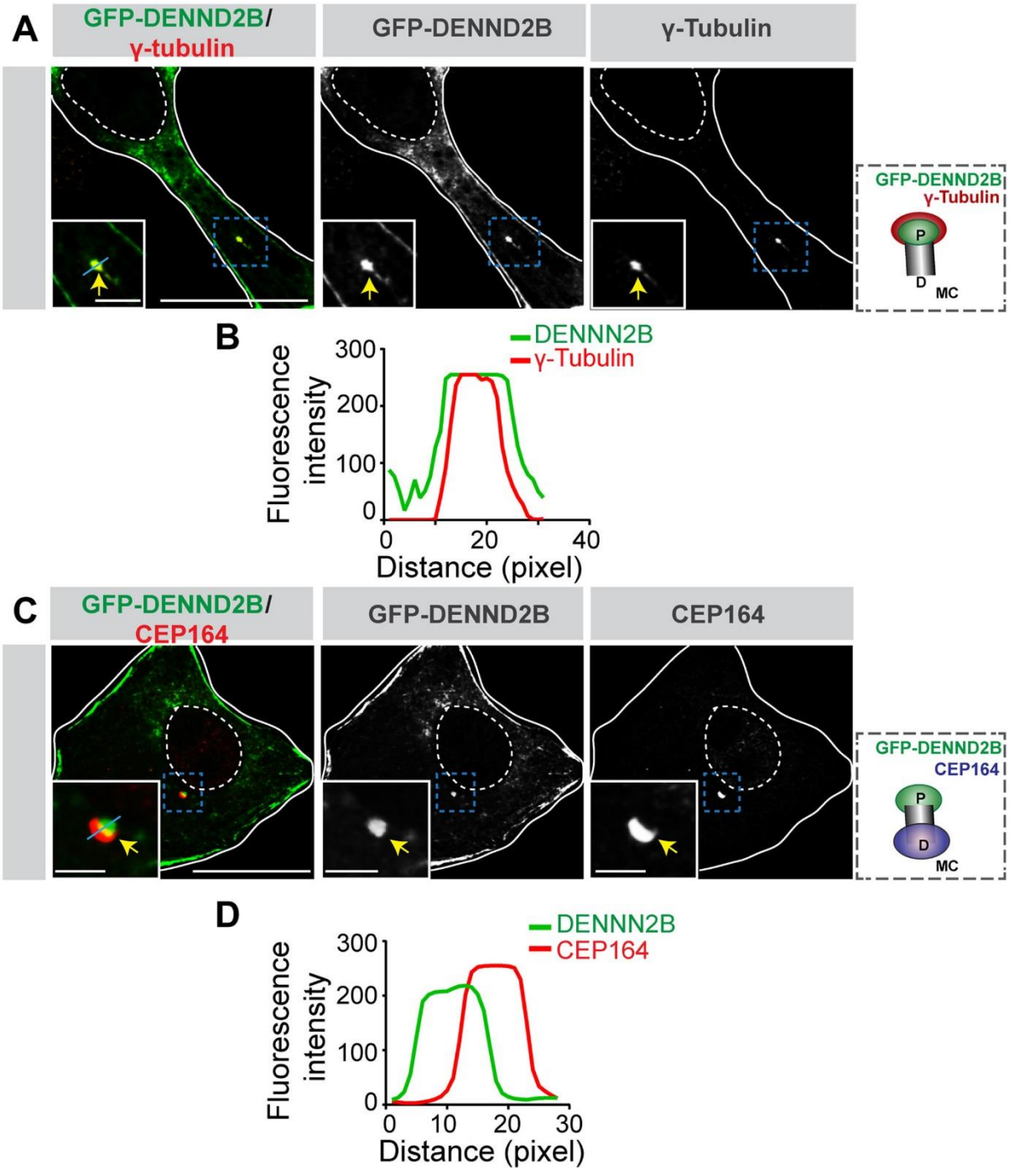
A
GFP-DENND2B/
γ-tubulin
GFP-DENND2B
γ-Tubulin
GFP-DENND2B
γ-Tubulin
P
D
MC
B
DENNN2B
γ-Tubulin
Fluorescence intensity
300
200
100
0
0
20
40
Distance (pixel)
C
GFP-DENND2B/
CEP164
GFP-DENND2B
CEP164
GFP-DENND2B
CEP164
P
D
MC
D
DENNN2B
CEP164
Fluorescence intensity
300
200
100
0
0
10
20
30
Distance (pixel)
E
DENND2B/
Ac-tubulin
DENND2B
Ac-tubulin

Figure 3: DENND2B localizes at the proximal end of the mother centriole.

(A) A549 cells with GFP-DENND2B were starved and then stained with γ-tubulin antibody to mark the basal body. The nucleus and cell periphery are outlined. Scale bars, 20 and 3 μm for low- and high-magnification images, respectively. (B) Intensity profiles along the straight blue line from the inset image in (A). (C) A549 cells with GFP-DENND2B were starved and then stained with CEP164 antibody to reveal the distal end of the mother centriole. The nucleus and cell periphery are outlined. Scale bars, 20 and 2.7 μm for low- and high-magnification images, respectively. The yellow arrows show localization of DENND2B proximal to the CEP164 staining. (D) Intensity profiles along the straight blue line from the inset image in (C). (E) A549 cells with GFP-DENND2B were starved and then stained with Ac-tubulin antibody to reveal primary cilia. The nucleus and cell periphery are outlined. Scale bars, 20 and 3.5 μm for low- and high-magnification images, respectively. The yellow arrows show localization of DENND2B at the base of primary cilia staining. For schematic representations of the mother centriole, “P,” proximal end of the centriole; “D,” distal end of the centriole; and “MC,” mother centriole.

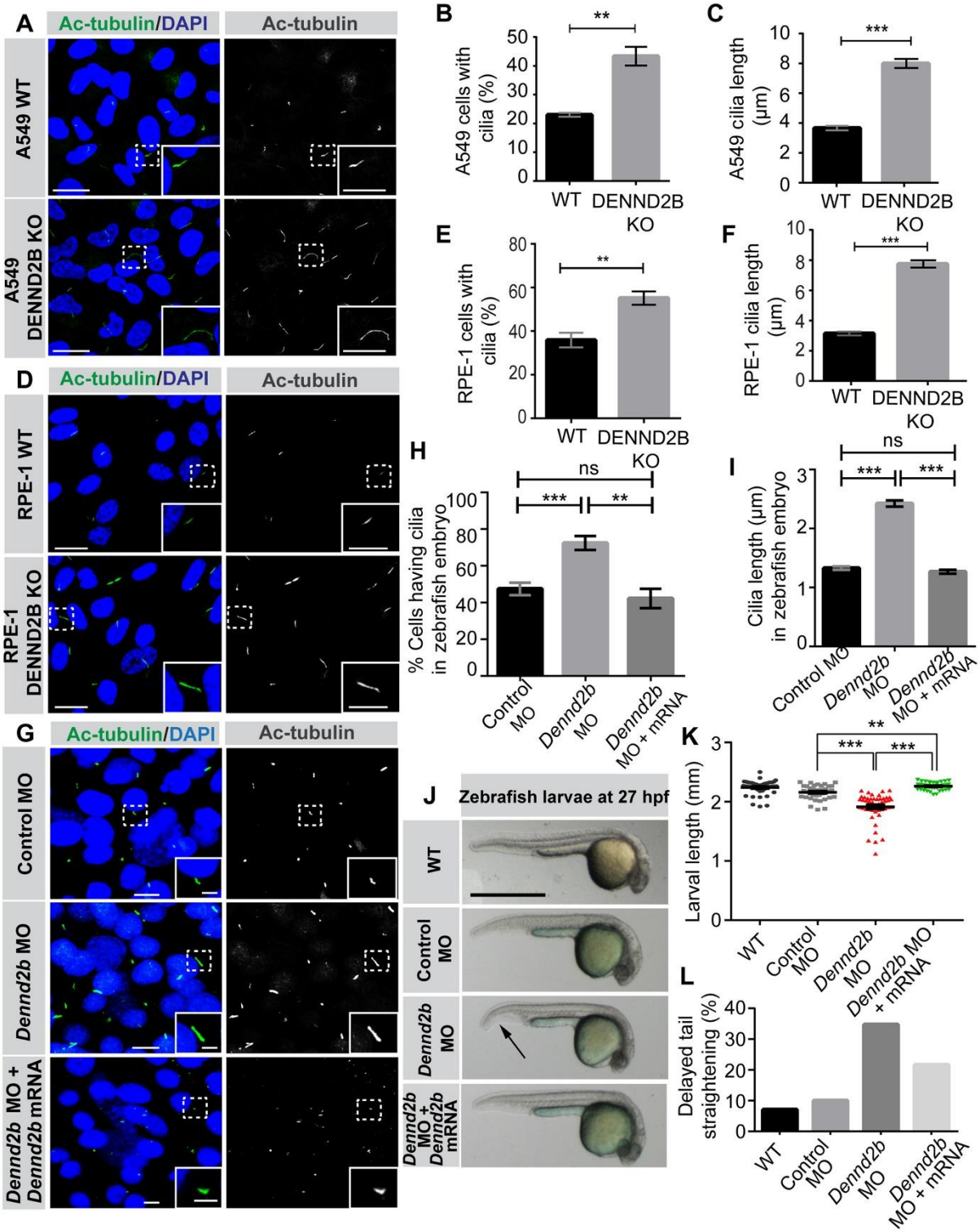
A
Ac-tubulin/DAPI
Ac-tubulin
A549 WT
A549 DENND2B KO
B
A549 cells with cilia (%)
WT
DENND2B KO
C
A549 cilia length (μm)
D
RPE-1 WT
RPE-1 DENND2B KO
E
RPE-1 cells with cilia (%)
F
RPE-1 cilia length (μm)
G
Control MO
Dennd2b MO
Dennd2b MO + Dennd2b mRNA
H
% Cells having cilia in zebrafish embryo
ns
Control MO
Dennd2b MO
Dennd2b MO + mRNA
I
Cilia length (μm) in zebrafish embryo
J
Zebrafish larvae at 27 hpf
WT
Control MO
Dennd2b MO
Dennd2b MO + Dennd2b mRNA
K
Larval length (mm)
L
Delayed tail straightening (%)

Figure 4: Loss of DENND2B enhances primary cilia formation and cilia length.

(A) Serum-starved A549 WT and DENND2B KO cells were fixed and stained with DAPI and Ac-tubulin antibody. Scale bars, 40 and 10 μm for the low- and high-magnification images, respectively. (B and C) Quantification of experiments as in (A); Mann-Whitney U test [>250 cells for (B) and 50 cells for (C)]. (D) Experiments were performed exactly as (A), except in RPE-1 cells. (E) Quantification of experiment in (D); unpaired t test (>250 cells). (F) Quantification of experiment as in (D); Mann-Whitney U test (>50 cells). (G) Zebrafish embryos at eight-somite stage injected with control or DENND2B MO or co-injected with DENND2B MO + DENND2B mRNA were stained with DAPI and Ac-tubulin antibody. Scale bars, 5 and 1.8 μm for the low- and high-magnification images, respectively. (H) Quantification of experiment as in (G); unpaired t test (>500 cells). (I) Quantification of experiment as in (G); Mann-Whitney U test (140 cells). (J) Example images of larval zebrafish at 27 hours post-fertilization (hpf). (K) Quantification of larval length; Kruskal-Wallis test, with pairwise multiple comparison (n = 42 for WT; n = 40 for control MO; n = 46 for DENND2B MO; n = 37 for DENND2B MO + DENND2B mRNA). (L) Percentage of larvae displaying delayed tail straightening. Means ± SEM. **P < 0.01 and ***P < 0.001

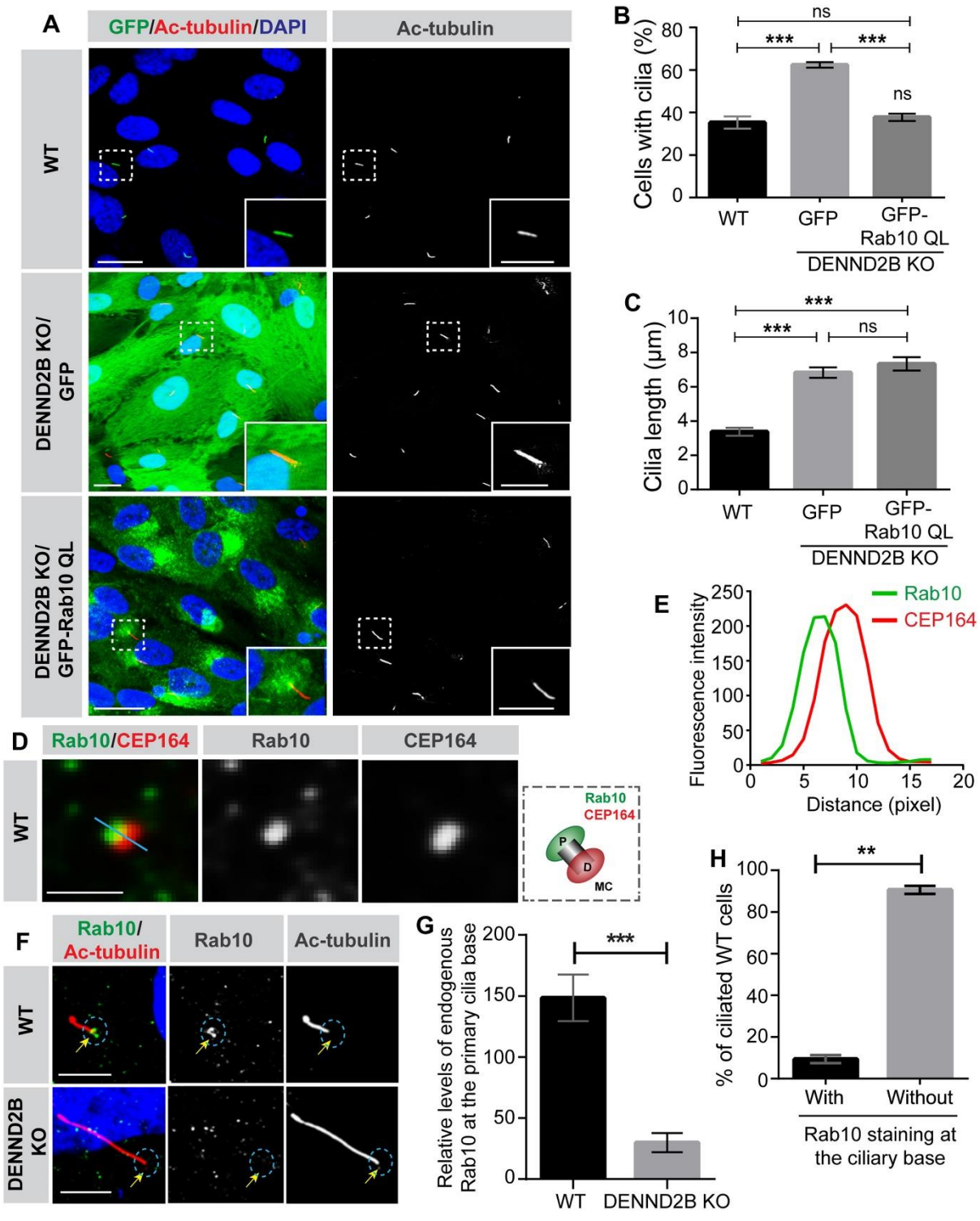
A
GFP/Ac-tubulin/DAPI
Ac-tubulin
WT
DENND2B KO/ GFP
DENND2B KO/ GFP-Rab10 QL
B
Cells with cilia (%)
ns
***
***
ns
WT
GFP
GFP-Rab10 QL
DENND2B KO
C
Cilia length (μm)
***
***
ns
WT
GFP
GFP-Rab10 QL
DENND2B KO
D
Rab10/CEP164
Rab10
CEP164
WT
Rab10
CEP164
P
D
MC
E
Rab10
CEP164
Fluorescence intensity
Distance (pixel)
F
Rab10/ Ac-tubulin
Rab10
Ac-tubulin
WT
DENND2B KO
G
Relative levels of endogenous Rab10 at the primary cilia base
***
WT
DENND2B KO
H
% of ciliated WT cells
**
With
Without
Rab10 staining at the ciliary base

Figure 5: Active Rab10 rescues defects in primary cilia formation but not length.

(A) RPE-1 cells expressing GFP or GFP-Rab10 QL (active mutant) were starved and stained with Ac-tubulin antibody to mark primary cilia. Scale bars, 20 and 10 μm for low- and high-magnification images, respectively. (B and C) Quantification of experiments as in (A); means ± SEM; one-way analysis of variance (ANOVA), with Tukey's posttest (***P < 0.001). n > 250 cells for (B) and 50 cells for (C). (D) Unstarved A459 WT cells were stained with Rab10 and CEP164 antibodies to reveal the mother centriole. Scale bar, 1.2 μm. (E) Intensity profiles along the straight blue line in (D). (F) Starved A549 cells were stained with Rab10 and Ac-tubulin antibodies for primary cilia (red). Scale bars, 5.5 μm. The yellow arrows in (F) represent the base of cilia (stained with anti–Ac-tubulin antibody). (G) Quantification of experiments as in (F). Means ± SEM; unpaired t test (***P < 0.001; n = 5). (H) Quantification of experiments as in (F); means ± SEM; Mann-Whitney U test (**P < 0.01; n > 50).

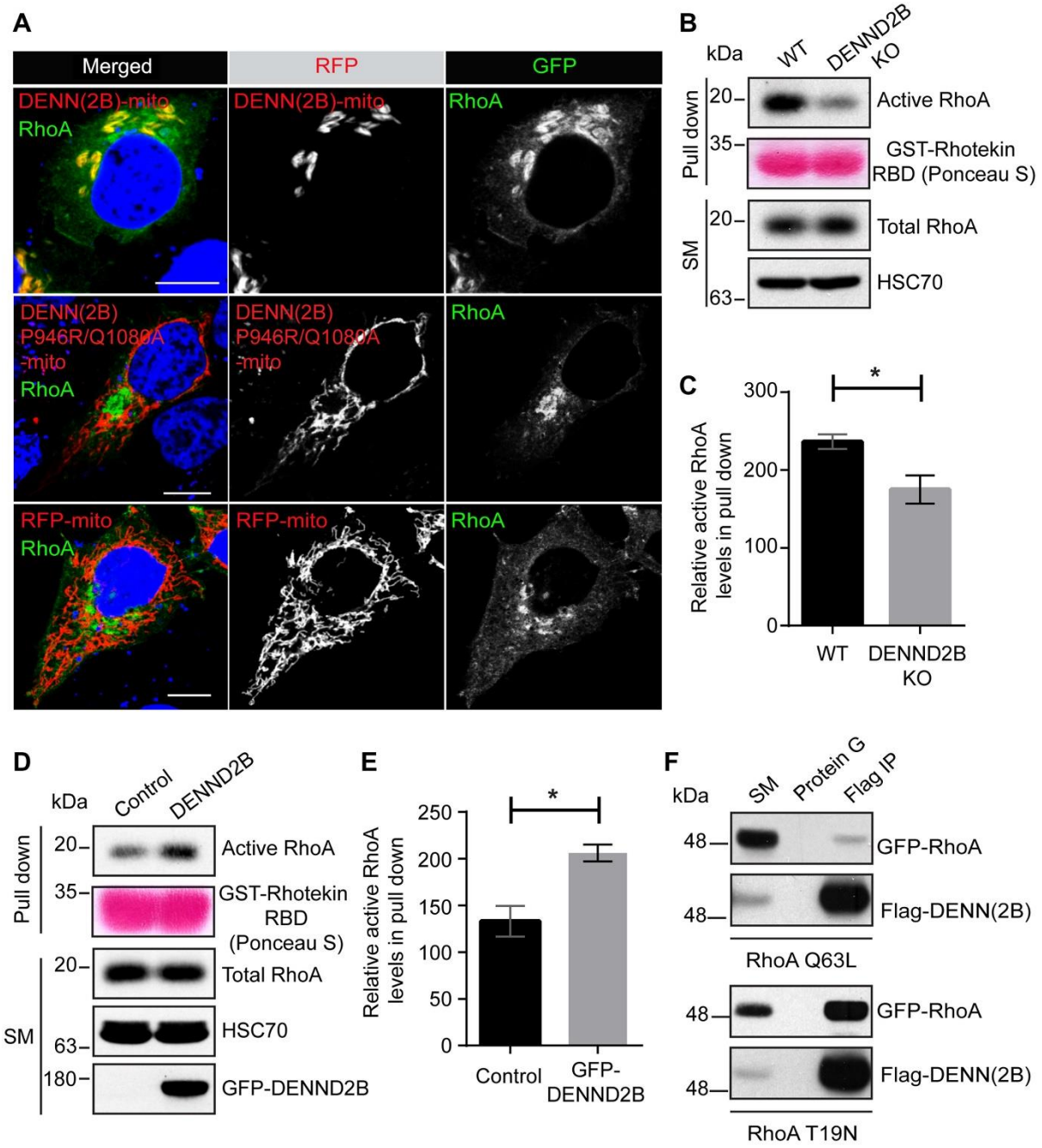
A
Merged
RFP
GFP
DENN(2B)-mito
RhoA
DENN(2B)-mito
RhoA
DENN(2B) P946R/Q1080A -mito
RhoA
DENN(2B) P946R/Q1080A -mito
RhoA
RFP-mito
RhoA
RFP-mito
RhoA
B
kDa
WT
DENND2B KO
Pull down
20
Active RhoA
35
GST-Rhotekin RBD (Ponceau S)
SM
20
Total RhoA
63
HSC70
C
Relative active RhoA levels in pull down
300
200
100
0
*
WT
DENND2B KO
D
kDa
Control
DENND2B
Pull down
20
Active RhoA
35
GST-Rhotekin RBD (Ponceau S)
SM
20
Total RhoA
63
HSC70
180
GFP-DENND2B
E
Relative active RhoA levels in pull down
250
200
150
100
50
0
*
Control
GFP-DENND2B
F
kDa
SM
Protein G
Flag IP
48
GFP-RhoA
48
Flag-DENN(2B)
RhoA Q63L
48
GFP-RhoA
48
Flag-DENN(2B)
RhoA T19N

Figure 6: The DENND2B DENN domain binds RhoA and functions as a RhoA GEF.

(A) HeLa cells cotransfected with GFP-RhoA WT and DENN(2B)-mito, DENN(2B)-mito with double mutations P946R/Q1080A predicted to inhibit GEF activity, or RFP-mito that were fixed and stained with DAPI (blue) to reveal nuclei. Scale bars, 10 μm. (B) WT or DENND2B KO A549 cell lysates were incubated with purified GST-Rhotekin RBD protein. Specifically bound proteins were detected by immunoblot with anti-RhoA antibody. The starting material (SM) was run in parallel to detect the total RhoA. Anti-HSC70 antibody was used as a loading control. (C) Quantification of experiment in (B); means ± SEM; unpaired t test (*P ≤ 0.05; n = 3). (D) HEK-293T cells were transfected with GFP-DENND2B. At 24 hours post-transfection, transfected or untransfected (control) cell lysates were incubated with purified GST-Rhotekin RBD. Specifically bound proteins were detected by immunoblot with anti-RhoA antibody or anti-GFP antibody recognizing DENND2B or anti-HSC70 antibody for loading control. (E) Quantification of experiment in (D); means ± SEM; unpaired t test (*P ≤ 0.05; n = 3). (F) HEK-293T cells were cotransfected with Flag-DENN(2B) and GFP-RhoA T19N or GFP-RhoA Q63L. At 24 hours post-transfection, cells were lysed and incubated with protein G–agarose alone (mock) or protein G–agarose with anti-Flag antibody (Flag IP). Specifically bound proteins were detected by immunoblot with anti-GFP antibody to detect active/inactive Rab10 or anti-Flag antibody recognizing DENN(2B).

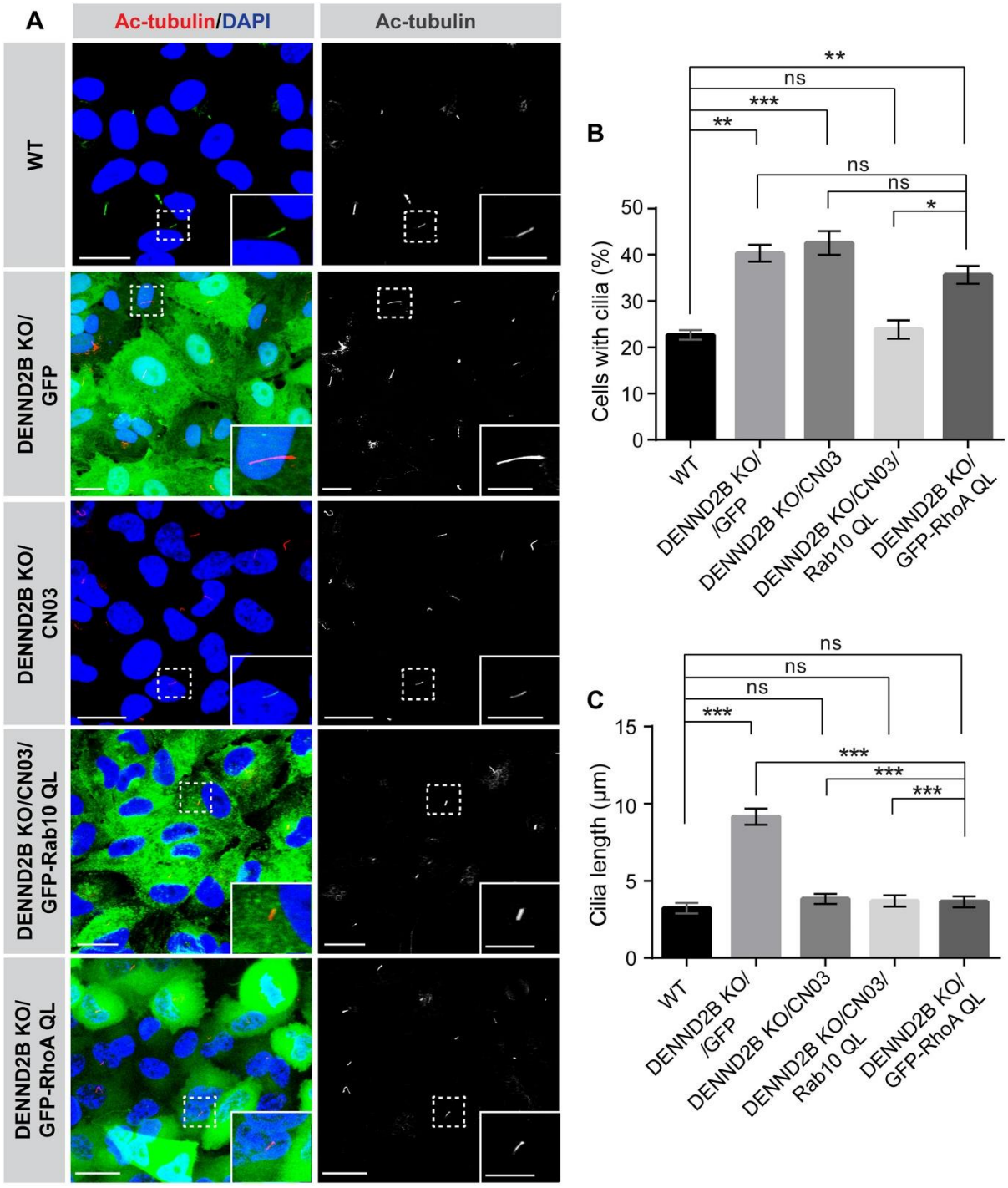
A
Ac-tubulin/DAPI
Ac-tubulin
WT
DENND2B KO/ GFP
DENND2B KO/ CN03
DENND2B KO/CN03/ GFP-Rab10 QL
DENND2B KO/ GFP-RhoA QL
B
Cells with cilia (%)
0
10
20
30
40
50
**
ns
***
**
ns
ns
*
WT
DENND2B KO/ /GFP
DENND2B KO/CN03
DENND2B KO/CN03/ Rab10 QL
DENND2B KO/ GFP-RhoA QL
C
Cilia length (µm)
0
5
10
15
ns
ns
ns
***
***
***
***
WT
DENND2B KO/ /GFP
DENND2B KO/CN03
DENND2B KO/CN03/ Rab10 QL
DENND2B KO/ GFP-RhoA QL

Figure 7: Overexpression of active RhoA mutant in DENND2B KO cells restores normal cilia length but not primary cilia formation.

(A) DENND2B KO A549 cells were transduced with lentivirus driving overexpression of either GFP alone, GFP-RhoA QL (active mutant), or GFP-Rab10 QL (active mutant). The cells were then treated or not treated with CN03 as indicated. All cells were then serum-starved for 24 hours and were then fixed and stained with DAPI to reveal nuclei and Ac-tubulin antibody for primary cilia (red). Scale bars, 20 μm for the low-magnification images and 10 μm for the higher-magnification insets. (B) Quantification of percentage of ciliated cells as shown in (A); means ± SEM; one-way ANOVA, with Tukey's posttest (***P ≤ 0.001, **P ≤ 0.01, and *P ≤ 0.05; n > 250 cells per condition). (C) Quantification of the ciliary length as shown in (A); means ± SEM; Kruskal-Wallis test, with pairwise multiple comparison posttest (***P ≤ 0.001; n > 20 cells per condition).

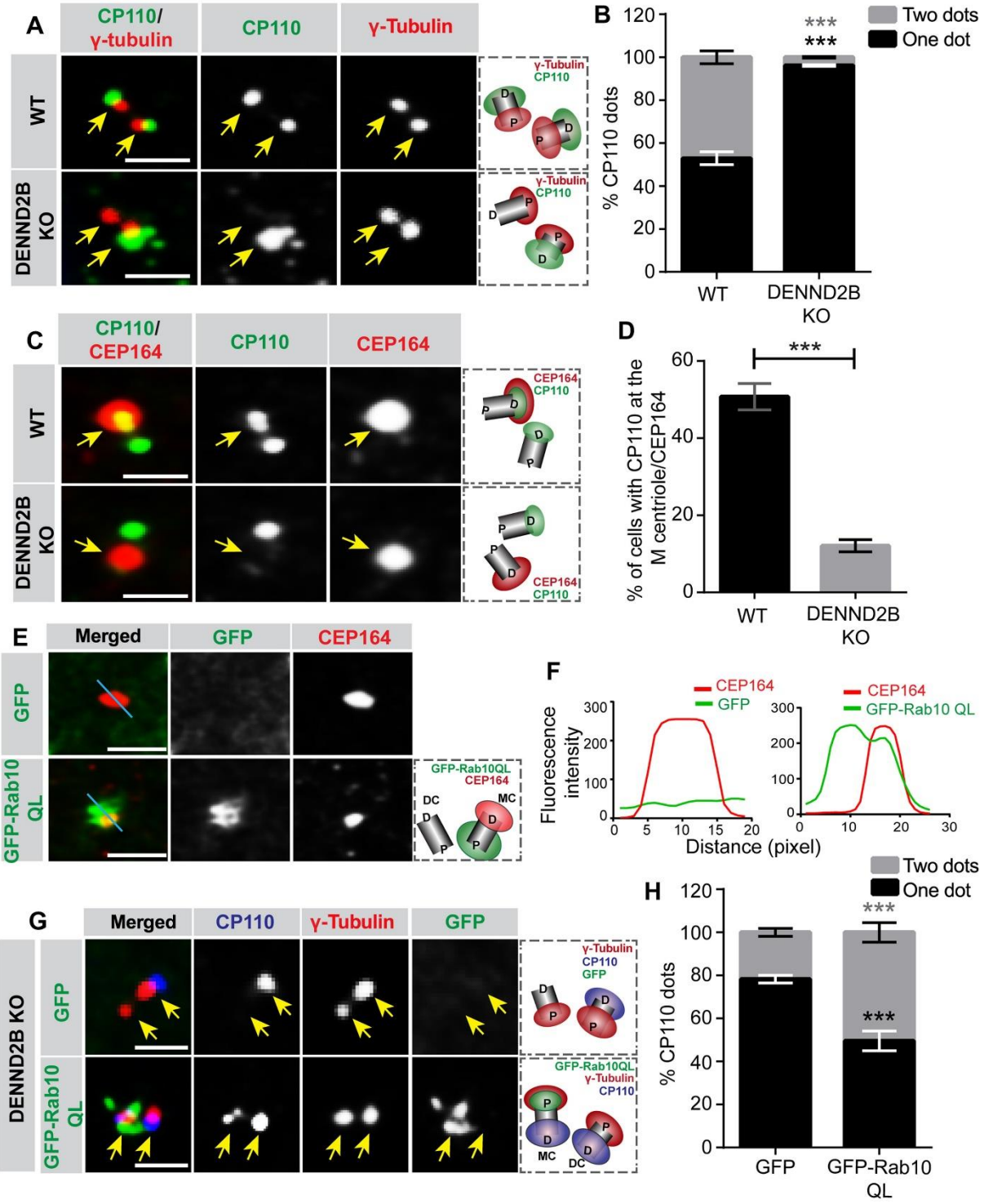
A
CP110/ γ-tubulin
CP110
γ-Tubulin
WT
DENND2B KO
γ-Tubulin CP110
B
Two dots
One dot
% CP110 dots
***
***
WT
DENND2B KO
C
CP110/ CEP164
CP110
CEP164
CEP164 CP110
D
% of cells with CP110 at the M centriole/CEP164
***
E
Merged
GFP
CEP164
GFP-Rab10 QL
GFP-Rab10QL CEP164
F
CEP164
GFP
GFP-Rab10 QL
Fluorescence intensity
Distance (pixel)
G
Merged
CP110
γ-Tubulin
GFP
DENND2B KO
γ-Tubulin CP110 GFP
GFP-Rab10QL γ-Tubulin CP110
H
Two dots
One dot
% CP110 dots
GFP
GFP-Rab10 QL

Figure 8: Inactivation of Rab10 impairs recruitment of CP110 to the mother centriole.

(A) A549 cells were starved and stained with CP110 and γ-tubulin antibodies. Scale bars, 1.57 μm (B) Quantification of experiments as in (A); means ± SEM; unpaired t test (***P ≤ 0.001; n > 70 cells per condition). (C) Cells as in (A) were stained with CP110 and CEP164 antibodies. Scale bars, 1.4 μm (D) Quantification of experiments as in (C); means ± SEM; unpaired t test (***P ≤ 0.001; n > 90 cells per condition). (E) A549 cells expressing GFP or GFP-Rab10 QL were starved and stained with CEP164 antibody for mother centriole. Scale bars, 2.10 μm. (F) Intensity profiles along the straight blue lines from the image in (E). (G) A549 cells expressing GFP or GFP-Rab10 QL were stained with CP110 and γ-tubulin antibodies for centrioles. Scale bars, 1.1 and 1.7 μm for GFP and GFP-Rab10 QL, respectively. (H) Quantification of experiments as in (G); means ± SEM; unpaired t test (***P ≤ 0.001; n > 45 cells per condition).

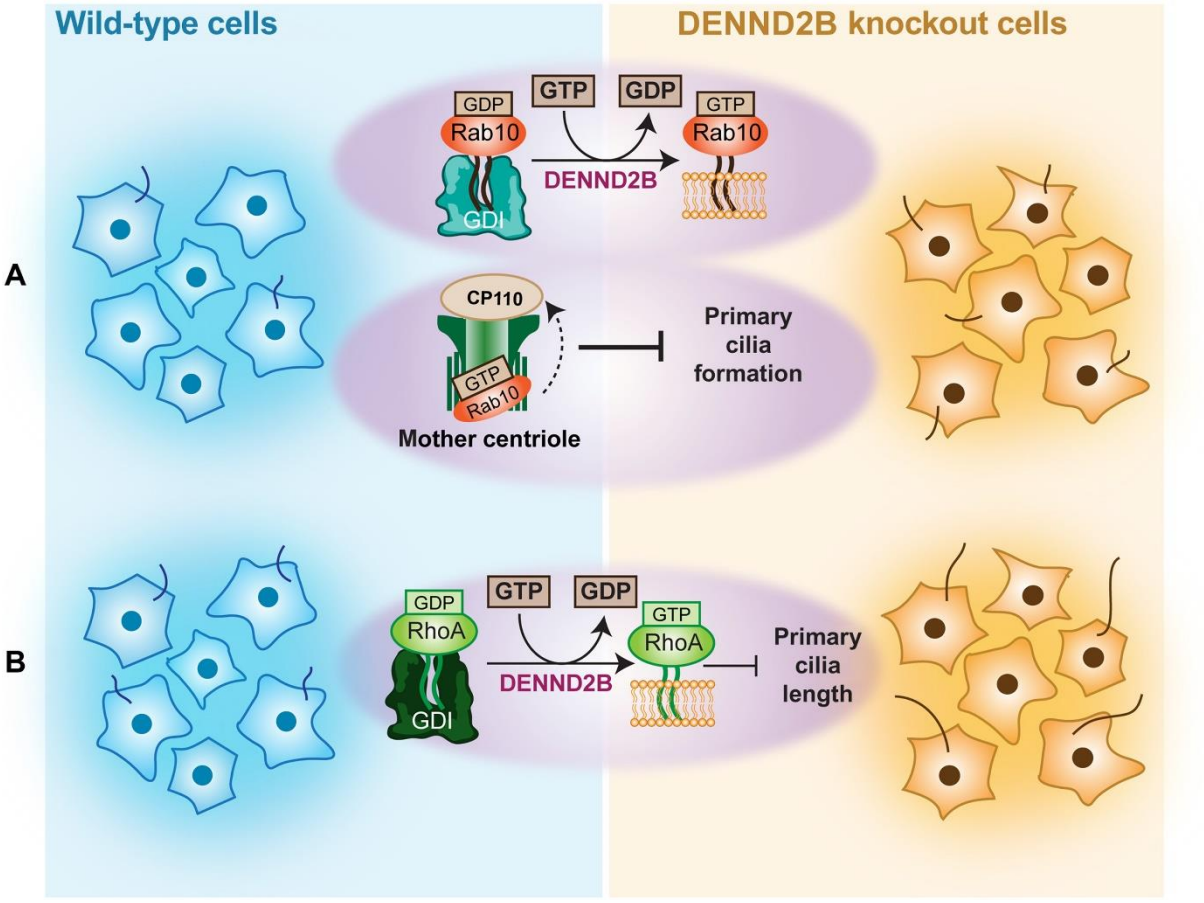

Figure 9: Model of DENND2B regulating primary cilia.

(A) Schematic representation of DENND2B regulating primary cilia via activation of Rab10. (B) DENND2B activating RhoA and controlling primary cilia length.

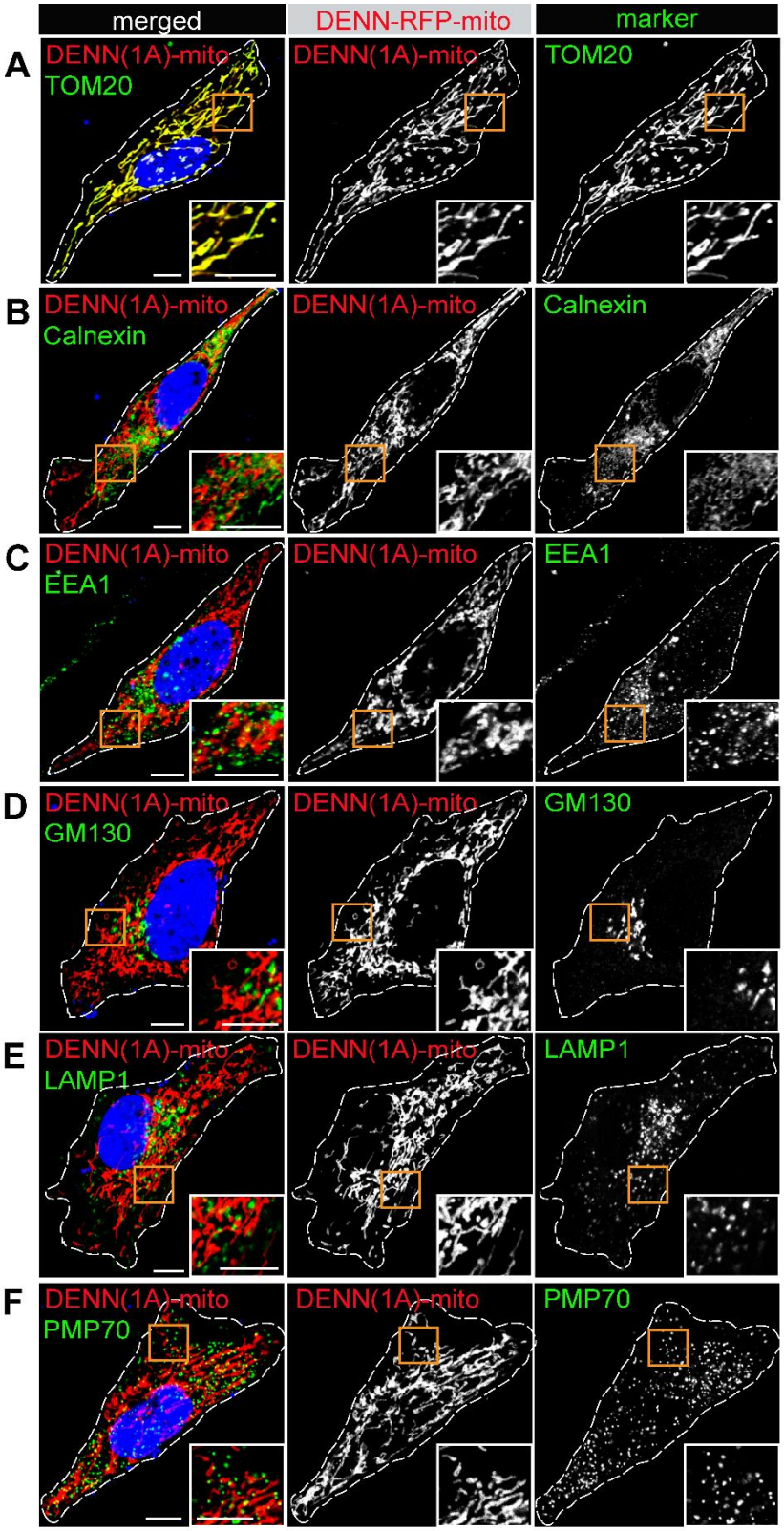

Supplementary figure 1: Mitochondrially targeted DENN domains specifically localize to mitochondria.

HeLa cells transfected with DENN(1A)-mito were fixed and stained with DAPI (blue) to reveal the nucleus and antibodies against organelle-specific proteins (A) TOM20 (mitochondria) (B) Calnexin (endoplasmic reticulum) (C) EEA1 (early endosomes) (D) GM130 (Golgi) (E) LAMP1 (lysosomess) (F) PMP70 (peroxisomes). Organelle-specific proteins were visualized by secondary antibody coupled to Alexa-488 (green). Scale bar = 8 µm.

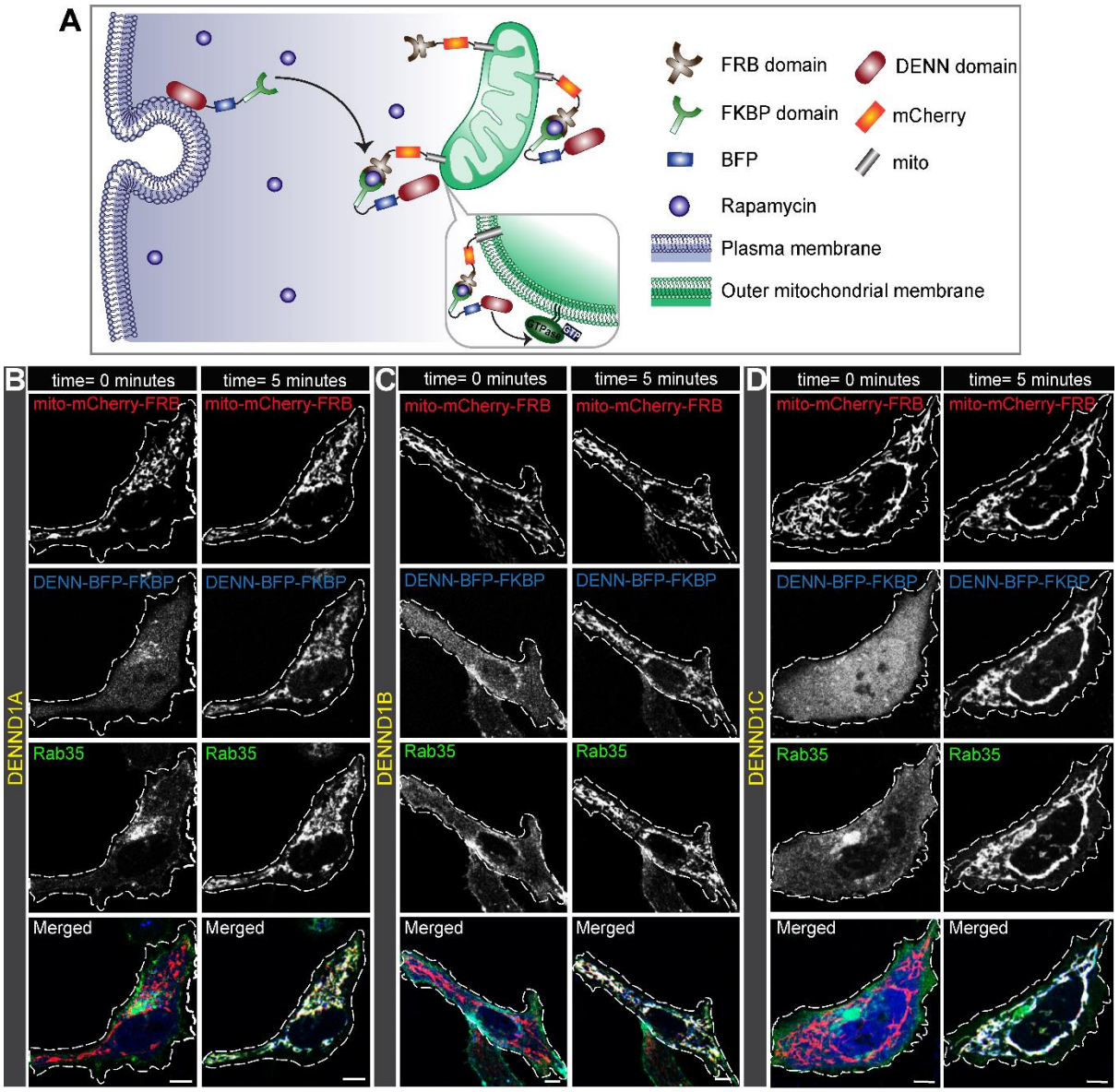

Supplementary figure 2: Time course of recruitment of Rab35 by DENND1 DENN domains.

(A) Schematic representation of rapamycin-induced relocalization of DENN domain proteins to the mitochondria. FKBP = FK506-binding protein domain; FRB = FKBP-rapamycin–binding domain. HeLa cells were transfected with **(B)** GFP-Rab35, mito-mCherry-FRB and DENN(1A)-BFP-FKBP, **(C)** GFP-Rab35, mito-mCherry-FRB, and

DENN(1B)-BFP-FKBP, **(D)** GFP-Rab35, mito-mCherry-FRB, and DENN(1C)-BFP-FKBP. For **B** through **D**, cells were imaged live with representative images at time=0 min (prior to rapamycin addition) and time=5 min (after rapamycin addition) are shown. Frames were captured every 8 sec. Scale bars = 10 μm.

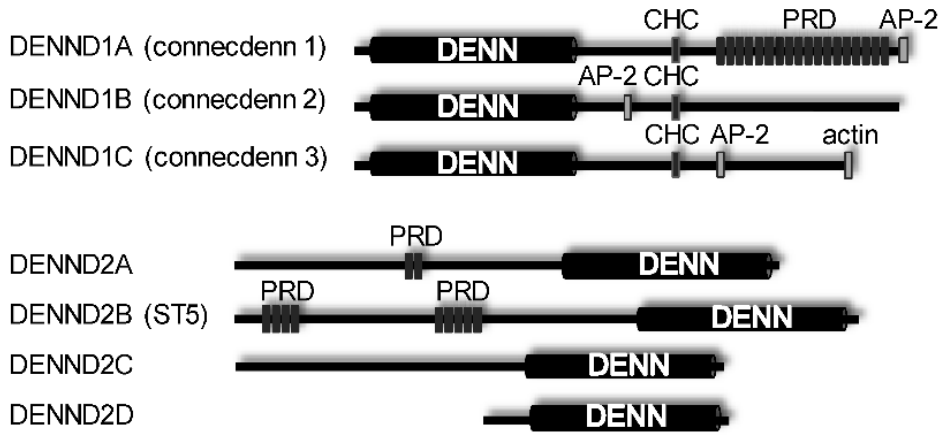

Supplementary figure 3: Schematics of domain models

Schematic of domain models of members of the DENND1/connecdenn and DENND2 families (adapted from (15)).

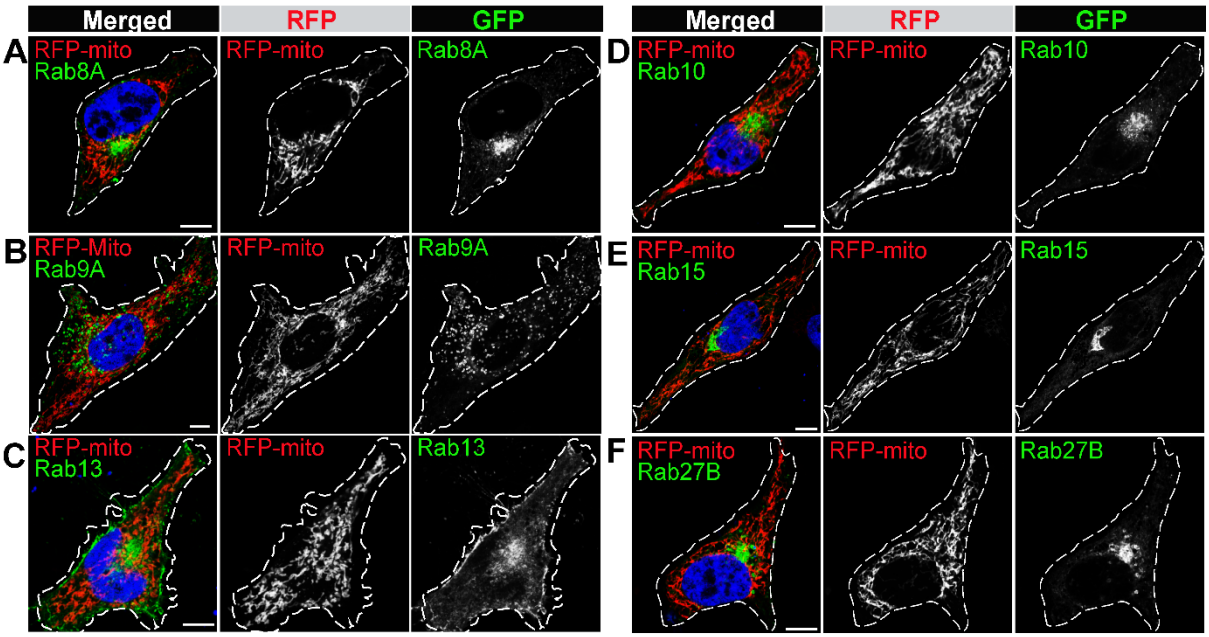

Supplementary figure 4: RFP-mito alone does not recruit GFP-Rabs to mitochondria.

(A-F) HeLa cells co-transfected with RFP-mito and **(A)** GFP-Rab8A or **(B)** GFP-Rab9A or **(C)** GFP-Rab13 or **(D)** GFP-Rab10 or **(E)** GFP-Rab15 or **(F)** GFP-Rab27B were fixed and stained with DAPI (blue) to reveal nuclei. Scale bar = 8 µm.

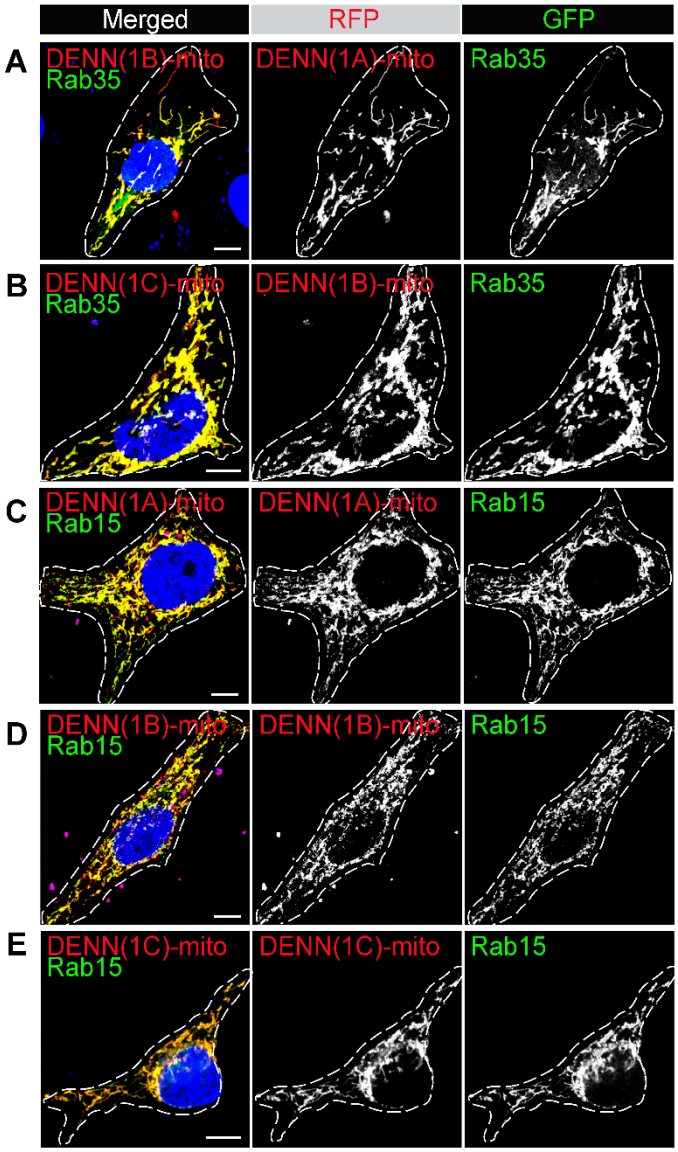

Supplementary figure 5: High-content screening results of DENN domain of DENND1.

(A-B) HeLa cells co-transfected with GFP-Rab35 and **(A)** DENN(1B)-mito or **(B)** DENN(1C)-mito were fixed and stained with DAPI (blue) to reveal nuclei. **(C-E)** HeLa cells co-transfected with GFP-Rab15 and **(C)** DENN(1A)-mito or **(D)** DENN(1B)-mito or **(E)** DENN(1C)-mito were fixed and stained with DAPI to reveal nucleus. Scale bar = 8 µm.

DENND1A									
Rab1A	Rab1B	Rab2A	Rab2B	Rab3A	Rab3B	Rab3C	Rab3D	Rab4A	Rab4B
Rab5A	Rab5B	Rab5C	Rab6A	Rab6B	Rab6C	Rab7A	Rab7B	Rab8A	Rab8B
Rab9A	Rab9B	Rab10	Rab11A	Rab11B	Rab12	Rab13	Rab14	Rab15	Rab17
Rab18	Rab19	Rab20	Rab21	Rab22A	Rab22B	Rab23	Rab24	Rab24	Rab25
Rab27A	Rab27B	Rab28	Rab29	Rab30	Rab32	Rab33A	Rab33B	Rab34	Rab35
Rab36	Rab37	Rab38	Rab39A	Rab39B	Rab40A	Rab40B	Rab40C	Rab42	Rab43

DENND1B									
Rab1A	Rab1B	Rab2A	Rab2B	Rab3A	Rab3B	Rab3C	Rab3D	Rab4A	Rab4B
Rab5A	Rab5B	Rab5C	Rab6A	Rab6B	Rab6C	Rab7A	Rab7B	Rab8A	Rab8B
Rab9A	Rab9B	Rab10	Rab11A	Rab11B	Rab12	Rab13	Rab14	Rab15	Rab17
Rab18	Rab19	Rab20	Rab21	Rab22A	Rab22B	Rab23	Rab24	Rab24	Rab25
Rab27A	Rab27B	Rab28	Rab29	Rab30	Rab32	Rab33A	Rab33B	Rab34	Rab35
Rab36	Rab37	Rab38	Rab39A	Rab39B	Rab40A	Rab40B	Rab40C	Rab42	Rab43

DENND1C									
Rab1A	Rab1B	Rab2A	Rab2B	Rab3A	Rab3B	Rab3C	Rab3D	Rab4A	Rab4B
Rab5A	Rab5B	Rab5C	Rab6A	Rab6B	Rab6C	Rab7A	Rab7B	Rab8A	Rab8B
Rab9A	Rab9B	Rab10	Rab11A	Rab11B	Rab12	Rab13	Rab14	Rab15	Rab17
Rab18	Rab19	Rab20	Rab21	Rab22A	Rab22B	Rab23	Rab24	Rab24	Rab25
Rab27A	Rab27B	Rab28	Rab29	Rab30	Rab32	Rab33A	Rab33B	Rab34	Rab35
Rab36	Rab37	Rab38	Rab39A	Rab39B	Rab40A	Rab40B	Rab40C	Rab42	Rab43

Supplementary figure 6: Screening results of DENND1 family.

Mitochondrially targeted DENN(1A/B/C) domain constructs were cotransfected with individual GFP-Rab constructs in a 96-well imaging plate. 24 hours post-transfection, cells were imaged and compared with control images (RFP targeted to the

mitochondria and corresponding GFP-Rab) for colocalization. Boxes in green represent positive hits.

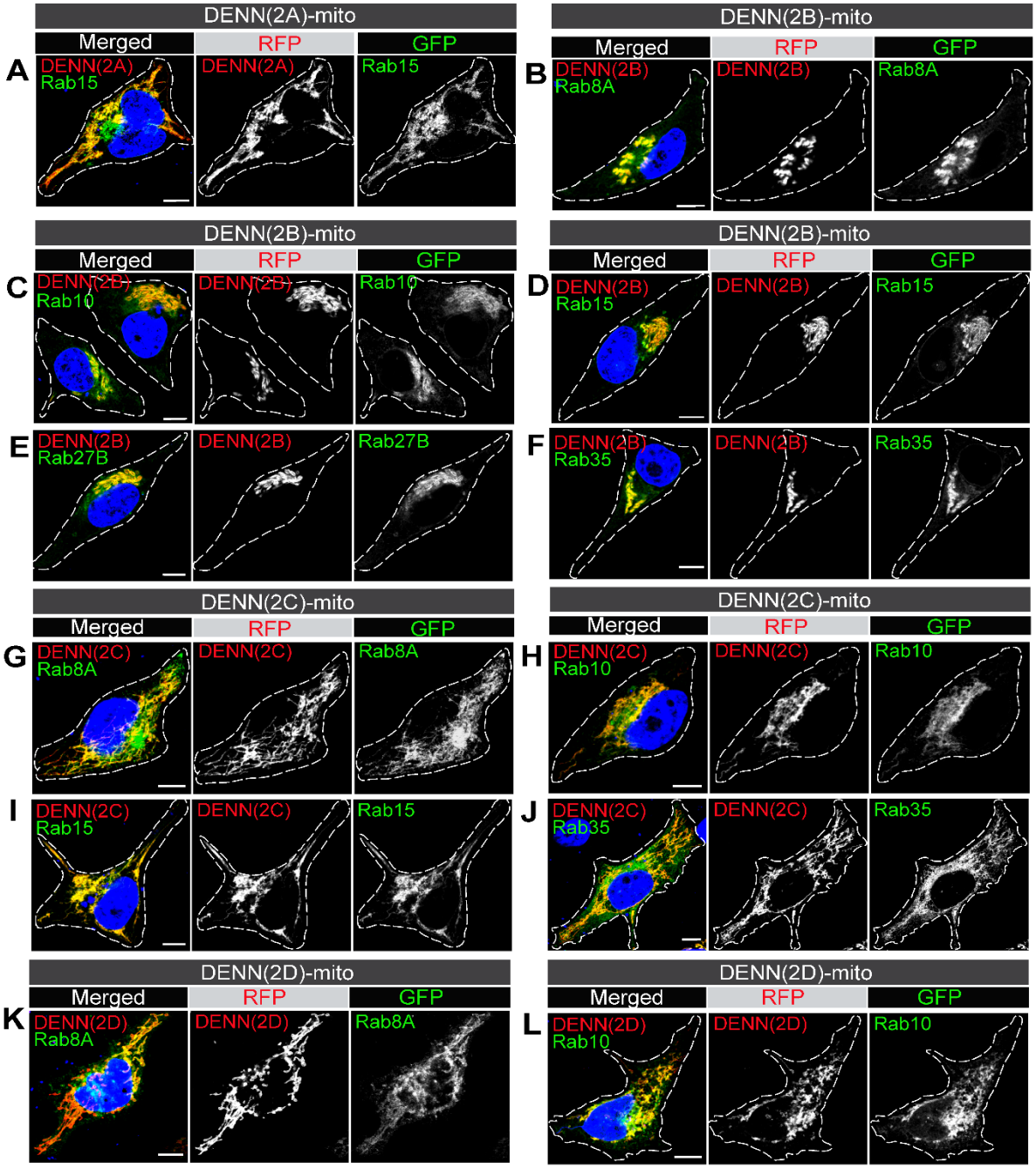

Supplementary figure 7: High-content screening results of DENN domain of DENND2.

(A) HeLa cells co-transfected with DENN(2A)-mito and GFP-Rab15 were fixed and stained with DAPI (blue) to reveal nuclei. **(B-F)** HeLa cells co-transfected with DENN(2B)-mito and **(B)** GFP-Rab8A or **(C)** GFP-Rab10 or **(D)** GFP-Rab15 or **(E)** GFP-Rab27B or **(F)** GFP-Rab35 were fixed and stained with DAPI (blue) to reveal

nuclei. **(G-J)** HeLa cells co-transfected with DENN(2C)-mito and **(G)** GFP-Rab8A or **(H)** GFP-Rab10 or **(I)** GFP-Rab15 or **(J)** GFP-Rab35 were fixed and stained with DAPI (blue) to reveal nuclei. **(K-L)** HeLa cells co-transfected with DENN(2D)-mito and **(K)** GFP-Rab8A or **(L)** GFP-Rab10 were fixed and stained with DAPI (blue) to reveal nuclei. Scale bar = 8 µm.

DENND2A									
Rab1A	Rab1B	Rab2A	Rab2B	Rab3A	Rab3B	Rab3C	Rab3D	Rab4A	Rab4B
Rab5A	Rab5B	Rab5C	Rab6A	Rab6B	Rab6C	Rab7A	Rab7B	Rab8A	Rab8B
Rab9A	Rab9B	Rab10	Rab11A	Rab11B	Rab12	Rab13	Rab14	Rab15	Rab17
Rab18	Rab19	Rab20	Rab21	Rab22A	Rab22B	Rab23	Rab24	Rab24	Rab25
Rab27A	Rab27B	Rab28	Rab29	Rab30	Rab32	Rab33A	Rab33B	Rab34	Rab35
Rab36	Rab37	Rab38	Rab39A	Rab39B	Rab40A	Rab40B	Rab40C	Rab42	Rab43

DENND2B									
Rab1A	Rab1B	Rab2A	Rab2B	Rab3A	Rab3B	Rab3C	Rab3D	Rab4A	Rab4B
Rab5A	Rab5B	Rab5C	Rab6A	Rab6B	Rab6C	Rab7A	Rab7B	Rab8A	Rab8B
Rab9A	Rab9B	Rab10	Rab11A	Rab11B	Rab12	Rab13	Rab14	Rab15	Rab17
Rab18	Rab19	Rab20	Rab21	Rab22A	Rab22B	Rab23	Rab24	Rab24	Rab25
Rab27A	Rab27B	Rab28	Rab29	Rab30	Rab32	Rab33A	Rab33B	Rab34	Rab35
Rab36	Rab37	Rab38	Rab39A	Rab39B	Rab40A	Rab40B	Rab40C	Rab42	Rab43

DENND2C									
Rab1A	Rab1B	Rab2A	Rab2B	Rab3A	Rab3B	Rab3C	Rab3D	Rab4A	Rab4B
Rab5A	Rab5B	Rab5C	Rab6A	Rab6B	Rab6C	Rab7A	Rab7B	Rab8A	Rab8B
Rab9A	Rab9B	Rab10	Rab11A	Rab11B	Rab12	Rab13	Rab14	Rab15	Rab17
Rab18	Rab19	Rab20	Rab21	Rab22A	Rab22B	Rab23	Rab24	Rab24	Rab25
Rab27A	Rab27B	Rab28	Rab29	Rab30	Rab32	Rab33A	Rab33B	Rab34	Rab35
Rab36	Rab37	Rab38	Rab39A	Rab39B	Rab40A	Rab40B	Rab40C	Rab42	Rab43

DENND2D									
Rab1A	Rab1B	Rab2A	Rab2B	Rab3A	Rab3B	Rab3C	Rab3D	Rab4A	Rab4B
Rab5A	Rab5B	Rab5C	Rab6A	Rab6B	Rab6C	Rab7A	Rab7B	Rab8A	Rab8B
Rab9A	Rab9B	Rab10	Rab11A	Rab11B	Rab12	Rab13	Rab14	Rab15	Rab17
Rab18	Rab19	Rab20	Rab21	Rab22A	Rab22B	Rab23	Rab24	Rab24	Rab25
Rab27A	Rab27B	Rab28	Rab29	Rab30	Rab32	Rab33A	Rab33B	Rab34	Rab35
Rab36	Rab37	Rab38	Rab39A	Rab39B	Rab40A	Rab40B	Rab40C	Rab42	Rab43

Supplementary figure 8: Screening results of DENND2 family.

Mitochondrially targeted DENN(2A/B/C/D) domain constructs were cotransfected with individual GFP-Rab constructs in a 96-well imaging plate. 24 hours post-transfection, cells were imaged and compared with control images (RFP targeted to the mitochondria and corresponding GFP-Rab) for colocalization. Boxes in green represent positive hits.

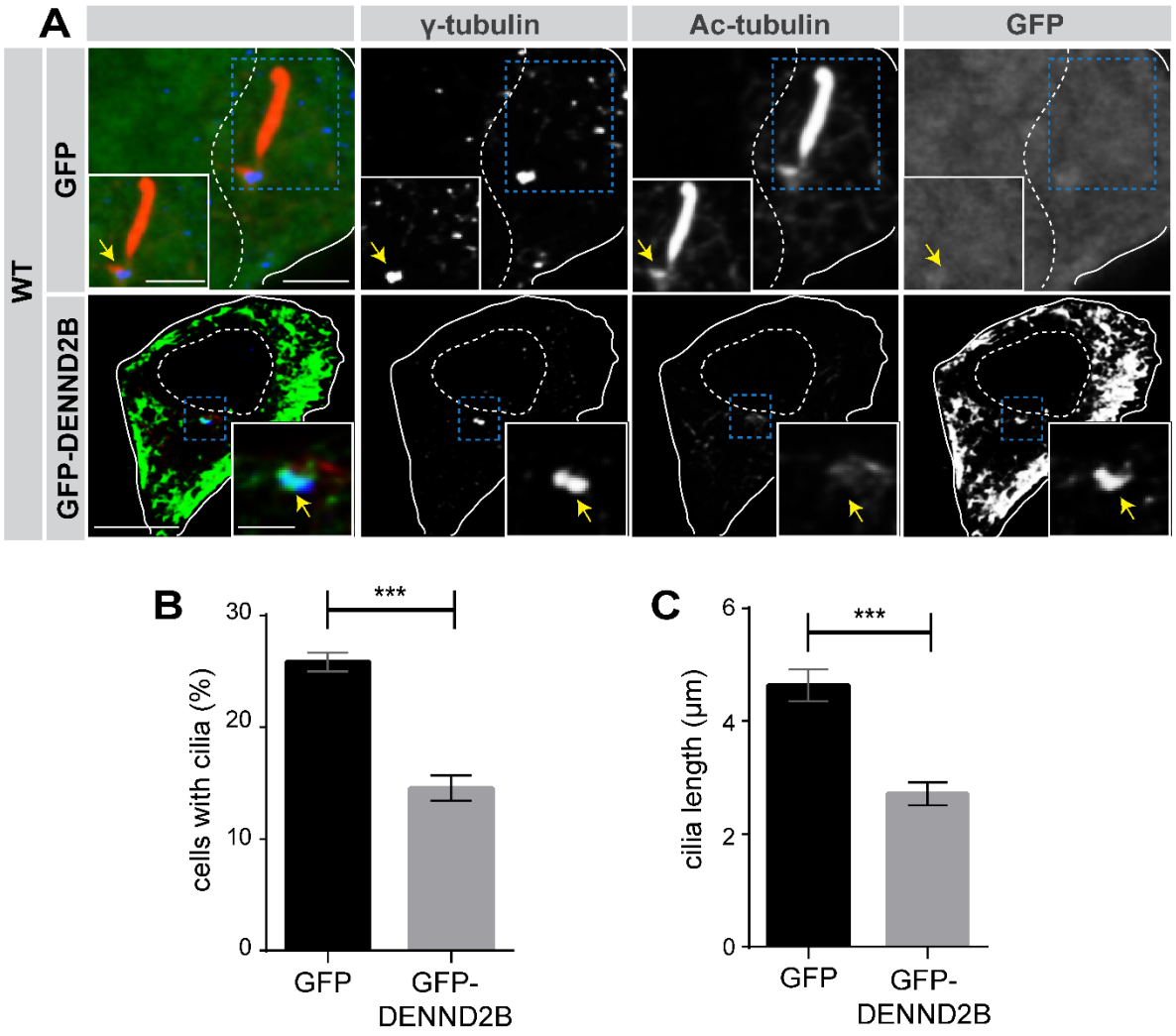

Supplementary figure 9: Overexpression of DENND2B suppresses primary cilia formation and ciliary length.

(A) A549 WT cells were either transfected with GFP or GFP-DENND2B construct and serum-starved for 24 h. Cells were then fixed and stained with γ-tubulin antibody to reveal the basal body and Ac-tubulin antibody for primary cilia. Scale bar = 2.5 μm for both the low and high -magnification images for GFP panel. Scale bars = 10 μm for the low-magnification images and 3.5 μm and 2.25 μm for the higher magnification insets for GFP-DENND2B panel. **(B)** graphical representation of quantification of the percentage of ciliated cells shown in **A**; mean ± SEM; unpaired t-test (***, $P < 0.001$;

>100 cells per condition). **(C)** Quantification of the length of ciliated cells shown in **A**; mean ± SEM; unpaired t-test (***, P < 0.001; >25 cells per condition).

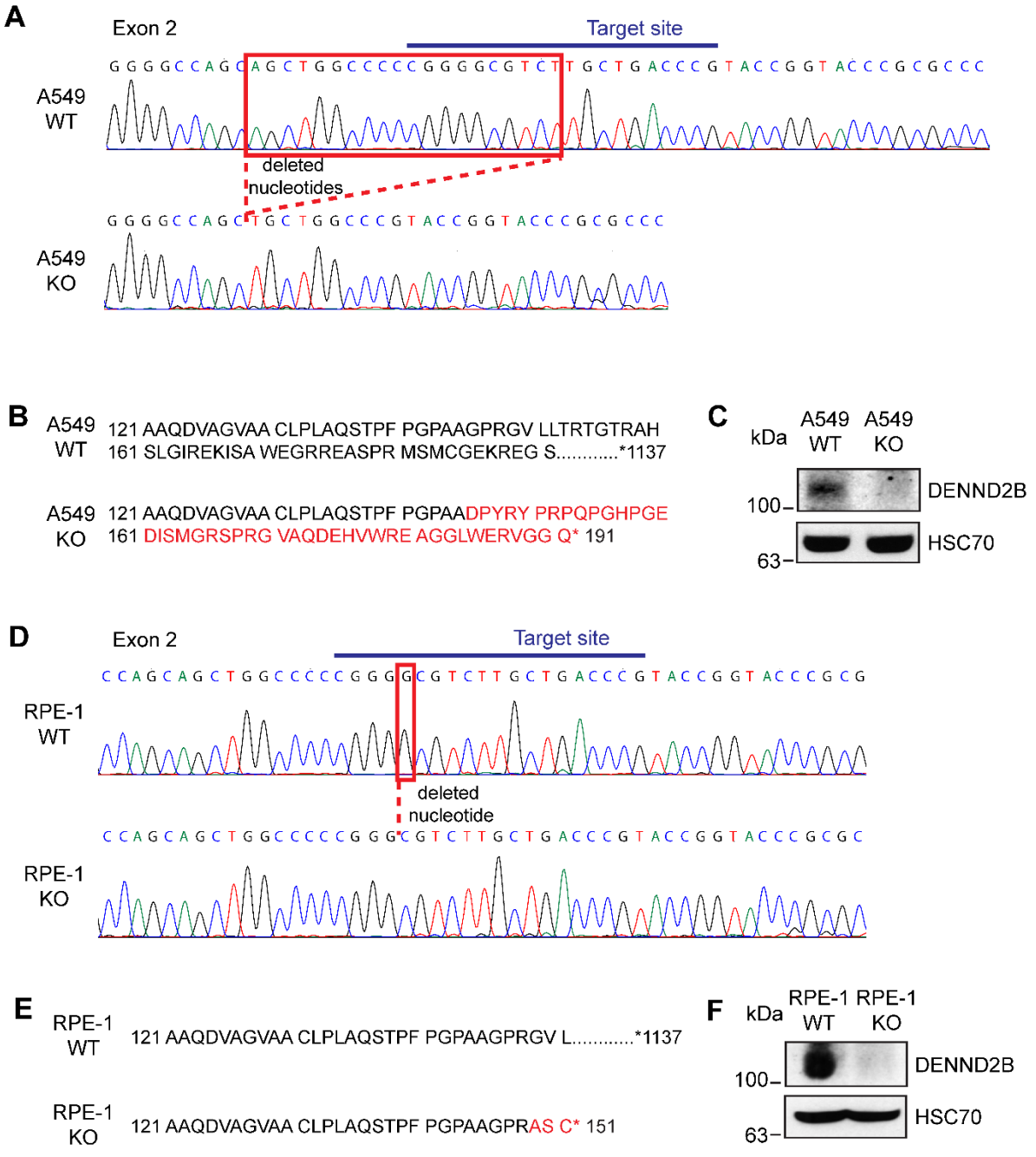

Supplementary figure 10: Generation of DENND2B KO cells.

DENND2B CRISPR target sites were designed in exon 2 of the DENND2B gene and screenings for CRISPR/Cas9-induced deletions of nucleotides were performed and selected further for maintenance. Genotype was analyzed using sequencing chromatograms of PCR-amplified DENND2B region, containing the target site. **(A)** DENND2B wild-type (WT) and KO A549 chromatogram sequencing results showing

deletion of 20 nucleotides. **(B)** Impact of CRISPR deletion in the A549 cell on the protein sequence. **(C)** Immunoblot showing loss of DENND2B protein in the A549 KO cells. Immunoblot probed with anti-DENND2B and anti-HSC70 antibody. A 7.5% polyacrylamide gel was used to resolve the band corresponding to DENND2B. **(D)** DENND2B wild-type (WT) and KO RPE-1 chromatogram sequencing results showing deletion of 1 nucleotide. **(E)** Impact of CRISPR deletion in the RPE-1 cell on the protein sequence. **(F)** Immunoblot showing loss of DENND2B protein in the RPE-1 KO cells. Immunoblot probed with anti-DENND2B and anti-HSC70 antibody. A 7.5% polyacrylamide gel was used to resolve the band corresponding to DENND2B.

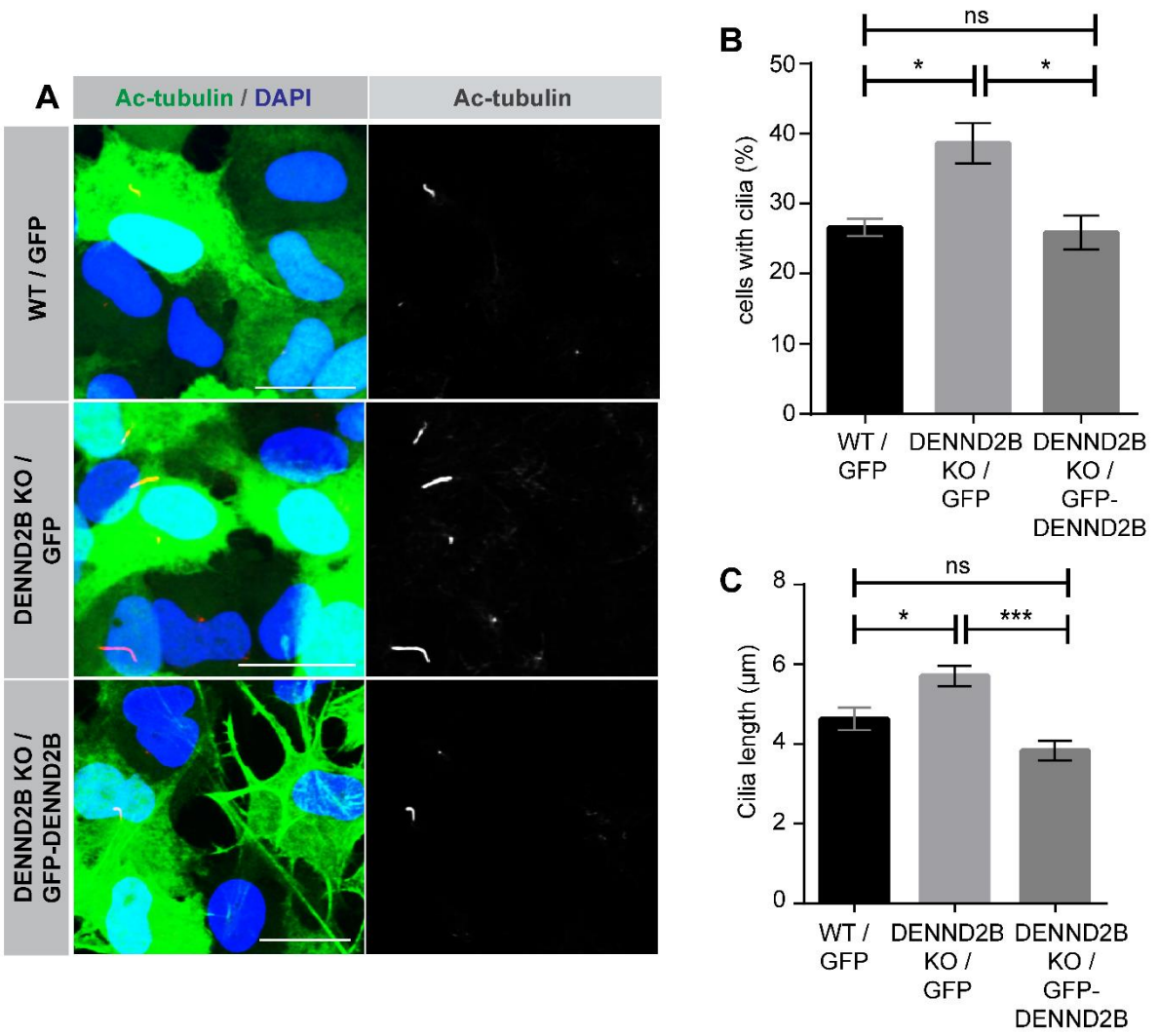

Supplementary figure 11: Overexpression of GFP-DENND2B rescues defects in cilia formation and ciliary length.

(A) WT or DENND2B KO A549 cells expressing GFP or GFP-DENND2B were serum-starved for 24 h. Cells were then fixed and stained with Ac-tubulin antibody for primary cilia. Scale bar = 20 µm. **(B)** graphical representation of quantification of the percentage of ciliated cells shown in **A**; mean ± SEM; one-way ANOVA, with Tukey's post-test (***, $P < 0.001$; >100 cells per condition). **(C)** Quantification of the length of ciliated cells shown in **A**; mean ± SEM; one-way ANOVA, with Tukey's post-test (***, $P < 0.001$; >25 cells per condition).

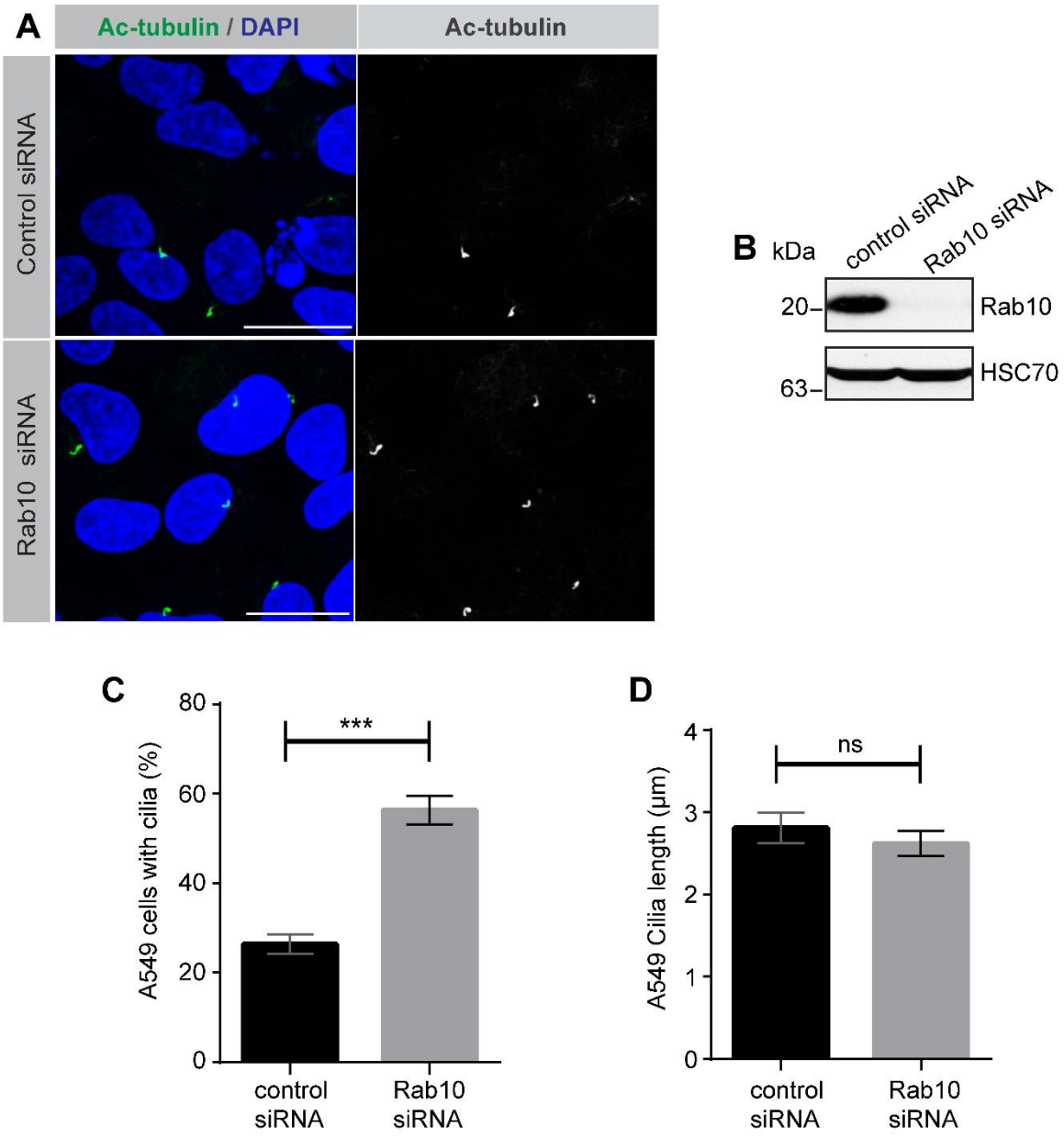

Supplementary figure 12: Depletion of Rab10 only enhances cilia formation.

(A) A549 cells were transfected with control siRNA or with an siRNA to selectively knockdown the expression of Rab10 and serum starved for 24 h post 48 h of siRNA treatment. Cells were then fixed and stained with Ac-tubulin antibody for primary cilia. Scale bar = 20 µm. **(B)** Immunoblot showing the level of Rab10 knockdown performed in **A**. Immunoblot probed with anti-Rab10 and anti-HSC70 antibody. **(C)** graphical

representation of quantification of the percentage of ciliated cells shown in **A**; mean ± SEM; unpaired t-test (***, P < 0.001; >230 cells per condition). **(D)** Quantification of the length of ciliated cells shown in **A**; mean ± SEM; unpaired t-test (ns, not significant; >45 cells per condition).

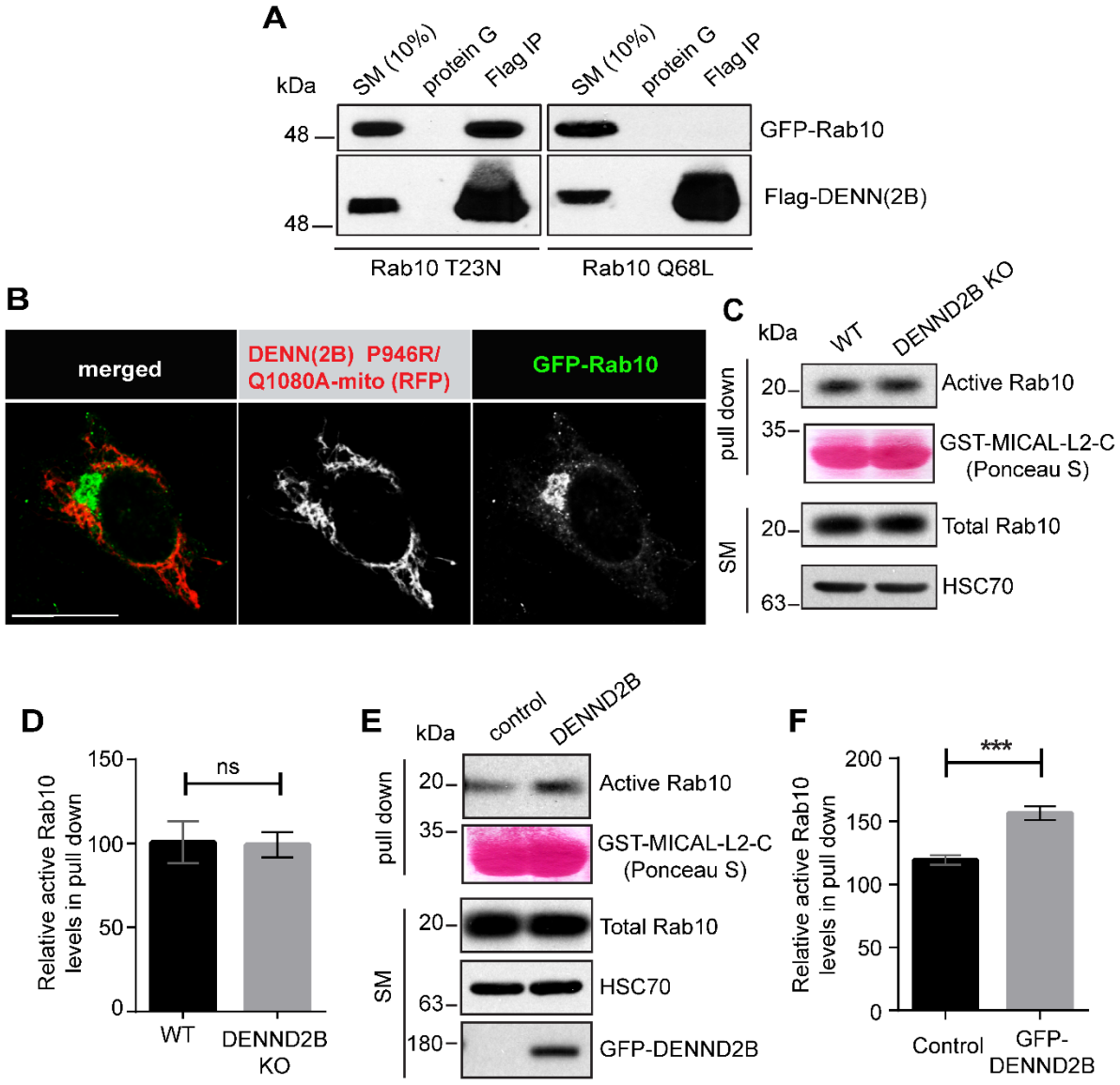

Supplementary figure 13: The DENND2B DENN domain binds Rab10 and functions as a GEF.

(A) HEK-293T cells were co-transfected with Flag-DENN(2B) and GFP-Rab10 T23N or GFP-Rab10 Q68L. At 24 h post-transfection, cells were lysed and incubated with protein G-agarose alone (mock) or protein G-agarose with anti-Flag antibody (Flag IP). Specifically bound proteins were detected by immunoblot with anti-GFP antibody to detect active/inactive Rab10 or anti-Flag antibody recognizing DENN(2B). **(B)** HeLa cells co-transfected with GFP-Rab10 WT and DENN(2B)-mito with double mutations

P946R/Q1080A were fixed and stained with DAPI (blue) to reveal nuclei. Scale bars = 20 μm. **(C)** A549 WT or DENND2B KO cell lysates were incubated with purified GST-MICAL-L2-C. Specifically bound proteins were detected by immunoblot with anti-Rab10 antibody and anti-HSC70 antibody for loading control. **(D)** Quantification of relative binding of active Rab10 with GST-MICAL-L2 C from experiments as in **C**; mean ± SEM; unpaired t-test (ns, not significant; n = 3). **(E)** HEK-293T cells were transfected with GFP-DENND2B. At 24 h post-transfection, transfected or untransfected (control) cell lysates were incubated with purified GST-MICAL-L2-C. Specifically bound proteins were detected by immunoblot with anti-Rab10 antibody or anti-GFP antibody recognizing DENND2B or anti-HSC70 antibody for loading control. **(F)** Quantification of relative binding of active Rab10 with GST-MICAL-L2 C from experiments as in **E**; mean ± SEM; unpaired t-test (***, $P < 0.001$; n = 4).

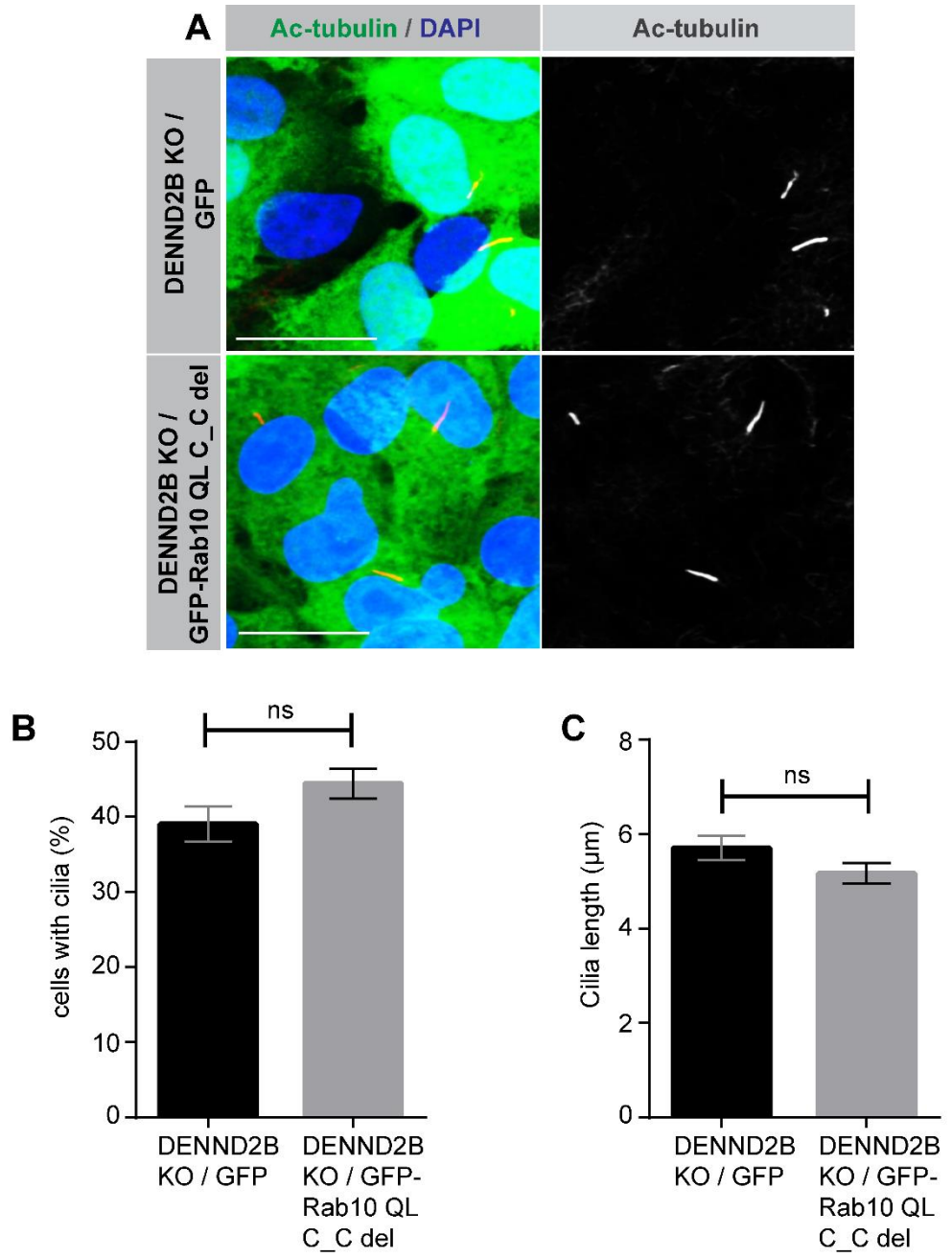

Supplementary figure 14: Overexpression of GFP-Rab10 QL C_C del (c-term deletion of cysteine residues) does not rescue defects in cilia formation and ciliary length.

(A) DENND2B KO A549 cells expressing GFP or GFP-Rab10 QL C_C del were serum-starved for 24 h. Cells were then fixed and stained with Ac-tubulin antibody for primary cilia. Scale bar = 20 µm. **(B)** graphical representation of quantification of the

percentage of ciliated cells shown in **A**; mean ± SEM; Mann-Whitney U test (ns, not significant; >100 cells per condition). **(C)** Quantification of the ciliary length shown in **A**; mean ± SEM; unpaired t-test (ns, not significant; >25 cells per condition).

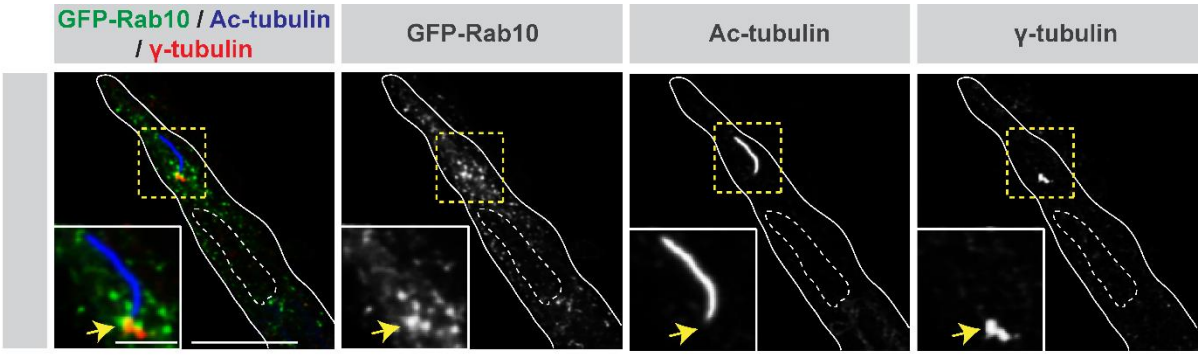

Supplementary figure 15: Rab10 localizes at the ciliary base.

A549 cells were transfected with GFP-Rab10 construct and serum-starved 24 hours post-transfection. Post starvation, cells were fixed and stained with γ-tubulin antibody for the basal body (red) and Ac-Tubulin for the primary cilia (blue). Dotted white lines represent the nucleus and solid white lines outline the cell periphery. Scale bars = 10 μm for the low-magnification images and 2.76 μm for the higher magnification insets (represented with blue dotted box). Yellow arrow indicates the ciliary base with Rab10 and γ-tubulin puncta.

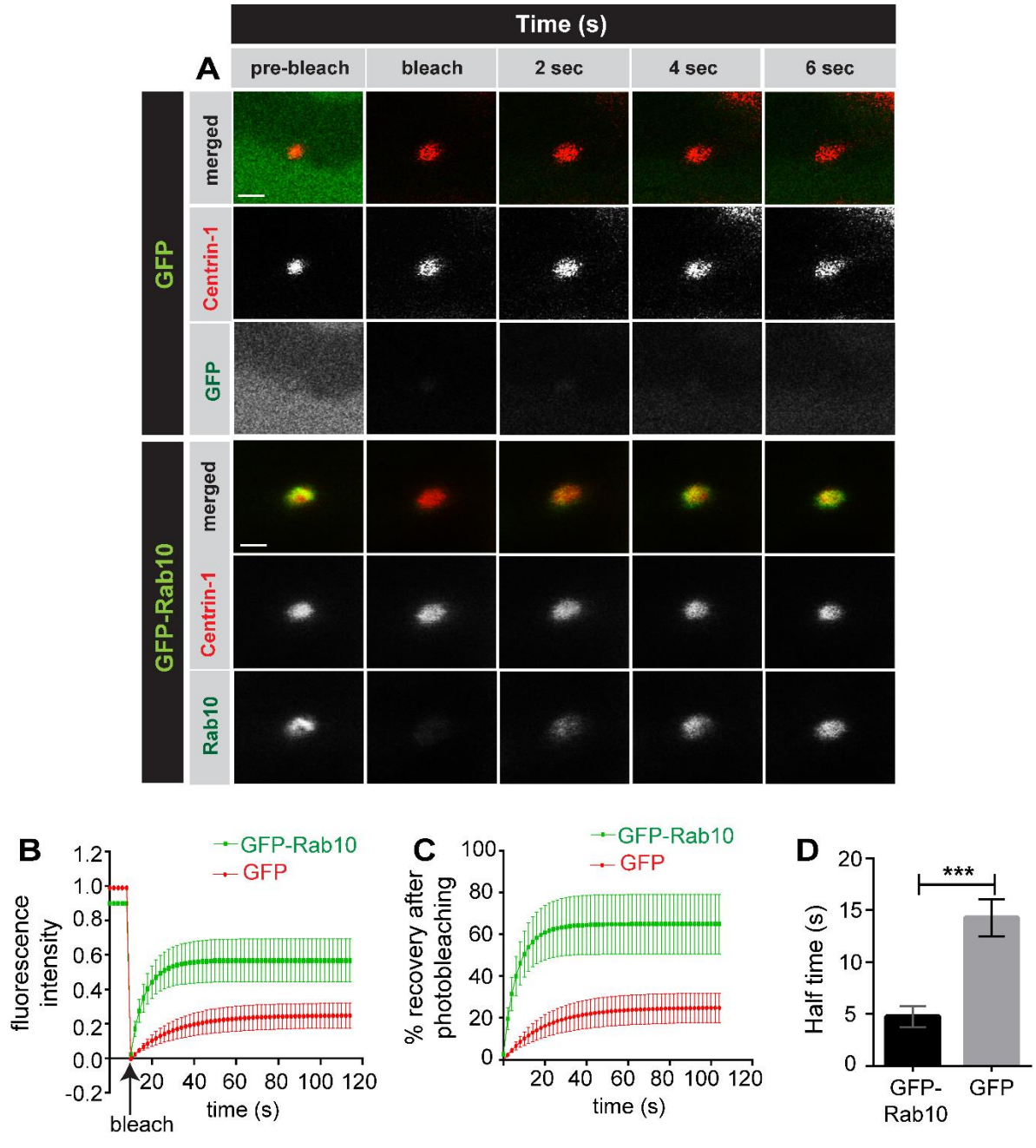

Supplementary figure 16: FRAP analysis of Rab10 dynamics at the centriole.

(A) A549 cells overexpressing dTomato-Centrin-1 and GFP or GFP-Rab10 were imaged at a region of interest encompassing the centriole (~2.3μm×2.3μm) and photobleached. Prebleach and postbleach time series images were collected at 2s intervals. Scale bars = 1 μm. **(B)** Average (SEM) fluorescence intensity curve of

the indicated bleached proteins in **A**. **(C)** Average (SEM) percentage recovery curve after photobleaching in **A**. **(D)** comparison of $t_{1/2}$ for the indicated proteins in **A**; mean ± SEM; unpaired t-test (***, $P < 0.001$; $n = 3$).

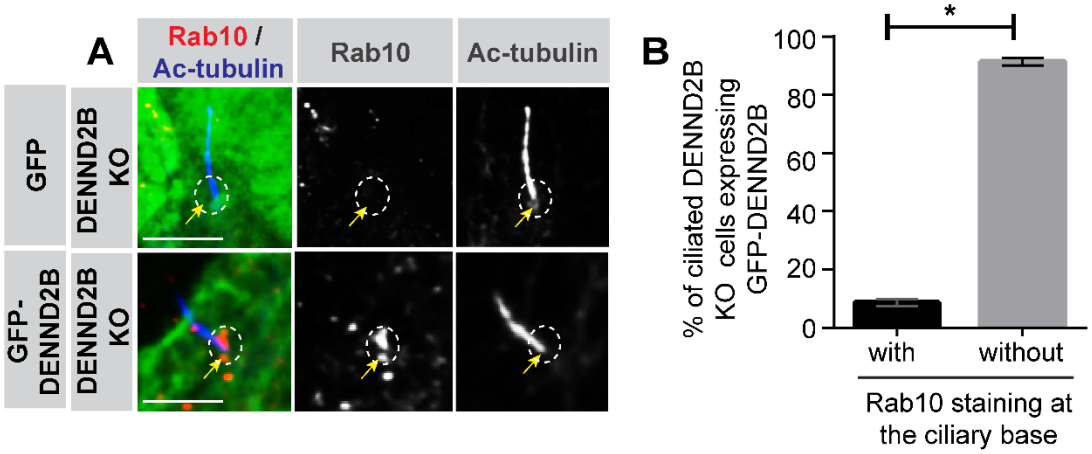

Supplementary figure 17: Overexpression of GFP-DENND2B in the DENND2B KO cells rescues the Rab10 localization.

(A) Serum starved (24 h) DENND2B KO A549 cells expressing GFP or GFP-DENND2B were fixed and stained with Rab10 antibody for endogenous Rab10 staining (red) and Ac-tubulin antibody for primary cilia (blue). Scale bars = 5.48 µm for the GFP panel and 2.73 µm for the GFP-DENND2B panel. The yellow arrow in **A** represents the base of cilia (stained with anti-Ac-tubulin antibody). **(B)** Quantification of percentage of ciliated DENND2B KO cells with or without Rab10 staining at the ciliary base in **A**; mean ± SEM; mann-whitney U test (*, $P < 0.05$; $n > 50$).

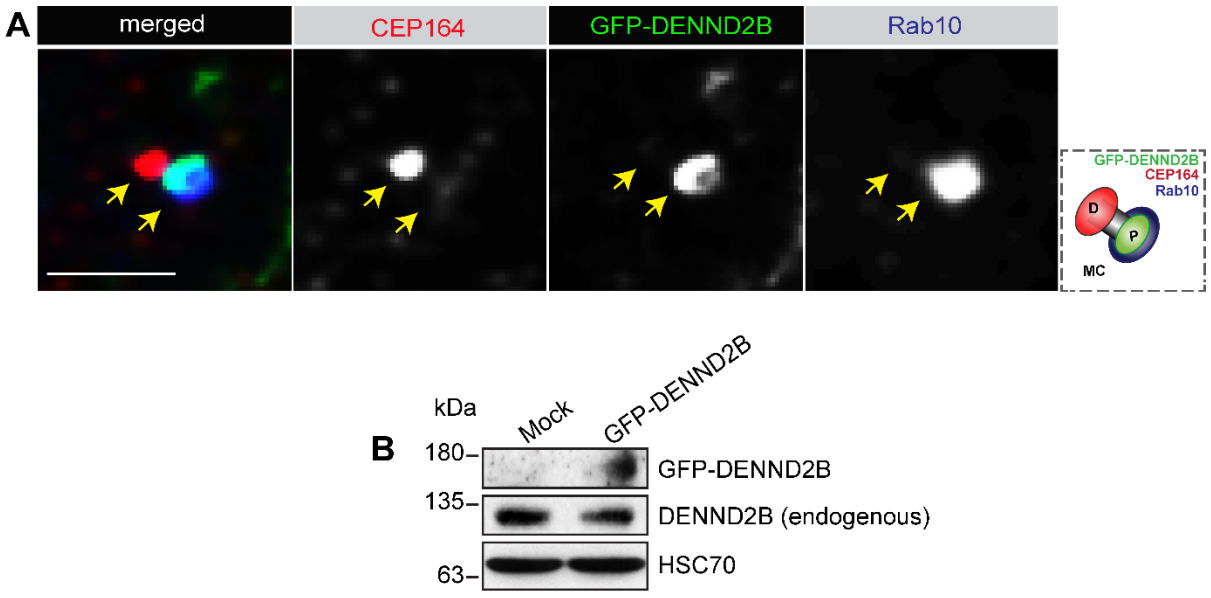

Supplementary figure 18: GFP-DENND2B and endogenous Rab10 colocalizes proximal to CEP164.

(A) Unstarved A459 WT cells expressing GFP-DENND2B were fixed and stained with Rab10 antibody and CEP164 antibody to reveal mother centriole. Scale bar 1.8 µm. Schematic representation of localization of proteins at the mother centriole are drawn in the dotted grey box in which 'P' stands for proximal end of the centriole, 'D' stands for distal end of the centriole, 'MC' stands for mother centriole. **(B)** Immunoblot showing level of overexpression of GFP-DENDN2B in A549 cells.

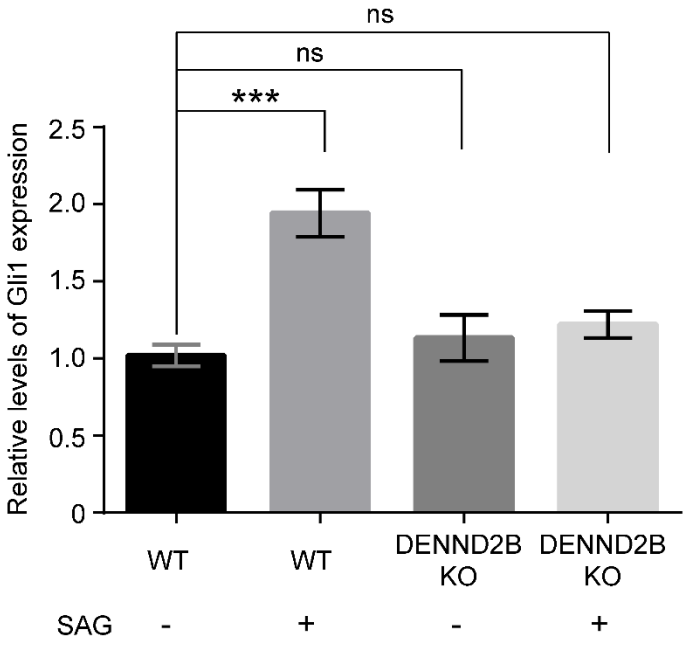

Supplementary figure 19: Absence of DENND2B inhibits sonic hedgehog signaling.

Unstarved and starved (24 h) A549 WT and DENND2B KO cells treated with 200nM of smoothened agonist (SAG) or H_2O (solvent for SAG) in serum-free media for another 24 h. SAG functions as an activator of receptor smoothened by direct binding and induces downstream Hh signaling that increases expression levels of Gli transcription factor (75). Cells were processed for RNA isolation and analyzed for the levels of Gli1 by qPCR; mean ± SEM; Kruskal-Wallis test, with pairwise multiple comparison post-test (***, $P \leq 0.001$; ns, not significant; n=3).

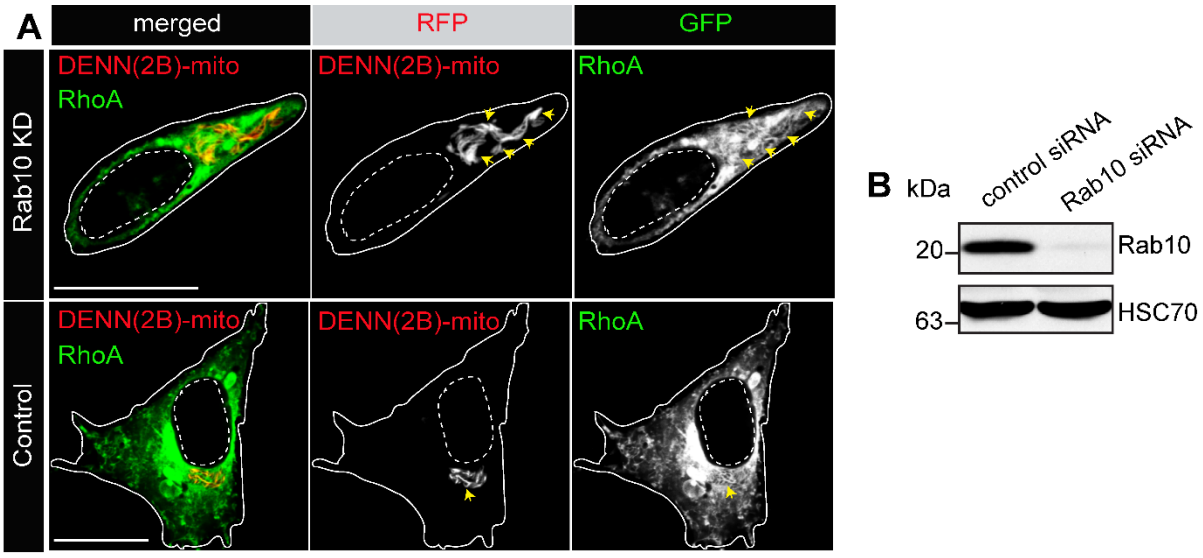

Supplementary figure 20: DENN domain of DENDN2B recruits RhoA to the mitochondria independent of Rab10.

(A) HeLa cells were transfected with control siRNA or with an siRNA to selectively knockdown the expression of Rab10. 48 h post siRNA transfection, cells were transfected with GFP-RhoA WT and DENN(2B)-mito. Scale bar = 20 µm. **(B)** Immunoblot showing the level of Rab10 knockdown performed in **A.** Immunoblot probed with anti-Rab10 and anti-HSC70 antibody.

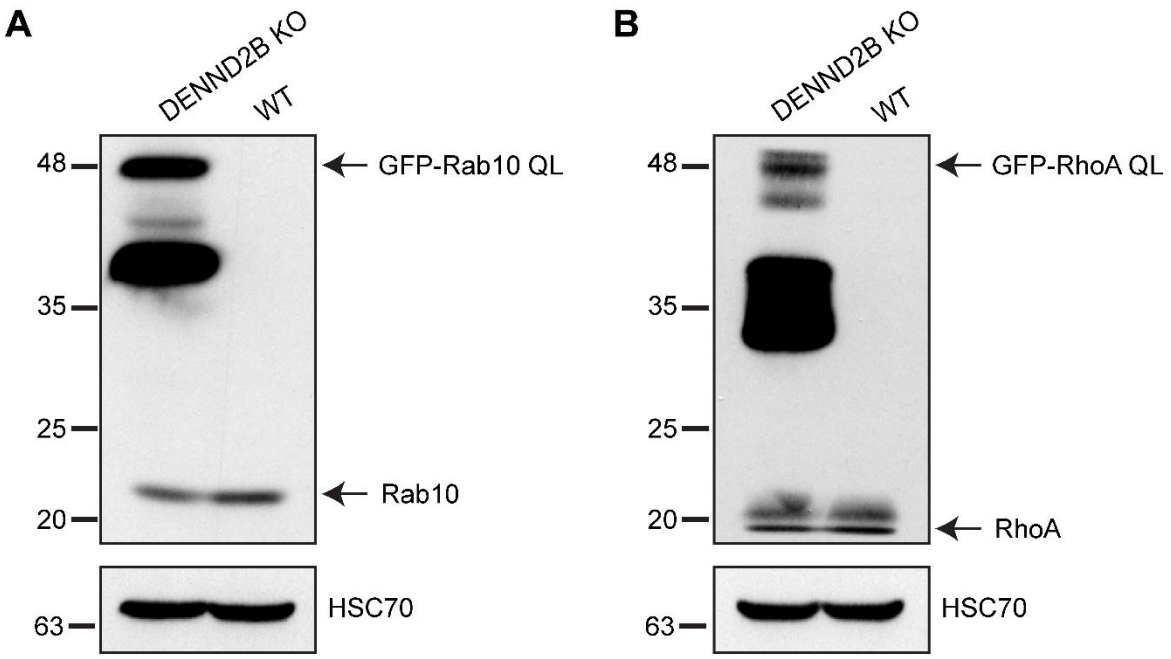

Supplementary figure 21: Levels of overexpression of Rab10 QL or RhoA QL in the rescue experiments.

(A) Immunoblot showing level of overexpression of GFP-Rab10 QL in A549 DENND2B KO cells versus WT alone. Immunoblot probed with anti-Rab10 and anti-HSC70 antibody. **(B)** Immunoblot showing level of overexpression of GFP-RhoA QL in A549 DENND2B KO cells versus WT alone. Immunoblot probed with anti-RhoA and anti-HSC70 antibody.

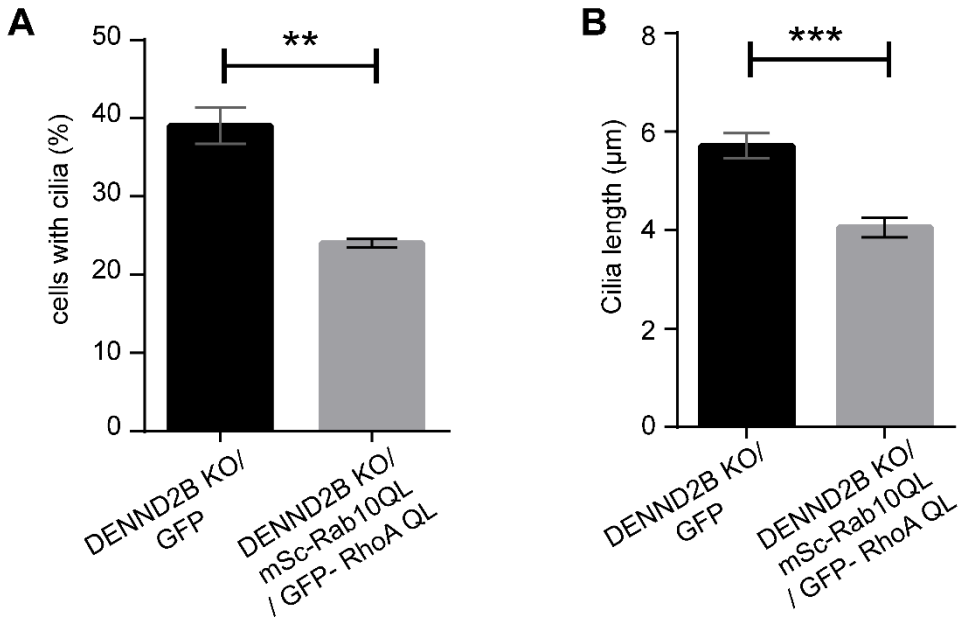

Supplementary figure 22: Overexpression of Rab10QL and RhoA QL in DENND2B KO cells rescues both cilia formation and ciliary length.

(A) Percentage of ciliated DENND2B KO A549 cells expressing GFP or GFP-RhoA QL/mSc-Rab10 QL; mean ± SEM; unpaired t-test (**, P ≤ 0.01; >80 cells per condition); **(B)** comparison of the ciliary length in the DENND2B KO A549 cells expressing GFP or GFP-RhoA QL/mSc-Rab10 QL; mean ± SEM; unpaired t-test (***, P ≤ 0.001; n > 22 cells per condition).

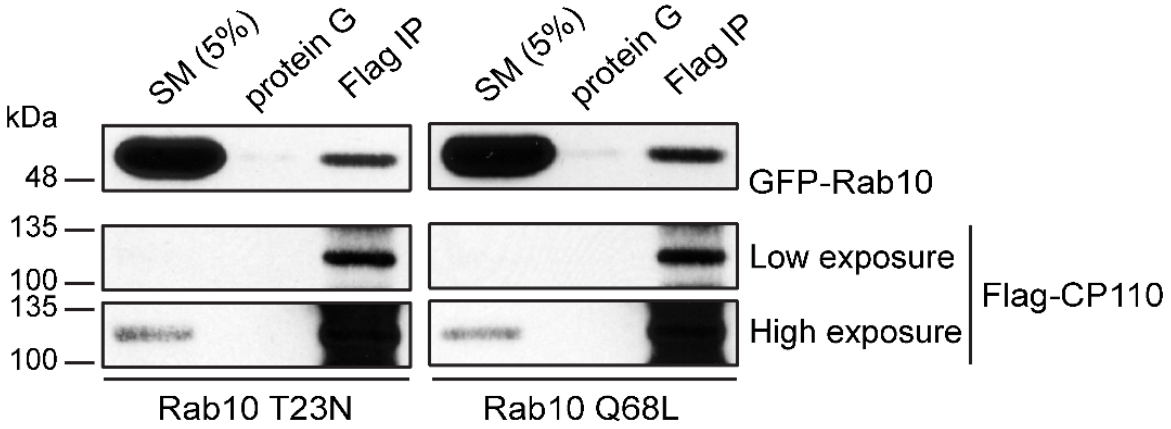

Supplementary figure 23: CP110 interacts with Rab10.

HEK-293T cells were co-transfected with Flag-CP110 and GFP-Rab10 T23N or GFP-Rab10 Q68L. At 24 h post-transfection, cells were lysed and incubated with protein G-agarose alone (mock) or protein G-agarose with anti-Flag antibody (Flag IP). Specifically bound proteins were detected by immunoblot with anti-GFP antibody to detect active/inactive Rab10 or anti-Flag antibody recognizing CP110.

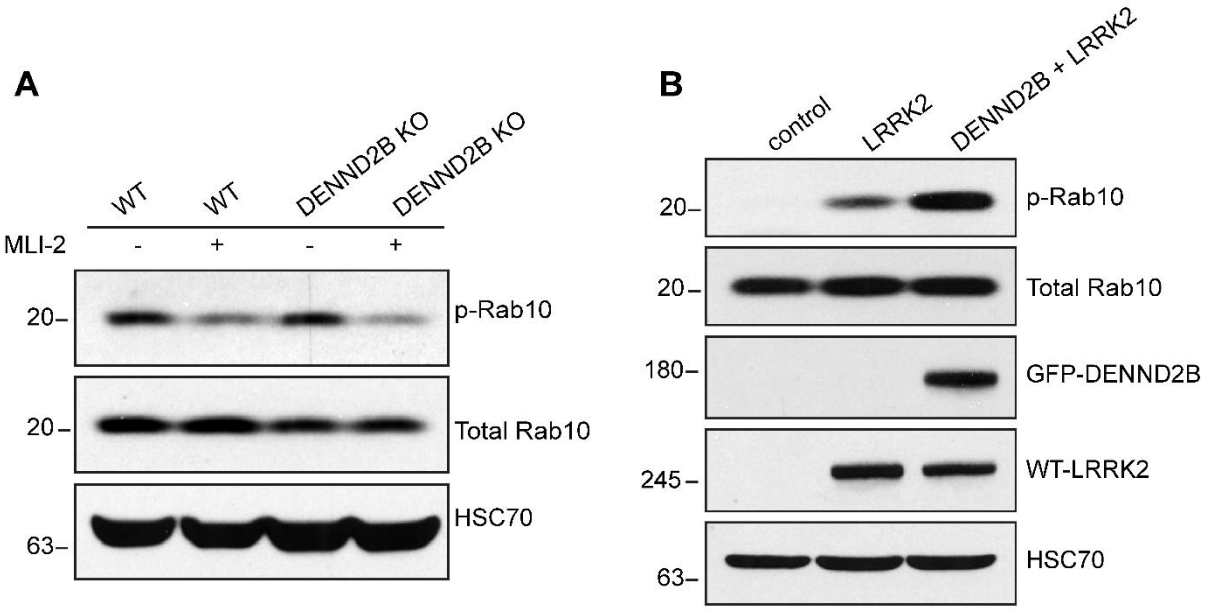

Supplementary figure 24: LRRK2 phosphorylates Rab10 in a DENND2B-dependent manner.

(A) WT or DENND2B KO A549 cells treated with 200 nM MLI-2 or DMSO for 60 minutes were lysed and analyzed for p-Rab10 levels. Proteins were detected by immunoblot with anti-Rab10 antibody or anti-p-Rab10 antibody or anti-HSC70 antibody for loading control. **(B)** HEK-293T cells were transfected with myc-LRRK2-WT and / or GFP-DENND2B. At 24 h post-transfection, transfected or untransfected (control) cell lysates were analyzed for p-Rab10 levels. Proteins were detected by immunoblot with anti-LRRK2 antibody or anti-GFP antibody or anti-Rab10 antibody or anti-p-Rab10 antibody or anti-HSC70 antibody for loading control.

PREFACE TO CHAPTER 4

By screening two major DENN protein families with all 60 Rab proteins, we confirmed already-known DENN/Rab pairs, provided new insights into disputed pairs, and discovered 19 new DENN/Rab relationships. This discovery also helps explain why there are fewer GEFs than Rabs, as a small number of DENN domain proteins can activate a broad range of Rab substrates. Thus, our findings have greatly improved our understanding of the function of Rab GEFs and their range of targets. Additionally, we have gained crucial insights into the development of primary cilia through the interplay of DENND2B, Rab10, and RhoA.

Despite our progress, we were still puzzled about how DENND2B is capable of activating various biological pathways through multiple Rab GTPases. Additionally, we observed that cells lacking DENND2B grow at a slower rate, which raised our curiosity about the possible involvement of DENND2B in cytokinesis. In Chapter 4 of our study, we thoroughly investigated this phenomenon and gained significant insights into the underlying cell biology.

Cytokinesis is the final step of cell division and defects in cytokinesis result in tetraploidy and genetically unstable cells that cause tumorigenesis, Lowe syndrome and neurodevelopmental disorders. Cytokinesis involves the formation of an intercellular cytokinetic bridge (ICB) connecting the two daughter cells followed by abscission, a step relying on depolymerization of microtubules and F-actin. Here we solve an outstanding question regarding control of upstream pathways driving actin depolymerization in cytokinesis. Cytokinesis depends on synchronized membrane trafficking regulated by Rab GTPases and their activators, guanine nucleotide

exchange factors (GEFs). Here we discover that DENND2B is a novel upstream regulator of cytokinesis.

During our investigation, we made a significant discovery:

1) DENND2B is a GEF for Rab35. Rab35 regulates cytokinetic abscission by recruiting its effector MICAL1 (an actin depolymerizing enzyme). KD of DENND2B leads to reduced recruitment of Rab35 and excess accumulation of F-actin at the intracellular bridge (ICB).

2) The DENN domain of DENND2B, located in the C-terminal region, functions as a GEF for Rab35 whereas the N-terminal region functions as a Rab35 effector. This suggests a positive feedback mechanism that enriches Rab35 at the ICB, where it persists for hours.

3) DENND2B localizes at the ICB in the presence of chromatin (chromatin bridge). The chromatin bridge is sensed by dividing cells as stress because it can lead to chromosome breaks or tetraploidy. In such situations, dividing cells have a conserved mechanism called the abscission checkpoint that delays abscission and ensures proper separation of chromatin. DENND2B KD causes an increase in chromatin bridges, and we discover that DENND2B regulates the abscission checkpoint.

CHAPTER 4

DENND2B activates Rab35 at the intercellular bridge regulating cytokinetic abscission and tetraploidy

Rahul Kumar*, Vincent Francis*, Maria S. Ioannou, Adriana Aguila, Emily Banks, Gopinath Kulasekaran, Maleeha Khan, Peter S. McPherson

* contributed equally

Department of Neurology and Neurosurgery, Montreal Neurological Institute (the Neuro), McGill University, Montreal, Quebec, Canada.

Preprint published in *BioRxiv*

DOI: https://doi.org/10.1101/2023.01.12.523789

Abstract

Cytokinesis is the final stage of cell division. Successful cytokinesis requires membrane trafficking pathways regulated by Rabs, molecular switches activated by guanine nucleotide exchange factors (GEFs). Late in cytokinesis, an intercellular cytokinetic bridge (ICB) connecting the two daughter cells undergoes abscission, which requires depolymerization of actin. Rab35 recruits MICAL1 to oxidate and depolymerize actin filaments. We report that DENND2B, a protein previously implicated in cancer, mental retardation and multiple congenital disorders functions as a GEF for Rab35 and recruits and activates the GTPase at the ICB. Unexpectedly, the N-terminal region of DENND2B interacts with an active mutant of Rab35, suggesting that DENND2B is both a Rab35 GEF and effector. KD of DENND2B delays abscission resulting in increased multinucleated cells and over-accumulation of F-actin at the ICB. F-actin accumulation leads to formation of a chromatin bridge, a process known to activate the NoCut/abscission checkpoint, and DENND2B KD actives Aurora B kinase, a hallmark of checkpoint activation. This study identifies DENND2B as a crucial player in cytokinetic abscission and provides insight into the multisystem disorder associated with DENND2B mutation.

Introduction

Membrane trafficking controls the localization and levels of proteins important for cell physiology and alterations in these pathways cause disease. Key to membrane trafficking pathways are small GTPases including Rabs [1], molecular switches that toggle between a guanosine diphosphate (GDP)–bound inactive state and a guanosine triphosphate (GTP)–bound active state [2]. Rabs are activated by guanine

nucleotide exchange factors (GEFs) [3], the largest family being the DENN domain-bearing proteins that comprise at least 18 members, most of which are poorly characterized [4]. Upon activation, Rabs in their GTP-bound state bind to effectors, proteins that carry out downstream steps in membrane trafficking [5].

Cytokinesis, the final step of cell division requires delivery and retrieval of select proteins to the site of daughter cell separation [6][7]. Defects in cytokinesis are associated with cancers, Lowe syndrome and neurodevelopmental disorders [8][9][10][11][12][13][14]. Cytokinesis involves the physical separation of two daughter cells at the end of mitosis/meiosis. Before abscission, the daughter cells remain attached through an intercellular bridge (ICB), which can persist for several hours [15]. The ICB contains an array of cytoskeletal components functioning in the ingression of the plasma membrane, which results in a cytokinetic furrow [6][16]. Successful abscission requires clearance of cytoskeletal elements such as microtubules and filamentous actin (F-actin) allowing for constriction of the plasma membrane by the ESCRT machinery [17][18][19]. The removal of microtubules from the ICB depends on ESCRT-mediated delivery of the microtubule-depolymerizing enzyme Spastin [20][21]. F-actin clearance involves the small GTPase Rab35. Rab35 prevents accumulation of F-actin through its effector Oculo-Cerebro-Renal syndrome of Lowe, an inositol (4,5)P2 5-phosphatase [12][22], and drives F-actin depolymerization through the effector MICAL1, which oxidates and depolymerizes F-actin [23][24]. Rab35/MICAL1-dependent actin depolymerization is also important for the recruitment of ESCRT [23][24]. A scaffold protein, Rab11FIP1, gets recruited to the ICB after recruitment of Rab35 and helps maintain Rab35 at this site [25]. The activation and recruitment of Rab35 at the ICB remains poorly understood.

There are pathophysiological conditions such as high membrane tension, defective nuclear pore complex integrity, and the presence of trapped chromatin in the cleavage plane (chromatin bridge) that trigger the abscission (NoCut) checkpoint machinery, which delays completion of abscission and leads to cytokinetic failure, tetraploidy and the development of cancer [26][27][28][29][30][31][31][32][33][34]. The activation of the checkpoint machinery is also observed with accumulation of F-actin at the ICB [31][35][36], although a recent report suggested F-actin accumulation may not coincide with checkpoint activation [37].

As Rabs become more commonly linked to disease [38][39], there is increased interest in identifying and characterizing their activators (GEFs). The largest family of GEFs contain an evolutionary conserved protein module, the DENN (differentially expressed in normal and neoplastic cells) domain [4]. There are minimally 18 DENN-domain bearing proteins and most are poorly characterized [4]. An in vitro screen based on purified Rabs and 16 DENN domain proteins led to the assignment of a single, unique Rab to each DENN domain subfamily [40]. Subsequent cell biological studies focusing on individual DENN domain proteins such as DENND1C [41] and DENND2B [42] revealed different Rab substrates than those identified in the in vitro screen. This disparity could stem from the fact that in vitro GEF assays are challenging as purification of recombinant Rabs can lead to their inactivation and altered nucleotide loading [43], and inactivation of purified DENN domains may also occur due to misfolding.

We developed a cell-based assay to identify Rab substrates for DENN domain proteins [44}. The basis of this assay is the finding that GEFs are primarily responsible for driving the spatial and temporal localization of Rab GTPases [44]. For example, when GEFs are artificially targeted to organelles such as mitochondria, Rab substrates

relocalize to these new sites [44]. Utilizing this approach, we discovered that DENN domain proteins activate a larger array of Rab substrates than previously thought [45]. Through investigation of newly identified DENN/Rab GEF/substrate pairs we discovered that DENND2B activates Rab10 to regulate primary cilia formation [45]. DENND2B is multifunctional in that it also acts as a GEF for Rab13, promoting the development of epithelial cancer [42]. Additionally, DENND2B functions in nervous system development and a loss of function mutation in DENND2B leads to severe mental retardation, seizures, bilateral sensorineural hearing loss, unilateral cystic kidney dysplasia, frequent infections and other congenital anomalies [46].

Here, we demonstrate that DENND2B interacts with Rab35 as both an effector and a GEF, and in so doing leads to enrichment of activated Rab35 at the ICB, allowing for actin depolymerization and cytokinesis. Disruption of DENND2B leads to increased formation of a chromatin bridge at the ICB and activates the NoCut/abscission checkpoint, delaying abscission. We suggest that these processes contribute to the role of DENND2B in cancer and neurodevelopmental disorders.

Results

Loss of DENND2B delays cytokinetic abscission

DENND2B is implicated in cancer and neurodevelopmental, processes involving cytokinetic defects [42][46][8][9][10][12][13][14]. We observed that loss of DENND2B causes cells to grow slowly and thus examined if DENND2B functions in cytokinesis. We performed phase contrast time-lapse microscopy imaging of HeLa cells comparing control and DENND2B KD using previously reported shRNA sequences [42][47]) that lead to a ~75% reduction in DENND2B mRNA levels (Fig. 1A). These shRNAs reduce

DENND2B protein levels in human cells [47]. Both control and KD cells form the ICB following furrow ingression (Fig. 1B) but control cells take on average 237 min to complete cytokinesis (as previously reported for HeLa cells [23]) whereas DENND2B KD cells require 472 min (Fig. 1B-D), similar to the delay observed for depletion of MICAL1 depletion [12][23]. DENND2B KD cells also have an increase in binucleated cells (Fig. S1A-B), a phenotype observed upon KD of Rab35 or Rab11FIP1 [25][48]. Thus, DENND2B is a positive regulator of cytokinetic abscission.

DENND2B regulates cytokinetic abscission via Rab35

A screen of the DENN domain of DENND2B against all 60 Rabs using a cell-based mitochondrial recruitment assay [45] revealed Rab8A, Rab8B, Rab10, Rab13, Rab15, Rab27A, Rab27B, and Rab35 as potential DENND2B GEF substrates [45]. Of these, Rab35 and Rab8 were identified in an unbiased proteomic analysis of the midbody, an organelle assembled at the center of the ICB [49][50], pointing our attention to these two Rab substrates. Expression of active mutants of Rab35 (Rab35 Q67L) but not Rab8 (Rab8 Q67L) in DENND2B KD cells rescued the cytokinetic abscission defect (Fig. 2A-B). Expressing a DENND2B construct resistant to DENND2B shRNA also rescues the cytokinetic abscission timing, supporting the specificity of DENND2B function in cytokinesis (Fig. 2A-B). Collectively, these data indicate that DENND2B controls cytokinetic abscission, likely through Rab35.

DENND2B functions as a GEF for Rab35

We next examined the potential GEF activity of DENND2B towards Rab35 using an assay in which GEFs can target substrates to the surface of mitochondria [44]. The mitochondrial targeted DENN domain of DENND2B [DENN(2B)-mito] leads to a near-complete steady-state re-localization of co-transfected GFP-Rab35 to mitochondria

(Fig. 3A). While the mitochondrially targeted DENN domain of DENND2B induces a morphological change in the mitochondria, this is not relevant to the study as the assay aims simply to identify candidate GTPase relocalized to the mitochondria.

We next co-transfected HeLa cells with DENN(2B)-mito and a non-prenylatable form of Rab35 lacking the two C-terminal cysteines (GFP-Rab35 C_C del). GFP-Rab35 C_C del is not recruited to mitochondria (Fig. 3A), suggesting that Rab recruitment requires insertion of prenyl groups, a process mediated by GEF activity. Structural alignments of the DENN domain of DENND1B [51] with the DENN domain of DENND2B predicted by AlphaFold [52] (Fig. 3C) revealed that of the seven residues in the DENN domain of DENND1B important for interaction with and GEF activity towards Rab35 [51], all are conserved in DENND2B with three identical. Mutation of two identical residues (P946R and Q1080A) abolished the mitochondrial recruitment of Rab35 (Fig. 3B), reinforcing that the catalytic GEF activity of DENND2B is required for the activation of Rab35 and mitochondrial recruitment. Finally, we performed an effector binding assay using a glutathione S-transferase (GST) fusion with a C-terminal fragment of MICAL-L1 (molecule interacting with CasL-like 1), which selectively binds the active form of Rab35 [53]. The active levels of Rab35 were increased with DENND2B overexpression (Fig. 4A-B).

A hallmark of GEF/Rab substrate relationships is that GEFs preferentially interact with the inactive, GDP-bound form of the Rab [51][54][55][56]. In coimmunoprecipitation experiments, full length (FL) Flag-DENND2B interacts with Rab35 but with no preference for active (QL) versus inactive (SN) mutants (Fig. 4C-D). In contrast, the DENN domain alone prefers inactive Rab35 whereas the N-terminal region (Fig. 4C) prefers the active form (QL) (Fig. 4E-H). Thus, through the N-terminal region, DENND2B appears to be an effector of Rab35. These data indicate that DENND2B is

both a GEF for Rab35 and an effector of the same GTPase. We speculate that these dual interactions could serve a positive feedback role allowing DENND2B to rapidly, and strongly, activate Rab35 at specific cellular locations.

DENND2B is localized in part to the midbody where it controls Rab35 recruitment and F-actin levels

We next investigated the localization of DENND2B in dividing cells. We expressed GFP-DENND2B in HeLa cells and stained with SiR-tubulin to visualize the progression of the ICB until complete scission [17][18]. Cleavage of the ICB is characterized by narrowing of either side of the midbody bulge (an organelle assembled at the center of the ICB) followed by scission, leaving behind a midbody remnant [17][18]. Upon furrow ingression, DENND2B accumulates at the cell-cell interface or the interface of the daughter cell and the ICB on either side (Fig. 5A). With the progression of the ICB, DENND2B accumulates at the cell-cell interface as revealed by the quantification of DENND2B fluorescence intensity from the marked representative regions (1 & 2) (Fig. 5A-B). Additionally, we detected a small fraction of DENNDB at the midbody as represented by the overlap of DENND2B and SiR-tubulin (Fig. 5A, C). The DENND2B intensity decreases at the cell-cell interface just before abscission (Fig. 5A-B). The midbody is an extremely dynamic structure. Therefore, we performed live-cell imaging on cells that were already dividing, and we were able to capture the midbody through multiple planes (Fig. 5D). DENND2B is present at the midbody throughout cytokinesis, even post cytokinetic abscission when the midbody has become a midbody remnant (Fig. 5D).

GFP-DENND2B shows a similar distribution as that of tagBFP-Rab35 at the cell-cell interface at the late ICB (Fig. S2A-B). The enrichment pattern of Rab35 at the diving cell interface was the same as that previously reported [25]. Co-localization at the bridge supports that DENND2B and Rab35 function together in cytokinesis. Finally, it is known that GEFs control the localization of their Rab substrates [57]. To analyze the localization of Rab35 in the absence of DENND2B, we performed DENND2B KD in HeLa cells stably expressing tagBFP-Rab35 and stained with β-tubulin to identify dividing cells with a late bridge [23]. Cells showing Rab35 enrichment at cell/ICB interface of the late bridge decreased significantly in the DENND2B KD cells as compared to the control (Fig. 6A-B). Quantitative analysis of fluorescence intensity of Rab35 at the bridge revealed a ~2.5-fold decrease of Rab35 recruitment in the DENND2B KD cells (Fig. 6A, C).

An important function of Rab35 at the ICB is to recruit MICAL1 to oxidate and depolymerize F-actin, facilitating cytokinetic abscission [23]. Since Rab35 recruitment at the late bridge is lost in the absence of DENND2B, we predicted that DENND2B depletion would alter F-actin levels at the bridge. There is an increase in the number of cells accumulating F-actin at the late bridge following DENND2B depletion (Fig. 6D-E) with a ~ 2-fold increase in F-actin levels within the bridge in DENDN2B KD cells (Fig. 6D, F). These data suggest that DENND2B activates Rab35 at the cytokinetic bridge with activated Rab35 driving downstream pathways causing F-actin depolymerization, facilitating cytokinetic abscission.

DENND2B is recruited in the presence of chromatin bridge and regulates the abscission checkpoint machinery

Cytokinetic abscission is a tightly coordinated process, the timing of which is surveilled by a conserved complex of proteins known as the abscission checkpoint machinery [30]. The checkpoint machinery is activated when dividing cells are experiencing stress such as the presence of trapped chromatin (chromatin bridge) at the ICB, high membrane tension, or nuclear pore defects [30]. These stresses can alter cytokinesis and lead to tetraploidy [31].

Activation of the abscission checkpoint correlates with the accumulation of F-actin at the ICB [31][35][36][58] although accumulation of F-actin at the ICB is not always a consequence of this process [37]. Given that DENND2B KD leads to F-actin accumulation at the ICB, we sought to test if DENND2B functions in abscission checkpoint. In HeLa cells expressing GFP-DENND2B and stained with LAP2-β (a nuclear envelope protein) to observe chromatin bridges [31][35], we found an enriched pool of DENND2B at the midbody region with the LAP2-β positive chromatin bridge (Fig. 7A) and that an increased percentage of DENND2B depleted cells had accumulation of F-actin at the chromatin bridge as compared to other cellular locations (Fig. 7B-C). Fluorescence intensity quantification revealed a ~2-fold increase of F-actin levels within the chromatin bridge in DENDN2B KD cells (Fig. 7B, D).

To further demonstrate that accumulation of F-actin at the bridge is due to a lack of Rab35 recruitment, we expressed tagBFP-Rab35 QL (active mutant) or tagBFP alone in DENND2B KD cells and analyzed dividing cells with or without chromatin bridges. We found that the Rab35 active mutant localized at cytokinetic bridges (Fig. S3A, D). The percentage of DENND2B KD cells with accumulation of high F-actin at the bridge

significantly decreased with the expression of Rab35 active mutant (Fig. S3B, E), and the F-actin intensities at the cytokinetic bridges were decreased by more than 2-fold in the presence of Rab35 active mutant, again suggesting that the activation and recruitment of Rab35 by DENND2B at the bridge with or without the chromatin is crucial for the maintenance of F-actin levels.

Lastly, we examined if DENND2B at the chromatin bridge regulates the abscission checkpoint. Aurora B kinase is a key regulator of abscission checkpoint that senses chromatin bridge at the ICB and delays abscission [30][31][33], which is dependent on the activating phosphorylation of Aurora B (pT232 Aurora B) [30][59]. We observed that a pool of DENND2B colocalizes with active, phosphorylated Aurora B at the midbody upon activation of checkpoint by the chromatin bridge at the ICB area (Fig. 8A). A hallmark of the activation of the abscission checkpoint is the concentration of phospho-Aurora B at the midbody in the presence of a chromatin bridge [31]. Indeed, we found that the percentage of cells with phospho-Aurora B at the midbody of the chromatin bridge increased significantly (~2-fold) in the DENND2B KD cells as compared to the control (Fig. 8B-C), suggesting DENDN2B and Aurora B are functionally related. Finally, we also found that the percentage of cytokinetic bridges with the chromatin bridges also increased in the DENND2B KD cells as compared to the control (Fig. 8D-E), another hallmark of activation of checkpoint [37]. In summary, these data reveal that DENND2B also regulates abscission checkpoint and may function in the same pathway as Aurora-B.

Discussion

Humans have ~60 Rabs and there is increasing interest to identify their activators given the growing association of altered membrane trafficking with human disease [60]. We identified multiple Rab GTPases as partners/substrates for DENN domain proteins [45]. We now report an important role of DENND2B in cytokinetic abscission.

Rab35 functions in various cellular contexts including cytokinesis [48][12][61], and yet, the mechanism by which Rab35 is activated and recruited at the cytokinetic bridge remains unknown. Here we demonstrate that DENND2B functions as a GEF for Rab35. Depletion of DENND2B leads to a delay in cytokinetic abscission and an increased number of binucleated cells [12][48]. F-actin clearance is required for the recruitment of ESCRT-III to allow timely abscission [23]. We observed accumulation of F-actin at the ICB upon loss of DENND2B. The idea that such phenotypes were caused by lost recruitment of Rab35 was validated by two findings. First, we observed a drastic reduction of cells with Rab35 at the cytokinetic bridge following DENND2B KD, and second, we could rescue the phenotype of F-actin accumulation at the bridge by expressing an active Rab35 mutant. Further, DENND2B and Rab35 colocalize at the cytokinetic bridge and show a similar enrichment pattern. Finally, we demonstrate that the DENN domain of DENND2B interacts with Rab35 in a nucleotide-dependent manner and that expression of DENND2B causes an increase in the levels of active Rab35 within the cell, further suggesting that DENND2B activates and recruits Rab35 at the cytokinetic bridge.

In addition to functioning as a GEF for Rab35, we find that DENND2B is a Rab35 effector. While effectors are recruited by Rab GTPases to help define the functional identity of the membrane [3], there are positive feedback loops caused by GEF–Rab-

effector complexes [5]. These loops help maintain the membrane anchored GTPases and downstream signaling [5]. A well-known example of a GEF-Rab-effector complex is Rabex5/Rab5/Rabaptin5 [62]. Rabex5 has GEF activity for Rab5 upon initial recruitment of Rab5 to the membrane [62]. Once Rab5 is activated on the membrane, it interacts with its effector Rabaptin5 [63]. Subsequently, Rabaptin5 binds to Rabex5 and increases its GEF activity, thus ensuring sustained GTPase activation and effector function [64]. Another example of such a positive feedback mechanism involves polarized trafficking in yeast by the Sec2/Sec4/Sec15 complex. Activation of the Rab GTPase Sec4 is mediated by its exchange factor Sec2 and Sec2 binds to the effector of Sec4, Sec15 which could generate a positive feedback loop [3][65]. The fact that a portion of the same GEF (N-terminal fragment) is functioning as an effector as observed here for DENND2B raises an intriguing possibility that the N-terminal fragment could function to drive a positive feedback loop to help maintain Rab35 at the cytokinetic bridge, given that the bridge persists for up to several hours. Future experiments will seek to understand whether the N-terminus of DENND2B plays a role in a similar positive feedback mechanism to help sustain Rab35 remain anchored to the membrane and cause prolonged downstream effector function.

We also demonstrate DENND2B-mediated regulation of the abscission checkpoint. The absence of DENND2B increases the proportion of cells with cytokinetic bridges containing chromatin. This, together with the fact that DENND2B colocalizes with active phospho-Aurora B, a key component of the abscission checkpoint and that absence of DENND2B increases the number of cells with active phospho-Aurora B at the midbody of the bridge, indicates that DENND2B plays a role in regulating abscission checkpoint. Questions regarding the detailed mechanistic role of

DENND2B in abscission checkpoint and potential DENND2B interaction with the checkpoint machineries remain unknown.

It is proposed that a balance of actin oxidation by MICAL1 and actin reduction by MsrB2 regulates F-actin levels at the cytokinetic bridge and controls abscission [35]. We propose that DENND2B activates Rab35 and recruits it to the cytokinetic bridge regardless of the presence of the chromatin bridge (Fig. 9). Recruited Rab35 contributes to F-actin oxidation mediated by MICAL1. In the absence of DENND2B, Rab35 recruitment is impaired resulting in elevated levels of F-actin at the bridge (Fig. 9). Accumulation of F-actin is not favorable for the recruitment of ESCRT-III, thus leading to delayed abscission [23]. The absence of DENND2B also activates abscission checkpoint in the presence of chromatin bridge (Fig. 9). An increased presence of activated checkpoint machinery (phospho-Aurora B) in the presence of chromatin at the bridge also contributes to the abscission delay [30] (Fig. 9).

With the identification of a new role of DENND2B/Rab35, we provide evidence supporting our previous findings that DENN domain proteins control a larger array of Rab GTPases in complex membrane trafficking pathways. Finally, this study leads to additional open questions. It appears that there are unknown contributing factors that define the context specific GEF activity of DENND2B for its activation at various cellular sites. While we have identified that DENND2B is crucial for the activation and recruitment of Rab35 at the bridge, the question regarding the upstream factors that cause the correct localization of DENND2B still needs to be determined.

In summary, we have uncovered that DENND2B functions as a GEF for Rab35 to control timely cytokinetic abscission and thereby prevents tetraploidy. We believe that

the identification of this crucial pathway is a step forward in understanding the various congenital anomalies associated with a DENND2B loss-of-function patient mutation.

Materials and Methods

Cell lines

HeLa and HEK-293T cells were from ATCC (CCL-2 and CRL-1573)

Cell culture

Cell lines were cultured in DMEM high-glucose (GE Healthcare cat# SH30081.01) containing 10% bovine calf serum (GE Healthcare cat# SH30072.03), 2 mM L-glutamate (Wisent cat# 609065), 100 IU penicillin and 100 µg/ml streptomycin (Wisent cat# 450201). Serum starvation media: DMEM high-glucose containing 2 mM L-glutamate, 100 IU penicillin and 100 µg/ml streptomycin. Cell lines were tested for mycoplasma contamination routinely using the mycoplasma detection kit (Lonza; cat# LT07-318).

DNA constructs

RFP-mito, DENN(2B)-mito, DENN(2B) P946R/Q1080A-mito, GFP-Rab35, GFP-Rab35 C_C del, Flag-DENND2B (DENN) and Flag-DENND2B (N-term) were described previously [45][42]. The following constructs were generated by SynBio Technologies: mScarlet-DENND2B (in pmScarlet-i_C1), tagBFP-Rab35 (Human Rab35; in lentivirus vector pLVX-M-puro (Addgene 125839)), tagBFP (in pLVX-M-puro), mScarlet-Rab8 Q67L (Human Rab8a; in pLVX-M-puro) and mScarlet-DENND2B resistant to DENND2B shRNA (Xenopus DENND2B; in pLVX-M-puro). Lenti tagBFP-Rab35 Q67L construct was generated using the QuickChange lightning site-directed mutagenesis (SDM) kit (Agilent Technologies) on lentivirus vector pLVX-M-puro containing GFP-Rab35 using following primers: Fwd- 5’ CACAGCGGGGCTGGAGCGCTTCC 3’ and Rev- 5’

GGAAGCGCTCCAGCCCCGCTGTG 3'. Successful cloning of constructs was verified by sequencing.

shRNA mediated KD of DENND2B

Production of control and DENND2B shRNA virus were described previously [42][47]. Briefly, the two shRNA sequences were used for control or DENND2B KD. The shRNA sequences were first cloned into pcDNA6.2/GW-emGFP–miR cassette and then the emGFP-miR cassette was PCR-amplified and subcloned into the pRRLsinPPT viral expression vector (Invitrogen). Control shRNA sequence: AATTCTCCGAACGTGTCACGT; DENND2B shRNA sequence:TGCTGCTTGGATGAAGCCAGCAAACAGTTTTGGCCACTGACTGACTG TTTGCTCTTCATCCAAG. The lentiviral particles were produced using shRNA containing pRRLsinPPT viral expression vector, pMD2.g, and pRSV-Rev as previously described [66].

Real-time quantitative PCR

Total RNA was extracted from HeLa cells using RNeasy Mini kit (Qiagen) and 500 ng of RNA was used for the cDNA synthesis using iScript™ Reverse Transcription Supermix (Bio-Rad Laboratories). Real-time quantitative PCR was performed using the Bio-Rad CFX Connect Real-Time PCR Detection System with SsoFast™ EvaGreen Supermix (Bio-Rad Laboratories). The values were expressed as fold change in mRNA expression in cells relative to control WT cells (untreated) using TATA-box binding protein (TBP) and beta-2-microglobulin (B2M) as endogenous controls. The primer sequences used in this study were:

DENND2B-Fwd 5' AGCAGAAAATCCTTTTGAGTTTG 3',

DENND2B-Rev 5' CTTTGGACAAGCTTGGGAATGC 3'.

Protein expression using lentivirus

For each virus, HEK-293T cells (90% confluency) were transfected with 30 µg of lentivirus construct expressing protein of interest, 30 µg of psPAX2 and 15 µg of pMD2 VSV-G using linear polyethylenimine (PEI) [67], 25,000 Da (1mg/ml; Polysciences, Inc.). The transfection ratio was 1 µg plasmid:3 µL PEI. At 8 h post-transfection, culture media was replaced with collection media (15 ml per plate; regular medium supplemented with 1× nonessential amino acids and 1 mM sodium pyruvate). The media was collected at 24 and 36 h and replaced with fresh media (15 ml per plate) with each collection. The collected media at 24 h was stored at 4oC until the last collection. The collected culture media were then filtered through a 0.45 µm PES membrane and concentrated by centrifugation (16 hour at 6800 rpm), and the resulting pellets were resuspended in DMEM in 1/5,000 of the original volume. Concentrated viruses were aliquoted and stored at −80°C.

Following virus production, concentrated lentivirus was added to the cells with minimum culture media (for example, 1 ml media in a well of 6-well dish), and the media was replaced with fresh culture media the following day (16-20h). The expression of the target protein was verified by fluorescence under microscope.

Antibodies and reagents

Mouse monoclonal Flag (M2) antibody was obtained from Sigma-Aldrich (F3165). Rabbit polyclonal GFP (A-6455) from Invitrogen, rat monoclonal HSC70 antibody (WB-1:10,000) is from Enzo (ADI-SPA-815-F). Phalloidin 647 (), Alexa Fluor 488 and 647-conjugated rabbit secondary antibodies are from Invitrogen. anti-Rab35 antibody (WB-1:1000) is from Abcam (ab152138), anti-β-tubulin antibody (IF- 1:2000) is from Invitrogen (32-2600), anti-LAP2-β (rabbit; IF- 1:300) antibody is from Proteintech

(14651-1-AP), anti-LAP2-β (mouse, IF- 1:500) antibody is from BD Biosciences (611000), phospho(T232)-Aurora B (IF- 1:200) is from Rockland (600-401-677). SiR-Tubulin (Cytoskeleton, Inc., CY-SC002) was used at 100 nM.

Imaging

Fixed cell imaging: HeLa cells following treatment as per the experimental condition were plated on poly-l-lysine coated coverslips. Cells were fixed with warm 4% paraformaldehyde for 10 min at 37°C, permeabilized for 5 min in 0.1% Triton X-100 and blocked for 1 h in 1% BSA in PBS (blocking buffer). Coverslips were incubated in blocking buffer containing diluted primary antibodies and incubated overnight at 4°C. Cells were washed 3 × 10 min with blocking buffer and incubated with corresponding Alexa Fluorophore-conjugated secondary antibodies diluted 1:1000 in blocking buffer for 1 h at room temperature. Cells were washed 3 × 10 min with blocking buffer and once with PBS. Coverslips were mounted on a microscopic slide using fluorescence mounting media (DAKO, Cat# S3023).

Imaging was performed using a Leica SP8 laser scanning confocal microscope. Image analysis was done using Image J. All the representative images in the figures were prepared for publication using Adobe Photoshop (adjusted contrast and applied 1-pixel Gaussian blur) and then assembled with Adobe Illustrator.

Phase contrast live cell microscopy: A Day before imaging, HeLa cells (treatment as per the experimental condition) were plated in a glass bottom 35mm MatTek dish (~35,000 cells per plate). 24-hour post cell seeding, MatTek dish containing cells were imaged using Zeiss live cell inverted microscope equilibrated in 5% CO2 and maintained at 37 °C. Timelapse phase contrast images were recorded every 10 min for ~30-hour using a 10X Air NA 0.45 objective (Zen software).

Widefield fluorescence Live cell imaging and deconvolution: A Day before imaging, HeLa cells (treatment as per the experimental condition) were plated in a glass bottom 35mm MatTek dish (~35,000 cells per plate) with media containing 100nM SiR-Tubulin. 24-hour post cell seeding, MatTek dish containing cells were imaged using Zeiss live cell inverted microscope equilibrated in 5% CO2 and maintained at 37 °C. Timelapse phase contrast images were recorded every 10 min for ~30-hour using a 63X Oil NA 1.4 objective (Zen software). The acquired live-cell images were processed with the fast iterative deconvolution module present in the Zen software to have increased resolution.

Generation of stable cell line

HeLa cells were transduced with lentivirus mediating expression of tagBFP-Rab35. 48-hour post transduction, cells were treated with media containing 2 µg/ml puromycin. Transduced cells were maintained in puromycin containing media for 8 days, with changing media every alternate day. Following this, resistant cells were sorted using FACS to enrich heterogenous population of cells having low to medium expression of Rab35. Sorted cells expressing Rab35 were maintained in media containing 2 µg/ml puromycin for a week and subsequently, experiments were conducted using these cells in media containing 1 µg/ml puromycin throughout.

Quantification of protein enrichment at the bridge

Each image frame was opened individually in ImageJ. Then a region of interest (ROI) was drawn using the custom region draw function either around the entire dividing cell using the outline of the cell periphery or the cell-cell interface. Subsequently, the average fluorescence signal was measured from both, and the fluorescence intensity of the entire dividing cell was used to normalize the intensity at the cell-cell interface.

Protein purification

GST-MICAL-L1-CC protein was expressed in Escherichia coli BL21 (500 µM isopropyl β-d-1-thiogalactopyranoside; Wisent Bioproducts; at room temperature for 16 h) and purified using standard procedure in Tris buffer (20 mM Tris, pH 7.4, 100 mM NaCl, 10 mM $MgCl_2$, and 1 mM dithiothreitol) supplemented with protease inhibitors (0.83 mM benzamidine, 0.20 mM phenylmethylsulfonyl fluoride, 0.5 mg/ml aprotinin and 0.5 mg/ml leupeptin).

Transfection

HEK-293T cells were transfected using calcium phosphate. HeLa cells were transfected using jetPRIME Transfection Reagent (Polyplus) according to the manufacturer's protocol.

Biochemical assays

Co-immunoprecipitation: HEK-293T cells grown to 60% confluency in 15-cm dishes were transfected with Flag-tagged and/or GFP-tagged constructs. At 24 h post-transfection, upon confirming >90% transfected cells using fluorescence microscope, cells were gently washed with PBS, scraped into lysis buffer (20 mM HEPES, 100 mM NaCl, 0.5 mM dithiothreitol, 10 mM $MgCl_2$, 1% Triton X-100 pH 7.4) supplemented with protease inhibitors (0.83 mM benzamidine, 0.20 mM phenylmethylsulfonyl fluoride, 0.5 mg/ml aprotinin and 0.5 mg/ml leupeptin), incubated for 20 min on a rocker at 4°C, and the lysates were centrifuged at 305,000 g for 15 min at 4°C. For Flag IP, supernatants were incubated with prewashed protein G beads–Sepharose beads (GE Healthcare) for 1.5 hour (preclearing step). Following preclearing, supernatants were incubated with protein G–Sepharose beads and the anti-Flag antibody for 2 h at 4°C. Beads coupled to the Flag antibody were washed three times with the same lysis

buffer, eluted in SDS-PAGE sample buffer, resolved by SDS-PAGE, and processed for immunoblotting.

Effector pull-down assay: Cells were gently washed with PBS, lyzed in lysis buffer (20 mM HEPES, 100 mM NaCl, 15 mM $MgCl_2$, 1% Triton X-100 pH 7.4) supplemented with protease inhibitors, incubated for 20 min on a rocker at 4°C, and the lysates were centrifuged at 305,000 g for 15 min at 4°C. For GST-pulldown experiments, supernatants were incubated with GST fusion proteins precoupled to glutathione–Sepharose beads for 1.5 h at 4°C. GST beads attached to the fusion proteins were washed three times with the same lysis buffer, eluted in SDS-PAGE sample buffer, resolved by SDS-PAGE, and processed for immunoblotting.

Immunoblot

Cell lysates were run on large 10% polyacrylamide gels and transferred to nitrocellulose membranes. Proteins on the blots were visualized by Ponceau staining. Blots were then blocked with 5% milk in Tris-buffered saline with 0.1% Tween 20 (TBST) for 1 h followed by incubation with antibodies overnight at 4°C diluted in 5% milk in TBST. Next day, blots were washed with TBST three times, each 10 minutes. Then, the peroxidase-conjugated secondary antibody was incubated in a 1:5000 dilution in TBST with 5% milk for 1 h at room temperature followed by washes (3 times, 10 minutes each).

Statistics

Graphs were prepared using GraphPad Prism software. All statistical tests were performed using SPSS. For all data, the normality test was performed before determining the appropriate statistical test. For normally distributed data, comparisons were made using either T-test or one-way ANOVA. For non-normally distributed data,

comparisons were made using Mann-Whitney U test or Kruskal-Wallis test. All data are shown as the mean +/- SEM with $P < 0.05$ considered statistically significant.

Acknowledgement for Chapter 4

We thank Jacynthe Philie and Maryam Fotouhi for their excellent technical assistance. We acknowledge the Neuro Microscopy Imaging Centre and Advanced BioImaging Facility at the McGill University. This work was supported by a Canadian Institutes of Health Research Foundation Grant to PSM. RK is supported by a studentship from ALS Canada. VF was supported by a fellowship from the Fonds de recherche du Quebec – Sante (FRQS). GK was supported by FRQS and a Jeanne Timmins Costello Fellowship. PSM is a Distinguished James McGill Professor and a Fellow of the Royal Society of Canada.

References for Chapter 4

[1] M. Zerial and H. McBride, “Rab proteins as membrane organizers,” Nature Reviews Molecular Cell Biology, vol. 2, no. 2. Nature Publishing Group, pp. 107–117, Feb. 2001. doi: 10.1038/35052055.

[2] H. Stenmark, “Rab GTPases as coordinators of vesicle traffic,” Nature Reviews Molecular Cell Biology, vol. 10, no. 8. Nature Publishing Group, pp. 513–525, Aug. 15, 2009. doi: 10.1038/nrm2728.

[3] P. Novick, “Regulation of membrane traffic by Rab GEF and GAP cascades,” https://doi-org.proxy3.library.mcgill.ca/10.1080/21541248.2016.1213781, vol. 7, no. 4, pp. 252–256, Oct. 2016, doi: 10.1080/21541248.2016.1213781.

[4] A. L. Marat, H. Dokainish, and P. S. McPherson, “DENN domain proteins: Regulators of Rab GTPases,” Journal of Biological Chemistry, vol. 286, no. 16. J Biol Chem, pp. 13791–13800, Apr. 22, 2011. doi: 10.1074/jbc.R110.217067.

[5] B. L. Grosshans, D. Ortiz, and P. Novick, “Rabs and their effectors: Achieving specificity in membrane traffic,” Proceedings of the National Academy of Sciences of the United States of America, vol. 103, no. 32. National Academy of Sciences, pp. 11821–11827, Aug. 08, 2006. doi: 10.1073/pnas.0601617103.

[6] S. Frémont and A. Echard, “Membrane Traffic in the Late Steps of Cytokinesis,” Curr. Biol., vol. 28, no. 8, pp. R458–R470, Apr. 2018, doi: 10.1016/J.CUB.2018.01.019.

[7] K. Nakayama, “Regulation of cytokinesis by membrane trafficking involving small GTPases and the ESCRT machinery,”

http://dx.doi.org/10.3109/10409238.2015.1085827, vol. 51, no. 1, pp. 1–6, Jan. 2015, doi: 10.3109/10409238.2015.1085827.

[8] T. I. Zack et al., “Pan-cancer patterns of somatic copy number alteration,” Nat. Genet., vol. 45, no. 10, pp. 1134–1140, Oct. 2013, doi: 10.1038/NG.2760.

[9] T. Fujiwara, M. Bandi, M. Nitta, E. V. Ivanova, R. T. Bronson, and D. Pellman, “Cytokinesis failure generating tetraploids promotes tumorigenesis in p53-null cells,” Nature, vol. 437, no. 7061, pp. 1043–1047, Oct. 2005, doi: 10.1038/NATURE04217.

[10] K. Sugimoto, H. Nishi, T. Miyazawa, S. Fujita, M. Okada, and T. Takemura, “A Novel OCRL1 Mutation in a Patient with the Mild Phenotype of Lowe Syndrome,” Tohoku J. Exp. Med., vol. 232, no. 3, pp. 163–166, 2014, doi: 10.1620/TJEM.232.163.

[11] S. C. Carim et al., “IPIP27 Coordinates PtdIns(4,5)P 2 Homeostasis for Successful Cytokinesis,” Curr. Biol., vol. 29, no. 5, pp. 775-789.e7, Mar. 2019, doi: 10.1016/J.CUB.2019.01.043/ATTACHMENT/81FF3F92-AE03-4CD1-B3C1-694BC9532FB3/MMC1.PDF.

[12] D. Dambournet et al., “Rab35 GTPase and OCRL phosphatase remodel lipids and F-actin for successful cytokinesis,” Nat. Cell Biol. 2011 138, vol. 13, no. 8, pp. 981–988, Jun. 2011, doi: 10.1038/ncb2279.

[13] N. Okamoto et al., “Disturbed chromosome segregation and multipolar spindle formation in a patient with CHAMP1 mutation,” Mol. Genet. Genomic Med., vol. 5, no. 5, p. 585, Sep. 2017, doi: 10.1002/MGG3.303.

[14] M. Garrity et al., “Neurodevelopmental phenotypes in individuals with pathogenic variants in CHAMP1,” Cold Spring Harb. Mol. Case Stud., vol. 7, no. 4, Aug. 2021, doi: 10.1101/MCS.A006092/-/DC1.

[15] P. Steigemann and D. W. Gerlich, “Cytokinetic abscission: cellular dynamics at the midbody,” Trends Cell Biol., vol. 19, no. 11, pp. 606–616, Nov. 2009, doi: 10.1016/J.TCB.2009.07.008.

[16] J. P. Fededa and D. W. Gerlich, “Molecular control of animal cell cytokinesis,” Nat. Cell Biol., vol. 14, no. 5, pp. 440–447, 2012, doi: 10.1038/NCB2482.

[17] N. Elia, R. Sougrat, T. A. Spurlin, J. H. Hurley, and J. Lippincott-Schwartz, “Dynamics of endosomal sorting complex required for transport (ESCRT) machinery during cytokinesis and its role in abscission,” Proc. Natl. Acad. Sci. U. S. A., vol. 108, no. 12, pp. 4846–4851, Mar. 2011, doi: 10.1073/PNAS.1102714108/-/DCSUPPLEMENTAL/PNAS.201102714SI.PDF.

[18] J. Guizetti et al., “Cortical constriction during abscission involves helices of ESCRT-III-dependent filaments,” Science, vol. 331, no. 6024, pp. 1616–1620, Mar. 2011, doi: 10.1126/SCIENCE.1201847.

[19] B. Mierzwa and D. W. Gerlich, “Cytokinetic abscission: molecular mechanisms and temporal control,” Dev. Cell, vol. 31, no. 5, pp. 525–538, Dec. 2014, doi: 10.1016/J.DEVCEL.2014.11.006.

[20] D. Yang, N. Rismanchi, B. Renvoisé, J. Lippincott-Schwartz, C. Blackstone, and J. H. Hurley, “Structural basis for midbody targeting of spastin by the ESCRT-III protein CHMP1B,” Nat. Struct. Mol. Biol. 2008 1512, vol. 15, no. 12, pp. 1278–1286, Nov. 2008, doi: 10.1038/nsmb.1512.

[21] J. W. Connell, C. Lindon, J. P. Luzio, and E. Reid, “Spastin couples microtubule severing to membrane traffic in completion of cytokinesis and secretion,” Traffic, vol. 10, no. 1, pp. 42–56, 2009, doi: 10.1111/J.1600-0854.2008.00847.X.

[22] C. Cauvin et al., “Rab35 GTPase Triggers Switch-like Recruitment of the Lowe Syndrome Lipid Phosphatase OCRL on Newborn Endosomes,” Curr. Biol., vol. 26, no. 1, pp. 120–128, Jan. 2016, doi: 10.1016/J.CUB.2015.11.040/ATTACHMENT/89BE4714-3190-476A-998D-B0F98E6AF393/MMC1.PDF.

[23] S. Frémont et al., “Oxidation of F-actin controls the terminal steps of cytokinesis,” Nat. Commun. 2017 81, vol. 8, no. 1, pp. 1–16, Feb. 2017, doi: 10.1038/ncomms14528.

[24] C. Addi, J. Bai, and A. Echard, “Actin, microtubule, septin and ESCRT filament remodeling during late steps of cytokinesis,” Curr. Opin. Cell Biol., vol. 50, pp. 27–34, Feb. 2018, doi: 10.1016/J.CEB.2018.01.007.

[25] N. V. G. Iannantuono and G. Emery, “Rab11FIP1 maintains Rab35 at the intercellular bridge to promote actin removal and abscission,” J. Cell Sci., vol. 134, no. 12, Jun. 2021, doi: 10.1242/JCS.244384/268385/AM/RAB11FIP1-MAINTAINS-RAB35-AT-THE-INTERCELLULAR.

[26] A. Caballe et al., “ULK3 regulates cytokinetic abscission by phosphorylating ESCRT-III proteins,” Elife, vol. 4, no. MAY, pp. 1–70, May 2015, doi: 10.7554/ELIFE.06547.

[27] J. Lafaurie-Janvore et al., “ESCRT-III assembly and cytokinetic abscission are induced by tension release in the intercellular bridge,” Science, vol. 339, no. 6127, pp. 1625–1629, Mar. 2013, doi: 10.1126/SCIENCE.1233866.

[28] M. Mendoza, C. Norden, K. Durrer, H. Rauter, F. Uhlmann, and Y. Barral, “A mechanism for chromosome segregation sensing by the NoCut checkpoint,” Nat. Cell Biol., vol. 11, no. 4, pp. 477–483, 2009, doi: 10.1038/NCB1855.

[29] N. Amaral et al., “The Aurora-B-dependent NoCut checkpoint prevents damage of anaphase bridges after DNA replication stress,” Nat. Cell Biol., vol. 18, no. 5, pp. 516–526, May 2016, doi: 10.1038/NCB3343.

[30] V. Nähse, L. Christ, H. Stenmark, and C. Campsteijn, “The Abscission Checkpoint: Making It to the Final Cut,” Trends Cell Biol., vol. 27, no. 1, pp. 1–11, Jan. 2017, doi: 10.1016/J.TCB.2016.10.001.

[31] P. Steigemann et al., “Aurora B-Mediated Abscission Checkpoint Protects against Tetraploidization,” Cell, vol. 136, no. 3, pp. 473–484, Feb. 2009, doi: 10.1016/J.CELL.2008.12.020/ATTACHMENT/B6FAD07F-297F-40E8-B286-0AF50C69E6D7/MMC16.MOV.

[32] E. Petsalaki and G. Zachos, “Clks 1, 2 and 4 prevent chromatin breakage by regulating the Aurora B-dependent abscission checkpoint,” Nat. Commun., vol. 7, Apr. 2016, doi: 10.1038/NCOMMS11451.

[33] J. G. Carlton, A. Caballe, M. Agromayor, M. Kloc, and J. Martin-Serrano, “ESCRT-III governs the Aurora B-mediated abscission checkpoint through CHMP4C,” Science, vol. 336, no. 6078, pp. 220–225, Apr. 2012, doi: 10.1126/SCIENCE.1217180.

[34] D. R. Mackay and K. S. Ullman, “ATR and a Chk1-Aurora B pathway coordinate postmitotic genome surveillance with cytokinetic abscission,” Mol. Biol. Cell, vol. 26, no. 12, pp. 2217–2226, Jun. 2015, doi: 10.1091/MBC.E14-11-1563.

[35] J. Bai, H. Wioland, T. Advedissian, F. Cuvelier, G. Romet-Lemonne, and A. Echard, “Actin reduction by MsrB2 is a key component of the cytokinetic abscission checkpoint and prevents tetraploidy,” Proc. Natl. Acad. Sci. U. S. A., vol. 117, no. 8,

pp. 4169–4179, Feb. 2020, doi: 10.1073/PNAS.1911629117/SUPPL_FILE/PNAS.1911629117.SM06.AVI.

[36] M. Dandoulaki, E. Petsalaki, D. Sumpton, S. Zanivan, and G. Zachos, “Src activation by Chk1 promotes actin patch formation and prevents chromatin bridge breakage in cytokinesis,” J. Cell Biol., vol. 217, no. 9, pp. 3071–3089, Sep. 2018, doi: 10.1083/JCB.201802102.

[37] V. Andrade et al., “Caveolae promote successful abscission by controlling intercellular bridge tension during cytokinesis,” Sci. Adv., vol. 8, no. 15, p. 5095, Apr. 2022, doi: 10.1126/SCIADV.ABM5095/SUPPL_FILE/SCIADV.ABM5095_MOVIES_S1_TO_S3.ZIP.

[38] F. R. Kiral, F. E. Kohrs, E. J. Jin, and P. R. Hiesinger, “Rab GTPases and Membrane Trafficking in Neurodegeneration,” Curr. Biol., vol. 28, no. 8, pp. R471–R486, Apr. 2018, doi: 10.1016/J.CUB.2018.02.010.

[39] G. Li, “Rab GTPases, Membrane Trafficking and Diseases,” Curr. Drug Targets, vol. 12, no. 8, p. 1188, Jul. 2011, doi: 10.2174/138945011795906561.

[40] S. I. Yoshimura, A. Gerondopoulos, A. Linford, D. J. Rigden, and F. A. Barr, “Family-wide characterization of the DENN domain Rab GDP-GTP exchange factors,” J. Cell Biol., vol. 191, no. 2, pp. 367–381, Oct. 2010, doi: 10.1083/jcb.201008051.

[41] A. L. Marat, M. S. Ioannou, and P. S. McPherson, “Connecdenn 3/DENND1C binds actin linking Rab35 activation to the actin cytoskeleton,” Mol. Biol. Cell, vol. 23, no. 1, pp. 163–175, Jan. 2012, doi: 10.1091/mbc.E11-05-0474.

[42] M. S. Ioannou et al., “DENND2B activates Rab13 at the leading edge of migrating cells and promotes metastatic behavior,” J. Cell Biol., vol. 208, no. 5, pp. 629–648, 2015, doi: 10.1083/jcb.201407068.

[43] A. K. Gillingham, R. Sinka, I. L. Torres, K. S. Lilley, and S. Munro, “Toward a Comprehensive Map of the Effectors of Rab GTPases,” Dev. Cell, vol. 31, no. 3, p. 358, Nov. 2014, doi: 10.1016/j.devcel.2014.10.007.

[44] J. Blümer et al., “RabGEFs are a major determinant for specific Rab membrane targeting,” J. Cell Biol., vol. 200, no. 3, pp. 287–300, Feb. 2013, doi: 10.1083/jcb.201209113.

[45] R. Kumar, V. Francis, G. Kulasekaran, M. Khan, G. A. B. Armstrong, and P. S. McPherson, “A cell-based GEF assay reveals new substrates for DENN domains and a role for DENND2B in primary ciliogenesis,” Sci. Adv., vol. 8, no. 8, p. 3088, Feb. 2022, doi: 10.1126/sciadv.abk3088.

[46] I. Göhring et al., “Disruption of ST5 is associated with mental retardation and multiple congenital anomalies,” J. Med. Genet., vol. 47, no. 2, pp. 91–98, Feb. 2010, doi: 10.1136/jmg.2009.069799.

[47] M. S. Ioannou et al., “Intersectin-s interaction with DENND2B facilitates recycling of epidermal growth factor receptor,” EMBO Rep., vol. 18, no. 12, pp. 2119–2130, Dec. 2017, doi: 10.15252/embr.201744034.

[48] K. I, S. M, A. N, G. B, and E. A, “Rab35 regulates an endocytic recycling pathway essential for the terminal steps of cytokinesis,” Curr. Biol., vol. 16, no. 17, pp. 1719–1725, Sep. 2006, doi: 10.1016/J.CUB.2006.07.020.

[49] C. Addi et al., “The Flemmingsome reveals an ESCRT-to-membrane coupling via ALIX/syntenin/syndecan-4 required for completion of cytokinesis,” Nat. Commun. 2020 111, vol. 11, no. 1, pp. 1–15, Apr. 2020, doi: 10.1038/s41467-020-15205-z.

[50] L. Capalbo et al., “The midbody interactome reveals unexpected roles for PP1 phosphatases in cytokinesis,” Nat. Commun. 2019 101, vol. 10, no. 1, pp. 1–17, Oct. 2019, doi: 10.1038/s41467-019-12507-9.

[51] X. Wu et al., “Insights regarding guanine nucleotide exchange from the structure of a DENN-domain protein complexed with its Rab GTPase substrate,” Proc. Natl. Acad. Sci. U. S. A., vol. 108, no. 46, pp. 18672–18677, Nov. 2011, doi: 10.1073/pnas.1110415108.

[52] J. Jumper et al., “Highly accurate protein structure prediction with AlphaFold,” Nat. 2021 5967873, vol. 596, no. 7873, pp. 583–589, Jul. 2021, doi: 10.1038/s41586-021-03819-2.

[53] H. Kobayashi and M. Fukuda, “Rab35 establishes the EHD1-association site by coordinating two distinct effectors during neurite outgrowth,” J. Cell Sci., vol. 126, no. Pt 11, pp. 2424–2435, Jun. 2013, doi: 10.1242/JCS.117846.

[54] M. Sato, K. Sato, W. Liou, S. Pant, A. Harada, and B. D. Grant, “Regulation of endocytic recycling by C. elegans Rab35 and its regulator RME-4, a coated-pit protein,” EMBO J., vol. 27, no. 8, pp. 1183–1196, Apr. 2008, doi: 10.1038/EMBOJ.2008.54.

[55] P. D. Allaire, A. L. Marat, C. Dall’Armi, G. Di Paolo, P. S. McPherson, and B. Ritter, “The Connecdenn DENN Domain: A GEF for Rab35 Mediating Cargo-Specific Exit from Early Endosomes,” Mol. Cell, vol. 37, no. 3, pp. 370–382, Feb. 2010, doi: 10.1016/j.molcel.2009.12.037.

[56] F. Barr and D. G. Lambright, “Rab GEFs and GAPs,” Curr. Opin. Cell Biol., vol. 22, no. 4, p. 461, Aug. 2010, doi: 10.1016/J.CEB.2010.04.007.

[57] M. Cabrera and C. Ungermann, “Guanine nucleotide exchange factors (GEFs) have a critical but not exclusive role in organelle localization of rab GTPases,” J. Biol. Chem., vol. 288, no. 40, pp. 28704–28712, Oct. 2013, doi: 10.1074/jbc.M113.488213.

[58] E. Petsalaki and G. Zachos, “The Abscission Checkpoint: A Guardian of Chromosomal Stability,” Cells, vol. 10, no. 12, Dec. 2021, doi: 10.3390/CELLS10123350.

[59] Y. Yasui et al., “Autophosphorylation of a newly identified site of Aurora-B is indispensable for cytokinesis,” J. Biol. Chem., vol. 279, no. 13, pp. 12997–13003, Mar. 2004, doi: 10.1074/JBC.M311128200.

[60] S. R. Pfeffer, “Rab GTPases: Master regulators that establish the secretory and endocytic pathways,” Molecular Biology of the Cell, vol. 28, no. 6. American Society for Cell Biology, pp. 712–715, Mar. 15, 2017. doi: 10.1091/mbc.E16-10-0737.

[61] R. Prekeris, “Actin regulation during abscission: unexpected roles of Rab35 and endocytic transport,” Cell Res. 2011 219, vol. 21, no. 9, pp. 1283–1285, Aug. 2011, doi: 10.1038/cr.2011.131.

[62] H. Horiuchi et al., “A novel Rab5 GDP/GTP exchange factor complexed to Rabaptin-5 links nucleotide exchange to effector recruitment and function,” Cell, vol. 90, no. 6, pp. 1149–1159, Sep. 1997, doi: 10.1016/S0092-8674(00)80380-3.

[63] H. Stenmark, G. Vitale, O. Ullrich, and M. Zerial, “Rabaptin-5 is a direct effector of the small GTPase Rab5 in endocytic membrane fusion,” Cell, vol. 83, no. 3, pp. 423–432, Nov. 1995, doi: 10.1016/0092-8674(95)90120-5.

[64] R. Lippé, M. Miaczynska, V. Rybin, A. Runge, and M. Zerial, “Functional Synergy between Rab5 Effector Rabaptin-5 and Exchange Factor Rabex-5 When Physically Associated in a Complex,” Mol. Biol. Cell, vol. 12, no. 7, p. 2219, 2001, doi: 10.1091/MBC.12.7.2219.

[65] M. Medkova, Y. E. France, J. Coleman, and P. Novick, “The rab exchange factor Sec2p reversibly associates with the exocyst,” Mol. Biol. Cell, vol. 17, no. 6, pp. 2757–2769, Jun. 2006, doi: 10.1091/MBC.E05-10-0917.

[66] B. Ritter, S. M. Ferguson, P. De Camilli, and P. S. McPherson, “A lentiviral system for efficient knockdown of proteins in neuronal cultures [version 1; referees: 2 approved],” MNI open Res., vol. 1, no. 2, p. 2, Dec. 2017, doi: 10.12688/MNIOPENRES.12766.1.

[67] S. E. Reed, E. M. Staley, J. P. Mayginnes, D. J. Pintel, and G. E. Tullis, “Transfection of mammalian cells using linear polyethylenimine is a simple and effective means of producing recombinant adeno-associated virus vectors,” J. Virol. Methods, vol. 138, no. 1–2, pp. 85–98, Dec. 2006, doi: 10.1016/J.JVIROMET.2006.07.024.

Figures for Chapter 4

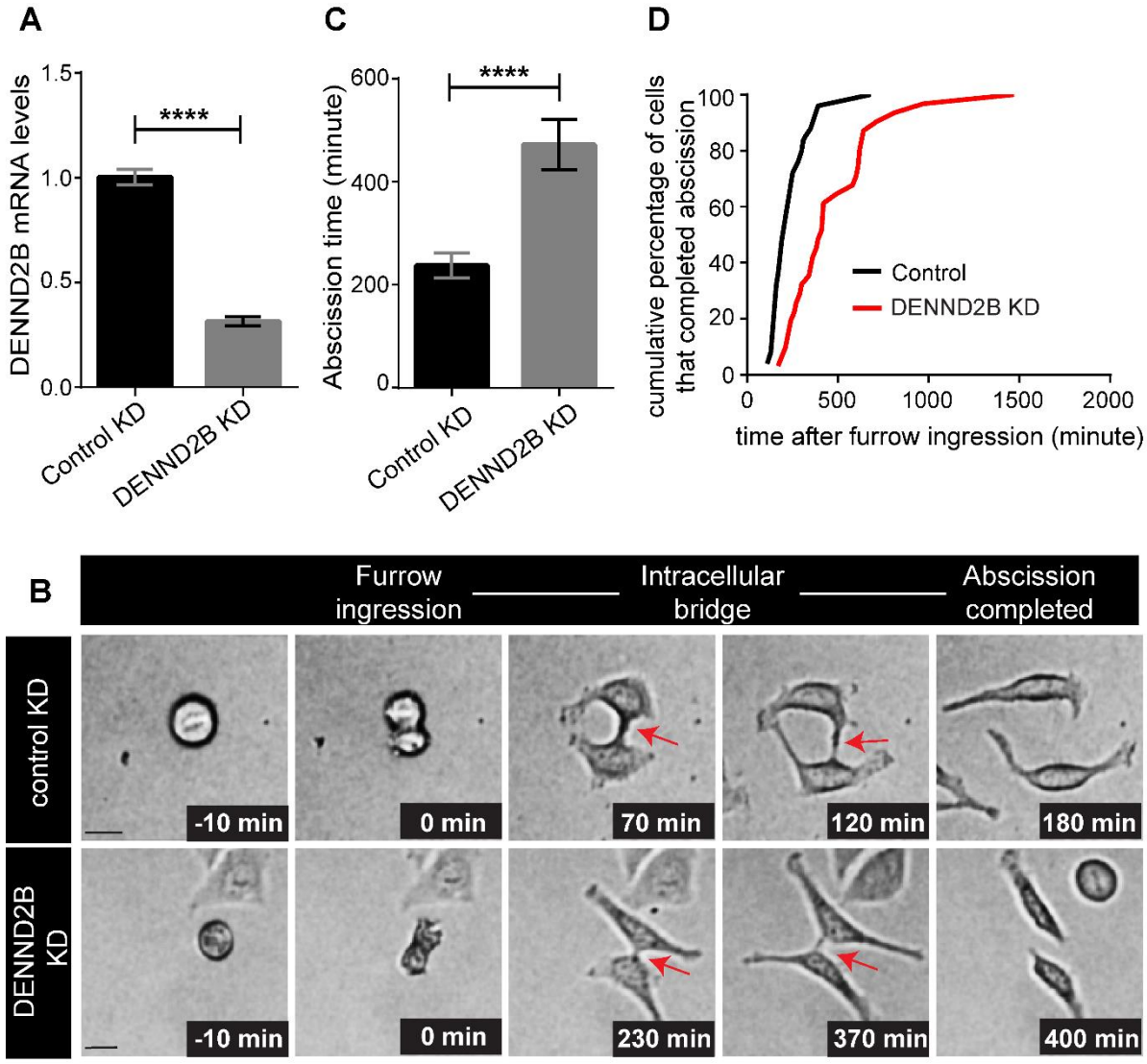

Figure 1. DENND2B is required for cytokinetic abscission.

(A) HeLa cells were transduced with control or DENND2B shRNA lentivirus and DENND2B mRNA levels were quantified by real-time PCR; mean ± SEM; unpaired t-test (****, P ≤ 0.0001). **(B)** Representative images of time-lapse phase-contrast microscopy of control or DENND2B KD HeLa cells. Time zero is set as the frame of furrow ingression. Scale bars = 20 μm. The red arrow represents the cytokinetic bridge. **(C)** Quantification of mean abscission timing of cytokinesis in control or

DENDN2B KD cells; mean ± SEM; Mann-Whitney U test (****, P < 0.0001; >30 cells per condition). **(D)** Control or DENND2B KD HeLa cells were imaged by time-lapse microscopy. The plot represents the cumulative percentage of cells that completed abscission (abscission time).

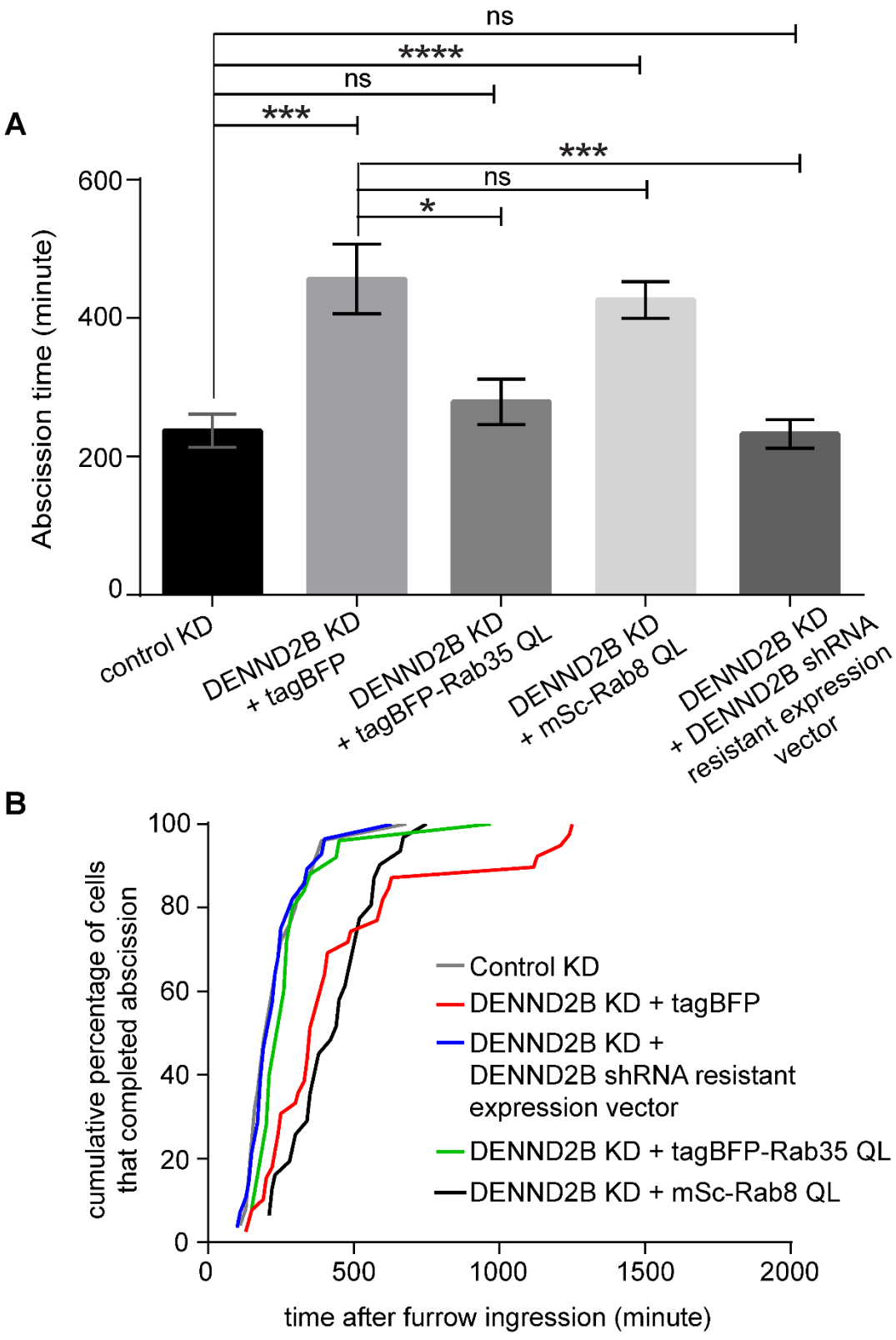
A
ns
****
ns
***
***
ns
*
600
400
200
0
Abscission time (minute)
control KD
DENND2B KD + tagBFP
DENND2B KD + tagBFP-Rab35 QL
DENND2B KD + mSc-Rab8 QL
DENND2B KD + DENND2B shRNA resistant expression vector
B
100
80
60
40
20
0
cumulative percentage of cells that completed abscission
0
500
1000
1500
2000
time after furrow ingression (minute)
Control KD
DENND2B KD + tagBFP
DENND2B KD + DENND2B shRNA resistant expression vector
DENND2B KD + tagBFP-Rab35 QL
DENND2B KD + mSc-Rab8 QL

Figure 2. Expression of Rab35 active mutant in DENND2B KD cells rescues cytokinesis.

(A) DENND2B KD HeLa cells were transduced with lentivirus mediating expression of tagBFP or tagBFP-Rab35 QL or mSc-Rab8 QL or mSc-DENND2B (resistant to DENND2B KD shRNA) and cytokinetic abscission timing was calculated using time-lapse phase contrast microscopy. The graph represents the quantification of mean abscission timing of cytokinesis; mean ± SEM; Kruskal-Wallis test, with pairwise multiple comparison test (****, $P < 0.0001$; ***, $P < 0.001$; **, $P < 0.01$; *, $P < 0.05$; >25 cells per condition) **(B)** HeLa cells in **A** were imaged by time-lapse microscopy. The data represents the cumulative percentage of cells that completed abscission (abscission time).

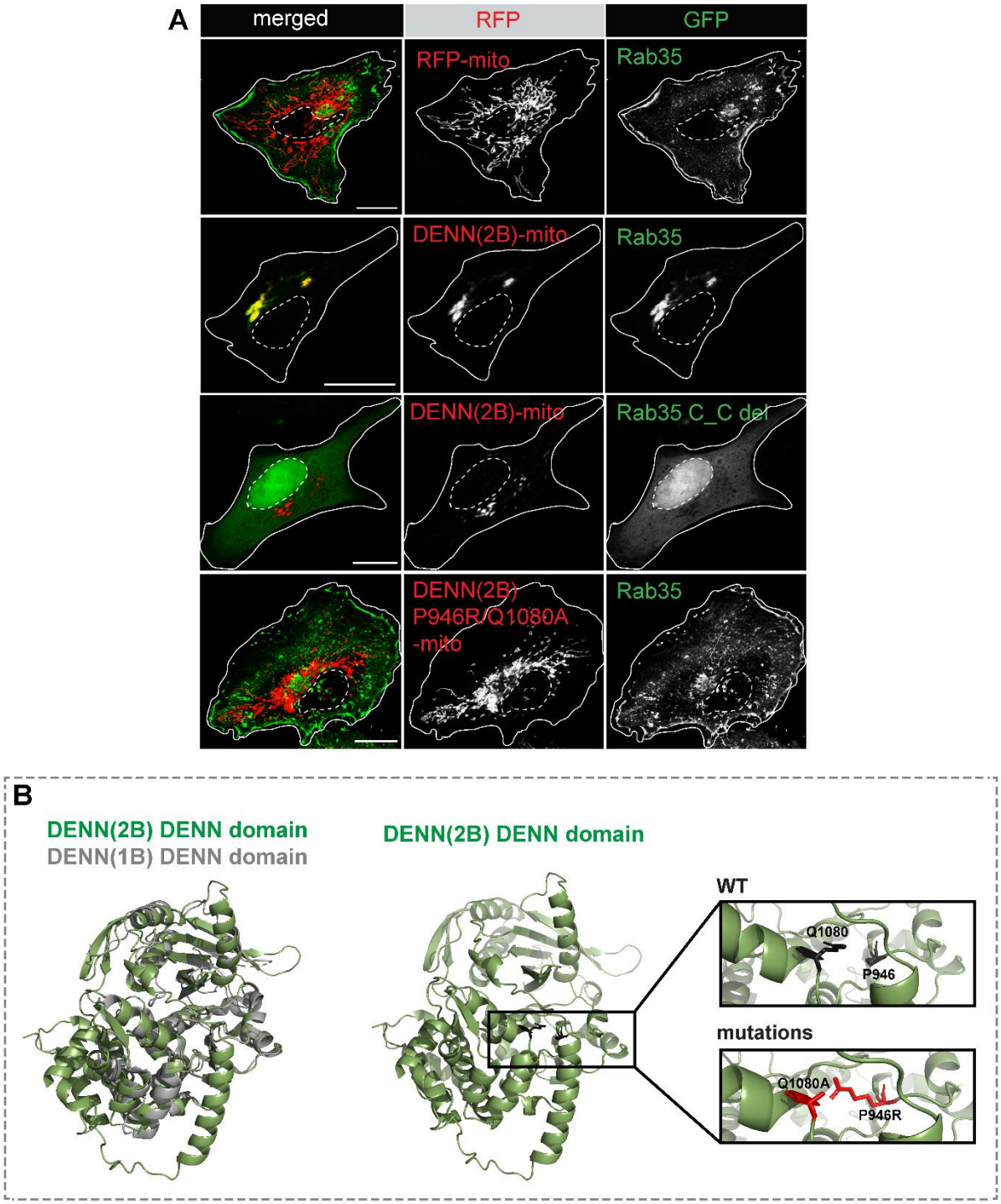
A
merged
RFP
GFP
RFP-mito
Rab35
DENN(2B)-mito
Rab35
DENN(2B)-mito
Rab35 C_C del
DENN(2B) P946R/Q1080A -mito
Rab35
B
DENN(2B) DENN domain
DENN(1B) DENN domain
DENN(2B) DENN domain
WT
Q1080
P946
mutations
Q1080A
P946R

Figure 3. DENND2B functions as a GEF for Rab35.

(A) HeLa cells co-transfected with GFP-Rab35 and RFP-mito or GFP-Rab35 and DENN(2B)-mito or DENN(2B)-mito and GFP-Rab35 C_C del or DENN(2B)-mito with double mutations P946R/Q1080A and GFP-Rab35. White solid line mark the cell periphery and dotted white line mark the nucleus. **(B)** Superposition of the crystal structure of the DENN domain of DENND1B [51] and an AlphaFold predicted structure of the DENN domain of DENND2B. Highlighted are two key residues involved in GEF activity and their mutation.

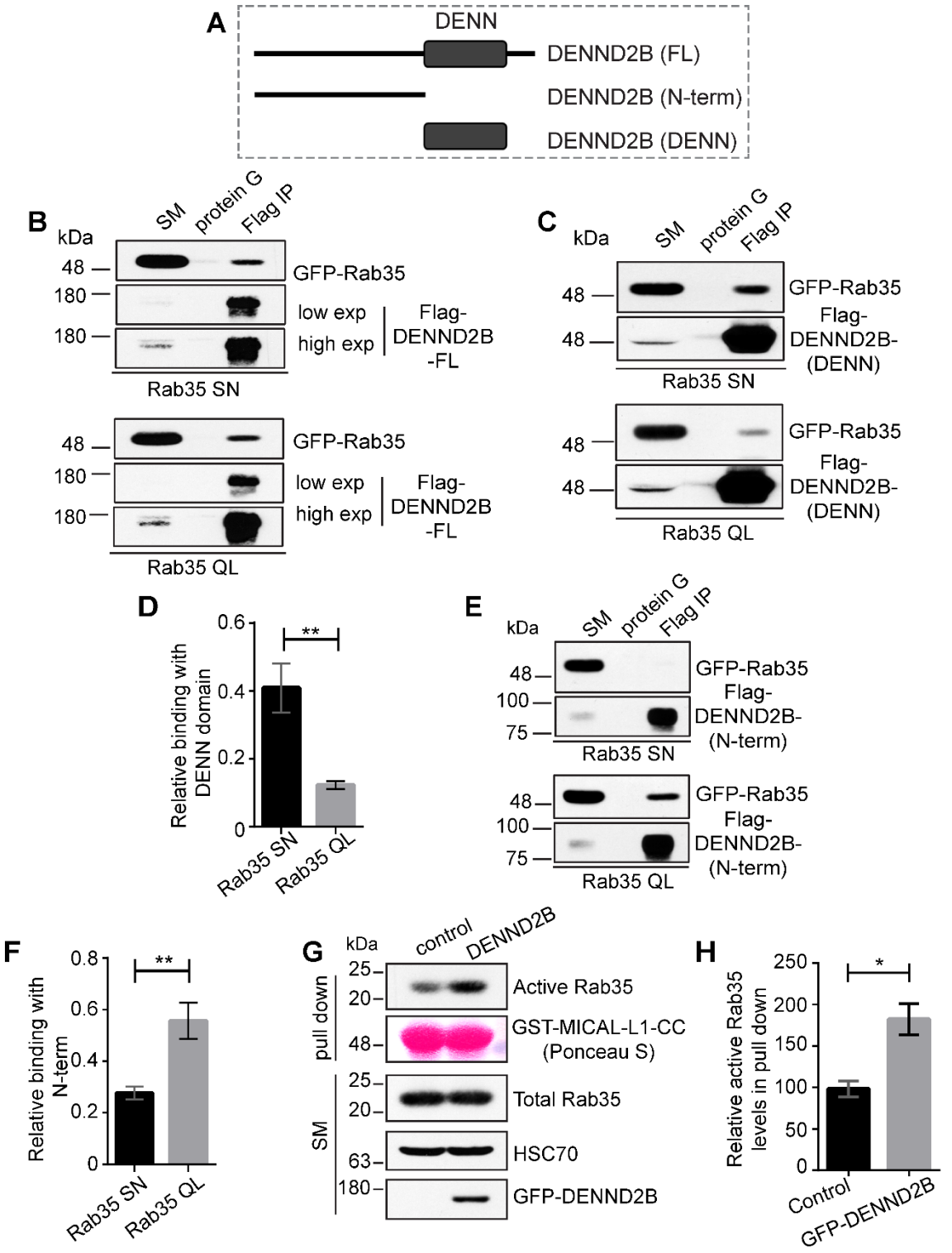
A
DENN
DENND2B (FL)
DENND2B (N-term)
DENND2B (DENN)
B
kDa
SM
protein G
Flag IP
48
180
180
GFP-Rab35
low exp
high exp
Flag-DENND2B-FL
Rab35 SN
48
180
180
GFP-Rab35
low exp
high exp
Flag-DENND2B-FL
Rab35 QL
C
kDa
SM
protein G
Flag IP
48
48
GFP-Rab35
Flag-DENND2B-(DENN)
Rab35 SN
48
48
GFP-Rab35
Flag-DENND2B-(DENN)
Rab35 QL
D
Relative binding with DENN domain
0.6
0.4
0.2
0
**
Rab35 SN
Rab35 QL
E
kDa
SM
protein G
Flag IP
48
100
75
GFP-Rab35
Flag-DENND2B-(N-term)
Rab35 SN
48
100
75
GFP-Rab35
Flag-DENND2B-(N-term)
Rab35 QL
F
Relative binding with N-term
0.8
0.6
0.4
0.2
0
**
Rab35 SN
Rab35 QL
G
kDa
control
DENND2B
pull down
25
20
48
Active Rab35
GST-MICAL-L1-CC (Ponceau S)
SM
25
20
63
180
Total Rab35
HSC70
GFP-DENND2B
H
Relative active Rab35 levels in pull down
250
200
150
100
50
0
*
Control
GFP-DENND2B

Figure 4. Nucleotide specificity of the DENN domain and the N-terminus of DENND2B interaction with Rab35.

(A) HEK-293T cells were transfected with GFP-DENND2B. At 24 h post-transfection, transfected or untransfected (control) cell lysates were incubated with purified GST-MICAL-L1-CC. Specifically bound proteins were detected by immunoblot with anti-Rab35 antibody or anti-GFP antibody recognizing DENND2B or anti-HSC70 antibody for loading control. **(B)** Quantification of relative binding of active Rab35 with GST-MICAL-L1-CC from experiments as in **G**; mean ± SEM; unpaired t-test (*, $P < 0.05$; n = 3). **(C)** Schematic representation of various DENND2B constructs used in the biochemical experiments. **(D)** HEK-293T cells were co-transfected with Flag-DENND2B FL and GFP-Rab35 SN or GFP-Rab35 QL. At 24 h post-transfection, cells were lysed and incubated with protein G-agarose alone (mock) or protein G-agarose with anti-Flag antibody (Flag IP). Specifically bound proteins were detected by immunoblot with anti-GFP antibody to detect active/inactive Rab35 or anti-Flag antibody recognizing DENND2B. **(E)** HEK-293T cells were co-transfected with Flag-DENND2B (DENN) and GFP-Rab35 SN or GFP-Rab35 QL. At 24 h post-transfection, cells were lysed and incubated with protein G-agarose alone (mock) or protein G-agarose with anti-Flag antibody (Flag IP). Specifically bound proteins were detected by immunoblot with anti-GFP antibody to detect active/inactive Rab35 or anti-Flag antibody recognizing DENND2B (DENN). **(F)** Quantification of experiments as in **E**; mean ± SEM; unpaired t-test (**, $P \leq 0.01$; n = 4). **(F)** HEK-293T cells were co-transfected with Flag-DENND2B (N-term) and GFP-Rab35 SN or GFP-Rab35 QL. At 24 h post-transfection, cells were lysed and incubated with protein G-agarose alone (mock) or protein G-agarose with anti-Flag antibody (Flag IP). Specifically bound proteins were detected by immunoblot with anti-GFP antibody to detect active/inactive

Rab35 or anti-Flag antibody recognizing DENND2B (N-term). **(G)** Quantification of experiment as in **F**; mean ± SEM; unpaired t-test (**, P ≤ 0.01; n = 4).

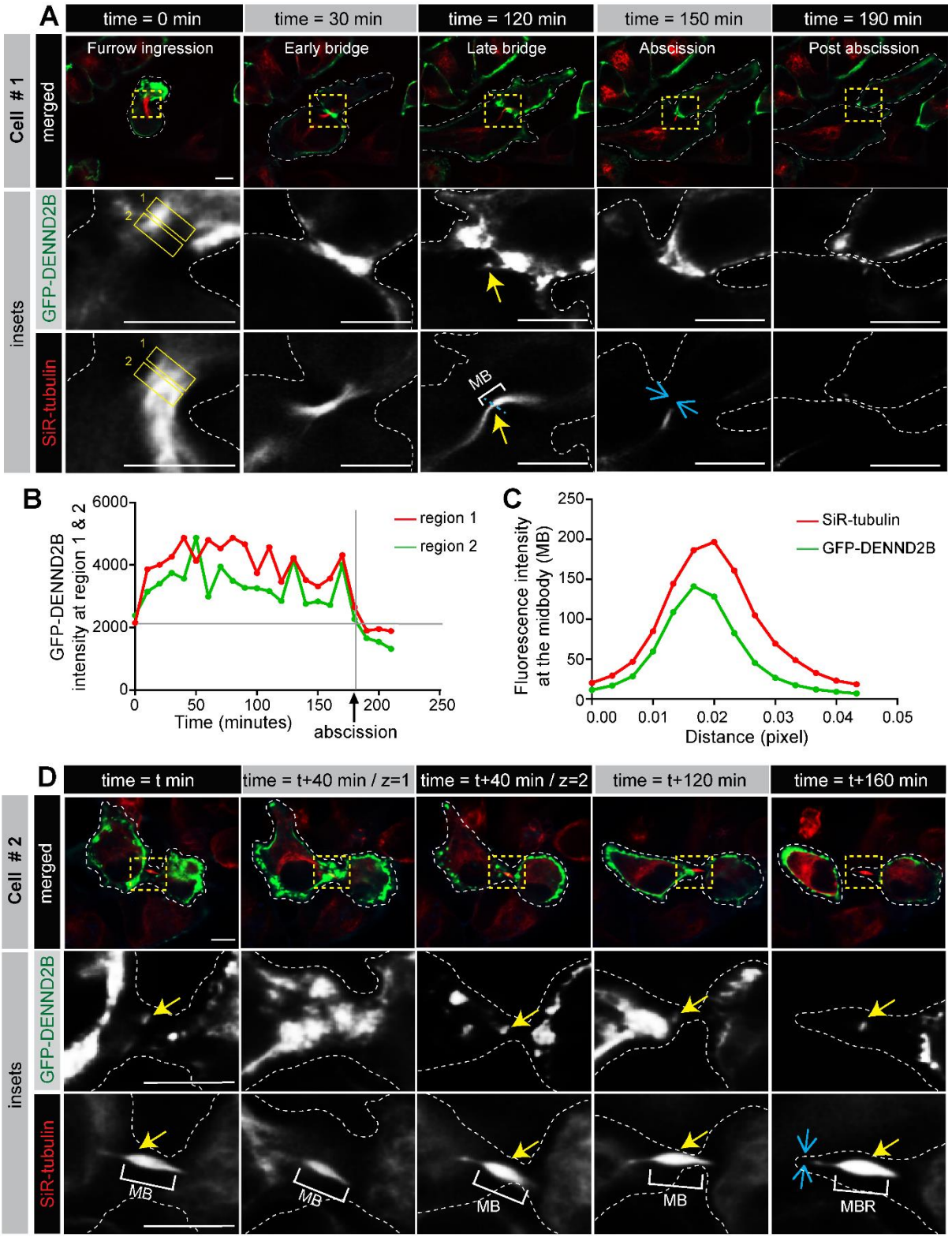
A
time = 0 min
time = 30 min
time = 120 min
time = 150 min
time = 190 min
Cell # 1
merged
Furrow ingression
Early bridge
Late bridge
Abscission
Post abscission
insets
GFP-DENND2B
SiR-tubulin
MB
B
GFP-DENND2B intensity at region 1 & 2
region 1
region 2
Time (minutes)
abscission
C
Fluorescence intensity at the midbody (MB)
SiR-tubulin
GFP-DENND2B
Distance (pixel)
D
time = t min
time = t+40 min / z=1
time = t+40 min / z=2
time = t+120 min
time = t+160 min
Cell # 2
MBR

Figure 5. Time course of DENND2B recruitment at the cell-cell interface and midbody.

(A) HeLa cells were transfected with GFP-DENND2B. At 24 h post transfection, cells were stained with SiR-tubulin and time-lapse imaging was performed using widefield fluorescence microscopy followed by deconvolution. Images represent frames of progressing cytokinesis over time, showing localization of DENND2B at the cell-cell interface and midbody. The yellow arrow represents localization of DENND2B at the midbody. The blue arrow represents completed abscission. Scale bars = 10 μm for the low-magnification images and 10 μm for the higher magnification insets (represented with yellow dotted box). The dotted white line marks the periphery of the dividing cell. **(B)** Plot of the fluorescence intensity of DENDN2B from the corresponding regions 1 and 2 drawn in **A** at the cell-cell interfaces throughout multiple frames over time. **(C)** Fluorescence intensity profiles along the dotted blue line from the inset image in **A** across the midbody (MB). **(D)** HeLa cells were processed as in **A** and already dividing cell was imaged over time and across multiple z-planes using widefield fluorescence microscopy followed by deconvolution. Images represent frames of progressing cytokinesis over time, showing localization of DENND2B at the cell-cell interface and midbody. The yellow arrow represents the localization of DENND2B at the midbody. The blue arrows represent completed abscission. Scale bars = 10 μm for the low-magnification images and 10 μm for the higher magnification insets (represented with yellow dotted box). Dotted white line marks the periphery of dividing cell.

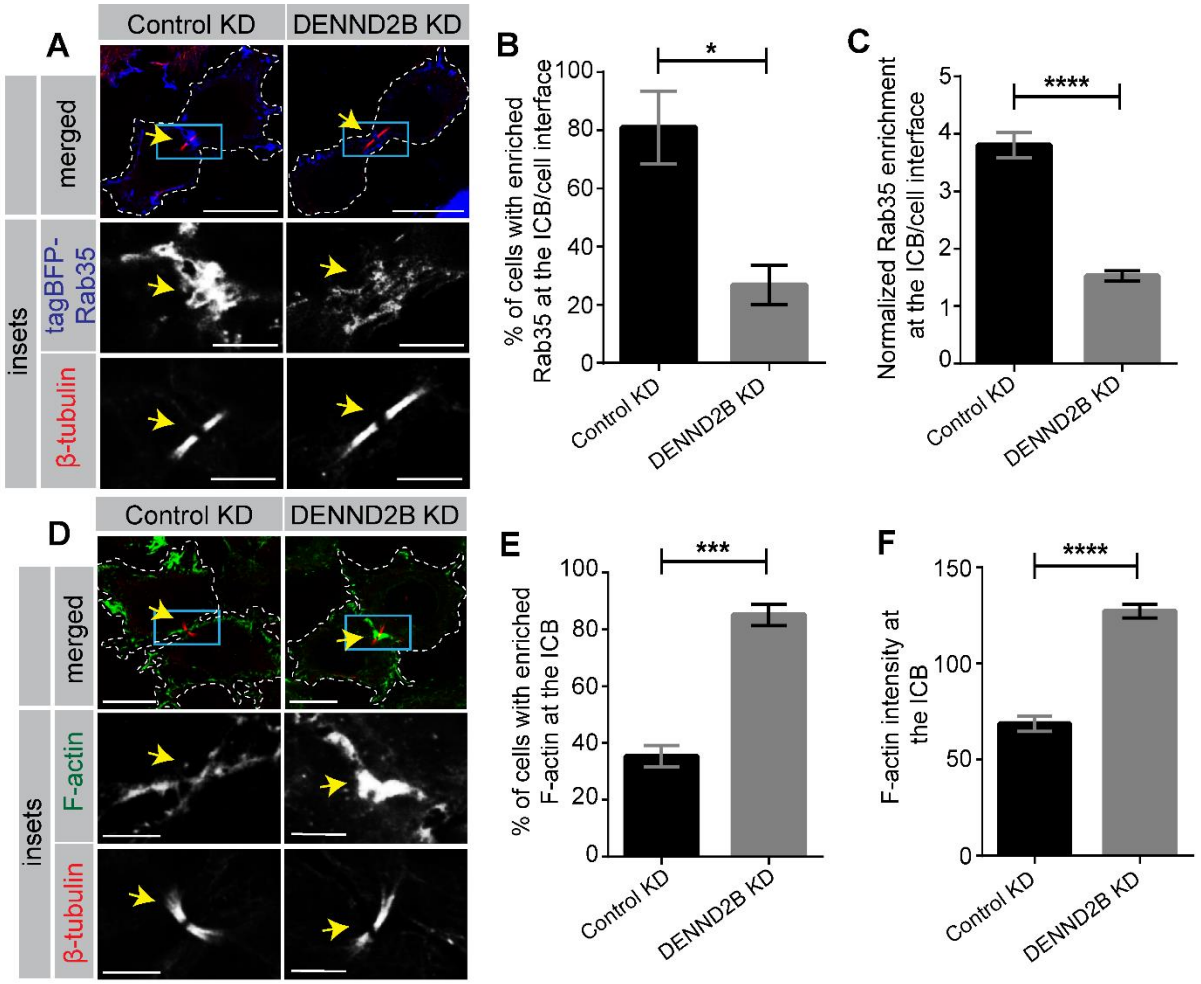

Figure 6. DENND2B KD causes loss of Rab35 and increased accumulation of F-actin at the cytokinetic bridge.

(A) HeLa cells stably expressing tagBFP-Rab35 were transduced with control or DENND2B shRNA lentivirus. Cells were fixed and stained with β-tubulin to identify cytokinetic bridge. Scale bars = 20 μm for the low-magnification images and, 5.93 μm and 5.78 μm for the higher magnification insets corresponding to control or DENND2B KD cells (represented with blue box). The dotted white line marks the periphery of dividing cells. The yellow arrows represent cytokinetic bridges. **(B)** Quantification of experiment as in **A**; mean ± SEM; unpaired t-test (*, P ≤ 0.05; >25 cells per condition) **(C)** Quantification of experiments as in **A**; mean ± SEM; Mann-Whitney U test (****, P

≤ 0.0001; >25 cells per condition) **(D)** HeLa cells were transduced with control or DENND2B shRNA lentivirus. Cells were fixed and stained with Phalloidin for F-actin and β-tubulin. Scale bars = 20 μm for the low-magnification images and 7 μm for the higher magnification insets (represented with blue box). Dotted white line marks the periphery of dividing cell. The yellow arrows represent cytokinetic bridges. **(E)** Quantification of experiment as in **D**; mean ± SEM; unpaired t-test (***, P ≤ 0.001; >25 cells per condition) **(F)** Quantification of experiments as in **D**; mean ± SEM; unpaired t-test (****, P ≤ 0.0001; >25 cells per condition)**.**

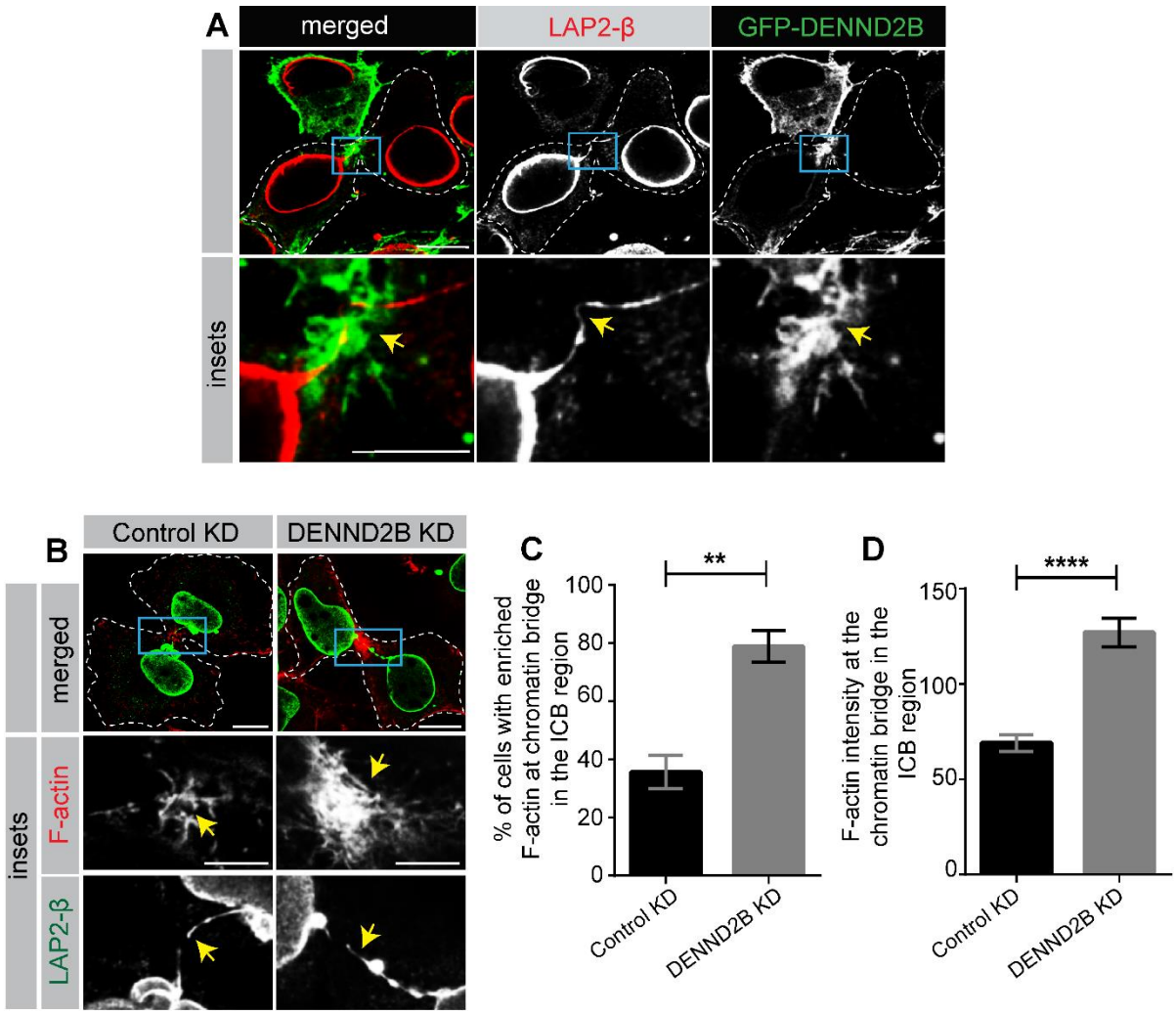

Figure 7. DENND2B is recruited to the midbody in the presence of chromatin bridges and controls F-actin levels.

(A) HeLa cells were transduced with lentivirus mediating expression of GFP-DENDN2B. Cells were fixed and stained with LAP2- β. Scale bars = 12.7 μm for the low-magnification images and 6.35 μm for the higher magnification insets (represented with blue box). Dotted white line marks the periphery of dividing cell. **(B)** HeLa cells were transduced with control or DENND2B shRNA lentivirus. Cells were fixed and stained with Phalloidin for F-actin and LAP2- β for chromatin bridge. Scale bars = 14.3 μm and 14.8 μm for the low-magnification images corresponding to control and

DENND2B KD cells and 7.15 µm and 7.4 µm for the higher magnification insets corresponding to control and DENND2B KD cells (represented with blue box). Dotted white lines mark the periphery of dividing cell. **(C)** Quantification of experiment in (B); mean ± SEM; unpaired t-test (**, P ≤ 0.01; >25 cells per condition) **(D)** Quantification of experiment in (B); mean ± SEM; unpaired t-test (****, P ≤ 0.01; >25 cells per condition)**.**

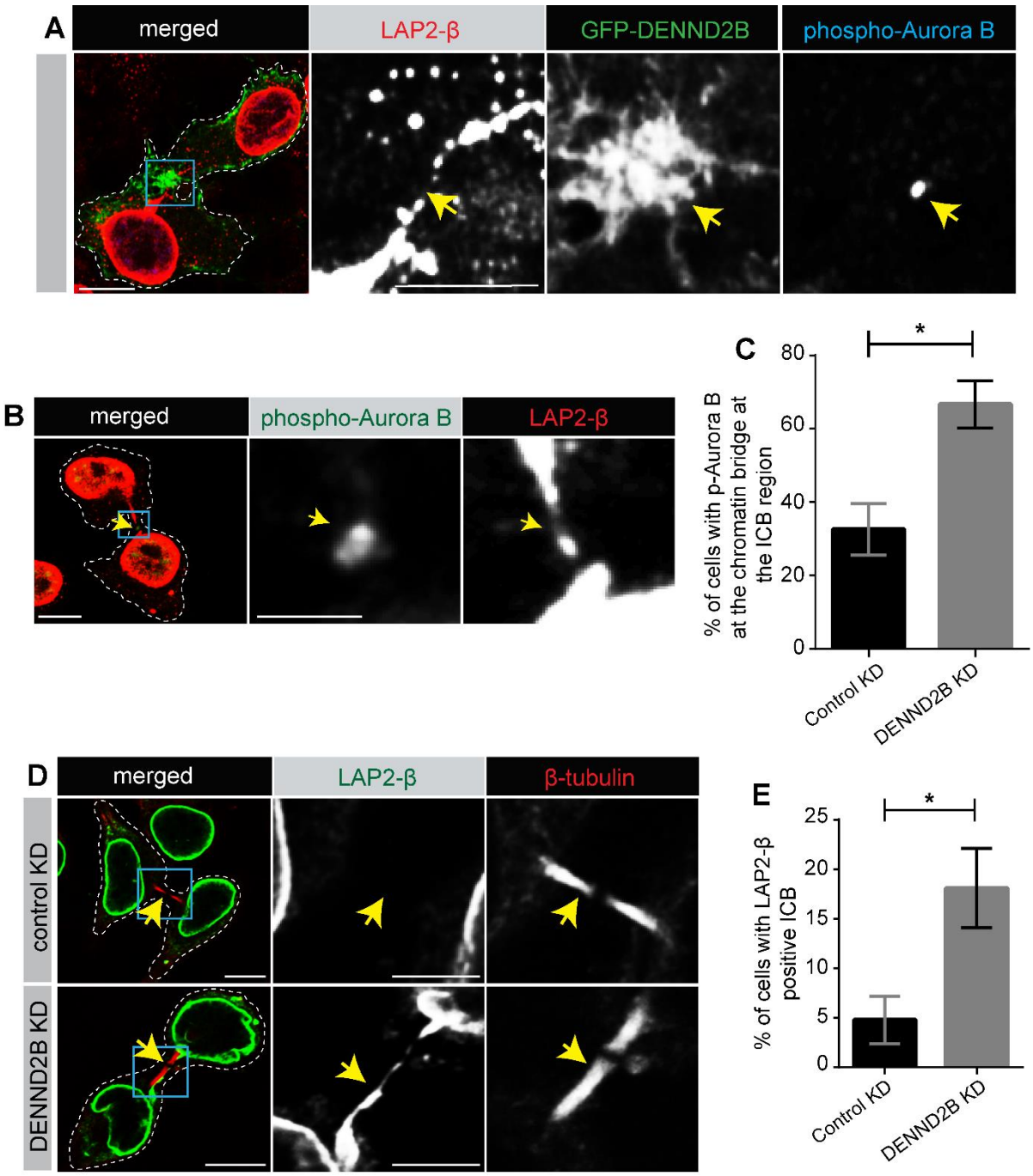

Figure 8. DENND2B colocalizes with Aurora B and functionally regulate abscission checkpoint.

(A) HeLa cells were transduced with lentivirus mediating expression of GFP-DENDN2B, Cells were fixed and stained with LAP2- β and phospho-Aurora B. Scale bars = 10 μm for the low-magnification images and 5 μm for the higher magnification

insets (represented with blue box). Dotted white line marks the periphery of dividing cell. Yellow arrow represents overlap of DENND2B, and phospho-Aurora B. **(B)** HeLa cells were fixed and stained with LAP2- β and phospho-Aurora B. Scale bars = 10 μm for the low-magnification images and 2.5 μm for the higher magnification insets (represented with blue box). Dotted white line marks the periphery of dividing cell. Yellow arrow represents presence of phospho-Aurora B at the chromatin bridge. **(C)** Quantification of experiment in (B); mean ± SEM; unpaired t-test (*, $P \leq 0.05$; >25 cells per condition)**. (D)** HeLa cells were transduced with control or DENND2B shRNA lentivirus. Cells were fixed and stained with β-tubulin and LAP2- β. Scale bars = 10 μm for the low-magnification images and 5 μm for the higher magnification insets (represented with blue box). Dotted white line marks the periphery of dividing cell. Yellow arrow represents presence or absence of chromatin bridge at the ICB marked by β-tubulin. **(E)** Quantification of experiment in (D); mean ± SEM; unpaired t-test (*, $P \leq 0.05$; >25 cells per condition)**.**

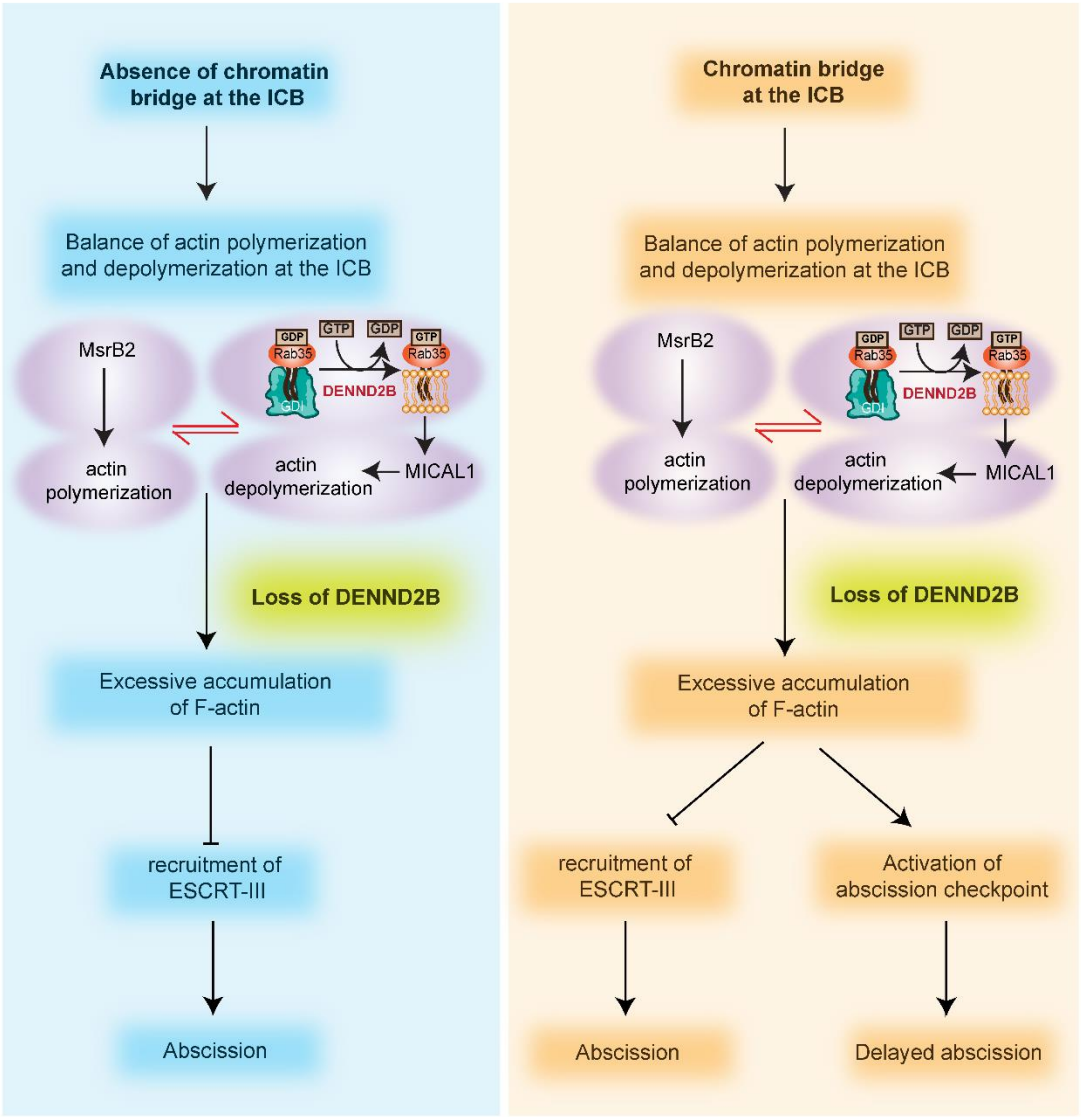

Figure 9. Proposed model of DENND2B regulation cytokinetic abscission.

DENND2B activates and recruits Rab35 at the ICB with or without chromatin bridge. Active Rab35 recruits MICAL1 which mediates depolymerization of F-actin. In the absence of DENND2B, F-actin accumulates at the bridge due to action of MsrB2 which polymerizes F-actin. F-actin accumulation inhibits ESCRT-III recruitment required for successful abscission. Whereas, in the presence of chromatin bridge, loss of DENND2B causes activation of abscission checkpoint which further contributes to delayed abscission.

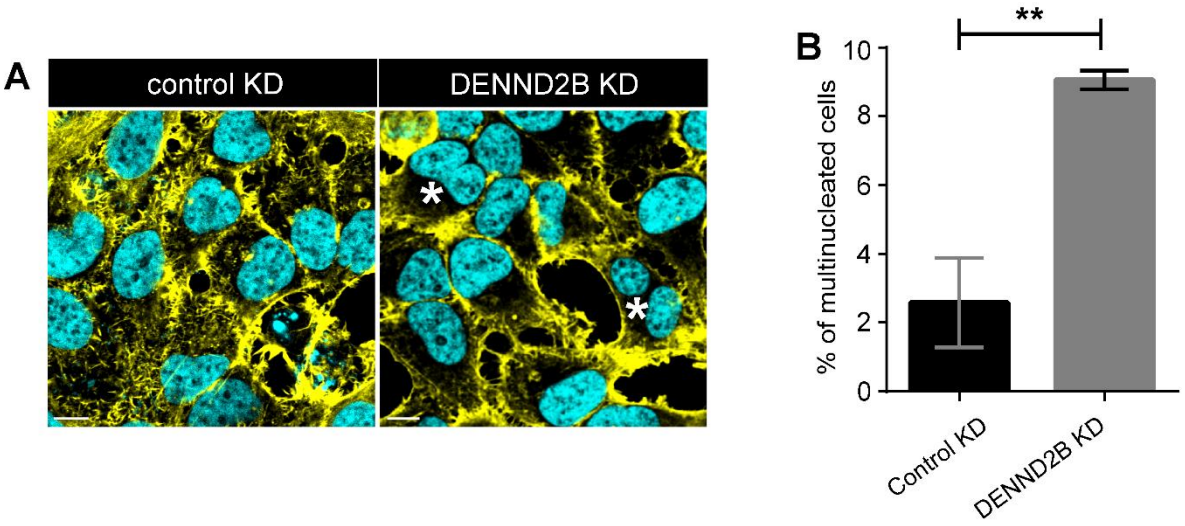

Supplementary figure 1. Loss of DENND2B increases number of binucleate cells.

(A) HeLa cells were transduced with control or DENND2B shRNA lentivirus. Cells were fixed and stained with DAPI and Phalloidin. Scale bars = 10 µm **(B)** Quantification of experiment in (A); mean ± SEM; unpaired t-test (**, P ≤ 0.01; >60 cells per condition)**.**

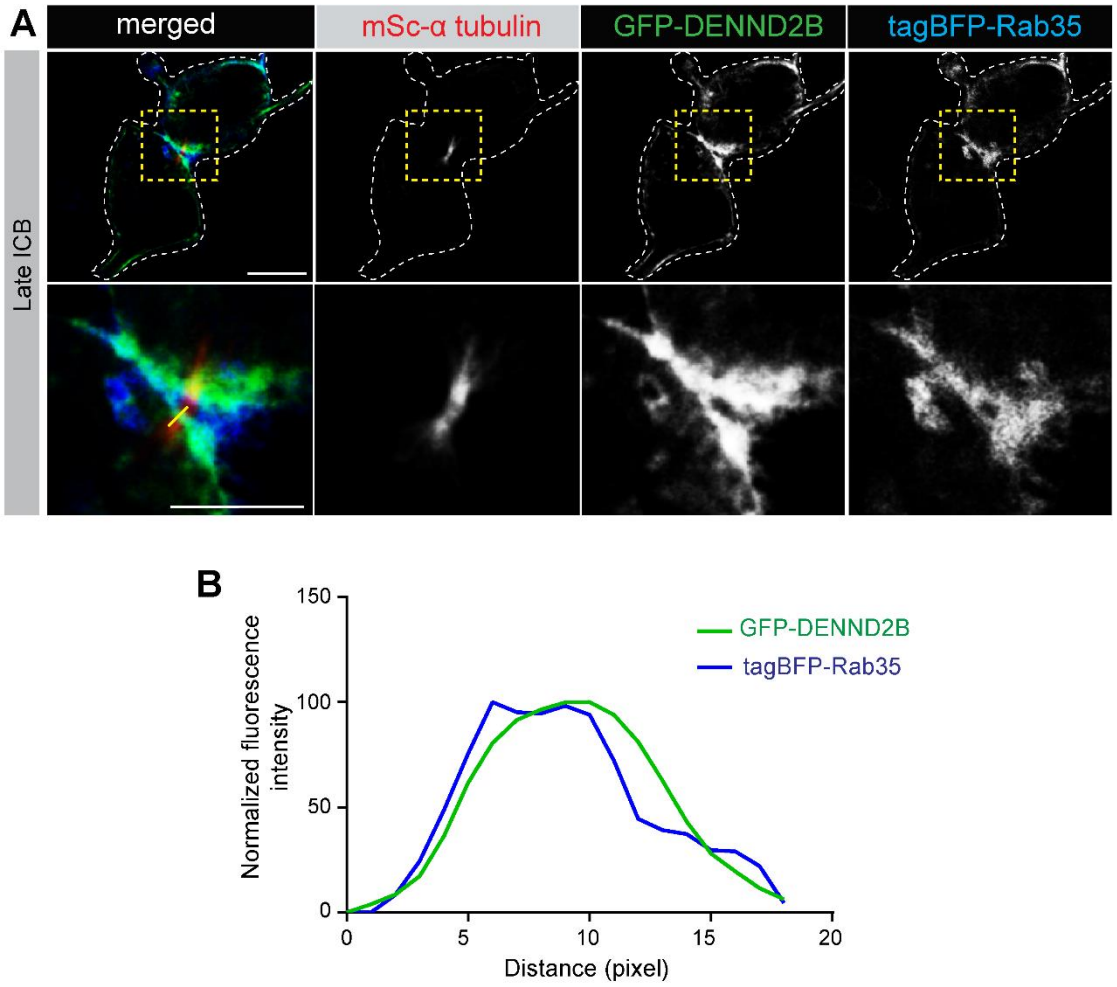

Supplementary figure 2. DENND2B and Rab35 colocalize at the cytokinetic bridge.

(A) HeLa cells were transduced with lentiviruses mediating expression of GFP-DENDN2B, mSc-alpha tubulin and tagBFP-Rab35. Cells were fixed and stained with LAP2- β. Scale bars = 13.2 μm for the low-magnification images and 6.25 μm for the higher magnification insets (represented with blue box). Dotted white line marks the periphery of dividing cell. **(B)** Normalized fluorescence intensity profiles along the yellow line from the inset image in (A) across the cytokinetic bridge.

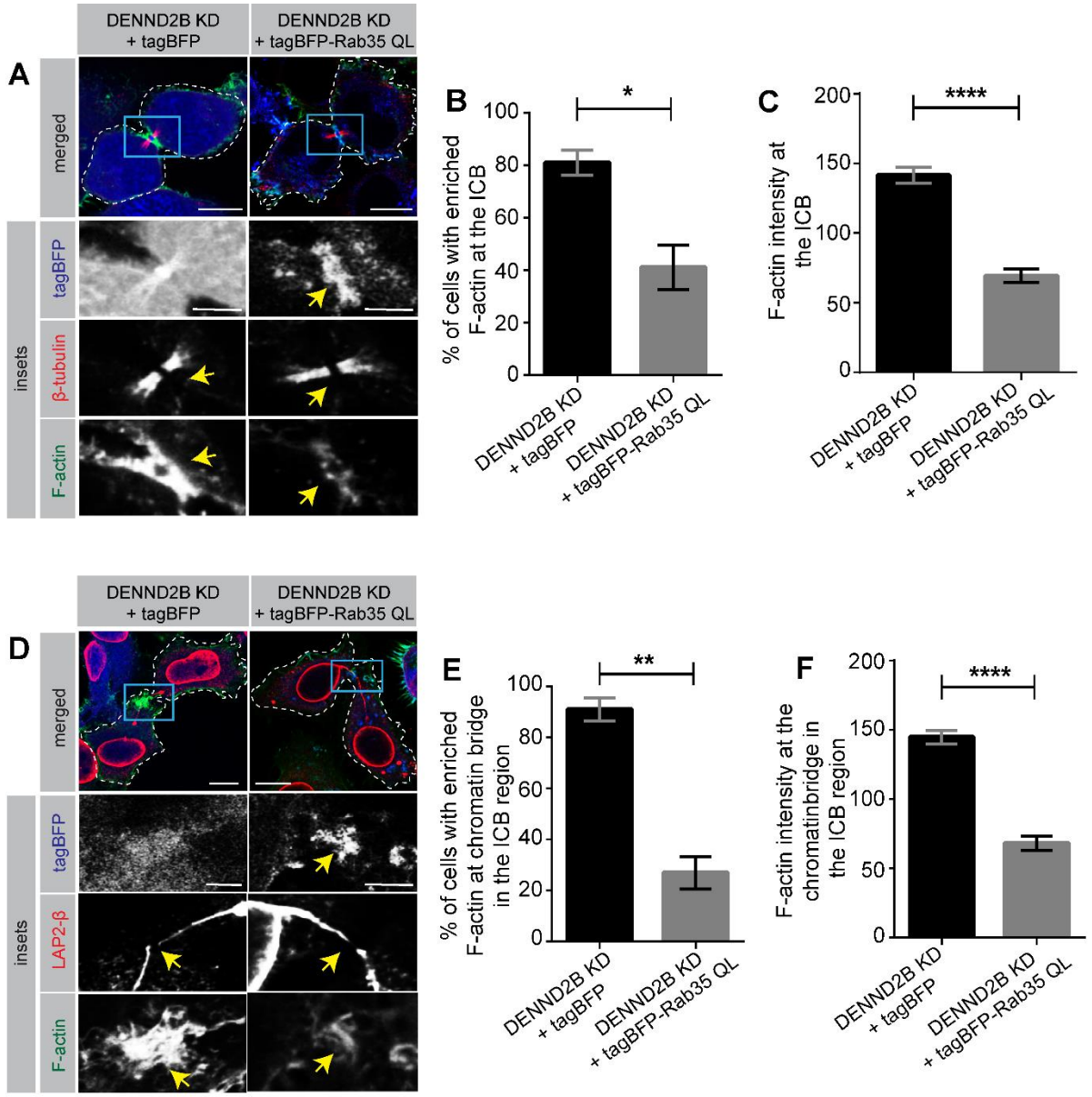

Supplementary figure 3. Expression of Rab35 active mutant rescues F-actin levels at the bridge with or without chromatin bridge.

(A) HeLa cells transduced with DENND2B shRNA lentivirus were further transduced with lentivirus mediating expression of tagBFP and tagBFP-Rab35 QL. Cells were fixed and stained with β-tubulin and Phalloidin. Scale bars = 10 μm for the low-magnification images and 4.25 μm for the higher magnification insets (represented with blue box). Dotted white line marks the periphery of dividing cell. Yellow arrow

represents the cytokinetic bridge. **(B)** Quantification of experiment in (A); mean ± SEM; unpaired t-test (*, P ≤ 0.05; >25 cells per condition)**. (C)** Quantification of experiment in (A); mean ± SEM; Mann-Whitney U test (****, P ≤ 0.0001; >25 cells per condition)**. (D)** HeLa cells transduced with DENND2B shRNA lentivirus were further transduced with lentivirus mediating expression of tagBFP and tagBFP-Rab35 QL. Cells were fixed and stained with LAP2-β and Phalloidin. Scale bars = 12 μm for the low-magnification images and 4.25 μm for the higher magnification insets (represented with blue box). Dotted white line marks the periphery of dividing cell. Yellow arrow represents the chromatin bridge. **(E)** Quantification of experiment in (C); mean ± SEM; unpaired t-test (**, P ≤ 0.01; >25 cells per condition)**. (F)** Quantification of experiment in (C); mean ± SEM; Mann-Whitney U test (****, P ≤ 0.0001; >25 cells per condition)**.**

CHAPTER 5

Discussion

Understanding the mechanisms of membrane trafficking and its connection to various human diseases is vital. Identifying GEFs for Rab GTPases is a key component of this effort. However, many of the GEFs for most mammalian Rabs have not yet been identified.In our study, we used a cell-based GEF assay to screen for all Rab substrates of the seven members of the DENND1 and DENND2 DENN domain–containing protein subfamilies which resulted in identification of new substrates (figure 1).

	Screening using DENN domains only	Previously reported Rab substrates	Newly identified and confirmed substrates
DENND1	DENND1A	Rab35	Rab35, Rab15
	DENND1B	Rab35	Rab35, Rab15
	DENND1C	Rab13 / Rab35	Rab35, Rab15
DENND2	DENND2A	Rab9	Rab15
	DENND2B	Rab9 / Rab13	Rab8A, Rab8B, Rab10, Rab13, Rab15, Rab27A, Rab27B, Rab35, RhoA
	DENND2C	Rab9	Rab8A, Rab8B, Rab10, Rab15, Rab35
	DENND2D	Rab9	Rab8A, Rab10

Figure 1: Tabular representation of previously known and newly identified GTPases. The table presents a comprehensive overview of GTPases newly identified or confirmed to be recruited by specific DENN domain proteins, in contrast to GTPases that were previously reported. *(Reproduced from Kumar et. al. 2022Science Advances, open access, licensed under a Creative Commons Attribution-NonCommercial 4.0)*

We chose to study these two families for three main reasons. Firstly, they are the largest subfamilies within the DENN domain family of proteins. Secondly, we had previously studied parts of these two subfamilies in our lab, which enabled us to start working quickly due to the availability of reagents. Finally, we were aware of the patient mutations in these subfamilies and their implications for human health. As a result of our approach, we identified a large number of substrates that were missed using traditional in vitro approaches. One of the major advantages of our cell-based system is that the Rab substrates retain their endogenous nucleotide status, which is often lost during purification. Our assay provides a more accurate representation of the in

vivo situation. However, we do acknowledge that the degree of overexpression of both the GEFs and the Rab substrates may lead to a lack of specificity in the results. For instance, DENND4C, which is a potent GEF for Rab10, is present at very low levels in multiple cell lines [133].

Additionally, some of the identified Rabs may be recruited to mitochondria as part of Rab cascades downstream of true Rab substrates. As an illustration, a hypothetical scenario involves DENNDx recruiting Rab "a," which in turn recruits protein Y. Protein Y, then, may function as a GEF for Rab "b." Nevertheless, our approach allowed the identification of an unexpected diversity in Rab substrates for the seven DENN domains tested. Despite this specific scenario, our experiments using biochemical binding assays and effector binding assays have revealed that DENND2B has multiple substrates. These results suggest that the total number of GEFs identified for Rab GTPases may be lower than the actual number [134], due to the limitations of traditional in vitro methods.

We found that Rab10 is involved in inhibiting the formation of primary cilia. Specifically, we discovered that the DENND2B protein activates Rab10 to prevent the formation of primary cilia by controlling the recruitment of CP110, a protein that represses ciliogenesis. We propose that DENND2B activates and recruits Rab10, which in turn recruits CP110 to the mother centriole, ultimately preventing cilia formation. We also discovered that DENND2B activates RhoA, which controls cilia length. Our findings indicate that DENND2B is a GEF for RhoA and expands the potential substrates for DENN domain proteins beyond Rab GTPases. Although we used standard protocols for identifying Rho GEFs, we cannot completely rule out the possibility of another Rab protein being recruited by DENND2B, which in turn recruits RhoA through a GTPase cascade. In addition, as highlighted by the reviewers, we were unable to perform an

in vitro exchange reaction due to our inability to purify the DENN domain fragment using conventional methods.

Our analysis demonstrates that the KD of DENND2B in zebrafish leads to developmental defects, including reduced larval length and a curved tail. The larvae's length and tail defects resemble those observed in other studies involving depletion of ciliary proteins in zebrafish, suggesting a potential ciliopathy. These findings indicate that dennd2b-mediated regulation of primary cilia is crucial for proper development. This observation is consistent with the severe anomalies related to ciliopathies seen in patients with a loss-of-function mutation in DENND2B. These disorders are caused by dysregulation of the Hedgehog (Hh) signaling pathway, which plays a crucial role in developmental processes [135]. Furthermore, our study suggests that DENND2B may be part of a common pathway involving M-phase phosphoprotein 9 (MPP9). KO mice for MPP9 exhibit decreased body weight/length and a twisted body axis at midgestation [136], suggesting that DENND2B and MPP9 may be involved in a shared pathway.

In addition to its role in regulating primary cilia, DENND2B recruits multiple other Rabs to the mitochondria, including Rab8A/B, Rab15, Rab35, and Rab27A/B. While the precise roles of the other GTPases recruited to the mitochondria by DENND2B are still not fully understood, we next decided to focus on investigating DENND2B/Rab35 pair in our next study. This decision was made because we observed that cells grow slower when DENND2B is lost, and we suspected that the DENND2B-Rab35 interaction may play a crucial role in cytokinesis.

In our subsequent investigations, we aimed to elucidate the mechanism by which DENND2B is involved in the regulation of cytokinesis. Our data indicated that

DENND2B interacts with Rab35 in a nucleotide-dependent manner, implying that the activation state of Rab35 is critical for its interaction with DENND2B. Moreover, we observed a marked increase in the levels of active Rab35 in the presence of DENND2B, suggesting that DENND2B acts as a GEF for Rab35.

Furthermore, the observation that DENND2B acts as both a GEF and an effector for Rab35 highlights the complexity of the regulatory mechanisms at the cytokinetic bridge. Rab GTPases recruit effector proteins to define the functional identity of the membrane. However, there are also positive feedback loops that occur as a result of GEF-Rab-effector complexes, which help to maintain membrane-anchored GTPases and downstream signaling. This is achieved by the effector protein binding back to the GEF, leading to an increase in GEF activity and thus sustained GTPase activation and effector function. One of the most well-known examples of a GEF-Rab-effector complex is Rabex5/Rab5/Rabaptin5 [66]. Rabex5 acts as a GEF for Rab5 and is initially recruited to the membrane to activate Rab5. Once activated, Rab5 interacts with its effector protein, Rabaptin5, which then binds back to Rabex5 to increase its GEF activity [68][137]. This positive feedback mechanism ensures that the GTPase remains active and that its effector function is sustained.

Another example of a positive feedback loop mediated by a GEF-Rab-effector complex involves polarized trafficking in yeast by the Sec2/Sec4/Sec15 complex [138]. In this complex, Sec2 activates the Rab GTPase Sec4, which in turn binds to its effector protein Sec15. Sec15 can then bind back to Sec2, generating a positive feedback loop that ensures sustained GTPase activation and effector function [138].

Overall, positive feedback loops mediated by GEF-Rab-effector complexes are essential for the maintenance of membrane-anchored GTPases and downstream

signaling. These loops allow for sustained GTPase activation and effector function, ensuring that the functional identity of the membrane is maintained.

The persistence of the bridge for several hours raises the possibility of a positive feedback loop involving the N-terminal fragment of DENND2B that could help maintain the presence of active Rab35 at the bridge. Such a positive feedback mechanism could involve the N-terminal fragment of DENND2B binding to activated Rab35, which in turn recruits more DENND2B to the bridge, resulting in even more activation of Rab35. This positive feedback loop could contribute to the robustness and stability of the cytokinetic bridge, which is critical for successful cytokinesis.

However, based on the current experiments provided, it may be premature to conclude the existence of a positive feedback loop involving the N-terminal fragment of DENND2B in maintaining Rab35 at the cytokinetic bridge. This is because performing experiments that involve deleting either the N-terminal or DENN domain to demonstrate this feedback loop is challenging. The N-terminal fragment of DENND2B is crucial for its subcellular localization, as reported by Ionnou et al. (2015). Figure 6 from their study demonstrated that the DENN domain alone is mostly soluble (cytosolic) and cannot cause the phenotype. Likewise, the N-term domain lacks the GEF domain (DENN) and thus cannot induce the phenotype. Therefore, deleting either the N-term or DENN domain to demonstrate the positive feedback loop in cytokinesis experiments is challenging. Furthermore, deleting the N-term domain is problematic since it determines both the subcellular localization and has effector binding properties, as demonstrated in the provided biochemical experiment. Previous reports on positive feedback loops caused by effectors were testable as the effector was a separate protein, not part of the same protein. Therefore, we could only speculate here about the potential role of the N-term domain as an effector in the discussion, based

on previously reported GEF-effector positive feedback loops. However, our findings are significant as they identify a biochemical interaction within the same GEF, which has not been observed previously in the field of membrane trafficking involving GEF/Rab cascade, to our knowledge.

In addition, our study also revealed that DENND2B may negatively regulate the presence of active checkpoint machinery, specifically phospho-Aurora B. We found that the absence of DENND2B leads to an increase in the active checkpoint machinery, indicating that the abscission checkpoint is activated in the absence of DENND2B. Moreover, our observation of colocalization between DENND2B and Aurora B suggests the possibility of crosstalk between the two proteins in this pathway. Our findings suggest that the absence of DENND2B leads to increased activation of the checkpoint machinery due to unknown player(s) in the pathway, rather than a direct interaction between DENND2B and abscission checkpoint proteins. Therefore, additional investigation is necessary to identify the player(s) responsible for regulating the abscission checkpoint in the absence of DENND2B.

DENND2B activates Rab35 and recruits it to the cytokinetic bridge, playing a crucial role in regulating F-actin levels and facilitating abscission. This is important because F-actin oxidation, mediated by MICAL1, and actin reduction, mediated by MsrB2, need to be balanced for proper regulation of F-actin levels at the cytokinetic bridge [35]. We propose that in the absence of DENND2B, Rab35 recruitment is impaired, resulting in elevated levels of F-actin at the bridge, which negatively impacts the recruitment of ESCRT-III, leading to delayed abscission [108]. Additionally, the absence of DENND2B leads to activation of the abscission checkpoint in the presence of chromatin bridge, which also contributes to the abscission delay [139]. In summary, our study sheds light on the role of DENND2B in regulating cytokinesis and abscission,

specifically by activating Rab35 and recruiting it to the cytokinetic bridge. Our findings also highlight the importance of proper regulation of F-actin levels at the bridge, and the negative impact of elevated levels of F-actin on abscission. This work opens up new avenues for future research, particularly regarding the upstream factors that determine the context-specific GEF activity of DENND2B.

Our findings support the idea that DENN domain-containing proteins are involved in the regulation of a larger array of Rab GTPases, playing a crucial role in complex membrane trafficking pathways. However, the question remains as to what factors define the context-specific GEF activity of DENND2B for its activation at various cellular sites. Further investigation is needed to understand the upstream factors that lead to the correct localization of DENND2B. The question of how multiple DENN domains can target a single Rab and how the same DENN domain can target multiple Rabs is still an intriguing one. One possible explanation is that different DENN domain proteins act on a common Rab but at different subcellular compartments. For instance, DENND1A/B activates Rab35 at endosomes, while DENND1C activates Rab35 at the actin cytoskeleton [140].

When it comes to Rab10, there are multiple GEFs that can activate it, including DENND2C and DENND2D, which were newly identified in this study, as well as DENND4C and Rabin8 [133][141]. It's possible that all of these GEFs are present in a given cell, but they activate Rab10 at different subcellular locations. However, when we knocked out DENND2B, we observed no change in the total cellular levels of the active form of Rab10, likely due to the presence of other Rab10 GEFs. Immunofluorescence analysis revealed that the pool of Rab10 at the centriole is a relatively minor component of the overall cellular pool of Rab10. This further highlights the specificity of DENND2B in activating Rab10 specifically at the centriole.

The role of DENND2B in membrane trafficking pathways have raised several questions regarding its function. One such question is whether the disrupted function of DENND2B could contribute to cancer phenotypes via defective primary cilia, given its inhibitory role in primary cilia. Previous studies have shown that numerous cancer cells lack primary cilia, and DENND2B is known to promote cancer invasion. Therefore, it would be interesting to investigate whether defective primary cilia resulting from DENND2B dysfunction could play a role in cancer invasion. Another important question relates to the context-specific GEF activity of DENND2B. We know that DENND2B activates both Rab8A and Rab10, but previous studies have shown that these two Rabs have opposite effects on cilia formation. It will be important to determine the factors that contribute to the context-specific GEF activity that leads to Rab10-specific phenotype, but not Rab8A.

The Parkinson's disease gene LRRK2 phosphorylates a subset of Rabs, and recent studies have associated Rab10 with an emerging Parkinson's disease cellular phenotype, inhibition of primary cilia formation by p-Rab10 [142]. Interestingly, overexpression of DENND2B increases the levels of Rab10 phosphorylated by LRRK2, while DENND2B KO cells show increased cilia formation. These findings fit with the model proposed by other groups, which suggests that increased LRRK2-mediated phosphorylation of Rab10 inhibits cilia formation [142][143]. Moreover, the diversity in substrate specificity within and between DENN domain families may be explained by the structure of individual DENN domains. Screening all remaining DENN domain family members using a similar approach would be necessary to understand the full complement of substrates, and since DENN domains may not be specific to Rabs, they must be screened across all small GTPase families in future studies.

Taking into account the latest discoveries and previously known functions (figure 2), we can summarize the role of DENND1A/B/C and DENND2B as follows: DENND1A/B are primarily located at clathrin-coated vesicles and the plasma membrane [47][144]. They play a key role in activating Rab35, which occurs at the level of endosomes situated between Clathrin-coated vesicles and early endosomes [47]. On the other hand, DENND1C binds to actin and has the ability to direct Rab35 towards actin [140]. Furthermore, DENND2B is found at the cell periphery, specifically on actin, and has a direct interaction with MICAL-L2 [20]. This coordination results in the activation of Rab13 and MICAL-L2, playing a crucial role in actin cytoskeleton function [20]. In the context of cell migration, Rab13 is initially delivered to the cell periphery in an inactive form via vesicles [4]. Upon local activation, Rab13 binds to MICAL-L2, leading to the alleviation of MICAL-L2's auto-inhibition [20]. Consequently, this promotes actin remodeling at the leading edge of migrating cells.

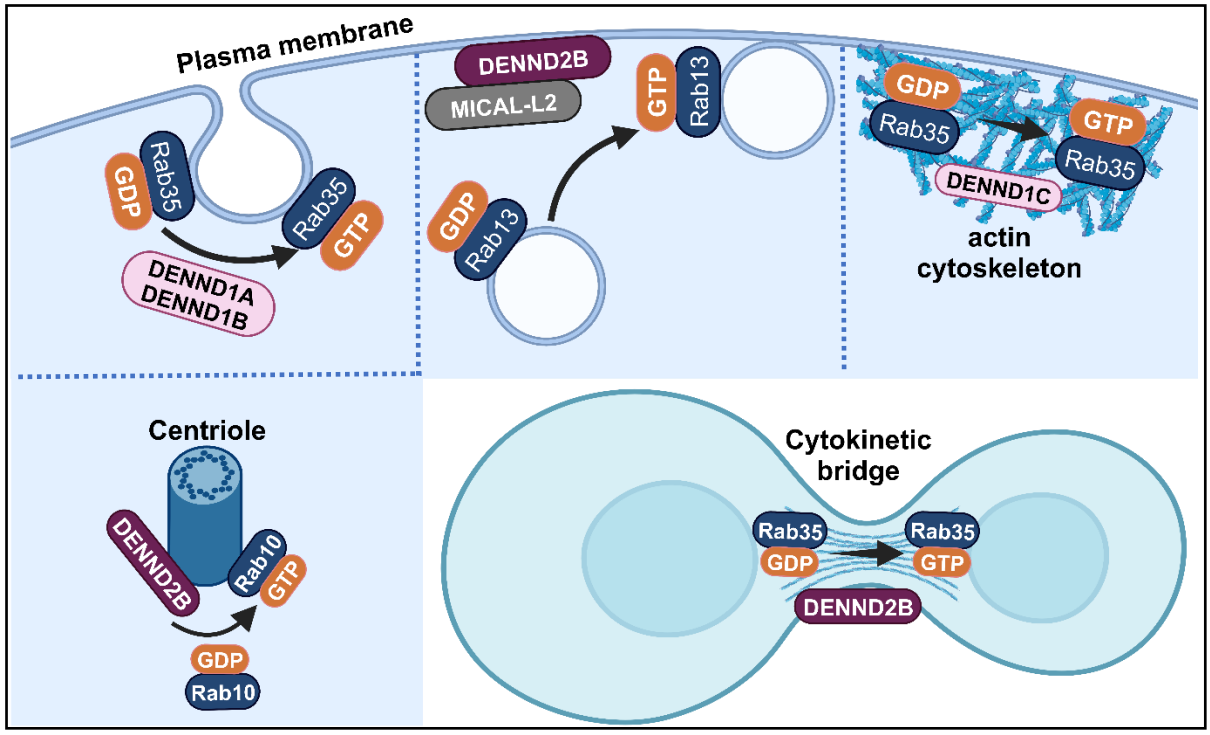

Figure 2: Representation of previously known and newly identified roles for DENN domain bearing proteins (DENND1A/B/C and DENND2B).

Additionally, recent findings uncovered the localization of DENND2B at the centriole. In this context, DENND2B activates Rab10, which is involved in regulating primary cilia formation [145]. Moreover, DENND2B is also present at the cytokinetic bridge [146]. Here, it activates Rab35 and facilitates the remodeling of actin filaments, thus contributing to the successful separation of cells during cytokinesis [146]. These findings shed light on the critical roles of DENND1A/B, DENND1C, and DENND2B in the cellular processes governing endosome function, actin dynamics, primary cilia formation, and cytokinesis.

The key question arising from these findings is whether DENN domain proteins target multiple Rab GTPases. Furthermore, do they activate a group of Rabs that would act together to favor a specific pathway or the specific trafficking of cargoes to a destination? Most likely, DENN domain proteins individually activate specific Rabs that drive specific cargo trafficking. For instance, Rab8 at the centriole promotes cilia formation, while Rab10 inhibits it. The clear inhibitory phenotype of loss of DENND2B in cilia formation likely explains the activity of Rab10 as opposed to Rab8. However, it's possible that there might be a mechanism specifically shutting down Rab8 activity at the centriole, such as phosphorylation in its active state. These scenarios need to be investigated in future studies.

Another significant question is how these GEFs are precisely targeted to the correct cellular compartments. Currently, the exact mechanisms responsible for DENND2B's localization at the centriole or the cytokinetic bridge remain unknown. A plausible speculation is that DENND2B could be recruited to the bridge through binding to a protein called IRSp5, which is known to function in the localization and activity of Rab35 [147]. However, this also requires further investigation.

We addressed the robustness of cell-based assays and their findings. It's worth noting that overexpressing Rab and DENN constructs may lead to nonspecific recruitment of Rabs on the mitochondrial outer membrane in the presence of DENN proteins. This raises the possibility that the level of overexpression could drive Rab recruitment that may not be physiologically relevant. Therefore, it is crucial to thoroughly characterize each pair being tested in terms of their cell biological function.

Finally, understanding the mechanisms underlying DENN domain specificity and how they interact with Rabs and other proteins will provide valuable insights into the complex network of regulatory pathways in the cell. The versatility of DENN domains makes them a promising target for further research, especially given their involvement in primary ciliopathies and other developmental disorders. Further research into the mechanisms of DENND2B and its downstream effectors could lead to the development of novel therapeutic strategies for these conditions.

Conclusion and summary

In this thesis, we aimed to comprehensively understand the functionality of DENN domain-bearing proteins. To achieve this, we transitioned from an in vitro system to an in vivo system where we targeted the DENN domain fragment to the outer mitochondrial surface and expressed GFP-tagged Rab GTPases to screen for potential substrates that would be recruited to the mitochondrial surface by DENN domain fragment. This approach confirmed some previously known pairs and discovered many new partners. We then sought to understand the biological pathways where they functioned, leading to the discovery of two new pathways regulated by DENND2B.

Firstly, we found that DENND2B regulates primary cilia formation through the activation of Rab10 and RhoA. Secondly, DENND2B activates Rab35 at the intercellular bridge, and regulates cytokinetic abscission. These findings shed light on the previously underappreciated implications of DENN-domain proteins, a major family of GEFs for Rab GTPases.

While our study discovered two pathways regulated by DENND2B, the remaining DENN domain-Rab pairs still represent a mystery as to where they interact and function. We speculate that further screening of the remaining members of the DENN domain family, combined with the use of bioinformatics and protein interaction screening methods such as BioID, could allow us to build a comprehensive network of interactions and pathways in membrane trafficking. This network could help us better understand the signaling events that occur during membrane trafficking and provide new insights into the role of DENN domain proteins in this process.

References

[1] H. Stenmark, “Rab GTPases as coordinators of vesicle traffic,” *Nature Reviews Molecular Cell Biology*, vol. 10, no. 8. Nature Publishing Group, pp. 513–525, Aug. 15, 2009. doi: 10.1038/nrm2728.

[2] Y. Zhen and H. Stenmark, “Cellular functions of Rab GTPases at a glance,” *J. Cell Sci.*, vol. 128, no. 17, pp. 3171–3176, Sep. 2015, doi: 10.1242/JCS.166074/260447/AM/CELLULAR-FUNCTIONS-OF-RAB-GTPASES-AT-A-GLANCE.

[3] S. R. Pfeffer, “Rab GTPases: Master regulators that establish the secretory and endocytic pathways,” *Molecular Biology of the Cell*, vol. 28, no. 6. American Society for Cell Biology, pp. 712–715, Mar. 15, 2017. doi: 10.1091/mbc.E16-10-0737.

[4] M. S. Ioannou, M. Girard, and P. S. McPherson, “Rab13 Traffics on Vesicles Independent of Prenylation,” *J. Biol. Chem.*, vol. 291, no. 20, p. 10726, May 2016, doi: 10.1074/JBC.M116.722298.

[5] R. M. Nottingham and S. R. Pfeffer, “Defining the boundaries: Rab GEFs and GAPs,” *Proceedings of the National Academy of Sciences of the United States of America*, vol. 106, no. 34. National Academy of Sciences, pp. 14185–14186, Aug. 25, 2009. doi: 10.1073/pnas.0907725106.

[6] F. Barr and D. G. Lambright, “Rab GEFs and GAPs,” *Curr. Opin. Cell Biol.*, vol. 22, no. 4, p. 461, Aug. 2010, doi: 10.1016/J.CEB.2010.04.007.

[7] B. T. Kinsella and W. A. Maltese, “rab GTP-binding proteins implicated in vesicular transport are isoprenylated in vitro at cysteines within a novel carboxyl-

terminal motif," *J. Biol. Chem.*, vol. 266, no. 13, pp. 8540–8544, May 1991, doi: 10.1016/S0021-9258(18)93008-5.

[8] J. P. Gorvel, P. Chavrier, M. Zerial, and J. Gruenberg, "rab5 controls early endosome fusion in vitro," *Cell*, vol. 64, no. 5, pp. 915–925, Mar. 1991, doi: 10.1016/0092-8674(91)90316-Q.

[9] L. Desnoyers, J. S. Anant, and M. C. Seabra, "Geranylgeranylation of Rab proteins," *Biochem. Soc. Trans.*, vol. 24, no. 3, pp. 699–703, 1996, doi: 10.1042/BST0240699.

[10] D. A. Andres *et al.*, "cDNA cloning of component A of Rab geranylgeranyl transferase and demonstration of its role as a Rab escort protein," *Cell*, vol. 73, no. 6, pp. 1091–1099, Jun. 1993, doi: 10.1016/0092-8674(93)90639-8.

[11] I. Schalk *et al.*, "Structure and mutational analysis of Rab GDP-dissociation inhibitor," *Nat. 1996 3816577*, vol. 381, no. 6577, pp. 42–48, May 1996, doi: 10.1038/381042a0.

[12] A. Rak *et al.*, "Structure of Rab GDP-Dissociation Inhibitor in Complex with Prenylated YPT1 GTPase," *Science (80-.).*, vol. 302, no. 5645, pp. 646–650, Oct. 2003, doi: 10.1126/SCIENCE.1087761/SUPPL_FILE/RAK.SOM.PDF.

[13] S. Pfeffer and D. Aivazian, "Targeting Rab GTPases to distinct membrane compartments," *Nat. Rev. Mol. Cell Biol. 2004 511*, vol. 5, no. 11, pp. 886–896, Nov. 2004, doi: 10.1038/nrm1500.

[14] H. Stenmark and V. M. Olkkonen, "The Rab GTPase family," *Genome Biology*, vol. 2, no. 5. BioMed Central, p. reviews3007.1, 2001. doi: 10.1186/gb-2001-2-5-reviews3007.

[15] K. Verhoeven *et al.*, “Mutations in the small GTP-ase late endosomal protein RAB7 cause Charcot-Marie-Tooth type 2B neuropathy,” *Am. J. Hum. Genet.*, vol. 72, no. 3, pp. 722–727, Mar. 2003, doi: 10.1086/367847.

[16] I. G. Ganley and S. R. Pfeffer, “Cholesterol Accumulation Sequesters Rab9 and Disrupts Late Endosome Function in NPC1-deficient Cells,” *J. Biol. Chem.*, vol. 281, no. 26, p. 17890, Jun. 2006, doi: 10.1074/JBC.M601679200.

[17] J. H. Brumell and M. A. Scidmore, “Manipulation of rab GTPase function by intracellular bacterial pathogens,” *Microbiol. Mol. Biol. Rev.*, vol. 71, no. 4, pp. 636–652, Dec. 2007, doi: 10.1128/MMBR.00023-07.

[18] V. A. Kelley and J. S. Schorey, “Modulation of cellular phosphatidylinositol 3-phosphate levels in primary macrophages affects heat-killed but not viable Mycobacterium avium’s transport through the phagosome maturation process,” *Cell. Microbiol.*, vol. 6, no. 10, pp. 973–985, Oct. 2004, doi: 10.1111/J.1462-5822.2004.00415.X.

[19] A. Ingmundson, A. Delprato, D. G. Lambright, and C. R. Roy, “Legionella pneumophila proteins that regulate Rab1 membrane cycling,” *Nature*, vol. 450, no. 7168, pp. 365–369, Nov. 2007, doi: 10.1038/NATURE06336.

[20] M. S. Ioannou *et al.*, “DENND2B activates Rab13 at the leading edge of migrating cells and promotes metastatic behavior,” *J. Cell Biol.*, vol. 208, no. 5, pp. 629–648, 2015, doi: 10.1083/jcb.201407068.

[21] M. S. Ioannou *et al.*, “Intersectin-s interaction with DENND2B facilitates recycling of epidermal growth factor receptor,” *EMBO Rep.*, vol. 18, no. 12, pp. 2119–2130, Dec. 2017, doi: 10.15252/embr.201744034.

[22] G. Kulasekaran *et al.*, “An Arf/Rab cascade controls the growth and invasiveness of glioblastoma,” *J. Cell Biol.*, vol. 220, no. 2, Feb. 2021, doi: 10.1083/JCB.202004229.

[23] P. Chavrier, J. P. Gorvel, E. Stelzer, K. Simons, J. Gruenberg, and M. Zerial, “Hypervariable C-termmal domain of rab proteins acts as a targeting signal,” *Nature*, vol. 353, no. 6346, pp. 769–772, 1991, doi: 10.1038/353769a0.

[24] B. R. Ali, C. Wasmeier, L. Lamoreux, M. Strom, and M. C. Seabra, “Multiple regions contribute to membrane targeting of Rab GTPases,” *J. Cell Sci.*, vol. 117, no. Pt 26, pp. 6401–6412, Dec. 2004, doi: 10.1242/JCS.01542.

[25] A. B. Dirac-Svejstrup, T. Sumizawa, and S. R. Pfeffer, “Identification of a GDI displacement factor that releases endosomal Rab GTPases from Rab-GDI,” *EMBO J.*, vol. 16, no. 3, pp. 465–472, Feb. 1997, doi: 10.1093/emboj/16.3.465.

[26] U. Sivars, D. Aivazian, and S. R. Pfeffer, “Yip3 catalyses the dissociation of endosomal Rab-GDI complexes,” *Nature*, vol. 425, no. 6960, pp. 856–859, Oct. 2003, doi: 10.1038/nature02057.

[27] J. Blümer *et al.*, “RabGEFs are a major determinant for specific Rab membrane targeting,” *J. Cell Biol.*, vol. 200, no. 3, pp. 287–300, Feb. 2013, doi: 10.1083/jcb.201209113.

[28] A. Gerondopoulos, L. Langemeyer, J. R. Liang, A. Linford, and F. A. Barr, “BLOC-3 mutated in Hermansky-Pudlak syndrome is a Rab32/38 guanine nucleotide exchange factor,” *Curr. Biol.*, vol. 22, no. 22, pp. 2135–2139, Nov. 2012, doi: 10.1016/j.cub.2012.09.020.

[29] M. Nordmann *et al.*, “The Mon1-Ccz1 complex is the GEF of the late endosomal

Rab7 homolog Ypt7," *Curr. Biol.*, vol. 20, no. 18, pp. 1654–1659, 2010, doi: 10.1016/J.CUB.2010.08.002.

[30] C. W. Wang, P. E. Stromhaug, E. J. Kauffman, L. S. Weisman, and D. J. Klionsky, "Yeast homotypic vacuole fusion requires the Ccz1-Mon1 complex during the tethering/docking stage," *J. Cell Biol.*, vol. 163, no. 5, pp. 973–985, Dec. 2003, doi: 10.1083/JCB.200308071.

[31] D. Poteryaev, S. Datta, K. Ackema, M. Zerial, and A. Spang, "Identification of the switch in early-to-late endosome transition," *Cell*, vol. 141, no. 3, pp. 497–508, 2010, doi: 10.1016/J.CELL.2010.03.011.

[32] J. Rink, E. Ghigo, Y. Kalaidzidis, and M. Zerial, "Rab conversion as a mechanism of progression from early to late endosomes," *Cell*, vol. 122, no. 5, pp. 735–749, Sep. 2005, doi: 10.1016/J.CELL.2005.06.043.

[33] N. Morozova *et al.*, "TRAPPII subunits are required for the specificity switch of a Ypt–Rab GEF," *Nat. Cell Biol. 2006 811*, vol. 8, no. 11, pp. 1263–1269, Oct. 2006, doi: 10.1038/ncb1489.

[34] K. Hattula, J. Furuhjelm, A. Arffman, and J. Peränen, "A Rab8-specific GDP/GTP exchange factor is involved in actin remodeling and polarized membrane transport," *Mol. Biol. Cell*, vol. 13, no. 9, pp. 3268–3280, Sep. 2002, doi: 10.1091/MBC.E02-03-0143.

[35] C. Walch-Solimena, R. N. Collins, and P. J. Novick, "Sec2p mediates nucleotide exchange on Sec4p and is involved in polarized delivery of post-Golgi vesicles," *J. Cell Biol.*, vol. 137, no. 7, pp. 1495–1509, Jun. 1997, doi: 10.1083/JCB.137.7.1495.

[36] G. Dong, M. Medkova, P. Novick, and K. M. Reinisch, “A catalytic coiled coil: structural insights into the activation of the Rab GTPase Sec4p by Sec2p,” *Mol. Cell*, vol. 25, no. 3, pp. 455–462, Feb. 2007, doi: 10.1016/J.MOLCEL.2007.01.013.

[37] M. V. Nachury *et al.*, “A Core Complex of BBS Proteins Cooperates with the GTPase Rab8 to Promote Ciliary Membrane Biogenesis,” *Cell*, vol. 129, no. 6, pp. 1201–1213, Jun. 2007, doi: 10.1016/j.cell.2007.03.053.

[38] S. Siniossoglou, S. Y. Peak-Chew, and H. R. B. Pelham, “Ric1p and Rgp1p form a complex that catalyses nucleotide exchange on Ypt6p,” *EMBO J.*, vol. 19, no. 18, pp. 4885–4894, Sep. 2000, doi: 10.1093/EMBOJ/19.18.4885.

[39] A. Delprato and D. G. Lambright, “Structural basis for Rab GTPase activation by VPS9 domain exchange factors,” *Nat. Struct. Mol. Biol.*, vol. 14, no. 5, p. 406, May 2007, doi: 10.1038/NSMB1232.

[40] A. Delprato, E. Merithew, and D. G. Lambright, “Structure, exchange determinants, and family-wide Rab specificity of the tandem helical bundle and Vps9 domains of Rabex-5,” *Cell*, vol. 118, no. 5, pp. 607–617, Sep. 2004, doi: 10.1016/j.cell.2004.08.009.

[41] S. Lee *et al.*, “Structural basis for ubiquitin recognition and autoubiquitination by Rabex-5,” *Nat. Struct. Mol. Biol.*, vol. 13, no. 3, pp. 264–271, Mar. 2006, doi: 10.1038/NSMB1064.

[42] L. Penengo *et al.*, “Crystal structure of the ubiquitin binding domains of rabex-5 reveals two modes of interaction with ubiquitin,” *Cell*, vol. 124, no. 6, pp. 1183–1195, Mar. 2006, doi: 10.1016/J.CELL.2006.02.020.

[43] A. L. Marat, H. Dokainish, and P. S. McPherson, “DENN domain proteins: Regulators of Rab GTPases,” *Journal of Biological Chemistry*, vol. 286, no. 16. J Biol Chem, pp. 13791–13800, Apr. 22, 2011. doi: 10.1074/jbc.R110.217067.

[44] M. Wada *et al.*, “Isolation and characterization of a GDP/GTP exchange protein specific for the Rab3 subfamily small G proteins.,” *J. Biol. Chem.*, vol. 272, no. 7, pp. 3875–8, Feb. 1997, doi: 10.1074/jbc.272.7.3875.

[45] A. R. Schievella, J. H. Chen, J. R. Graham, and L. L. Lin, “MADD, a novel death domain protein that interacts with the type 1 tumor necrosis factor receptor and activates mitogen-activated protein kinase.,” *J. Biol. Chem.*, vol. 272, no. 18, pp. 12069–75, May 1997, doi: 10.1074/jbc.272.18.12069.

[46] M. Sato, K. Sato, W. Liou, S. Pant, A. Harada, and B. D. Grant, “Regulation of endocytic recycling by C. elegans Rab35 and its regulator RME-4, a coated-pit protein,” *EMBO J.*, vol. 27, no. 8, pp. 1183–1196, Apr. 2008, doi: 10.1038/EMBOJ.2008.54.

[47] P. D. Allaire, A. L. Marat, C. Dall’Armi, G. Di Paolo, P. S. McPherson, and B. Ritter, “The Connecdenn DENN Domain: A GEF for Rab35 Mediating Cargo-Specific Exit from Early Endosomes,” *Mol. Cell*, vol. 37, no. 3, pp. 370–382, Feb. 2010, doi: 10.1016/j.molcel.2009.12.037.

[48] A. L. Marat and P. S. McPherson, “The connecdenn family, Rab35 guanine nucleotide exchange factors interfacing with the clathrin machinery,” *J. Biol. Chem.*, vol. 285, no. 14, pp. 10627–10637, Apr. 2010, doi: 10.1074/jbc.M109.050930.

[49] S. I. Yoshimura, A. Gerondopoulos, A. Linford, D. J. Rigden, and F. A. Barr, “Family-wide characterization of the DENN domain Rab GDP-GTP exchange

factors," *J. Cell Biol.*, vol. 191, no. 2, pp. 367–381, Oct. 2010, doi: 10.1083/jcb.201008051.

[50] K. S. Carroll *et al.*, "Facilitating Receptor Recruitment by TIP47," *Science (80-.).*, 2001.

[51] T. Matsui, K. Noguchi, and M. Fukuda, "Dennd3 functions as a guanine nucleotide exchange factor for small GTPase Rab12 in mouse embryonic fibroblasts.," *J. Biol. Chem.*, vol. 289, no. 20, pp. 13986–95, May 2014, doi: 10.1074/jbc.M113.546689.

[52] J. Xu, M. Fotouhi, and P. S. McPherson, "Phosphorylation of the exchange factor DENND3 by ULK in response to starvation activates Rab12 and induces autophagy.," *EMBO Rep.*, vol. 16, no. 6, pp. 709–18, Jun. 2015, doi: 10.15252/embr.201440006.

[53] S. Schuck *et al.*, "Rab10 is involved in basolateral transport in polarized Madin-Darby canine kidney cells.," *Traffic*, vol. 8, no. 1, pp. 47–60, Jan. 2007, doi: 10.1111/j.1600-0854.2006.00506.x.

[54] H. Sano *et al.*, "Rab10, a target of the AS160 Rab GAP, is required for insulin-stimulated translocation of GLUT4 to the adipocyte plasma membrane.," *Cell Metab.*, vol. 5, no. 4, pp. 293–303, Apr. 2007, doi: 10.1016/j.cmet.2007.03.001.

[55] I. Janoueix-Lerosey, F. Jollivet, J. Camonis, P. N. Marche, and B. Goud, "Two-hybrid System Screen with the Small GTP-binding Protein Rab6," *J. Biol. Chem.*, 1995, doi: 10.1074/jbc.270.24.14801.

[56] A. Boulet *et al.*, "Rab6-interacting protein 1 links Rab6 and Rab11 function," *Traffic*, 2007, doi: 10.1111/j.1600-0854.2007.00612.x.

[57] R. Recacha *et al.*, “Structural basis for recruitment of Rab6-interacting protein 1 to Golgi via a RUN domain.,” *Structure*, vol. 17, no. 1, pp. 21–30, Jan. 2009, doi: 10.1016/j.str.2008.10.014.

[58] C. E. Becker, E. M. Creagh, and L. A. J. O’Neill, “Rab39a binds caspase-1 and is required for caspase-1-dependent interleukin-1beta secretion.,” *J. Biol. Chem.*, vol. 284, no. 50, pp. 34531–7, Dec. 2009, doi: 10.1074/jbc.M109.046102.

[59] M. Giannandrea *et al.*, “Mutations in the small GTPase gene RAB39B are responsible for X-linked mental retardation associated with autism, epilepsy, and macrocephaly.,” *Am. J. Hum. Genet.*, vol. 86, no. 2, pp. 185–95, Feb. 2010, doi: 10.1016/j.ajhg.2010.01.011.

[60] A. Linford *et al.*, “Rab14 and Its Exchange Factor FAM116 Link Endocytic Recycling and Adherens Junction Stability in Migrating Cells,” *Dev. Cell*, 2012, doi: 10.1016/j.devcel.2012.04.010.

[61] J. H. Lumb, K. F. Leung, K. N. DuBois, and M. C. Field, “Rab28 function in trypanosomes: interactions with retromer and ESCRT pathways,” *J. Cell Sci.*, 2011, doi: 10.1242/jcs.079178.

[62] S. Niwa, Y. Tanaka, and N. Hirokawa, “KIF1Bbeta- and KIF1A-mediated axonal transport of presynaptic regulator Rab3 occurs in a GTP-dependent manner through DENN/MADD.,” *Nat. Cell Biol.*, vol. 10, no. 11, pp. 1269–79, Nov. 2008, doi: 10.1038/ncb1785.

[63] T. R. Mahoney *et al.*, “Regulation of synaptic transmission by RAB-3 and RAB-27 in Caenorhabditis elegans.,” *Mol. Biol. Cell*, vol. 17, no. 6, pp. 2617–25, Jun. 2006, doi: 10.1091/mbc.e05-12-1170.

[64] Y. Homma, S. Hiragi, and M. Fukuda, “Rab family of small GTPases: an updated view on their regulation and functions,” *FEBS J.*, vol. 288, no. 1, pp. 36–55, Jan. 2021, doi: 10.1111/febs.15453.

[65] M. Rubino, M. Miaczynska, R. Lippé, and M. Zerial, “Selective membrane recruitment of EEA1 suggests a role in directional transport of clathrin-coated vesicles to early endosomes,” *J. Biol. Chem.*, vol. 275, no. 6, pp. 3745–3748, Feb. 2000, doi: 10.1074/JBC.275.6.3745.

[66] H. Horiuchi *et al.*, “A novel Rab5 GDP/GTP exchange factor complexed to Rabaptin-5 links nucleotide exchange to effector recruitment and function,” *Cell*, vol. 90, no. 6, pp. 1149–1159, Sep. 1997, doi: 10.1016/S0092-8674(00)80380-3.

[67] V. Rybin *et al.*, “GTPase activity of Rab5 acts as a timer for endocytic membrane fusion,” *Nature*, vol. 383, no. 6597, pp. 266–269, 1996, doi: 10.1038/383266A0.

[68] H. Stenmark, G. Vitale, O. Ullrich, and M. Zerial, “Rabaptin-5 is a direct effector of the small GTPase Rab5 in endocytic membrane fusion,” *Cell*, vol. 83, no. 3, pp. 423–432, Nov. 1995, doi: 10.1016/0092-8674(95)90120-5.

[69] R. Lippé, H. Horiuchi, A. Runge, and M. Zerial, “Expression, purification, and characterization of Rab5 effector complex, rabaptin-5/rabex-5,” *Methods Enzymol.*, vol. 329, pp. 132–145, 2001, doi: 10.1016/S0076-6879(01)29074-0.

[70] D. F. Seals, G. Eitzen, N. Margolis, W. T. Wickner, and A. Price, “A Ypt/Rab effector complex containing the Sec1 homolog Vps33p is required for homotypic vacuole fusion,” *Proc. Natl. Acad. Sci. U. S. A.*, vol. 97, no. 17, pp. 9402–9407, Aug. 2000, doi: 10.1073/PNAS.97.17.9402.

[71] B. L. Grosshans, D. Ortiz, and P. Novick, “Rabs and their effectors: Achieving specificity in membrane traffic,” *Proceedings of the National Academy of Sciences of the United States of America*, vol. 103, no. 32. National Academy of Sciences, pp. 11821–11827, Aug. 08, 2006. doi: 10.1073/pnas.0601617103.

[72] G. Jedd, J. Mulholland, and N. Segev, “Two new Ypt GTPases are required for exit from the yeast trans-Golgi compartment,” *J. Cell Biol.*, vol. 137, no. 3, pp. 563–580, May 1997, doi: 10.1083/jcb.137.3.563.

[73] D. Ortiz, M. Medkova, C. Walch-Solimena, and P. Novick, “Ypt32 recruits the Sec4p guanine nucleotide exchange factor, Sec2p, to secretory vesicles; evidence for a Rab cascade in yeast,” *J. Cell Biol.*, vol. 157, no. 6, pp. 1005–1015, Jun. 2002, doi: 10.1083/JCB.200201003.

[74] A. Salminen and P. J. Novick, “A ras-like protein is required for a post-Golgi event in yeast secretion,” *Cell*, vol. 49, no. 4, pp. 527–538, May 1987, doi: 10.1016/0092-8674(87)90455-7.

[75] S. E. Rieder and S. D. Emr, “A novel RING finger protein complex essential for a late step in protein transport to the yeast vacuole,” *Mol. Biol. Cell*, vol. 8, no. 11, pp. 2307–2327, 1997, doi: 10.1091/MBC.8.11.2307.

[76] S. Caplan, L. M. Hartnell, R. C. Aguilar, N. Naslavsky, and J. S. Bonifacino, “Human Vam6p promotes lysosome clustering and fusion in vivo,” *J. Cell Biol.*, vol. 154, no. 1, pp. 109–121, Jul. 2001, doi: 10.1083/JCB.200102142.

[77] B. Y. Kim, H. Krämer, A. Yamamoto, E. Kominami, S. Kohsaka, and C. Akazawa, “Molecular characterization of mammalian homologues of class C Vps proteins that interact with syntaxin-7,” *J. Biol. Chem.*, vol. 276, no. 31, pp. 29393–29402, Aug. 2001, doi: 10.1074/JBC.M101778200.

[78] S. C. W. Richardson, S. C. Winistorfer, V. Poupon, J. P. Luzio, and R. C. Piper, “Mammalian late vacuole protein sorting orthologues participate in early endosomal fusion and interact with the cytoskeleton,” *Mol. Biol. Cell*, vol. 15, no. 3, pp. 1197–1210, Mar. 2004, doi: 10.1091/MBC.E03-06-0358.

[79] I. B. Rogozin, M. K. Basu, M. Csürös, and E. V. Koonin, “Analysis of Rare Genomic Changes Does Not Support the Unikont–Bikont Phylogeny and Suggests Cyanobacterial Symbiosis as the Point of Primary Radiation of Eukaryotes,” *Genome Biol. Evol.*, vol. 1, p. 99, Jan. 2009, doi: 10.1093/GBE/EVP011.

[80] D. R. Mitchell, “Evolution of Cilia,” *Cold Spring Harb. Perspect. Biol.*, vol. 9, no. 1, Jan. 2017, doi: 10.1101/CSHPERSPECT.A028290.

[81] B. P. Piasecki, J. Burghoorn, and P. Swoboda, “Regulatory Factor X (RFX)-mediated transcriptional rewiring of ciliary genes in animals,” *Proc. Natl. Acad. Sci. U. S. A.*, vol. 107, no. 29, pp. 12969–12974, Jul. 2010, doi: 10.1073/PNAS.0914241107/-/DCSUPPLEMENTAL.

[82] P. Satir and S. T. Christensen, “Overview of structure and function of mammalian cilia,” *Annual Review of Physiology*, vol. 69. Annual Reviews, pp. 377–400, Feb. 16, 2007. doi: 10.1146/annurev.physiol.69.040705.141236.

[83] G. Wheway, L. Nazlamova, and J. T. Hancock, “Signaling through the primary cilium,” *Front. Cell Dev. Biol.*, vol. 6, no. FEB, p. 8, Feb. 2018, doi: 10.3389/FCELL.2018.00008/BIBTEX.

[84] E. A. Otto *et al.*, “Mutations in INVS encoding inversin cause nephronophthisis type 2, linking renal cystic disease to the function of primary cilia and left-right axis determination,” *Nat. Genet.*, vol. 34, no. 4, pp. 413–420, Aug. 2003, doi:

10.1038/NG1217.

[85] V. Singla and J. F. Reiter, “The primary cilium as the cell’s antenna: signaling at a sensory organelle,” *Science*, vol. 313, no. 5787, pp. 629–633, Aug. 2006, doi: 10.1126/SCIENCE.1124534.

[86] J. M. Gerdes, E. E. Davis, and N. Katsanis, “The vertebrate primary cilium in development, homeostasis, and disease,” *Cell*, vol. 137, no. 1, pp. 32–45, Apr. 2009, doi: 10.1016/J.CELL.2009.03.023.

[87] D. Huangfu, A. Liu, A. S. Rakeman, N. S. Murcia, L. Niswander, and K. V. Anderson, “Hedgehog signalling in the mouse requires intraflagellar transport proteins,” *Nature*, vol. 426, no. 6962, pp. 83–87, Nov. 2003, doi: 10.1038/NATURE02061.

[88] P. Satir and S. T. Christensen, “Overview of structure and function of mammalian cilia,” *Annu. Rev. Physiol.*, vol. 69, pp. 377–400, 2007, doi: 10.1146/ANNUREV.PHYSIOL.69.040705.141236.

[89] D. K. Breslow and A. J. Holland, “Mechanism and Regulation of Centriole and Cilium Biogenesis,” *Annual Review of Biochemistry*, vol. 88. Annual Reviews Inc., pp. 691–724, Jun. 20, 2019. doi: 10.1146/annurev-biochem-013118-111153.

[90] A. Knödler *et al.*, “Coordination of Rab8 and Rab11 in primary ciliogenesis,” *Proc. Natl. Acad. Sci. U. S. A.*, vol. 107, no. 14, pp. 6346–6351, Apr. 2010, doi: 10.1073/pnas.1002401107.

[91] A. Gerondopoulos *et al.*, “Planar Cell Polarity Effector Proteins Inturned and Fuzzy Form a Rab23 GEF Complex,” *Curr. Biol.*, vol. 29, no. 19, pp. 3323-

3330.e8, Oct. 2019, doi: 10.1016/j.cub.2019.07.090.

[92] A. Onnis *et al.*, “The small GTPase Rab29 is a common regulator of immune synapse assembly and ciliogenesis,” *Cell Death Differ. 2015 2210*, vol. 22, no. 10, pp. 1687–1699, Mar. 2015, doi: 10.1038/cdd.2015.17.

[93] M. E. Oguchi, K. Okuyama, Y. Homma, and M. Fukuda, “A comprehensive analysis of Rab GTPases reveals a role for Rab34 in serum starvation-induced primary ciliogenesis,” *J. Biol. Chem.*, vol. 295, no. 36, pp. 12674–12685, Sep. 2020, doi: 10.1074/JBC.RA119.012233.

[94] A. K. Ganga *et al.*, “Rab34 GTPase mediates ciliary membrane formation in the intracellular ciliogenesis pathway,” *Curr. Biol.*, vol. 31, no. 13, pp. 2895-2905.e7, Jul. 2021, doi: 10.1016/J.CUB.2021.04.075.

[95] M. W. Stuck, W. M. Chong, J. C. Liao, and G. J. Pazour, “Rab34 is necessary for early stages of intracellular ciliogenesis,” *Curr. Biol.*, vol. 31, no. 13, pp. 2887-2894.e4, Jul. 2021, doi: 10.1016/J.CUB.2021.04.018.

[96] S. I. Yoshimura, J. Egerer, E. Fuchs, A. K. Haas, and F. A. Barr, “Functional dissection of Rab GTPases involved in primary cilium formation,” *J. Cell Biol.*, vol. 178, no. 3, pp. 363–369, Jul. 2007, doi: 10.1083/JCB.200703047.

[97] T. Sato *et al.*, “The Rab8 GTPase regulates apical protein localization in intestinal cells,” *Nature*, vol. 448, no. 7151, pp. 366–369, Jul. 2007, doi: 10.1038/NATURE05929.

[98] T. Sato *et al.*, “Rab8a and Rab8b are essential for several apical transport pathways but insufficient for ciliogenesis,” *J. Cell Sci.*, vol. 127, no. Pt 2, pp. 422–431, Jan. 2014, doi: 10.1242/JCS.136903.

[99] C. J. Westlake *et al.*, “Primary cilia membrane assembly is initiated by Rab11 and transport protein particle II (TRAPPII) complex-dependent trafficking of Rabin8 to the centrosome,” *Proc. Natl. Acad. Sci. U. S. A.*, vol. 108, no. 7, pp. 2759–2764, Feb. 2011, doi: 10.1073/pnas.1018823108.

[100] C. Boehlke *et al.*, “Differential role of Rab proteins in ciliary trafficking: Rab23 regulates smoothened levels,” *J. Cell Sci.*, vol. 123, no. Pt 9, pp. 1460–1467, May 2010, doi: 10.1242/JCS.058883.

[101] Y. S. Lim and B. L. Tang, “A role for Rab23 in the trafficking of Kif17 to the primary cilium,” *J. Cell Sci.*, vol. 128, no. 16, pp. 2996–3008, Aug. 2015, doi: 10.1242/JCS.163964.

[102] A. Leaf and M. Von Zastrow, “Dopamine receptors reveal an essential role of IFT-B, KIF17, and Rab23 in delivering specific receptors to primary cilia,” *Elife*, vol. 4, no. JULY2015, Jul. 2015, doi: 10.7554/ELIFE.06996.

[103] J. H. Lumb and M. C. Field, “Rab23 is a flagellar protein in Trypanosoma brucei,” *BMC Res. Notes*, vol. 4, 2011, doi: 10.1186/1756-0500-4-190.

[104] G. B. Carballo, J. R. Honorato, G. P. F. De Lopes, and T. C. L. D. S. E. Spohr, “A highlight on Sonic hedgehog pathway,” *Cell Communication and Signaling*, vol. 16, no. 1. BioMed Central Ltd., pp. 1–15, Mar. 20, 2018. doi: 10.1186/s12964-018-0220-7.

[105] K. Fuller, J. T. O’Connell, J. Gordon, O. Mauti, and J. Eggenschwiler, “Rab23 regulates Nodal signaling in vertebrate left-right patterning independently of the Hedgehog pathway,” *Dev. Biol.*, vol. 391, no. 2, pp. 182–195, Jul. 2014, doi: 10.1016/J.YDBIO.2014.04.012.

[106] J. P. Fededa and D. W. Gerlich, “Molecular control of animal cell cytokinesis,” *Nat. Cell Biol.*, vol. 14, no. 5, pp. 440–447, 2012, doi: 10.1038/NCB2482.

[107] B. Mierzwa and D. W. Gerlich, “Cytokinetic abscission: molecular mechanisms and temporal control,” *Dev. Cell*, vol. 31, no. 5, pp. 525–538, Dec. 2014, doi: 10.1016/J.DEVCEL.2014.11.006.

[108] S. Frémont *et al.*, “Oxidation of F-actin controls the terminal steps of cytokinesis,” *Nat. Commun. 2017 81*, vol. 8, no. 1, pp. 1–16, Feb. 2017, doi: 10.1038/ncomms14528.

[109] I. Goliand *et al.*, “Resolving ESCRT-III Spirals at the Intercellular Bridge of Dividing Cells Using 3D STORM,” *Cell Rep.*, vol. 24, no. 7, pp. 1756–1764, Aug. 2018, doi: 10.1016/J.CELREP.2018.07.051.

[110] J. Guizetti *et al.*, “Cortical constriction during abscission involves helices of ESCRT-III-dependent filaments,” *Science*, vol. 331, no. 6024, pp. 1616–1620, Mar. 2011, doi: 10.1126/SCIENCE.1201847.

[111] D. Yang, N. Rismanchi, B. Renvoisé, J. Lippincott-Schwartz, C. Blackstone, and J. H. Hurley, “Structural basis for midbody targeting of spastin by the ESCRT-III protein CHMP1B,” *Nat. Struct. Mol. Biol. 2008 1512*, vol. 15, no. 12, pp. 1278–1286, Nov. 2008, doi: 10.1038/nsmb.1512.

[112] C. Addi, J. Bai, and A. Echard, “Actin, microtubule, septin and ESCRT filament remodeling during late steps of cytokinesis,” *Curr. Opin. Cell Biol.*, vol. 50, pp. 27–34, Feb. 2018, doi: 10.1016/J.CEB.2018.01.007.

[113] D. Dambournet *et al.*, “Rab35 GTPase and OCRL phosphatase remodel lipids and F-actin for successful cytokinesis,” *Nat. Cell Biol. 2011 138*, vol. 13, no. 8,

pp. 981–988, Jun. 2011, doi: 10.1038/ncb2279.

[114] C. Cauvin *et al.*, “Rab35 GTPase Triggers Switch-like Recruitment of the Lowe Syndrome Lipid Phosphatase OCRL on Newborn Endosomes,” *Curr. Biol.*, vol. 26, no. 1, pp. 120–128, Jan. 2016, doi: 10.1016/J.CUB.2015.11.040/ATTACHMENT/89BE4714-3190-476A-998D-B0F98E6AF393/MMC1.PDF.

[115] N. V. G. Iannantuono and G. Emery, “Rab11FIP1 maintains Rab35 at the intercellular bridge to promote actin removal and abscission,” *J. Cell Sci.*, vol. 134, no. 12, Jun. 2021, doi: 10.1242/JCS.244384/268385/AM/RAB11FIP1-MAINTAINS-RAB35-AT-THE-INTERCELLULAR.

[116] J. A. Schiel and R. Prekeris, “Membrane dynamics during cytokinesis,” *Curr. Opin. Cell Biol.*, vol. 25, no. 1, pp. 92–98, 2013, doi: 10.1016/J.CEB.2012.10.012.

[117] S. Sechi *et al.*, “Rab1 interacts with GOLPH3 and controls Golgi structure and contractile ring constriction during cytokinesis in Drosophila melanogaster,” *Open Biol.*, vol. 7, no. 1, 2017, doi: 10.1098/RSOB.160257.

[118] T. Pellinen *et al.*, “Integrin trafficking regulated by Rab21 is necessary for cytokinesis,” *Dev. Cell*, vol. 15, no. 3, pp. 371–385, Sep. 2008, doi: 10.1016/J.DEVCEL.2008.08.001.

[119] V. S. Lalioti, A. Ilari, D. J. O’Connell, E. Poser, I. V. Sandoval, and G. Colotti, “Sorcin links calcium signaling to vesicle trafficking, regulates Polo-like kinase 1 and is necessary for mitosis,” *PLoS One*, vol. 9, no. 1, Jan. 2014, doi: 10.1371/JOURNAL.PONE.0085438.

[120] E. E. Kelly *et al.*, “Class I Rab11-family interacting proteins are binding targets for the Rab14 GTPase,” *Biol. cell*, vol. 102, no. 1, pp. 51–62, Jan. 2009, doi: 10.1042/BC20090068.

[121] R. D. Militello *et al.*, “Rab24 is required for normal cell division,” *Traffic*, vol. 14, no. 5, pp. 502–518, May 2013, doi: 10.1111/TRA.12057.

[122] A. Sakaguchi *et al.*, “REI-1 Is a Guanine Nucleotide Exchange Factor Regulating RAB-11 Localization and Function in C. elegans Embryos,” *Dev. Cell*, vol. 35, no. 2, pp. 211–221, Oct. 2015, doi: 10.1016/J.DEVCEL.2015.09.013.

[123] G. R. X. Hickson *et al.*, “Arfophilins are dual Arf/Rab 11 binding proteins that regulate recycling endosome distribution and are related to Drosophila nuclear fallout,” *Mol. Biol. Cell*, vol. 14, no. 7, pp. 2908–2920, Jul. 2003, doi: 10.1091/MBC.E03-03-0160.

[124] C. P. Horgan, M. Walsh, T. H. Zurawski, and M. W. McCaffrey, “Rab11-FIP3 localises to a Rab11-positive pericentrosomal compartment during interphase and to the cleavage furrow during cytokinesis,” *Biochem. Biophys. Res. Commun.*, vol. 319, no. 1, pp. 83–94, Jun. 2004, doi: 10.1016/j.bbrc.2004.04.157.

[125] A. B. Fielding *et al.*, “Rab11-FIP3 and FIP4 interact with Arf6 and the exocyst to control membrane traffic in cytokinesis,” *EMBO J.*, vol. 24, no. 19, pp. 3389–3399, Oct. 2005, doi: 10.1038/SJ.EMBOJ.7600803.

[126] G. M. Wilson *et al.*, “The FIP3-Rab11 protein complex regulates recycling endosome targeting to the cleavage furrow during late cytokinesis,” *Mol. Biol. Cell*, vol. 16, no. 2, pp. 849–860, Feb. 2005, doi: 10.1091/MBC.E04-10-0927.

[127] K. Kasahara, Y. Nakayama, Y. Nakazato, K. Ikeda, T. Kuga, and N. Yamaguchi, “Src signaling regulates completion of abscission in cytokinesis through ERK/MAPK activation at the midbody,” *J. Biol. Chem.*, vol. 282, no. 8, pp. 5327–5339, Feb. 2007, doi: 10.1074/JBC.M608396200.

[128] B. Riggs *et al.*, “Actin cytoskeleton remodeling during early Drosophila furrow formation requires recycling endosomal components Nuclear-fallout and Rab11,” *J. Cell Biol.*, vol. 163, no. 1, pp. 143–154, Oct. 2003, doi: 10.1083/JCB.200305115.

[129] M. G. Giansanti, G. Belloni, and M. Gatti, “Rab11 is required for membrane trafficking and actomyosin ring constriction in meiotic cytokinesis of Drosophila males,” *Mol. Biol. Cell*, vol. 18, no. 12, pp. 5034–5047, Dec. 2007, doi: 10.1091/MBC.E07-05-0415.

[130] G. Polevoy *et al.*, “Dual roles for the Drosophila PI 4-kinase four wheel drive in localizing Rab11 during cytokinesis,” *J. Cell Biol.*, vol. 187, no. 6, pp. 847–858, Dec. 2009, doi: 10.1083/JCB.200908107.

[131] F. R. Kiral, F. E. Kohrs, E. J. Jin, and P. R. Hiesinger, “Rab GTPases and Membrane Trafficking in Neurodegeneration,” *Curr. Biol.*, vol. 28, no. 8, pp. R471–R486, Apr. 2018, doi: 10.1016/J.CUB.2018.02.010.

[132] G. Li, “Rab GTPases, Membrane Trafficking and Diseases,” *Curr. Drug Targets*, vol. 12, no. 8, p. 1188, Jul. 2011, doi: 10.2174/138945011795906561.

[133] H. Sano, G. R. Peck, A. N. Kettenbach, S. A. Gerber, and G. E. Lienhard, “Insulin-stimulated GLUT4 Protein Translocation in Adipocytes Requires the Rab10 Guanine Nucleotide Exchange Factor Dennd4C,” *J. Biol. Chem.*, vol. 286, no. 19, p. 16541, May 2011, doi: 10.1074/JBC.C111.228908.

[134] J. Cherfils and M. Zeghouf, “Regulation of small GTPases by GEFs, GAPs, and GDIs,” *Physiological Reviews*, vol. 93, no. 1. American Physiological Society Bethesda, MD, pp. 269–309, Jan. 01, 2013. doi: 10.1152/physrev.00003.2012.

[135] E. M. Valente, R. O. Rosti, E. Gibbs, and J. G. Gleeson, “Primary cilia in neurodevelopmental disorders,” *Nature Reviews Neurology*, vol. 10, no. 1. NIH Public Access, pp. 27–36, Jan. 2014. doi: 10.1038/nrneurol.2013.247.

[136] N. Huang *et al.*, “M-Phase Phosphoprotein 9 regulates ciliogenesis by modulating CP110-CEP97 complex localization at the mother centriole,” *Nat. Commun.*, vol. 9, no. 1, Dec. 2018, doi: 10.1038/s41467-018-06990-9.

[137] R. Lippé, M. Miaczynska, V. Rybin, A. Runge, and M. Zerial, “Functional Synergy between Rab5 Effector Rabaptin-5 and Exchange Factor Rabex-5 When Physically Associated in a Complex,” *Mol. Biol. Cell*, vol. 12, no. 7, p. 2219, 2001, doi: 10.1091/MBC.12.7.2219.

[138] M. Medkova, Y. E. France, J. Coleman, and P. Novick, “The rab exchange factor Sec2p reversibly associates with the exocyst,” *Mol. Biol. Cell*, vol. 17, no. 6, pp. 2757–2769, Jun. 2006, doi: 10.1091/MBC.E05-10-0917.

[139] V. Nähse, L. Christ, H. Stenmark, and C. Campsteijn, “The Abscission Checkpoint: Making It to the Final Cut,” *Trends Cell Biol.*, vol. 27, no. 1, pp. 1–11, Jan. 2017, doi: 10.1016/J.TCB.2016.10.001.

[140] A. L. Marat, M. S. Ioannou, and P. S. McPherson, “Connecdenn 3/DENND1C binds actin linking Rab35 activation to the actin cytoskeleton,” *Mol. Biol. Cell*, vol. 23, no. 1, pp. 163–175, Jan. 2012, doi: 10.1091/mbc.E11-05-0474.

[141] Y. Homma and M. Fukuda, “Rabin8 regulates neurite outgrowth in both GEF

activity-dependent and -independent manners," *Mol. Biol. Cell*, vol. 27, no. 13, pp. 2107–2118, Jul. 2016, doi: 10.1091/mbc.E16-02-0091.

[142] H. S. Dhekne *et al.*, "A pathway for parkinson's disease LRRK2 kinase to block primary cilia and sonic hedgehog signaling in the brain," *Elife*, vol. 7, Nov. 2018, doi: 10.7554/eLife.40202.

[143] Y. Sobu, P. S. Wawro, H. S. Dhekne, W. M. Yeshaw, and S. R. Pfeffer, "Pathogenic LRRK2 regulates ciliation probability upstream of tau tubulin kinase 2 via Rab10 and RILPL1 proteins," *Proc. Natl. Acad. Sci.*, vol. 118, no. 10, Mar. 2021, doi: 10.1073/PNAS.2005894118.

[144] P. D. Allaire *et al.*, "Connecdenn, a novel DENN domain-containing protein of neuronal clathrin-coated vesicles functioning in synaptic vesicle endocytosis," *J. Neurosci.*, vol. 26, no. 51, pp. 13202–13212, Dec. 2006, doi: 10.1523/JNEUROSCI.4608-06.2006.

[145] R. Kumar, V. Francis, G. Kulasekaran, M. Khan, G. A. B. Armstrong, and P. S. McPherson, "A cell-based GEF assay reveals new substrates for DENN domains and a role for DENND2B in primary ciliogenesis," *Sci. Adv.*, vol. 8, no. 8, p. 3088, Feb. 2022, doi: 10.1126/sciadv.abk3088.

[146] R. Kumar *et al.*, "DENND2B activates Rab35 at the intercellular bridge, regulating cytokinetic abscission and tetraploidy," *Cell Rep.*, vol. 42, no. 7, p. 112795, Jul. 2023, doi: 10.1016/J.CELREP.2023.112795.

[147] S. Bisi *et al.*, "IRSp53 controls plasma membrane shape and polarized transport at the nascent lumen in epithelial tubules," *Nat. Commun. 2020 111*, vol. 11, no. 1, pp. 1–23, Jul. 2020, doi: 10.1038/s41467-020-17091-x.